

17. SITE 685¹

Shipboard Scientific Party²

HOLE 685A

Date occupied: 1350 L, 22 November 1968

Date departed: 0930 L, 30 November 1968

Time on hole: 187 hr 40 min

Position: 9°06.78'S, 80°35.01'W

Water depth (sea level; corrected m, echo-sounding): 5070.8

Water depth (rig floor; corrected m, echo-sounding): 5081.3

Bottom felt (m, drill pipe): 5093.4

Penetration (m): 468.6

Number of cores: 51

Total length of cored section (m): 468.6

Total core recovered (m): 278.65

Core recovery (%): 59.5

Oldest sediment cored

Depth (mbsf): 468.6

Nature: Conglomeratic sandy siltstone

Age: early late Miocene

Measured velocity (km/s): 1.8

Principal results: Site 685 (9°06.78'S, 80°35.01'W) on the lower slope of the Peru Trench was located at a water depth of 5070 m, about 1200 m above the trench floor. Here, our main objective was to establish the nature and age of the transition between the accreted sediments at the front of the margin and the continental crust drilled previously. The frontal part of the transition was inferred to be a landward-dipping boundary that transects the entire upper plate. We sampled shorter landward-dipping reflections 1 km downslope, where thin slope deposits allowed sufficient penetration.

The two main lithologies found in the 468 m cored were (1) slope deposits and (2) the accreted complex. The slope deposits (0–200 m) consist of 80-m-thick diatomaceous mud having small normal faults overlying a diatomaceous mud having folding, locally developed fissility and a fabric that cuts the beds at high angles. Fossils are of Pleistocene age, and most were transported from the shelf. The age range is well-constrained and yields a sedimentation rate of 100 m/m.y.

A hiatus having a minimum duration of 4.3 m.y. separates the lower Pleistocene slope deposits from the early upper Miocene accreted complex. The dominantly diatomaceous mudstones are variably calcareous. In the upper part, the rocks showed a moderate-to-strong, scaly fabric parallel to the dipping beds. Toward the bottom of the cored section the well-lithified parts are intensely fractured and show compressional structure. The apparent dips of bedding cluster between 45° and 60°, whereas those of the reflections in the seismic record are from 10° to 20° and thus indicate tectonic thickening. The hole bottomed in sand and in sedimentary breccias having Eocene to late Miocene clasts. The lower unit contained transported fauna, and diatom assemblages were from a single zone (6.1 to 6.8 Ma). A minimum sedimentation rate (not corrected for tectonic thickening) was about 250 m/m.y., but only one-half of the thrust packet was penetrated.

Methane gas hydrate was recovered at 99 mbsf and was observed visually to 165 mbsf. This hydrate occurrence is consistent with the shallow generation of considerable amounts of biogenic methane that starts at only 11.6 mbsf. Total organic carbon contents are lower at this site than in the other Leg 112 sites because of dilution by biogenic and clastic components from rapid sedimentation rates. This rapid sedimentation is responsible for extreme concentration gradients of chemical species dissolved in pore water. Maxima in alkalinity (156 mmol/L), phosphate (0.826 mmol/L), and ammonia (31.7 mmol/L) were the highest reported up until then for DSDP and ODP cruises. Despite the extreme chemical gradients, the amounts of diagenetic minerals that form per unit volume of sediment are small.

The stratigraphy and fabric of the cored section are consistent with the accretionary nature apparent in the seismic section. The change from upper Miocene nonaccretionary to accretionary sediments along the Peru Trench occurs after the Nazca Ridge was subducted at the latitude of the site. At the same time, sedimentation increased dramatically following the onset of coastal upwelling.

BACKGROUND AND SCIENTIFIC OBJECTIVES

Site 685 was located so as to sample the oldest part of the sediment accreted at the Peru Trench during the Andean orogeny. Sites 685 and 683 straddle the transition from the continental crust to the accretionary complex (Fig. 1). This transition occurs beneath the midslope, where a broad terrace dominates the morphology (Fig. 2). Beneath this terrace, seismic imaging in CDP-2, the primary record that best illustrates the tectonic structure across the northern transect (see "Background and Scientific Objectives" section, Site 683 chapter, and "Geophysics" section, Site 685 chapter, this volume), indicates a complex tec-

¹ Suess, E., von Huene, R., et al., 1988. *Proc. ODP, Init. Repts.*, 112: College Station, TX (Ocean Drilling Program).

² Erwin Suess (Co-Chief Scientist), Oregon State University, College of Oceanography, Corvallis, OR 97331; Roland von Huene (Co-Chief Scientist), U.S. Geological Survey, Branch of Pacific Marine Geology, 345 Middlefield Rd. M/S 999, Menlo Park, CA 94025; Kay-Christian Emeis (ODP Staff Scientist), Ocean Drilling Program, Texas A&M University, College Station, TX 77843; Jacques Bourgois, Département de Géotectonique, Université Pierre et Marie Curie, 4 Place Jussieu, 75230 Paris Cedex 05, France; José del C. Cruzado Castañeda, Petroleos del Peru S. A., Paseo de la Republica 3361, San Isidro, Lima, Peru; Patrick De Wever, CNRS, Laboratoire de Stratigraphie, Université Pierre et Marie Curie, 4 Place Jussieu, 75230 Paris Cedex 05, France; Geoffrey Eglinton, University of Bristol, School of Chemistry, Cantock's Close, Bristol BS8 1TS, England; Robert Garrison, University of California, Earth Sciences, Applied Sciences Building, Santa Cruz, CA 95064; Matt Greenberg, Lamont-Doherty Geological Observatory, Columbia University, Palisades, NY 10964; Elard Herrera Paz, Petroleos del Peru, S. A., Paseo de la Republica 3361, San Isidro, Lima, Peru; Phillip Hill, Atlantic Geoscience Centre, Bedford Institute of Oceanography, Box 1006, Dartmouth, Nova Scotia B2Y 4A2, Canada; Masako Ibaraki, Geoscience Institute, Faculty of Science, Shizuoka University, Shizuoka 422, Japan; Miriam Kastner, Scripps Institution of Oceanography, SVH, A-102, La Jolla, CA 92093; Alan E. S. Kemp, Department of Oceanography, The University, Southampton SO9 5NH, England; Keith Kvenvolden, U.S. Geological Survey, Branch of Pacific Marine Geology, 345 Middlefield Rd., M/S 999, Menlo Park, CA 94025; Robert Langridge, Department of Geological Sciences, Queen's University at Kingston, Ontario K7L 3A2, Canada; Nancy Lindsley-Griffin, University of Nebraska, Department of Geology, 214 Bessey Hall, Lincoln, NE 68588-0340; Janice Marsters, Department of Oceanography, Dalhousie University, Halifax, Nova Scotia B3H 4J1, Canada; Erlend Martini, Geologisch-Paläontologisches Institut der Universität Frankfurt, Senckenberg-Anlage 32-34, D-6000, Frankfurt/Main, Federal Republic of Germany; Robert McCabe, Department of Geophysics, Texas A&M University, College Station, TX 77843; Leonidas Ocola, Laboratorio Central, Instituto Geofísico del Peru, Lima, Peru; Johanna Resig, Department of Geology and Geophysics, University of Hawaii, Honolulu, HI 96822; Agapito Wilfredo Sanchez Fernandez, Instituto Geológico Minero y Metalúrgico, Pablo Bermúdez 211, Lima, Peru; Hans-Joachim Schrader, College of Oceanography, Oregon State University, Corvallis, OR 97331 (currently at Department of Geology, University of Bergen, N-5000 Bergen, Norway); Todd Thornburg, College of Oceanography, Oregon State University, Corvallis, OR 97331; Gerold Wefer, Universität Bremen, Fachbereich Geowissenschaften, Postfach 330 440, D-2800 Bremen 33, Federal Republic of Germany; Makoto Yamano, Earthquake Research Institute, University of Tokyo, Bunkyo-ku, Tokyo 113, Japan.

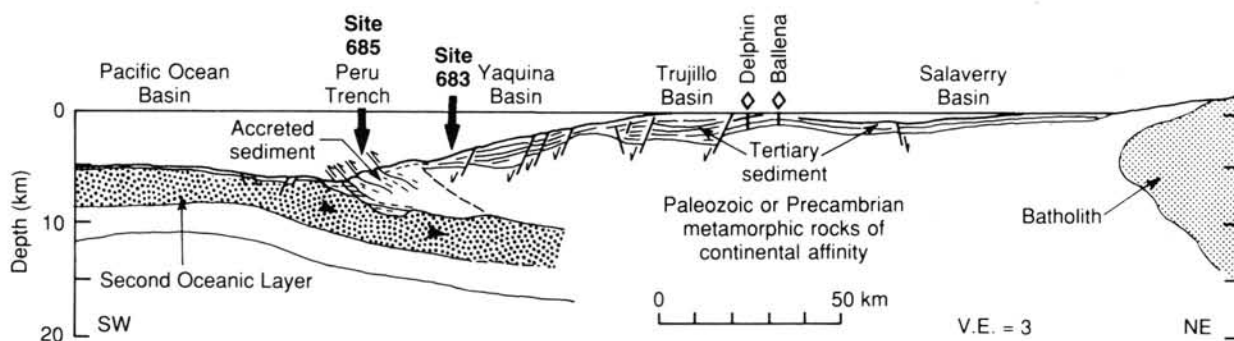


Figure 1. Diagrammatic cross section of structures across the central Peruvian margin near 9°S latitude.

tonic transition from the edge of truncated continental crust to an accretionary prism. Site 685 was located seaward of the transition zone in an area where the seismic record clearly displays a pattern of landward-dipping strata, which are considered typical of an accretionary complex. At this site, these strata were shallow enough to be drilled by the *JOIDES Resolution*.

The studies that develop the tectonic overview of a Peruvian convergent margin "type" are discussed in the Site 683 "Background and Scientific Objectives" section (this volume) and are not repeated here. The major tectonic objectives at Site 685 were to document the extent of the accretionary complex and its age. The age when tectonic erosion ended and accretion began is important for constraining the reasons why some convergent margins are accretionary and others are nonaccretionary. Thus, the studies of cores from this site focused on identifying the stratigraphy and structures that separate accreted sediment from an overlying cover of slope deposits that may have already been involved in the deformation associated with accretion. The age when accretion began can then be related to plate tectonic history. Perhaps slight changes in the relative direction and rate of convergence affect tectonic processes, or perhaps the time when the Nazca Ridge first collided and passed the latitude of the northern transect affect tectonic history of the margin. The effects of the collision of a 2-km-high ridge may provide insight into the role of subducting topographic features in the tectonic processes at the front of the Andean subduction zone. The history of accretion or of erosion may also be related to the general supply of sediment to the margin, as documented by the sedimentation rates from Leg 112 sites. The history of subduction may be related to the Cenozoic history of andesitic volcanism in the Andes and to times of mineralization. The timing of the change from erosion to accretion at the front of the Peru margin thus may provide insights into the reasons for that change.

OPERATIONS

The *JOIDES Resolution* departed Site 684 at 0915 L, 22 November 1986, and steamed west to intercept the track along which seismic record CDP-2 had been made at a point about 6 nmi from Site 685. The first pass downslope failed to produce seismic records or other information from which the correct location could be positively identified, and so the ship passed beyond the location to an adjacent distinctive topographic point. Once that point was identified, the ship reversed course and steamed upslope to drop a beacon. The survey lasted about 1.5 hr, and a beacon was dropped at 1311 (1811 UTC), 22 November. After passing a short distance beyond the drop point, the geophysical gear was retrieved. When the ship became stationary over the beacon, the coordinates from our global positioning system agreed with those of the site.

At a water depth of slightly more than 5 km, deployment of the drill string took about 10 hr. The hole was spudded on 23 November, and after only four cores (32.6 mbsf) the overpull on

the APC system became excessive and required us to change to the XCB drilling mode. Drilling proceeded normally, and care was exercised to condition the hole with mud and wiper trips (Table 1). On 28 November, we encountered obvious deterioration of hole conditions. Continuing high torque and caving signaled the end of drilling at 1400 hr on 28 November, which was forced by stuck drill string after retrieval of Core 112-685A-51X at a total depth of 468.6 mbsf. The hole was conditioned, the bit released, and logging began. We made three logging runs at ever-decreasing depths because of continued caving. On 30 November, the ship departed the site for a 30-hr transit to Site 686.

LITHOSTRATIGRAPHY

Lithological Units

The sediments recovered at Site 685 are subdivided into two lithological units on the basis of visual core descriptions, smear-slide analysis, carbonate determinations, and biostratigraphic data. These units are further subdivided into subunits, which are described in detail next (Figs. 3 and 4 and Table 2).

Unit I

Cores 112-685A-1H through 112-685A-22X; depth, 0–203.6 mbsf; age, Quaternary.

Subunit IA

Cores 112-685A-1H through 112-685A-9X-3; depth, 0–74.0 mbsf; age, Quaternary.

Subunit IA is composed of mostly diatomaceous muds ranging in color from dusky yellow green to dark greenish gray and dark olive gray. The component of diatom frustules in the dominant lithology ranges from 25% to 35% and generally increases downsection from 25% in Cores 112-685A-1H and 112-685A-2H to values of between 30% and 35% in Core 112-685A-4H and below. Moderate bioturbation persists throughout the unit. Small (~1 mm) spots and streaks of monosulfide and pyrite (see "Diagenesis" discussion next) occur from Core 112-685A-1H (Fig. 5) and become more abundant and denser down to Cores 112-685A-6X and 112-685A-7X, where the sediment is mottled with very dark gray. Core 112-685A-8X was initially very dark gray to black, but as was the case with Cores 112-685A-6X and 112-685A-7X, the color faded rapidly from dark olive gray to dark greenish gray. The muds at this level contain up to 13% pyrite.

The terrigenous proportion (quartz, feldspar, lithics) of the diatomaceous muds generally varies from 5% to 15%. The clays of Core 112-685A-1X have lower than average terrigenous component (5%), while the muds of Cores 112-685A-2H and 112-685A-3H have a higher than average (20%–25%) terrigenous component. Authigenic carbonate values are generally very low throughout Subunit IA and vary from 0% to 5%. A small, friable,

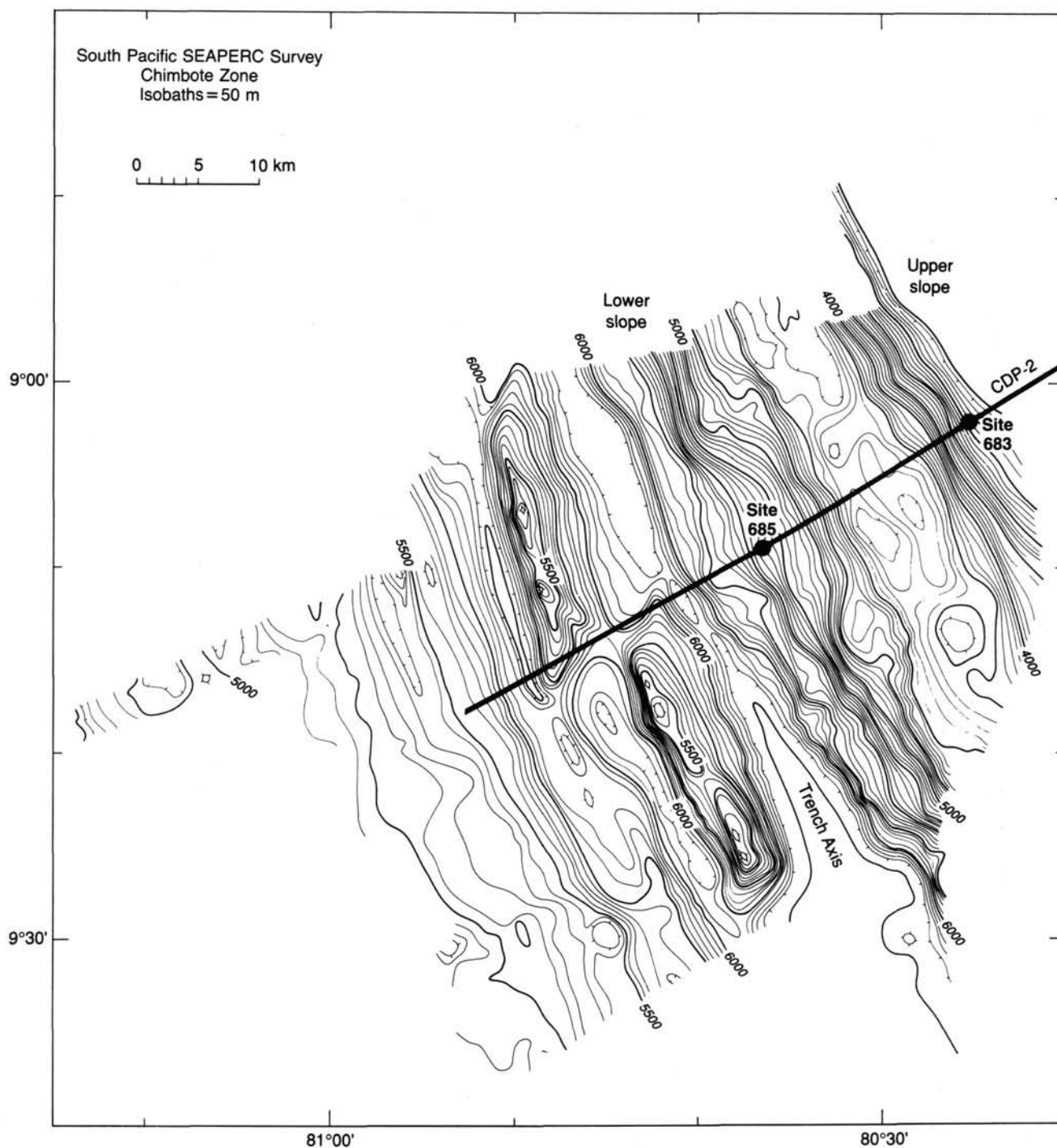


Figure 2. Seabeam bathymetry of the middle and lower slope, showing the location of CDP-2 and Site 685.

ble, dolomicrite nodule occurs in Core 112-685A-2H-1. An isolated dolomite nodule showing internal deformation occurs in Core 112-685A-2H-3 (Fig. 6) and is probably allochthonous (see "Diagenesis" discussion).

Calcareous microfossils were not observed in the diatomaceous muds of Cores 112-685A-1H to 112-685A-4H. Foraminifers were identified in trace amounts in Cores 112-685A-5X through 112-685A-8X. Nannofossils were noted in only two smear slides from Cores 112-685A-5X and 112-685A-7X.

Beds of glauconitic and glauconite-bearing terrigenous sand and silty mud occur in Cores 112-685A-1H (two separate beds)

and 112-685A-4H (a single bed). In Sample 112-685A-1H-2, 91-111 cm, a composite glauconitic and foraminifer sand exhibits multiple grading to a silty mud (Fig. 7). These beds are commonly bioturbated along their upper surface (Fig. 7) or, in the case of thin beds, throughout (Fig. 8). Scattered, small (<1 mm) patches of glauconite also occur sporadically in Cores 112-685A-1H through 112-685A-3H.

The diatomaceous muds also are punctuated by 1- to 10-cm-thick beds of olive muddy nannofossil ooze, nannofossil-foraminifer ooze, and nannofossil- and foraminifer-bearing muddy silts (olive facies). These invariably have sharp bases and gener-

Table 1. Coring summary for Hole 685A.

Core/section	Date (Nov. 1986)	Time (L)	Depth (mbsf)	Length cored (m)	Length recovered (m)	Recovery (%)
112-685A-1H	23	0340	0-4.1	4.1	4.17	102.0
2H	23	0437	4.1-13.6	9.5	9.68	102.0
3H	23	0540	13.6-23.1	9.5	9.81	103.0
4H	23	0645	23.1-32.6	9.5	10.12	106.5
5X	23	0835	32.6-42.1	9.5	7.70	81.0
6X	23	1005	42.1-51.6	9.5	9.48	99.8
7X	23	1145	51.6-61.1	9.5	4.70	49.5
8X	23	1325	61.1-70.6	9.5	9.65	101.0
9X	23	1505	70.6-80.1	9.5	11.52	121.2
10X	23	1640	80.1-89.6	9.5	8.09	85.1
11X	23	1830	89.6-99.1	9.5	9.66	101.0
12X	23	2055	99.1-108.6	9.5	11.07	116.5
13X	23	2220	108.6-118.1	9.5	3.87	40.7
14X	24	0224	118.1-127.6	9.5	5.18	54.5
15X	24	0400	127.6-137.1	9.5	6.39	67.2
16X	24	0540	137.1-146.6	9.5	5.21	54.8
17X	24	0720	146.6-156.1	9.5	11.72	123.3
18X	24	0915	156.1-165.6	9.5	12.83	135.0
19X	24	1115	165.6-175.1	9.5	0.91	9.6
20X	24	1535	175.1-184.6	9.5	10.70	112.6
21X	24	1855	184.6-194.1	9.5	11.14	117.2
22X	24	2040	194.1-203.6	9.5	5.96	62.7
23X	24	2250	203.6-213.1	9.5	0.19	2.0
24X	25	0135	213.1-222.6	9.5	0.00	0.0
25X	25	0400	222.6-232.1	9.5	0.55	5.8
26X	25	0630	232.1-233.6	1.5	0.13	8.7
27X	25	0915	233.6-243.1	9.5	1.77	18.6
28X	25	1125	243.1-252.6	9.5	12.75	134.2
29X	25	1405	252.6-262.1	9.5	4.20	44.2
30X	25	1645	262.1-271.6	9.5	3.10	32.6
31X	25	1830	271.6-281.1	9.5	0.45	4.7
32X	25	2255	281.1-290.6	9.5	5.84	61.5
33X	26	0340	290.6-300.1	9.5	0.63	6.6
34X	26	0605	300.1-309.6	9.5	10.19	107.2
35X	26	0820	309.6-319.1	9.5	9.50	100.0
36X	26	1040	319.1-328.6	9.5	11.81	124.3
37X	26	1310	328.6-338.1	9.5	3.90	41.0
38X	26	1550	338.1-347.6	9.5	0.74	7.8
39X	26	2110	347.6-357.1	9.5	11.42	120.2
40X	27	0310	357.1-366.6	9.5	3.86	40.6
41X	27	0715	366.6-376.1	9.5	0.91	9.6
42X	27	1005	376.1-385.6	9.5	2.89	30.4
43X	27	1220	385.6-392.6	7.0	0.90	12.8
44X	27	1510	392.6-402.1	9.5	3.86	40.6
45X	27	1750	402.1-411.6	9.5	0.71	7.5
46X	27	2025	411.6-421.1	9.5	2.25	23.7
47X	27	2310	421.1-430.6	9.5	1.66	17.5
48X	28	0140	430.6-440.1	9.5	2.27	23.9
49X	28	0425	440.1-449.6	9.5	0.74	7.8
50X	28	0740	449.6-459.1	9.5	1.39	14.6
51X	28	1355	459.1-468.6	9.5	0.48	5.1

H = hydraulic piston. X = extended-core barrel. L = local time.

ally have tops whose color grades from olive to the dark greenish-gray of the dominant diatomaceous muds. The top contact of these muds is commonly bioturbated. In Core 112-685A-3H, the basal contact with diatomaceous mud is commonly marked by a 1- to 2-cm-thick zone enriched with bluish-black monosulfide/pyrite in the diatomaceous mud. These interbeds are most abundant in Cores 112-685A-2H and 112-685A-3H and, at these levels, are commonly grouped at intervals of 20 to 50 cm in packets of beds separated by intervals of 1 to 3 cm thick. These persist until Core 112-685A-9X-1. In addition, a single, 8-cm-thick bed of nannofossil ooze occurs in Sample 112-685A-8X-2, 25 cm.

In Cores 112-685A-4H and 112-685A-5X, several 1- to 15-cm-thick interbeds of brownish, dark olive gray, sandy, foraminifer-bearing or nannofossil- and foraminifer-bearing silts and silty muds occur (brown facies). These commonly display size-grading from sharp bases to diffuse tops whose color grades to the dark greenish-gray of the enclosing muds. These are commonly bioturbated, particularly along the top surface (Fig. 9).

Subunit IA is further characterized by the ubiquitous presence of small (generally less than 1 mm) patches of sponge spicules (Figs. 5 and 8). These are composed mainly of monaxones

(see "Biostratigraphy" section, this chapter). Spicules occur only rarely below lithologic Unit I.

Subunit IB

Cores 112-685A-9X-4 through 112-685A-22X; depth, 74.0-203.6 mbsf; age, Quaternary.

The diatomaceous muds of Subunit IB differ from those of Subunit IA in having a generally higher, more constant content of diatom frustules (35%-40%). The upper boundary of Subunit IB also coincides with the loss of diatoms from the coarse fraction of the paleontological core-catcher sample (see "Biostratigraphy" section, this chapter). This absence persists through Cores 112-685A-9X to 112-685A-23X. The greater diatom abundance, together with the absence of diatoms from the coarse fraction, is explained by the presence of long thin species that can pass through a sieve. Light-to-moderate bioturbation was observed at several levels (Fig. 10) and may occur throughout, although we could not determine the extent of bioturbation because of the poor quality of recovered cores. The initial color of the muds in Cores 112-685A-9X through 112-685A-19X was black to very dark gray, but this faded rapidly to olive gray and dark olive gray. Cores 112-685A-20X through 112-685A-22X were less dark initially, but also faded to olive gray and dark olive gray. Cores 112-685A-9X to 112-685A-14X are unusually enriched in pyrite (up to 20%). There is little variation in the terrigenous component of the unit, other than for Cores 112-685A-20X to 112-685A-22X, which contain a relatively large proportion (15%-25%) of terrigenous grains. The amount of authigenic carbonate is generally very low and ranges from 0% to 5%, with the exception of Cores 112-685A-12X and 112-685A-19X, where values of up to 17% are recorded.

Calcareous microfossils were observed in the dominant (diatomaceous mud) lithology throughout Subunit IB; these occur sporadically in Cores 112-685A-9X to 112-685A-15X and regularly in Cores 112-685A-16X to 112-685A-22X.

Gas hydrates were observed at two levels within Subunit IB; the first occurrence was noted in Section 112-685A-12X-1 and the second in Section 112-685A-17X, CC (see "Organic Geochemistry" section, this chapter). The abundance of gas within Cores 112-685A-12X, 112-685A-17X, 112-685A-18X, 112-685A-20X, and 112-685A-21X resulted in explosive decompression upon opening the core barrel and, consequently, a loss in core quality.

Thin (1 mm to 2 cm) beds of foraminifer- and sometimes glauconite-bearing sandy silt or sandy mud were present in Sections 112-685A-9X-4 through 112-685A-20X-5 (Fig. 10, see also Fig. 27). Their overall frequency is difficult to establish because of the poor quality of recovered core at this interval. The thicker beds sometimes display grading, which generally is a distribution grading (Fig. 10). The distinctive "salt-and-pepper" texture of this lithology is a characteristic feature of Subunit IB.

Cores 112-685A-19X through 112-685A-22X exhibit partial induration with pieces of mudstone as well as mud.

Unit II

Cores 112-685A-23X through 112-685A-51X; depth, 203.6-468.6 mbsf; age, earliest late Miocene.

The lithologies of Unit II vary more than those of lithologic Unit I and include diatomaceous mudstones, diatom-bearing mudstones, and calcareous mudstones (Subunit IIB), with sedimentary breccias and sands occurring in the lower part. The unit is divided into two subunits, described in detail as follows.

Subunit IIA

Cores 112-685A-23X through 112-685A-42X; depth, 203.6-383.1 mbsf; age, earliest late Miocene (NN11-NN10).

The diatomaceous to diatom-bearing mudstones of Subunit IIA vary from dark greenish-gray to dark olive gray and black,

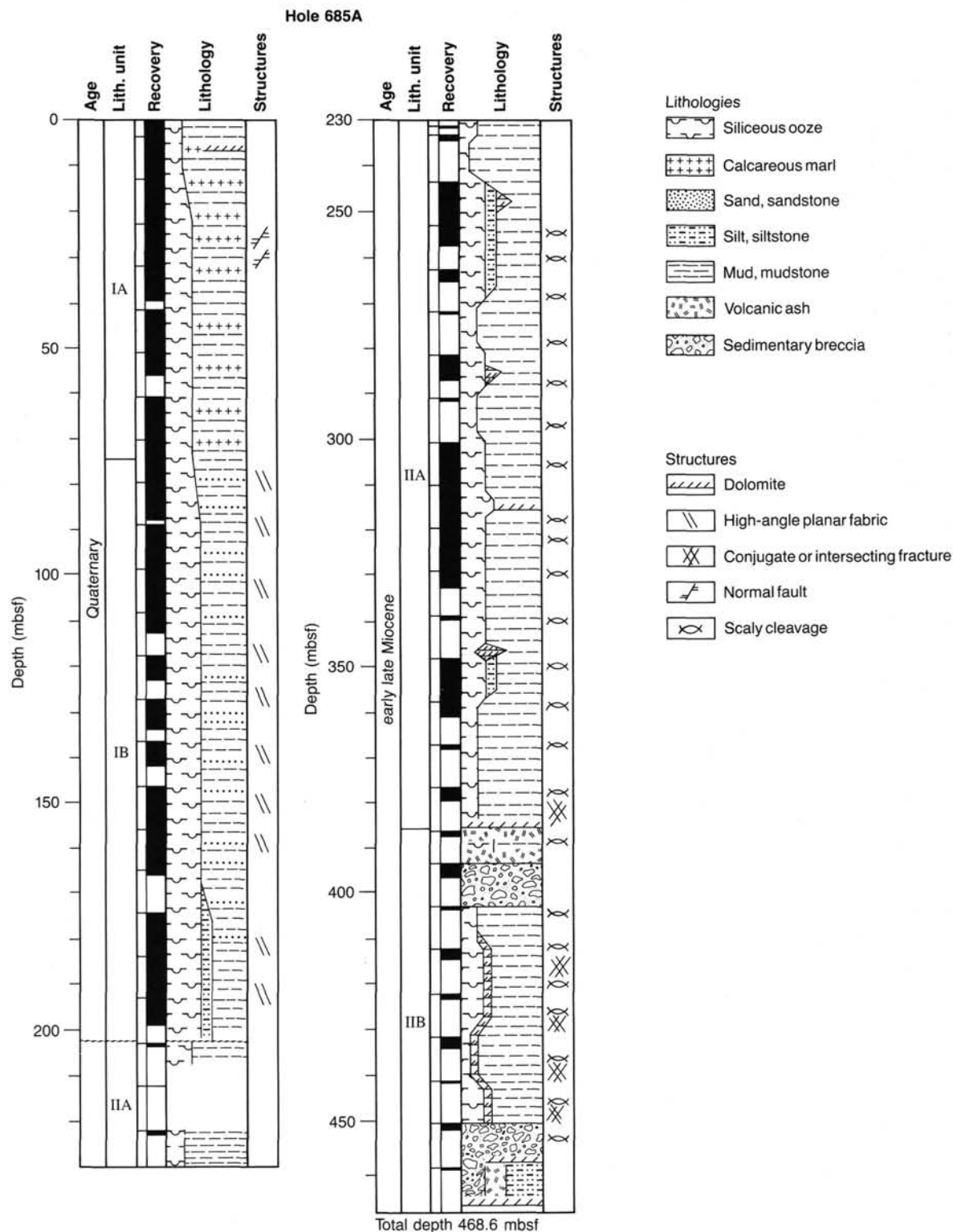


Figure 3. Generalized stratigraphic column for Site 685.

although systematic color variation was not recognized. Sporadic alternating pale and dark laminae on a scale of 0.1 to 0.5 mm were recognized from Cores 112-685A-28X to 112-685A-35X (Figs. 11 and 12). The darker layers at these levels generally contained more clay or terrigenous material and less diatoms. The diatom frustule content of the mudstones varies from lows of less than 10% to highs of 35%. Cores 112-685A-25X to 112-

685A-27X are particularly low in diatoms. Diatoms return to the coarse fraction of Section 112-685A-25X, CC after their absence in Subunit IB. Bioturbation was frequently difficult to detect because of the poor quality of cores, but we did recognize light-to-moderate bioturbation in several zones (Fig. 12).

The terrigenous component of the mudstones was generally higher than those in lithologic Unit I. In addition, we observed

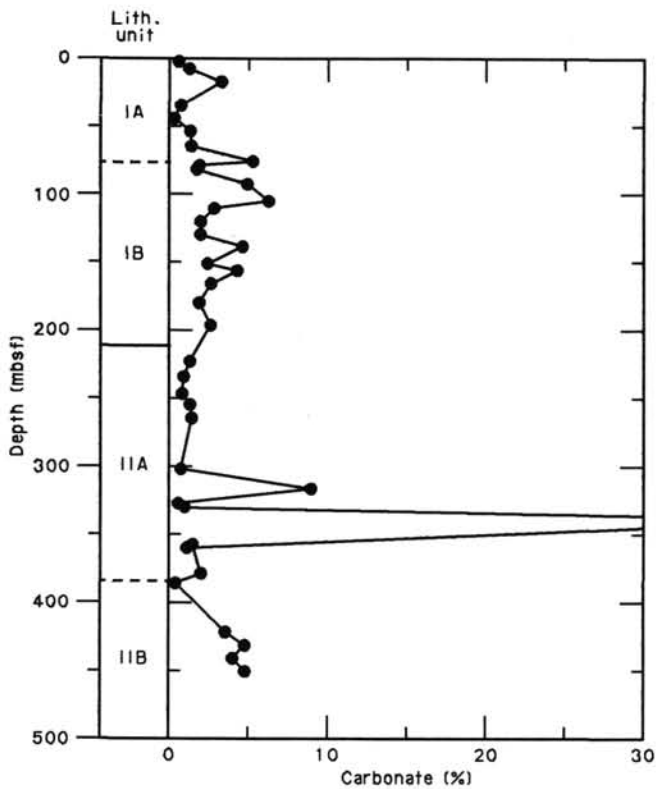


Figure 4. Carbonate contents at Site 685. Note the generally lower carbonate content of Subunit IIA and relatively high carbonate content of the lower part of Subunit IIB.

two prominent terrigenous clastic intervals. One interval occurred from Cores 112-685A-28X to 112-685A-30X, which contained a sequence of glauconite-bearing muddy sands and silts, and the second one was found in Core 112-685A-39X, where sandy muds occur. Explosive decompression of gassy cores made the search for primary structures in the terrigenous intervals impossible.

The authigenic carbonate content is generally low and ranges from 0% to 7%, but two short intervals in Cores 112-685A-28X and 112-685A-32X contain muds having up to 30% carbonate. Discrete carbonate beds are very rare and occur only in Cores 112-685A-35X (8-cm-thick dolomitic bed), 112-685A-39X (6-cm-thick micrite), and 112-685A-42X (8-cm-thick dolomicrite). The dolomicrite observed in Sample 112-685A-42X, CC (24–28 cm) (Fig. 13) is pervasively veined and recrystallized and as it was completely cored, must be of some lateral extent. Calcareous nannofossils were noted in only three cores: in trace amounts in isolated samples from Cores 112-685A-31X and 112-685A-34X

and in four samples (from trace to 5%) in Core 112-685A-38X. Foraminifers were noted in trace amounts in Cores 112-685A-23X, 112-685A-25X, 112-685A-27X, and 112-685A-40X.

Subunit IIB

Cores 112-685A-43X through 112-685A-51X; depth, 383.1–468.6 mbsf; age, earliest late Miocene (NN10).

Subunit IIB is distinctive in that it contains vitric tuffaceous material and prominent sedimentary breccia zones. In addition, the dominant lithology of dark olive gray diatomaceous mudstone contains an average of 10% authigenic carbonate down-hole from Core 112-685A-46X, based on smear-slide determinations. Carbonate determinations also indicate an elevated carbonate content from this level (Fig. 4). Discrete minor (about 0.5 cm) blebs of olive, muddy, nannofossil-bearing micrite occur in Cores 112-685A-46X and 112-685A-48X. The diatomaceous mudstones of Cores 112-685A-46X through 112-685A-48X also contain calcareous nannofossils. The diatom frustule content of the mudstones does not vary significantly and ranges from 15% to 25%; an exception is Core 112-685A-43X, which is relatively diatom-rich (35%–40%).

Two tuff bands composed mostly of volcanic glass occur in Core 112-685A-43X. The diatomaceous mud matrix of the breccia in Core 112-685A-50X and the sandy silt matrix of the pebbly sandstone in Core 112-685A-51X also contain significant quantities (30%–40%) of volcanic glass.

The sedimentary breccias of Cores 112-685A-44X and 112-685A-50X are compositionally and texturally similar and both contain a variety of clasts of differing ages (Figs. 14 through 17). The size of the clasts ranges from less than 0.1 mm to 4 cm in diameter, with the commonest range from 0.1 to 1 cm. The breccia in Core 112-685A-44X is mostly supported by clasts, with a few areas supported by matrix as well as small patches of ill-defined matrix material formed in part by disintegration of the more labile clasts. No imbrication of clasts was observed. In Core 112-685A-50X, the matrix is more abundant, and this breccia is supported locally by matrix. The shape of the clasts in both breccias is mainly subangular, although some subrounded clasts occur in both.

These clasts are mainly diatomaceous and diatom-bearing mudstones of Eocene and early and middle to late Miocene age, but also include nannofossil- and foraminifer-bearing mudstones and oozes, micrites, and dolomites (Table 3). The lower breccia (112-685A-50X) also includes a large (4 × 3 cm) clast of a calcareous feldspathic sandstone that contains foraminifers and other minor bioclastic material. Several clasts indicate evidence for deformation before incorporation, which includes veining, mud-filled fissures, and boudinage structures. The clay part of the Eocene clasts appears to be substantially recrystallized relative to that of the Miocene material. Definition of the matrix material in Core 112-685A-44X was difficult because of disaggregation of clasts to form local matrix. In Core 112-685A-50X,

Table 2. Lithologic units at Site 685.

Lith. unit	Lithology	Core/section	Depth (mbsf)
I	-----	112-685A-1H-1-22X, CC	0-203.6
IA	Diatomaceous muds with silty marl interbeds	112-685A-1H-1-9X-3	0-74.0
IB	Diatomaceous muds with very thin sandy mud interbeds	112-685A-9X-4-22X, CC	74.0-203.6
II	-----	112-685A-23X, CC-51X, CC	203.6-468.6
IIA	Diatomaceous and diatom-bearing mudstones	112-685A-23X, CC-42X, CC	203.6-383.1
IIB	Diatomaceous mudstones with interbedded ash layers and sedimentary breccias	112-685A-43X-1-51X, CC	383.1-468.6

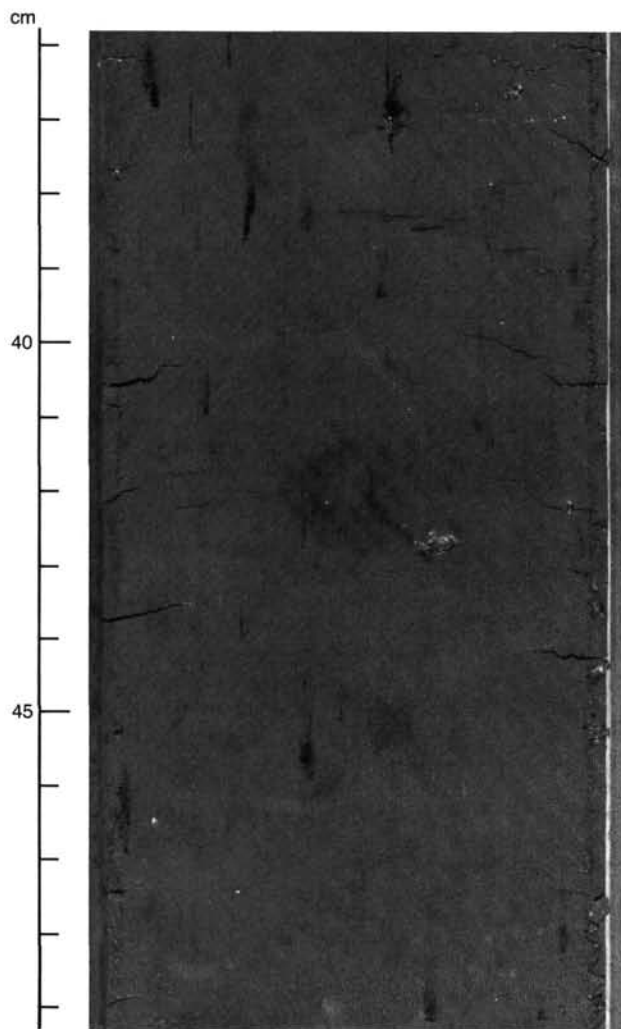


Figure 5. Spots of pyrite and patches of ?monosulfide and sponge spicules in massive diatomaceous mud, Subunit IA (Sample 112-685A-2H-7, 35.8–49.3 cm).

the matrix is a diatom-bearing, ashy, silty mudstone of earliest late Miocene age. A 5-cm-thick, laminated, foraminifer-bearing dolomitic mudstone occurs at the base of Core 112-685A-50X and is probably a clast in the breccia, rather than a continuous zone (Fig. 17).

The last core recovered at Site 685 (Core 112-685A-51X) is composed of a pebbly, ashy, sandy silt. This breccia contains a few mudstone clasts similar to those found in Cores 112-685A-44X and 112-685A-50X, but encompasses predominantly coarser clastic material. It includes lithic, ashy silts and sandstones, a silty bioclastic calcarenite, and a carbonate-cemented feldspathic sandstone (prominent well-lithified clast at Sample 112-685A-51X, CC, [42–43 cm]) similar to the calcareous feldspathic sandstone clast found in Core 112-685A-50X.

Carbonate Measurements

Carbonate measurements from Site 685 are listed in Table 4 and illustrated in Figure 4. Apart from localized carbonate-rich layers or nodules, the following general patterns emerge. Subunit IB has higher carbonate values than Subunit IA; Subunit IIA has the lowest carbonate values, and Subunit IIB has uniformly higher values of around 4%, corresponding to the higher carbonate recorded in smear-slide analyses. The significance of

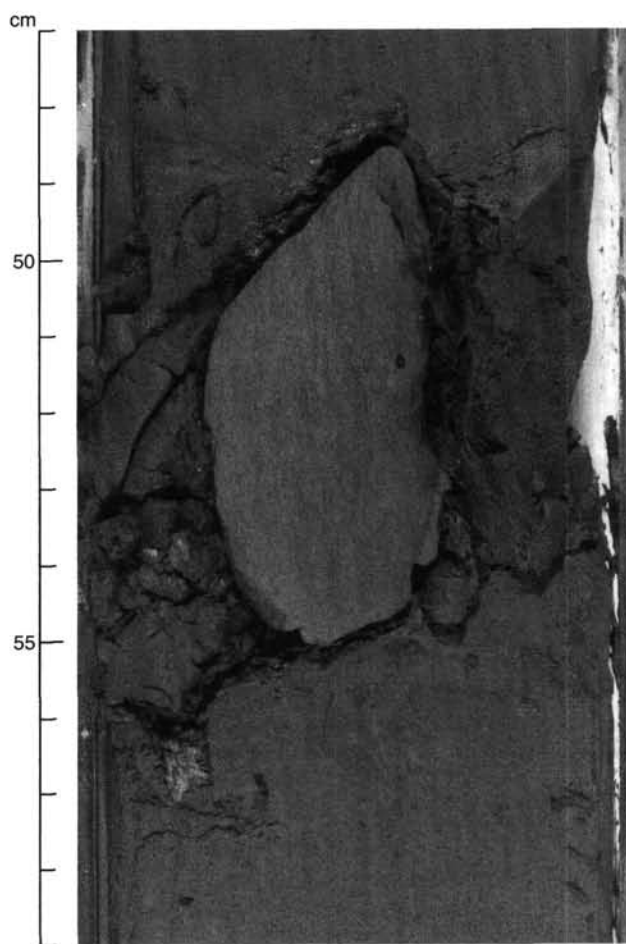


Figure 6. Allochthonous dolomite cobble showing pervasive extensional deformation, Subunit IA (Sample 112-685A-2H-2, 47–59 cm).

the variation in carbonate content is discussed in the “Depositional Environments” and “Structure” sections (this chapter).

Diagenesis

Compared to most other sites drilled during Leg 112, comparatively few diagenetic products were noted at Site 685. In addition, moderate-to-severe drilling disturbance of cores from this site hindered systematic study.

Phosphate and Glauconite

Although very small amounts of phosphatic and especially glauconitic grains are present in most parts of the sediment column at Site 685, only a few thin layers having abundant phosphate and/or glauconite were noted. A thin layer with 68% glauconite peloids occurs in Sample 112-685A-4H-7, 85 cm, and thin layers with 2%–15% glauconite and 5%–12% phosphatic grains are present in Cores 112-685A-28X and 112-685A-29X. These layers appear to be the basal coarse parts of thin turbidite beds, and we concluded that most, if not all, of the phosphate and glauconite at Site 685 was redeposited from shallower water.

A reworked mudstone clast in Sample 112-685A-20X-6, 141 cm, contains a distinctive form of pale green, authigenic apatite. This type of apatite was observed at present burial depths in excess of 410 m at Site 683, where it was tentatively interpreted as a product of relatively late burial diagenesis (see “Lithostratigraphy” section, Site 683 chapter). We believe that this clast was buried to at least comparable depths before it was exhumed and redeposited.

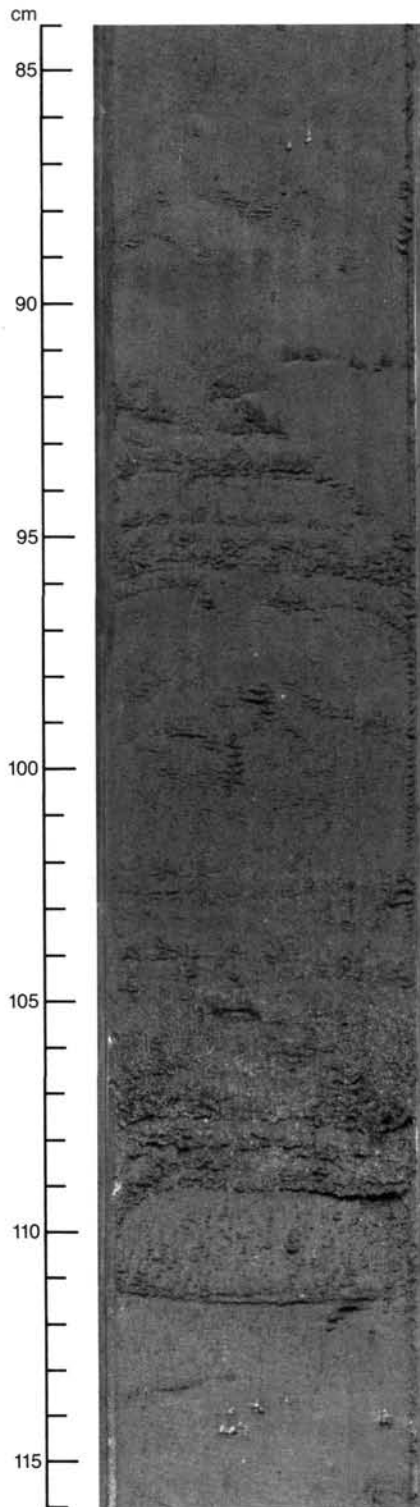


Figure 7. Multiple grading in glauconitic, foraminifer sandy silt and mud, Subunit I (Sample 112-685A-1H-2, 84–116 cm).

Authigenic Carbonates

Authigenic carbonates are comparatively sparse at Site 685, an observation in accord with the low concentrations of calcium and magnesium in pore waters. As noted in the "Inorganic Geochemistry" section (this chapter), the rapid sedimentation rates for the section in Hole 685A may have created an unfavorable

chemical environment for the buildup of these ions and for extensive precipitation of calcite or dolomite.

Those authigenic carbonates that are present can be divided into (1) *in-situ* carbonates in unlithified sediments and (2) redeposited lithified carbonate rocks. The distribution of *in-situ* authigenic carbonate phases in Hole 685A is irregular. Based on smear-slide observations, we recognized five zones in which these phases are abundant, compared to the intervening parts of the section.

Zone	Depth (mbsf)	Cores	Description
1	0–70	1H-8X	Main phase is anhedral calcite, accompanied in places by small amounts of dolomite rhombs. Authigenic carbonate values in the diatomaceous muds vary from 0%–5% and in the calciturbidites are commonly around 10%.
2	108–118	11X–12X	5%–10% authigenic calcite.
3	185–204	21X–22X	This interval contains layers with 3%–8% authigenic carbonate, either calcite with traces of dolomite or only dolomite.
4	232–383	23X–42X	Both authigenic calcite and dolomite are present, but dolomite is more abundant than higher in the section. Values generally between 0%–5% dolomite or calcite were observed in the diatomaceous muds. Enriched carbonate values of up to 10%–20% and rarely 60% occur in isolated zones in Cores 112-685A-31X, 112-685A-32X, 112-685A-38X, 112-685A-41X, and 112-685A-42X.
5	421–450	46X–49X	Values of 10%–15% authigenic calcite and dolomite are common.

Of these five zones, carbonate diagenesis is significant only in zones 4 and 5, where carbonates act sporadically as cements for calcitic or dolomitic mudstones. The generally uneven distribution of authigenic carbonates may reflect variations in the calcite content of the primary sediments (for example, the carbonate-enriched zone in Cores 112-685A-46X to 112-685A-49X coincides with the development of thin, nannofossil-bearing micrites). Examples in zone 4 include a 10-cm-thick bed of partly dolomitized diatomaceous mud (60% dolomite) in Section 112-685A-35X-7; a layer of diatomaceous mud with 50% authigenic calcite (and 20% nannofossils) in Section 112-685A-38X, CC; and a calcite-cemented mudstone in Section 112-685A-48X-1 having 55% authigenic calcite and 15% nannofossils.

Some of the calcite cements in zones 4 and 5 are very fine-grained, with subsequent slightly elongated crystals ranging from 1 to 3 μ m (examples include Samples 112-685A-28X-2, 78 cm, 112-685A-30X-1, 67 cm, 112-685A-32X, CC [21 cm], and 112-685A-38, CC [18 cm]). This may reflect relatively late cementation when calcite cement crystals grew in the tiny pores of partly compacted muds.

Redeposited lithified carbonate rocks occur sporadically within the sediments recovered from Hole 685A. These first appear in Sections 112-685A-2H-1 and 112-685A-2H-2, which contain two small pieces of hard dolomite, one of which has small-scale flaser or boudinage structure resulting from solution seams or microfaulting (Fig. 6). Similar structures in Cretaceous chalks in southern England appear to have formed at burial depths of several hundred meters (Garrison and Kennedy, 1977), in contrast to today's burial depth for the dolomite clasts of 4 to 6 m. An intensely fractured dolomicrite having white secondary carbonate veins (Fig. 18) occurs in Section 112-685A-42X, CC (depth of about 386 mbsf); the provenance of this rock is somewhat uncertain; it may be an *in-situ* bed, rather than a redeposited clast. The largest concentrations of reworked carbonate clasts occur in the lower part of lithologic Unit II, particularly in Cores 112-685A-44X and 112-685A-50X, which contain conglomerate beds having numerous clasts of micritic limestone,

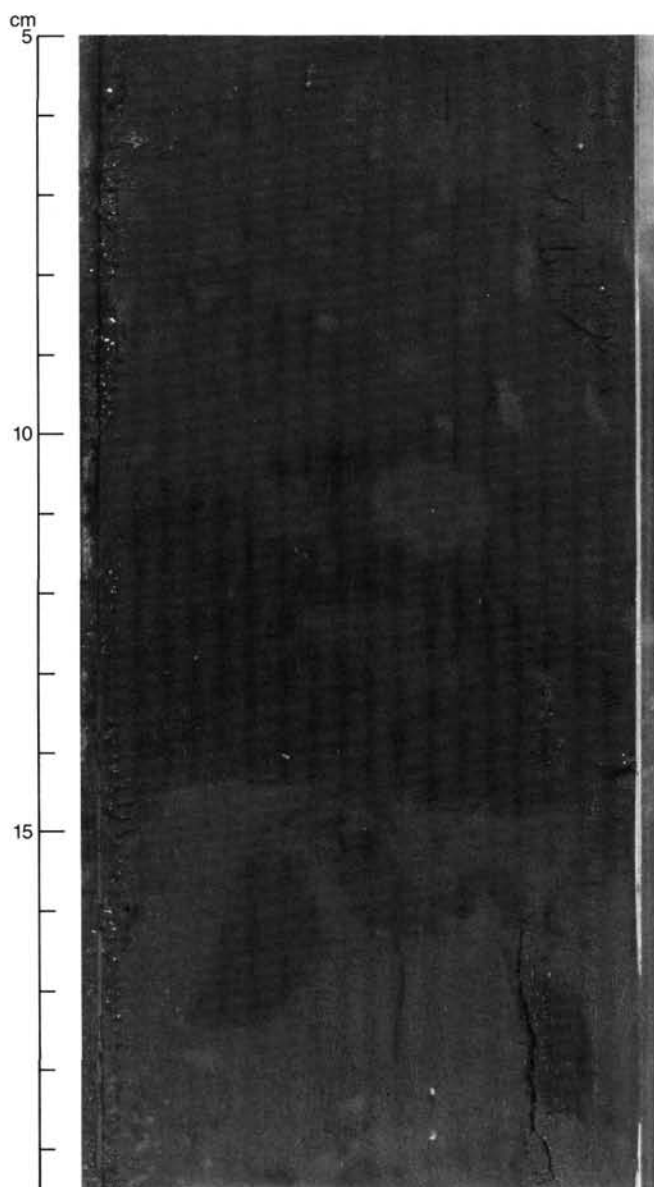


Figure 8. Bioturbated muddy turbidite layer, with patches of small white sponge spicules visible at the top and bottom, Subunit IA (Sample 112-685A-1H-3, 5-19.5 cm).

dolomitic and carbonate-cemented sandstones, along with mudstone clasts.

Iron Sulfides

Pyrite framboids are present in small to abundant amounts throughout the section at Site 685. Their abundance ranges mostly between 5% and 10%, but locally, pyrite attains abundances of 55% to 65% (e.g., Samples 112-685A-2H-6, 80 cm, 60% pyrite; 112-685A-20X-3, 143 cm, 55% pyrite; and 112-685A-34X, CC [11 cm], 65% pyrite). In addition to framboids, pyrite also replaces microfossils and lithic fragments in these heavily pyritized intervals. Pyritized worm tubes were noted in Sections 112-685A-4H, CC and 112-685A-7H, CC. A thin pyrite vein occurred in Section 112-685A-10X-2, and small pyrite nodules were found in Sections 112-685A-22X-1 and 112-685A-43X, CC. Figure 19 represents an X-ray diffractogram of a pyrite-rich sample.

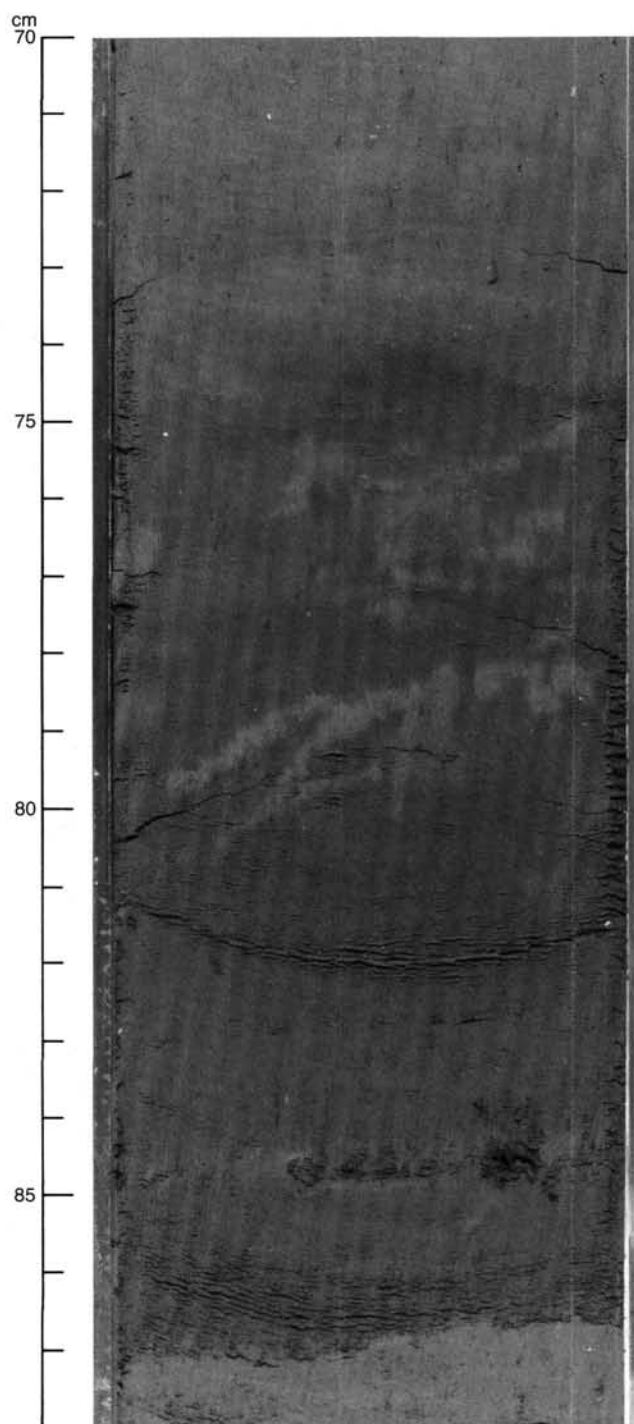


Figure 9. Muddy turbidite of "brown" facies showing relatively sharp base and gradational, bioturbated top, Subunit I (Sample 112-685A-4H-7, 70-88 cm).

Cores 112-685A-4H to 112-685A-13X, 112-685A-20X, and 112-685A-21X contain (in addition to framboidal pyrite) fine, clay-sized, opaque particles that we believe may be iron monosulfides, possibly either amorphous iron sulfide (Goldhaber and Kaplan, 1974), mackinawite (FeS_{1-x}), or greigite (Fe_3S_4), or some combination of these phases. This distinctive material has a sooty consistency that causes it to stick to the hands of those who touch it, a property consistent with the description of greigite

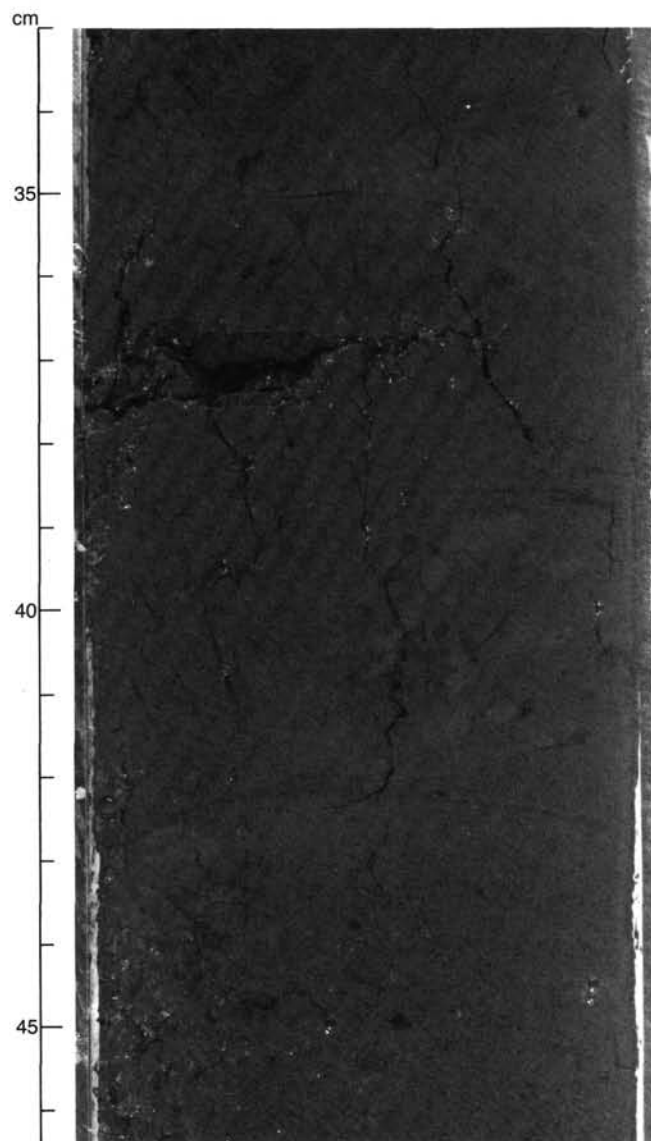


Figure 10. Bioturbation and (lower right) "salt-and-pepper"-textured sandy mud dips about 20° from right to left, Subunit IB (Sample 112-685A-9X-6, 33–46.4 cm). Note also the spaced, high-angle, planar fabric perpendicular to bedding.

by Ward (1970). An attempt to identify greigite or mackinawite on a slow-scanning X-ray diffractogram proved inconclusive in that the major peaks for these two minerals could not be identified with certainty; however, the extremely small grain size of this sooty material, coupled with its presence in small amounts, makes X-ray analysis difficult, so that further investigation is warranted. Greigite has strong magnetic properties (Ward, 1970) and significantly, the intensity of the magnetic signal through the interval noted above was very weak, with the exception of an interval between about 75 and 85 mbsf (Cores 112-685A-9X and 112-685A-10X; see "Paleomagnetism" section, this chapter). This suggests that if greigite is present, it most likely will occur in this latter interval.

Restriction of this sooty material to the upper part of the section in Hole 685A may reflect the metastability of iron monosulfides, which should transform to stable pyrite at deeper burial levels (Goldhaber and Kaplan, 1974).

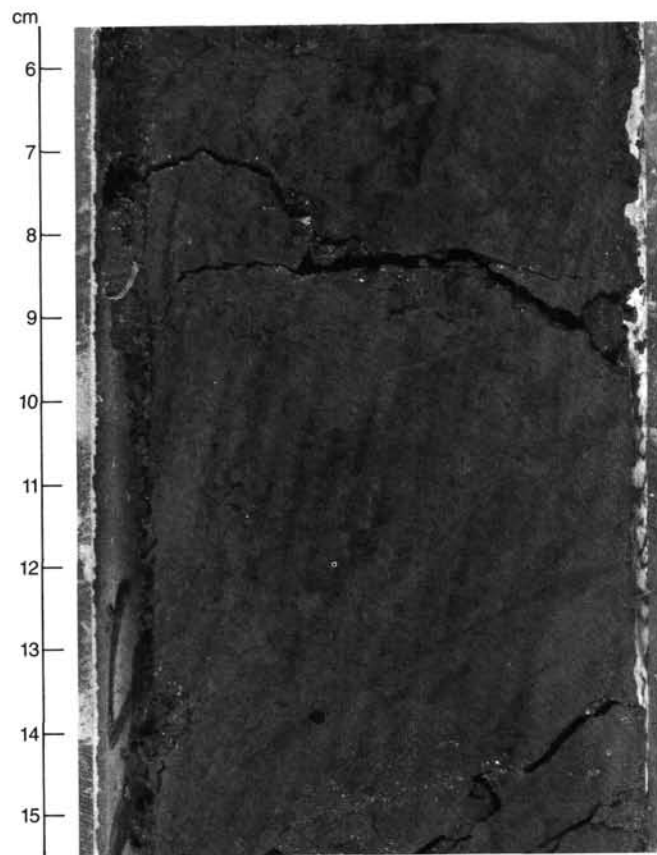


Figure 11. Deformed, color-banded mudstones with bioturbation, possibly post-dating disruption and extension of bedding.

Depositional Environments

The sediments of Subunit IA represent an 80-m-thick, lower-slope sequence. As we detected no magnetic reversal up to Core 112-685A-14X (where palaeomagnetic measurements ceased), this sequence was deposited entirely in the Brunhes Chron, giving a minimum sedimentation rate of 110 m/m.y.

The low (authigenic) carbonate content and the absence of calcareous fossils from the diatomaceous muds in Cores 112-685A-1H through 112-685A-4H were consistent with a location beneath the carbonate compensation depth (CCD). The trace quantities of calcareous microfossils noted in Cores 112-685A-5X to 112-685A-8X suggest a location in the vicinity of the CCD. The foraminifer-nannofossil silty marls and oozes interbedded with the muds display sharp basal contacts, size grading (in the case of thicker units), and upward color gradation to that of the background muds and bioturbated tops. These features are characteristic of muddy biogenic turbidites (Stow, 1984). Introduction by turbidity current and rapid burial has preserved the calcareous biogenic fraction below the CCD. The foraminifer-rich muddy turbidites (brown facies) contain a variety of benthic foraminifers ranging from outer shelf through lower abyssal forms, which suggests that the turbidity currents originated near the shelf-break and scavenged material during their downward path from intermediate depths. An origin near the shelf edge may also be probable for the glauconitic foraminifer sands and silty muds. The muddy turbidites, whose biogenic fraction is composed mainly of nannofossils (olive facies), may



Figure 12. Bioturbation of color-banded mudstones with bioturbation, possibly post-dating disruption and extension of bedding.

have originated at more intermediate depths on the slope above the CCD.

We could not estimate a reliable sedimentation rate for Subunit IB because bedding in this sequence was highly variable and because folding probably was extensive, although values may be similar to those of Subunit IA. This deformation observed in Subunit IB may relate to slumping (see "Structure" below).

Significantly, both calcareous nannoplankton and foraminifers are present throughout Subunit IB in the diatomaceous muds, which suggests deposition above the CCD.

The very thin (1 mm to 2 cm) beds of foraminifer- and glauconite-bearing sandy mud in Subunit IIB are distinctly different from the muddy turbidites of Subunit IA. While the material within these beds originates substantially from the shelf edge, little evidence exists to support a density-current origin for these layers. An alternative origin may be from winnowing currents that resuspended the muddy matrix and concentrated the coarser grains (glauconite and foraminifers) that are scattered throughout the diatomaceous muds of Subunit IB.

The dominance of outer shelf- to upper slope-dwelling foraminifers throughout Unit I suggests continuous transporting of sediment from this area during the Quaternary.

The sediments of Subunit IIA are substantially more variable in diatom content than those of Unit I, which suggests more variable influx. The absence of calcareous nannofossils after Core 112-685A-27X (other than Core 112-685A-38X) and of benthic foraminifers (except in Cores 112-685A-23X and 112-



Figure 13. Intensely fractured and multiple-veined dolomite layer with carbonate veins, Subunit IIA (Sample 112-685A-42X, CC [22.2-28.2 cm]).

685A-38X) suggests deposition below the CCD (or strictly speaking, the lysocline). In contrast to lithologic Unit I, the meager foraminifer faunas identified are mainly of lower abyssal to bathyal species (see "Biostratigraphy" section, this chapter). Thus, little evidence exists of transportation to the depositional area from shallower depths, other than the terrigenous, glauconite-bearing sandy interval in Cores 112-685A-28X to 112-685A-30X. These data suggest that the sediments of Subunit IIA were deposited farther below the CCD than the overlying Quaternary sequence. Furthermore, these sediments also apparently accumulated in an area that did not receive an influx of density currents from the upper to midslope areas above the CCD. The depth implications of this depend on knowledge of variations in CCD depth. However, the lack of influx from slope sources could suggest an original location outward from the trench.

The ashy material in Subunit IIB (Cores 112-685A-43X, 112-685A-50X, and 112-685A-51X) is the only record of vulcanism at Site 685. The presence of calcareous nannofossils *in-situ* lithologies in Cores 112-685A-43X and 112-685A-46X through 112-685A-48X, together with the elevated carbonate content in this interval, suggests deposition above the CCD.

A submarine-slide or "rock-fall" origin for the sedimentary breccias is suggested by their dominantly clast-supported framework, subordinate matrix, and mainly subangular clast shape. The angular clast shape and the dominance of older clasts argue for a "first-generation" origin for the breccias.

This type of deposit is most common adjacent to scarps that may be related to margin foundering or block-faulting (Johns, 1978). Breccias of this sort can also be associated with large-block olistostromes, forming talus around blocks (Naylor, 1982). Proximity to source cannot be inferred directly from the breccia fabric as the breccias encountered may be distal portions of a large slide unit. However, the age range and lithology of the clasts (Table 3) indicates the foundering of a slope sequence of



Figure 14. Sedimentary breccia in Subunit IIB (Sample 112-685A-44X-2, 35–78 cm).

Eocene, early Miocene, and mid- to late Miocene age (there are no purely middle Miocene dates). The diagenetic state of some of the Eocene material further suggests the exhumation of a sequence of substantial thickness (see “Diagenesis” section, this chapter).

In summary, the sediments of Subunit IIB indicate substantial tectonism and volcanic activity along the margin in early late Miocene time.

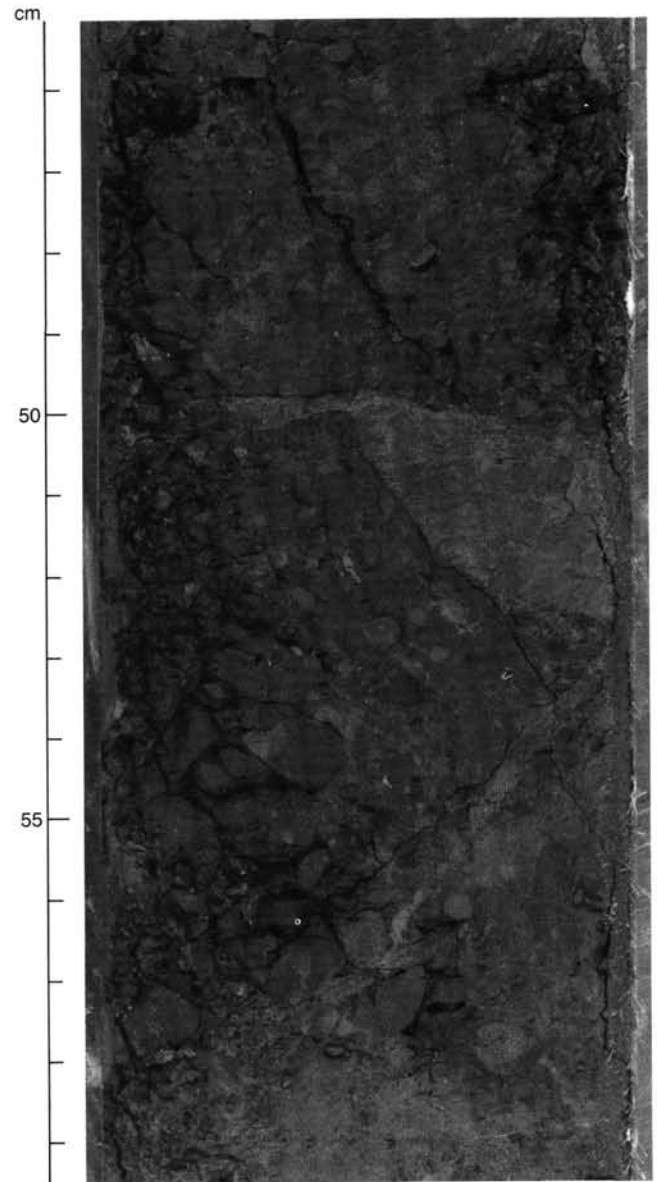


Figure 15. Detail of sedimentary breccia showing a clast with preexisting breccia fabric, Subunit IIB (Sample 112-685A-44X-2, 45.2–59.5 cm).

Structure

Structural studies at Site 685 focused on identifying variations in structural style that might distinguish slope and accreted material. The poor quality of some of the gassy cores made identification of structural features difficult in some intervals. However, sufficient material was recovered intact to characterize contrasting deformational zones. Orientation of measured bedding (Fig. 20) is generally inferred as apparent dips, except for Subunit IA. In biscuited sections, where several determinations exist, true dip is probably represented as considerable rotation exists between biscuits.

Drilling-Induced Structures

The quality of recovery throughout Subunit IA was good. Biscuiting was first observed in Core 112-685A-9X (70 mbsf) and persisted below this level. An X-ray radiograph made of a slab of core 20 cm × 1 cm (Sample 112-685A-18X-1, 5–24 cm) gave us insight into the biscuiting process (Fig. 21). The slurry



Figure 16. Clasts in sedimentary breccia, including pale micritic limestone, Subunit IIB (Section 112-685A-44X, CC [10–21.5 cm]).

formed from biscuit disaggregation shows up as a darker matrix for the paler, fractured, biscuited sediment. Invasion of the disaggregated matrix into the biscuits can be clearly seen by the contrast in shade. Rotation within individual biscuits as well as between biscuits was observed in several intervals in Subunit IB. In Unit II several core sections were effectively reduced to “drilling breccias,” but disintegration obviously took place along pre-existing planes of weakness, such as scaly cleavage surfaces. In some cores a gradation from intact sediment to “drilling breccia” was observed.

Deformational Structure

Subunit IA

The sediments of Subunit IA (Cores 112-685A-1H through 112-685A-9X-3 [0–74 mbsf]) are only lightly deformed. One interval from Sections 112-685A-3H-7 to 112-685A-4H-7 (22–30 mbsf) shows gentle dips of 5°–25° and is cut by small-scale normal faults. The faults have observed displacements of between 0.5 and 8 cm and generally have dips of between 30° and 80° (Fig. 22). One set of faults has a 90°–110° dip (i.e., are overturned) (Fig. 23), and two faults apparently have opposing dip and throw to that of the majority. These faults are frequently filled in by thin (<1 mm) seams of dark bluish-black iron monosulfide and pyrite.

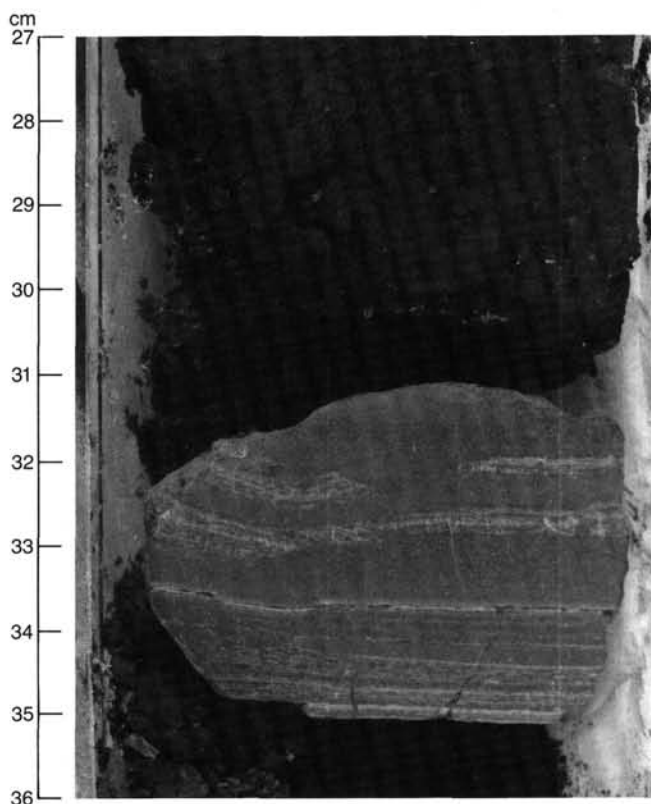


Figure 17. Laminated dolomite ?clast in lower sedimentary breccia unit, Subunit IIB (Section 112-685A-50X, CC [27–36 cm]).

Orientation studies on this interval (see “Paleomagnetism” section, this chapter) indicate that the beds are tilted and the faults downthrow toward the west.

A minor fault dipping at 50° in massive muds in Section 112-685A-8X-6 (69 mbsf) has well-developed slickensides that indicate reverse movement. Interestingly, we did not observe any mud-filled vein arrays like those of the upper slope and shelf sequences.

Subunit IB

In contrast to the overlying sediments, Subunit IB (Cores 112-685A-9X-4 through 112-685A-2X [74–203.6 mbsf]) shows evidence of extensive deformation. The measured bedding orientations vary widely (Fig. 20) and include vertical dips (Cores 112-685A-14X-3 at 123 mbsf and 112-685A-16X-2 at 139 mbsf) and local overturning (140° dip in 112-685A-16X-1, 137 mbsf), which suggest folding. Small-scale, open-to-closed folding was observed directly in Sections 112-685A-10X-3 (84 mbsf), 112-685A-16X-2 (139 mbsf), and 112-685A-18X-2 (157 mbsf).

A developed incipient fissility was observed in Core 112-685A-9X, which became stronger, although was still sporadically developed, through Core 112-685A-15X (Fig. 24).

The boundary between Subunits IA and IB in Core 112-685A-9X coincides with the development of a planar fabric that cuts the bedding at high angles. Figure 25 shows the split halves of core when viewed uphole. Section 112-685A-9X-2 (Subunit IA) displays a crude, coring-related radial fabric, but Section 112-685A-9X-8 (Subunit IB) shows a planar fabric of uniform orientation that cuts the entire core. Examination of the fabric planes (Fig. 26) shows them to be discrete, polished surfaces having oriented grooves and subvertical displacement. The spac-

Table 3. Type and age of clasts within sedimentary breccias of lithologic Subunit IIB, Hole 685A.

Core/section interval (cm)	Type	Age
112-685A-44X, CC, 6	Diatom-bearing mudstone	middle to early Miocene
50X-1, 36	Diatomaceous mudstone	late early to early late Miocene
50X-1, 49.5	Nannofossil and diatom-bearing mudstone	late early to early late Miocene
50X, CC (25.5)	Diatomaceous mudstone	late early to early late Miocene
44X, CC (16.5)	Diatom-foraminifer-nannofossil mudstone	late early Miocene
44X, CC (18.5)	Dolomite	early Miocene
50X-1, 53	Diatom-bearing muddy micrite	early Miocene
44X, CC (16)	Muddy, pyritic, nannofossil-diatom ooze	early Miocene (with some Eocene forms)
44X-1, 113	Chloritic, diatom-bearing mudstone	Eocene
44X-2, 15	Sandy, pyritic, diatom-bearing mudstone	Eocene
44X-2, 72	Diatomaceous mudstone	Eocene
44X, CC (33)	Diatomaceous mudstone	Eocene
44X, CC (33.5)	Diatomaceous mudstone	Eocene
50X-1, 66	Micritic limestone	Eocene
50X-1, 81.5	Calcareous mudstone	Eocene

Table 4. Carbonate measurements at Site 685.

Core/section interval (cm)	Depth (mbsf)	Carbonate (%)
112-685A-1H-2, 40-41	1.90	0.58
2H-3, 44-45	7.54	1.25
3H-3, 35-36	16.95	3.25
5X-2, 41-42	34.51	0.75
6X-2, 22-23	43.82	0.33
7X-2, 33-34	53.43	1.33
8X-3, 55-56	64.65	1.42
9X-5, 70-71	76.17	5.25
9X-7, 30-31	78.77	1.92
10X-2, 30-31	81.90	1.75
11X-3, 10-11	92.70	4.92
12X-5, 30-31	105.40	6.26
13X-2, 65-66	110.75	2.84
14X-2, 71-72	120.31	2.00
15X-3, 47-48	129.87	2.00
16X-2, 19-20	138.79	4.59
17X-4, 45-46	151.05	2.42
18X-1, 31-32	156.41	4.25
19X-1, 23-23	165.83	2.67
20X-4, 72-73	180.04	1.92
22X-2, 91-92	196.51	2.59
25X-CC, 5-6	223.00	1.33
27X-1, 49-50	234.09	0.92
28X-3, 48-49	246.58	0.83
29X-2, 14-15	254.24	1.33
30X-2, 49-50	264.09	1.42
34X-2, 26-27	301.86	0.75
35X-6, 29-30	316.13	8.99
36X-7, 40-41	327.40	0.58
37X-1, 146-147	330.06	1.00
38X-CC, 20-21	338.82	42.10
40X-2, 99-100	359.59	1.09
40X-1, 1-2	357.11	1.50
42X-CC, 9-10	378.79	2.00
43X-1, 30-31	385.90	0.42
47X-1, 39-40	421.49	3.58
48X-1, 61-62	431.21	4.75
49X-CC, 9-10	440.59	4.00
50X-1, 52-53	450.12	4.75

H = hydraulic piston. X = extended-core barrel.

ing of the fabric planes at this level typically ranges from 0.5 to 3 mm (Fig. 27). This fabric rapidly increases in intensity and becomes more closely spaced downhole (Fig. 28), although the apparent spacing varies widely. Locally, very thin mud seams occur within the fabric planes. On surfaces cut by the saw, the fabric was seen to be locally anastomosing and commonly resembled the closely spaced, mud-filled vein arrays of the upper slope and shelf sites (Fig. 28), although it is pervasively developed at Site 685. Small offsets along fabric surfaces are common and provide further evidence of movement along fabric planes (Fig. 29). These offsets resemble the microfaults observed in the shallower sites.

The orientation of the planar fabric varies widely and typically ranges from 30° to 60°. However, the fabric appears everywhere to be bedding-perpendicular (Figs. 27 and 29). In one observed example (Section 112-685A-10X-3, [84 mbsf]) a fold in bedding also folds the fabric. Thus, the fabric appears, at least locally, to pre-date the folding of Subunit IB. This distinctive, high-angle planar fabric is present down to and including Core 112-685A-21X.

Cores 112-685A-19X to 112-685A-22X exhibit partial induration and include both mud and mudstone. Core 112-685A-22X contains a developed, incipient scaly cleavage.

Subunit IIA

Subunit IIA encompasses Cores 112-685A-23X through 112-685A-42X (203.6-383.1). No meaningful statement can be made about deformation in Cores 112-685A-23X to 112-685A-27X because of the minimal, low-quality recovery. Cores 112-685A-28X to 112-685A-30X were highly brecciated by drilling. However, they appear to be fragmented along a partly blocky fissility that is transitional in places to a scaly cleavage. This fissility locally follows minor bedding anisotropies whose orientation, in some cases, appears to be controlled by a preexisting deformation (see next section) (Figs. 30 and 31).

A scaly cleavage was noted in Core 112-685A-31X (272 mbsf) that persists throughout Subunit IIA, where its development is moderate (Fig. 32) to intense (Fig. 33). Where most intense, some cleavage surfaces appear highly polished. The scaly cleavage appears generally subparallel to bedding, but in cases where bedding/cleavage relationships can be clearly observed, the scaly cleavage dips between 10° and 30° shallower than the bedding

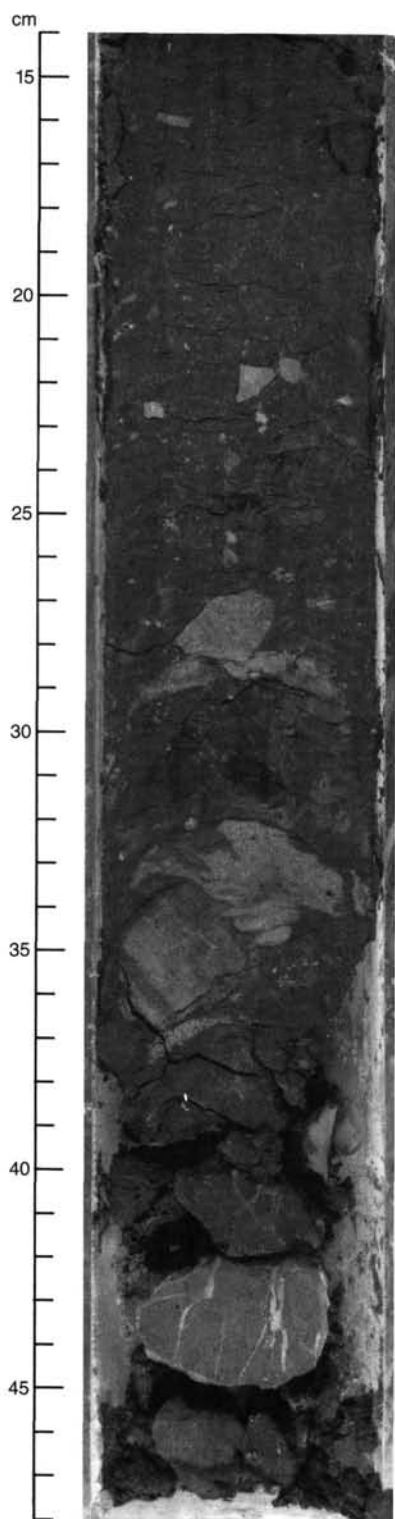


Figure 18. Pebbly, ashy, sandy silt showing crude grading, Subunit IIB (Section 112-685A-51X, CC [14–48 cm]).

(Sections 112-685A-32X, CC at 290 mbsf; 112-685A-39X-1 at 348 mbsf; and 112-685A-44X-1 at 393 mbsf).

Well-preserved sections display a range of brittle to ductile deformation, which includes microfaulting, boudinage, extreme necking, and disaggregation of beds to form clast-in-matrix textures that record the (mainly extensional) disruption of partially

lithified sediment (Figs. 30 and 31). The microfaults are generally closely spaced and, although most are extensional faults, some thrust faults also occur. This style of deformation is particularly well developed in Cores 112-685A-29X, 112-685A-32X, 112-685A-37X, and 112-685A-41X.

An exclusively brittle brecciation was only rarely observed in Subunit IIA, but a striking example did occur in Section 112-685A-42X, CC. Here, a brecciated mudstone is adjacent to a cored bed of intensely brecciated and veined dolomite (Fig. 13).

Subunit IIB

A moderate to strong scaly cleavage persists throughout most of Subunit IIB. However, a significant contrast in deformational style occurs in Cores 112-685A-46X to 112-685A-49X. In this zone we observed an intense fracturing that apparently is superimposed on a scaly cleavage (Fig. 34). In addition to the scaly cleavage surfaces, at least three intersecting fracture planes have developed. These planes are pervasively polished and grooved. Many of these surfaces display compression normal to the core axis (Figs. 35 through 37). Figures 35 through 37 show a conjugate pair of faults in Sample 112-685A-48X-1, 94 cm, and the results of an attempt to orient the fault planes using paleomagnetic measurements. Analysis indicates that the faults strike southeast and northwest ($306^\circ \pm 15^\circ$). If we assume that the axis of maximum compressive stress would make an angle of 30° with the two planes, a northeast/southwest orientation should result. Compressive stress indicated a probable relationship with the interaction of the Nazca and South American plates.

Within the sedimentary breccias (Cores 112-685A-44X and 112-685A-50X), there is evidence for significant internal deformation, including the smearing out of more labile clasts. A scaly cleavage is locally developed, particularly in zones of smaller clasts.

Discussion

The gentle oceanward dips and oceanward-facing normal faults of the upper slope sequence (Subunit IA) are consistent with gravitational processes operating on the slope. The disruption of bedding and folding within the lower part of the slope sequence (Subunit IB) could have formed in response to downslope slumping or possibly could relate to the upward propagation of deformation from Unit II ("tectonic kneading"). The fabric in Subunit IA is transitional between the mud-filled microfaults and the *en-echelon* mud-filled vein arrays observed at Site 679; both of these were related to fluid escape. However, in contrast to previously observed examples, the fabric of Subunit IA is pervasively developed. The generation of pervasive fluid-escape features suggests that the deformation observed in Subunit IB may be related to downslope mass movement. Interestingly, the sediments of Subunit IB contain abundant calcareous microfossils (in contrast to those of Subunit IA) an observation that supports a possible shallower-water origin for the sediment of Subunit IB.

The moderate-to-strong scaly cleavage present in most of lithologic Unit II marks a distinctive change in structural style from the overlying slope sediments and a contrast to deformation encountered in the other slope sites. The development of this fabric is consistent with underthrusting during accretion. The early deformation structures observed, particularly in the middle of Subunit IIA, may also relate to underthrusting, although their dominantly extensional character suggests a slumping origin.

The bedding dips observed in Unit II are significantly higher than those estimated from the seismic-reflection profile. The surfaces imaged on the reflection record may represent faults, and the steeper bedding orientation can be explained either by

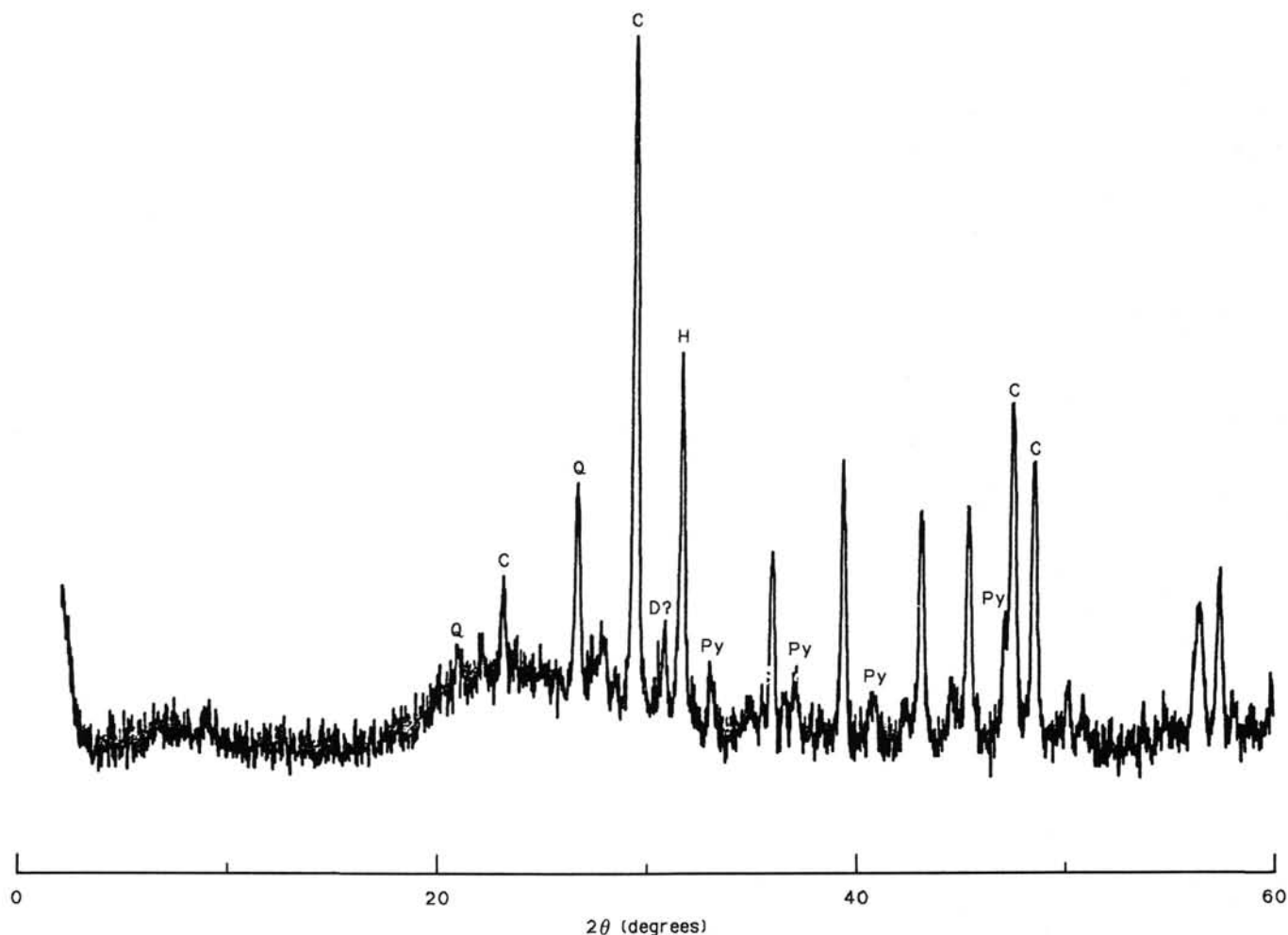


Figure 19. X-ray diffractogram of a pyrite-rich diatomaceous mud, Subunit IB (Sample 112-685A-12X-1, 84 cm). Peak symbols are Py = pyrite, Q = quartz, C = calcite, D = dolomite, H = halite, an artifact.

re-imbrication of the thrust stack or duplex formation during initial underthrusting. The dips of cleavage that are shallower than bedding can also be accounted for in this way.

The intense fracturing in Subunit IIB, which caused the abandonment of the hole, is obviously related to compression. The development of this fracturing coincides with an increase in carbonate content and an increase in water content, with commensurate decreased bulk density and increased porosity (see "Physical Properties" section, this chapter). The higher water content and increased porosity may result from a fracture porosity induced in the sediment. This would account for the decreased bulk density, which otherwise would be expected to increase with carbonate cementation. Alternatively, if the increased porosity is in the rock, then the fracturing coupled with the elevated water contents may suggest hydraulic fracturing.

The deformational styles encountered at Site 685 are summarized and related to tectonic environments in Table 5.

BIOSTRATIGRAPHY

Hole 685A was drilled in a water depth of 5070.8 m to a depth of 468.6 mbsf into the lower-slope sediment prism. The hole penetrated 200 m of Quaternary hemipelagic, diatom-rich mud and mudstone overlying 250 m of upper Miocene diatomaceous mudstone that contains various clasts in the lower part of the section. Transported shallow-water benthic diatoms and ben-

thic foraminifers occurring throughout the section indicate that part of the sediment was derived from the continental shelf and slope.

Diatoms, radiolarians, and silicoflagellates are present throughout. Calcareous microfossils are not present in the uppermost core-catcher sample, as the site lies below the carbonate compensation depth (CCD). However, their presence in most of the Quaternary samples and in a few of the upper Miocene samples can be attributed to sediment transport. Age assignments based on the various microfossils are shown in Figure 38.

Sedimentation rates, as determined from diatom and nannoplankton events, are greater than 100 m/m.y. for the Quaternary. A hiatus with a minimum duration of 4.3 m.y. separates the lower Pleistocene, found in Section 112-685A-22X, CC (199.8 mbsf), from the lower upper Miocene, found in Section 112-685A-23X, CC (203.6 mbsf). Diatoms, radiolarians, and planktonic foraminifers show an admixture of specimens of late Miocene age, with the Quaternary assemblage above the hiatus. Calcareous nannofossils, planktonic foraminifers, silicoflagellates, radiolarians, and diatoms of early Miocene and Eocene age occur with late Miocene microfossils in the lower part of the cored section. Some of these are derived from clasts. Diatoms in the upper Miocene samples are representative of a single zone having a duration of 6.1–6.8 Ma. Radiolarians in the upper Miocene samples are also representative of a single zone. Rapid deposition, the mixture of microfossils of different ages, and the

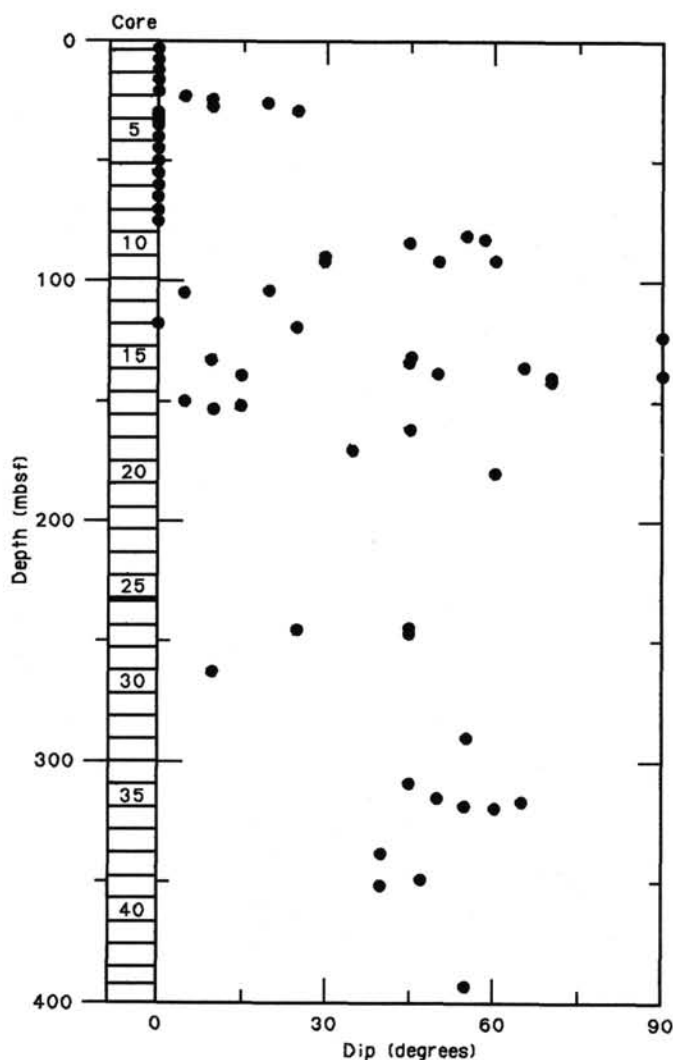


Figure 20. Bedding dips in Hole 685A. Dips measured are apparent dips.

sediment texture all suggest that slumping was the emplacement mode of these upper Miocene deposits.

Diatoms

Marine planktonic diatoms are abundant to common in most core-catcher samples of Hole 685A. They are moderately well to well preserved in the Quaternary through Miocene sections and poorly preserved in the clasts of Eocene, reworked, siliceous-rich mudstones. A hiatus (685-H-1) was found between Cores 112-685A-22X and 112-685A-23X (199.79–203.6 mbsf) that all of the Pliocene and most of the upper Miocene encompassed (around 4.3 m.y. missing, minimum value). The section between 203.6 to 440.5 mbsf represents sediments that belong to one zone of very short duration (6.1 to 6.8 Ma) and document sedimentation in one "big" and/or several "small" slump deposits with occasional injection of older material. Sedimentation rates for the Quaternary interval are 100 m/m.y. or higher.

The following diatom zones and datums could be identified: *Nitzschia reinholdii* (LAD: 0.6 Ma, Koizumi, 1986) and *Thalassiosira leptopus* var. *ellipticus* were last seen in Section 112-685A-6X, CC (51.4 mbsf). The acme of *Delphineis ossiformis* (new species) occurred in Section 112-685A-8X, CC (70.4 mbsf) and correlates with similar intervals at the other Leg 112 sites

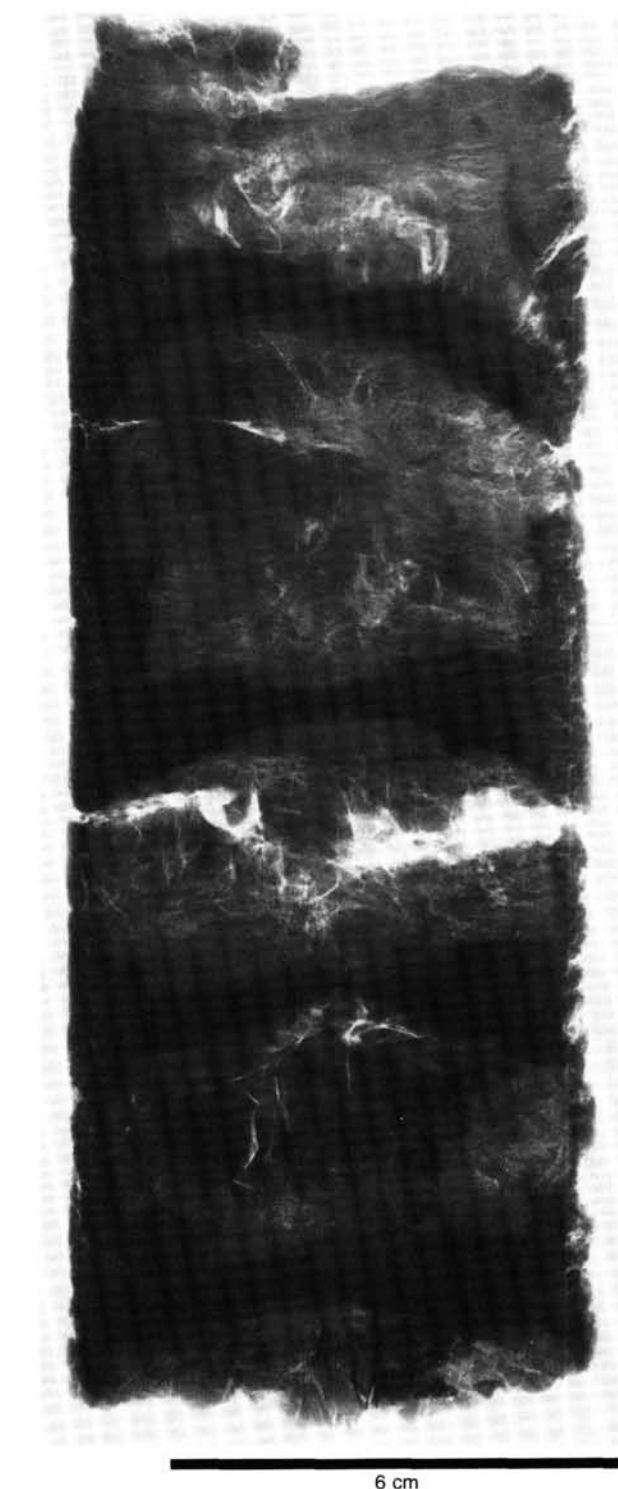


Figure 21. X-ray radiograph of slab of core 1 cm × 20 cm, showing dark disaggregated slurry material progressively attacking fractured paler biscuits (Sample 112-685A-18X-1, 5–24 cm).

(i.e., Section 112-680A-3H, CC). *Rhizosolenia barboi*, the precursor of *Rhizosolenia curvirostris*, was seen in Section 112-685A-16X, CC (142.15 mbsf). This species was reported by Koizumi (1973), Schrader (1973), and Barron (1980) to range through the *Rhizosolenia curvirostris* Zone of Koizumi (1973) and was dated as 0.26 to 0.9 Ma by Barron (1980).

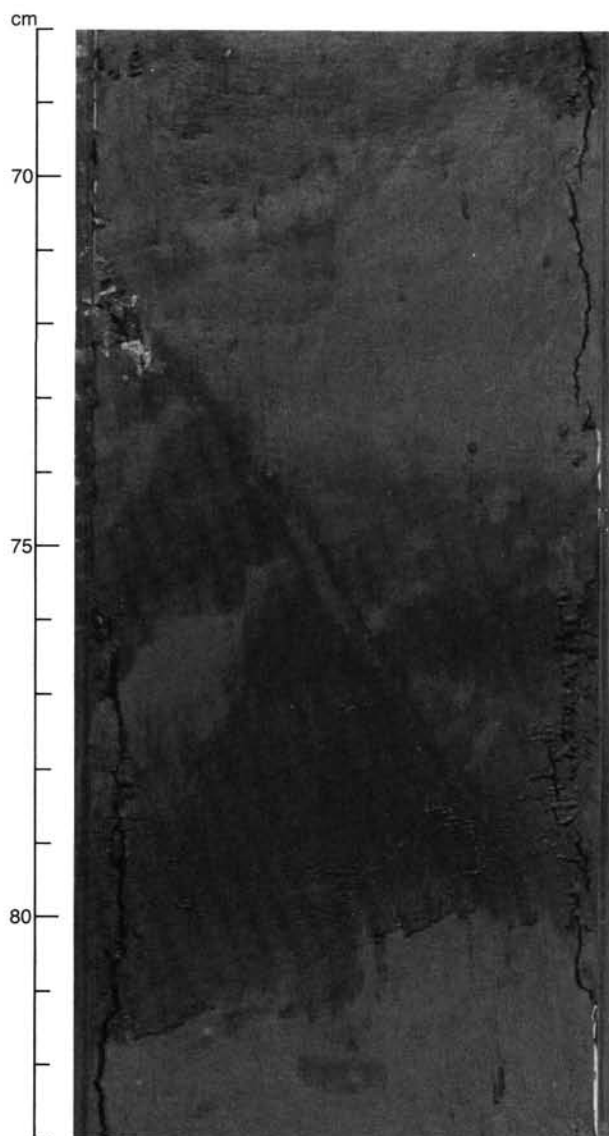


Figure 22. Normal fault-cutting turbidite bed. Infill of fault is a pyrite-rich mud (Sample 112-685A-4H-3, 68–83 cm).

Late Miocene mixed with true Quaternary species did occur in Section 112-685A-22X, CC (199.79 mbsf). This assemblage included *Pseudoeunotia doliolus*, *Thalassiosira oestrupii*, *Nitzschia miocenica*, *Coscinodiscus deformans*, and *Denticulopsis hustedtii*. The presence of *Pseudoeunotia doliolus* in Section 112-685A-22X, CC indicates that this sample is no older than the FAD of *P. doliolus*, which is around 1.9 Ma (Koizumi, 1986).

The *Nitzschia miocenica* Zone (6.1 to 6.8 Ma) of Barron (1985) was recognized in Sections 112-685A-23X, CC through 112-685A-27X, CC (203.6–235.2 mbsf). A questionable *Nitzschia porteri* Zone (6.8 to 7.65 Ma, Barron, 1985) was recognized in Sections 112-685A-28X, CC and 112-685A-29X, CC (255.73–256.5 mbsf). This section contained *Coscinodiscus nodulifer* var. *cyclopus* in addition to rare *Nitzschia porteri* specimens. The *Coscinodiscus nodulifer* var. *cyclopus* acme was reported by Barron (1985) to occur around 7.1 Ma within the *Nitzschia porteri* Zone in equatorial Pacific sites of DSDP Leg 85.

Sections 112-685A-30X, CC through 112-685A-32X, CC (264.97–286.4 mbsf) were assigned to the *Coscinodiscus yabei*

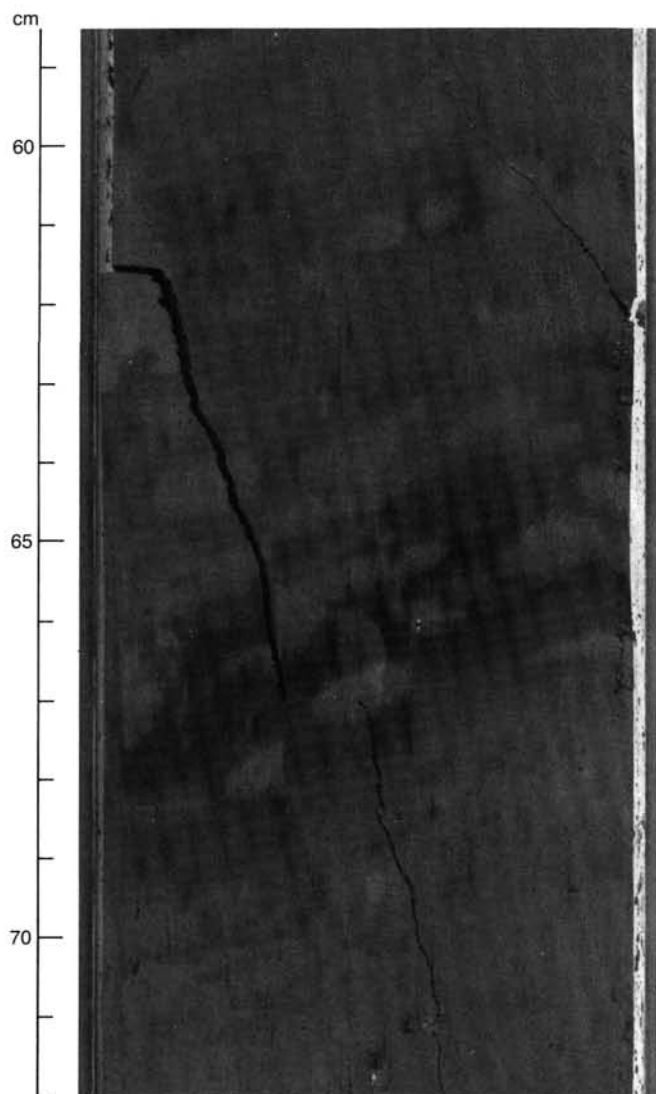


Figure 23. Vertical to overturned "normal" faults cutting turbidite layers. Note displacement of burrows across faults.

Zone (7.65 to 8.9 Ma) of Barron (1985) because *Thalassiosira yabei*, *Nitzschia cylindrica*, *Denticulopsis hustedtii*, and no *Nitzschia porteri* specimens were found. This interval contains abundant "diatom frustule hash."

The *Nitzschia miocenica* Zone (6.1 to 6.8 Ma) of Barron (1985) was found in Sections 112-685A-35X, CC through 112-685A-42X, CC (318.7–378.7 mbsf).

Opal-rich clasts of Eocene age were found in Core 112-685A-43X (385.6–386.25 mbsf). These contained *Pyxilla reticulata*, *Melosira architecturalis*, *Trochosira trochlea*, *Hemiaulus kljushnikovii* fragments, and *Hemiaulus* spp., among others. Fenner (1985) illustrated a restricted range of *Trochosira trochlea* and *Hemiaulus kljushnikovii* in her *Triceratium kanayae* Zone, which is correlated with calcareous nannoplankton Zones NP14 and NP15 and is of middle Eocene age (Fenner, 1984). Based on the assumption that the ranges of the two species are correct, these "Eocene" clasts were tentatively placed in Fenner's (1984) *Triceratium kanayae* Zone, even though the zonal marker was not determined. Other zonal markers were not detected. The admixture of lower Miocene diatomaceous material and the injection of *Synedra jouseana* into poorly preserved Eocene material gave some material the appearance of late Oligocene age; *Synedra jouseana* ranged from the middle Miocene through the upper

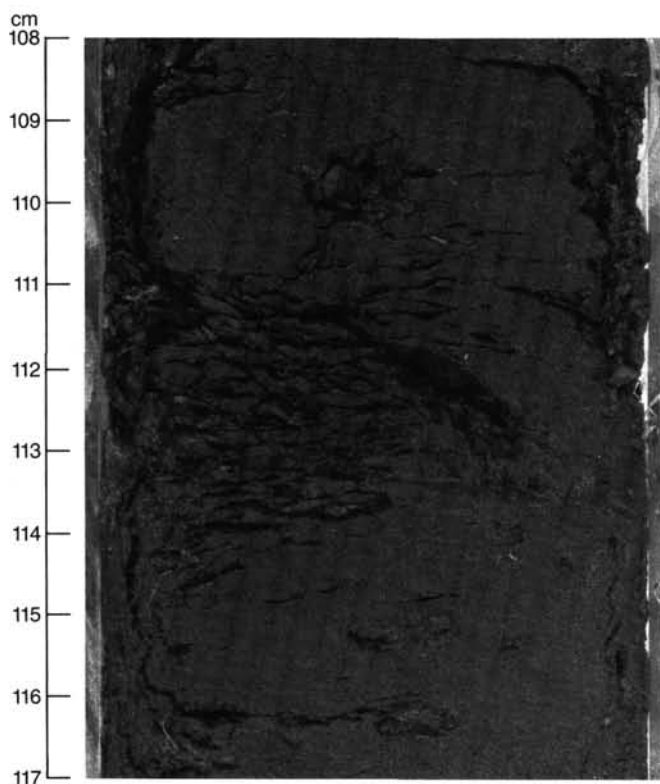


Figure 24. Irregular fissility (parallel to bedding) that was developed in Subunit IB (Sample 112-685A-15X-3, 108–117 cm).

Oligocene. Lower Miocene of the *Coscinodiscus lewisianus*/*Cestodiscus peplum* Zones was found in one clast (medium brown clast from Sample 112-685A-44X, CC [17 cm]).

Sections 112-685A-46X, CC through 112-685A-49X, CC (413.6–440.5 mbsf) were assigned to the *Nitzschia miocenica* Zone (6.1 to 6.8 Ma) of Barron (1985). Core-catcher samples of Cores 112-685A-50X to 112-685A-51X (450.62–459.1 mbsf) contained a mixed lower Miocene and Eocene assemblage.

Displaced shallow-water marine benthic diatoms were found throughout the section; no displaced freshwater diatoms were encountered. *Ethmodiscus rex* fragments were commonly found in the *Nitzschia miocenica* Zone. Antarctic species that have not been reported this far north did occur in the *Nitzschia miocenica* Zone, including *Coscinodiscus deformans*, *Nitzschia denticuloides*, and *Denticulopsis antarctica* (for species description see Schrader, 1976). The occurrence of these antarctic species may indicate an enhanced and more vigorous northward-flowing current system in the *Nitzschia miocenica* Zone of early late Miocene. No antarctic diatom species currently migrate with the Peru Current system north of the subtropical convergence at about 40°S latitude (Fenner et al., 1976).

The abundance of *Thalassiothrix longissima*, *Thalassiothrix robusta*, and *Thalassionema nitzschioides* in the absence or only minor presence of coastal upwelling neritic species (Schuette and Schrader, 1979, 1981; DeVries and Schrader, 1981) classifies these Quaternary and late Miocene diatom assemblages as offshore Humboldt Current assemblages. No association with true coastal upwelling could be made when using the autochthonous component of the diatom assemblages. The abundance of good biostratigraphic indicators common to the low latitudes is further evidence that Site 685A has a more oceanic-temperate character, compared with the more shoreward sites drilled previously.

Coscinodiscus nodulifer occurs in high enough numbers in the Quaternary section to allow application of the *Coscinodiscus*

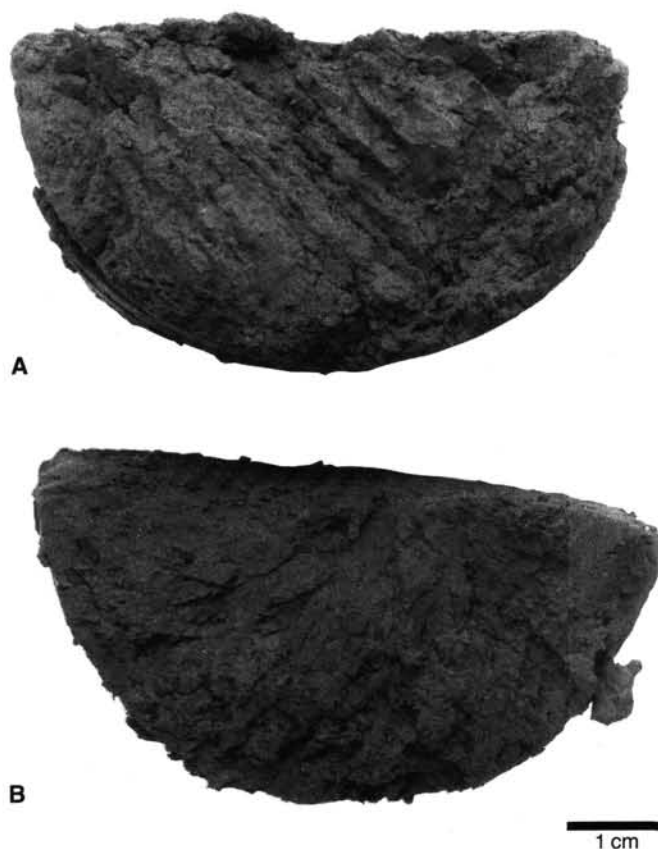


Figure 25. Split halves of core from Core 112-685A-9X (viewed uphole) showing A) uniform planar fabric cutting core surfaces that dip steeply to lower left, Subunit IA (Sample 112-685A-9X-2, 105 cm) contrasted with B) crude coring-related, radial fabric, Subunit IB (Sample 112-685A-9X-8, 30 cm).

nodulifer size range stratigraphy developed by Burckle (1978), which can be substituted for oxygen-isotope stratigraphy.

The Eocene diatom-bearing clasts in Cores 112-685A-44X, 112-685A-50X, and 685A-51X seem to be embedded in a lower Miocene diatom-bearing mud. The clast- and matrix-bearing interval in Core 112-685A-44X again is embedded in upper Miocene diatomaceous sediments, whereas the lower boundary of the clast- and matrix-bearing section in Cores 112-685A-50X and 112-685A-51X was not recovered.

The occurrence of Eocene diatomaceous material in this area is new. Dissolution of diatoms may have occurred in sections of the lower Chira Formation exposed on land, while Eocene diatoms at Site 685A may have been preserved because they were embedded in highly diatomaceous sediments above and below. The Eocene assemblages are similar to those described from DSDP Site 149 (Caribbean), Site 338 (Norwegian Sea), Site 94 (Gulf of Mexico), and Site 390A (western North Atlantic). We can make no environmental interpretations, except to infer that these sediments were produced by increased diatom production in the photic zone. *Pyxilla* spp. were occasionally found during the routine smear-slide diatom preparation. This species is thought to represent contamination.

Silicoflagellates

All core-catcher and some additional samples in Hole 685A were studied for silicoflagellates and other siliceous microfossils. Cores 112-685A-1H to 112-685A-22X (0–199.8 mbsf) con-

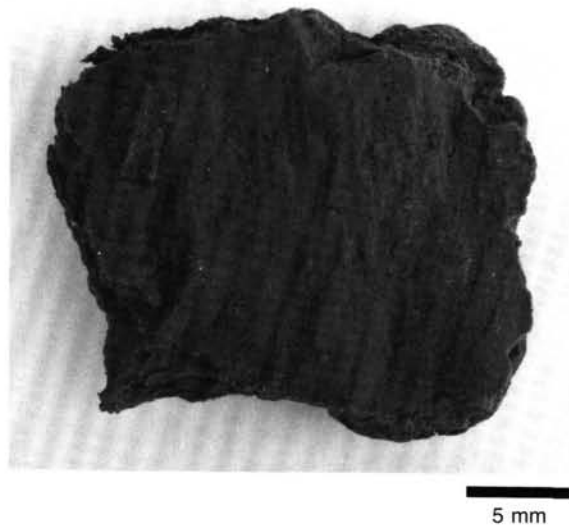


Figure 26. Detail of planar fabric of Figure 25A, showing development of smooth, grooved planes (Sample 112-685A-9X-8, 6.1–8.9 cm).

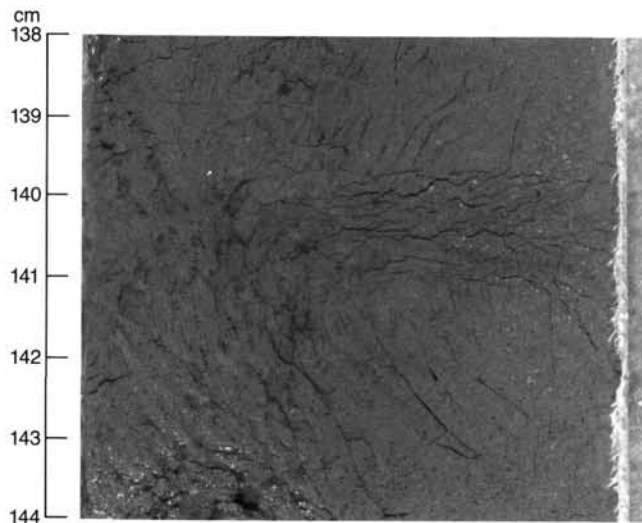


Figure 27. Spaced, high-angle planar fabric near top of Subunit IB. Curvature is caused by rotation between biscuits. (Biscuit boundary is centrally located and picked out by darker gray film and horizontal parting, Sample 112-685A-9X-6, 138–144 cm.)

tain Quaternary silicoflagellate assemblages that are associated with abundant diatoms, frequent sponge spicules, and occasional actiniscidians. The most common silicoflagellates belong to the *Dictyocha messanensis* group, with *Dictyocha messanensis aculeata* (indicating a late Quaternary age) found in Sections 112-685A-5X, CC (40.2 mbsf), 112-685A-6X, CC (51.4 mbsf), and 112-685A-11X, CC (99 mbsf). *Mesocena quadrangula* was observed in Section 112-685A-8X, CC (70.5 mbsf), but is more common in the interval from Core 112-685A-16X down to Core 112-685A-22X, and has its lowest occurrence in Section 112-685A-22X, CC (199.8 mbsf). *Distephanus bioctonarius bioctonarius* is present in Core 112-685A-2H and in Section 112-685A-16X, CC (142.2 mbsf).

Small whitish clusters are scattered throughout Cores 112-685A-1H to 112-685A-9X. Samples 112-685A-2H-2, 135 cm (7

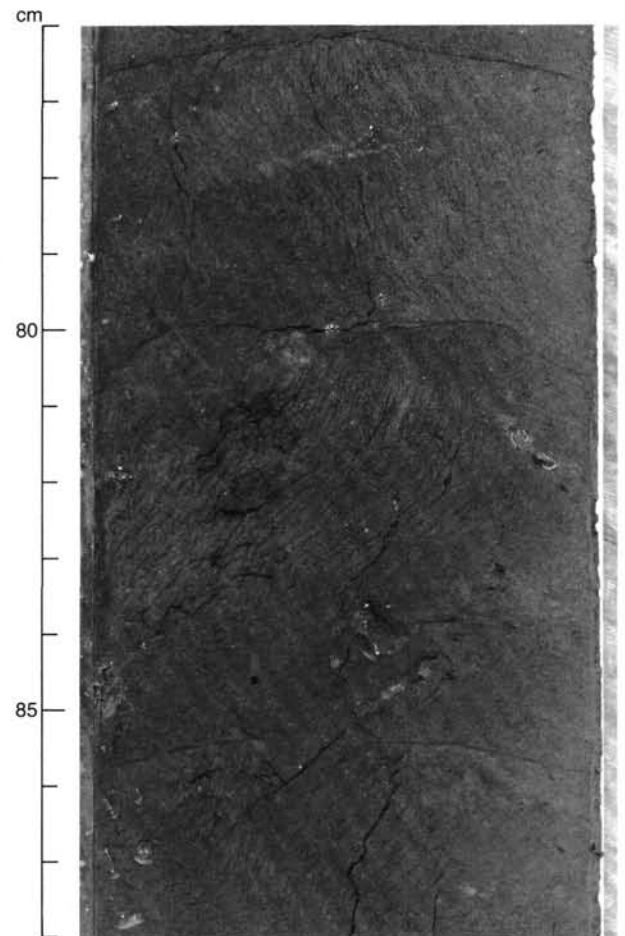


Figure 28. Closely spaced, anastomosing, subvertical planar fabric in Subunit IB. The very thin fissures are filled with concentrated fines. The principal cause of the contrasting orientations is rotation between biscuits (Sample 112-685A-10X-5, 76–88 cm).

mbsf), 112-685A-4H-1, 89 cm (24 mbsf), and 112-685A-4H-1, 71 cm (23.8 mbsf) contain abundant sponge spicules, mostly monaxonones of various shapes, which will be studied later in detail.

Between Cores 112-685A-22X and 112-685A-23X at approximately 200 mbsf, a hiatus (about 4.3 m.y. duration) divides the lower Pleistocene from the upper Miocene. The silicoflagellate assemblages between Sections 112-685A-23X, CC and 112-685A-51X, CC (203.6–459.1 mbsf) contain *Dictyocha varia*, members of the *Distephanus crux* group, and *Distephanus speculum speculum* f. *speculum* in most samples. *Dictyocha messanensis stapedia* was noted in a few samples, and *Paramesocena apiculata* was found in Sections 112-685A-28X, CC (255.7 mbsf) and 112-685A-32X, CC (286.6 mbsf) during this study. This interval seems to represent the late middle to early upper Miocene *Dictyocha varia* Zone (Locker and Martini, 1986). From Section 112-685A-34X, CC (310 mbsf) downward, silicoflagellates and diatoms are highly fractured and not well preserved.

Reworked middle or upper Miocene silicoflagellates occur in Section 112-685A-13X, CC (112.3 mbsf) of Quaternary age, and reworked *Naviculopsis* species from the upper Oligocene/lower Miocene occur in the upper Miocene Section 112-685A-29X, CC (256.5 mbsf). In the basal part of Core 112-685A-43X as well as in Cores 112-685A-44X (386.3–396.1 mbsf) and 112-685A-50X (450.6 mbsf) lower Miocene and Paleogene silicoflagellates like *Naviculopsis biapiculata*, *N. lata*, *N. foliacea*, and

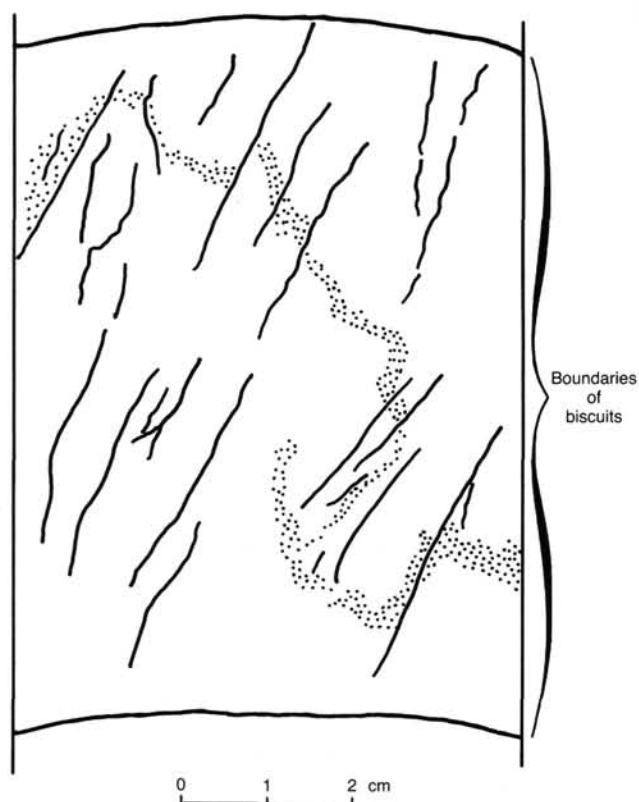


Figure 29. Displacement of base of "salt-and-pepper"-textured sandy mud layer along high-angle, planar fabric surfaces (Sample 112-685A-16X-3, 86-93 cm).

Corbisema hexacantha outnumber the upper Miocene silico-flagellates and indicate downslope slumping during the late Miocene.

Actiniscidians were found occasionally but seem to occur more frequently in the Miocene interval. These include *Actiniscus pentasterias* and *A.? elongatus*. Ebridians were noted in Sections 112-685A-10X, CC (88 mbsf) and 112-685A-26X, CC (232.1 mbsf). Displaced Eocene ebridians were found frequently in the lowest part of Core 112-685A-43X and in 112-685A-44X.

Calcareous Nannoplankton

All core-catcher and some additional samples of Hole 685A were studied for calcareous nannoplankton. Cores 112-685A-1H to 112-685A-22X (199.8 mbsf) contained meager Quaternary nannoplankton assemblages at some levels, but commonly were barren or yielded only a few badly preserved *Gephyrocapsa* specimens. Some better preserved assemblages were found in Sections 112-685A-4H, CC (33 mbsf) and 112-685A-16X, CC (142.2 mbsf), including *Gephyrocapsa oceanica*, *G. aperta*, *Helicosphaera carteri*, and *Cyclococcolithus leptoporus*. We were unable to assign certain nannoplankton zones in the Quaternary because of low diversity and barren intervals.

A hiatus of approximately 4.3 m.y. was noted between Cores 112-685A-22X and 112-685A-23X at approximately 200 mbsf that divided the Quaternary from the upper Miocene. In Section 112-685A-23X, CC (203.6 mbsf) and Sample 112-685A-25X-1, 3 cm (222.6 mbsf), *Discoaster quinquaramus* was frequently found together with *Reticulofenestra pseudoumbilica*, *Reticulofenestra* sp. (small), and rare *Sphenolithus abies*, *Coccolithus pelagicus*, *Cyclococcolithus leptoporus*, and some unidentified six-rayed discoasters having an overgrowth of calcite. In Section 112-685A-25X, CC (223 mbsf) only a few *Discoaster quinquaramus* were observed. Based on nannoplankton

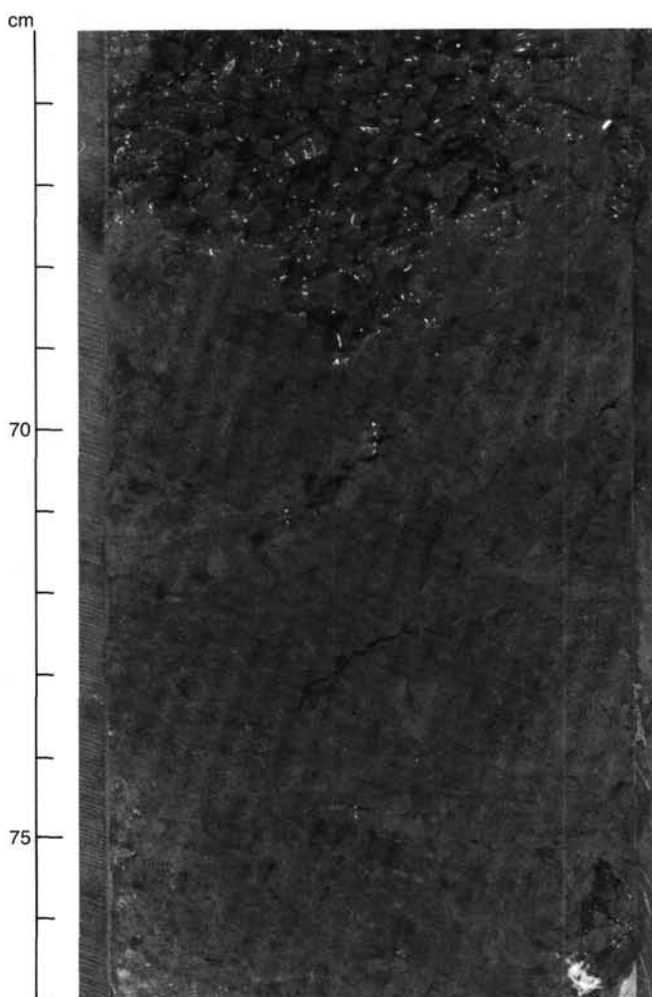


Figure 30. Extension-related disaggregation of layering in mudstone of Subunit IIA. Note blocky parting fissility exploiting clast and layer boundaries (Sample 112-685A-28X-3, 65-77 cm).

occurrences, the interval between Cores 112-685A-23X and 112-685A-25X (Core 112-685A-24X had no recovery) were placed in the late Miocene nannoplankton Zone NN11 (*Discoaster quinquaramus* Zone). Section 112-685A-26X, CC (232.1 mbsf) contained only few, well-preserved *Discoaster calcaris* and, as *Discoaster quinquaramus* was not found, was assigned to the late Miocene nannoplankton Zone NN10 (*Discoaster calcaris* Zone). Cores 112-685A-27X through 112-685A-51X (235.2-459.1 mbsf) are barren of calcareous nannoplankton, with the exception of Cores 112-685A-38X, 112-685A-44X, 112-685A-48X, and 112-685A-50X. In Cores 112-685A-38X and 112-685A-48X a poorly preserved, partially recrystallized nannoplankton assemblage was observed in a snowflakelike background of tiny calcite particles. A single specimen of *Discoaster calcaris* was noted among frequent *Reticulofenestra* sp. and rare *Sphenolithus abies*, as well as *Coccolithus pelagicus* in Sample 112-685A-38X-1, 36 cm (338.6 mbsf), which indicates that this level may still belong to nannoplankton Zone NN10.

In Cores 112-685A-44X (392.6-396.1 mbsf) and 112-685A-50X (449.6-450.6 mbsf) slumped material was recovered that contains a mixture of upper and lower Miocene as well as middle to upper Eocene nannoplankton. We did not find Oligocene calcareous nannoplankton. Nannoplankton in selected clasts from Core 112-685A-44X revealed that besides exclusively lower Miocene and Eocene clasts, a number of lower Miocene fragments

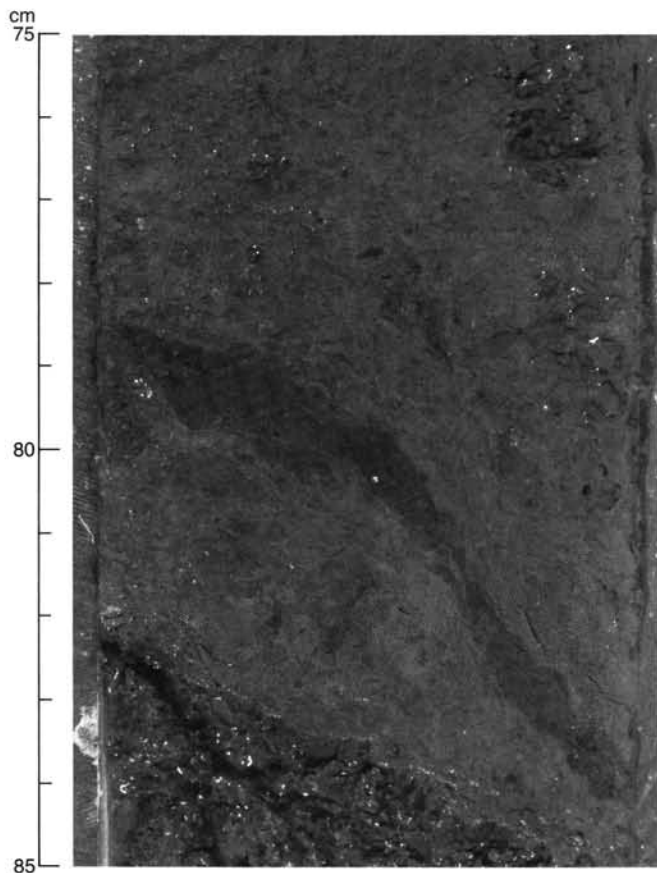


Figure 31. Extensional disruption of bedding in Subunit IIA mudstones, Sample 112-685A-28X-2, 75–85 cm.



Figure 32. Poorly developed, scaly cleavage in Subunit IIA mudstones, Sample 112-685A-35X, CC, 12–17 cm.

are present that also contain Eocene nannoplankton obviously reworked in early Miocene time from older strata.

Based on the occurrence of only discoaster-bearing samples, poorly preserved coccolith assemblages, and barren samples, most of the sequence was deposited well below the local CCD. The interval between Cores 112-685A-23X to 112-685A-26X (203.6–232.1 mbsf), however, was deposited at approximately the local CCD, with Sections 112-685A-25X, CC (223 mbsf) and 112-

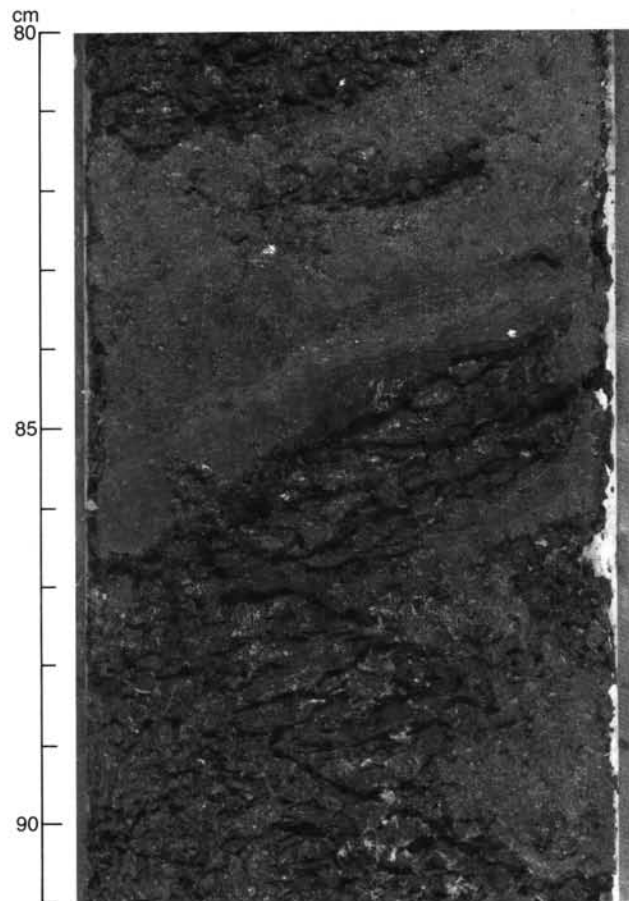


Figure 33. Strongly developed scaly cleavage in Subunit IIA mudstones showing anastomosing cleavage surfaces, Sample 112-685A-31X-3, 80–91 cm.

685A-26X, CC (232.1 mbsf) just below the local CCD. The same seems to apply for Cores 112-685A-38X (338.1–338.6 mbsf) and 112-685A-48X (430.6–440.5 mbsf). In the Quaternary, coccolith-bearing layers are associated, in most cases, with turbidites and are displaced from shallower areas.

Based on nannoplankton data, the sedimentation rate in the Quaternary (NN19 to NN21) may exceed 107 m/m.y. (interval at 0–199.8 mbsf) and 168 m/m.y. in the late Miocene (NN10) (interval at 232.1–459.1 mbsf) at this site. Dip of the sediments was not considered in these calculations.

Radiolarians

One hiatus can be documented by radiolarians between lower Quaternary and lower upper Miocene sediments, and between Sections 112-685A-22X, CC (199.8 mbsf) and 112-685A-25X, CC (223 mbsf). Reworked radiolarians were suspected in Sections 112-685A-22X, CC, 112-685A-23X, CC, 112-685A-34X, CC, and 112-685A-38X, CC and were documented in Sections 112-685A-43X, CC (386.3 mbsf) and 112-685A-44X, CC (396.1 mbsf).

To extract radiolarians from Sections 112-685A-39X, CC to 112-685A-51X, CC (358.9–459.1 mbsf), we had to employ the techniques used for Mesozoic rocks (De Wever et al., 1979; De Wever, 1982).

All core-catcher samples from Hole 685A were studied for radiolarians. These are well to moderately preserved in all samples and are generally few, but sometimes common, except in Sections 112-685A-47X, CC (422.5 mbsf) and 112-685A-52X, CC (459.1 mbsf), where they are rare.

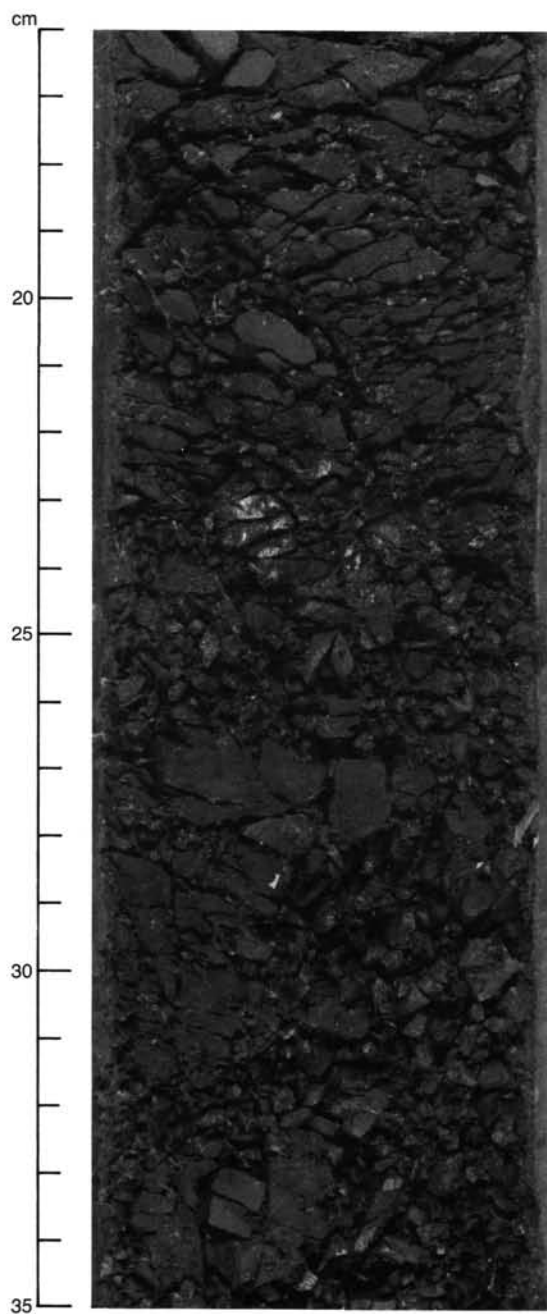


Figure 34. Intense conjugate fracturing developed in Subunit IIB. Note reflection on polished and grooved surface (center) and preexisting scaly cleavage (visible in the upper right), Sample 112-685A-48X-2, 16–35 cm.

A radiolarian assemblage with *Lamprocyclus nigrinae* was found in Sections 112-685A-1H, CC to 112-685A-21X, CC (4–195.3 mbsf); it indicates a Quaternary age. *Didymocyrtis tetralthalmus* was found in Sections 112-685A-8X, CC through 112-685A-17X, CC. *L. nigrinae* was common in Section 112-685A-8X, CC. *Lamprocyclus neoheteroporos* was found in Sections 112-685A-19X, CC to 112-685A-21X, CC (166.3–195.3 mbsf); it indicates the lower part of the Quaternary. No collospherids were found; therefore, we could not subdivide the Quaternary stage.

Botryostrobus aquilonaris, *Theocorythium trachelium*, and *Lamprocyclus neoheteroporos* were found in Sections 112-685A-22X, CC (199.8 mbsf) and 112-685A-23X, CC (203.6 mbsf). This assemblage indicates a Quaternary age. *Didymocyrtis hughesi*

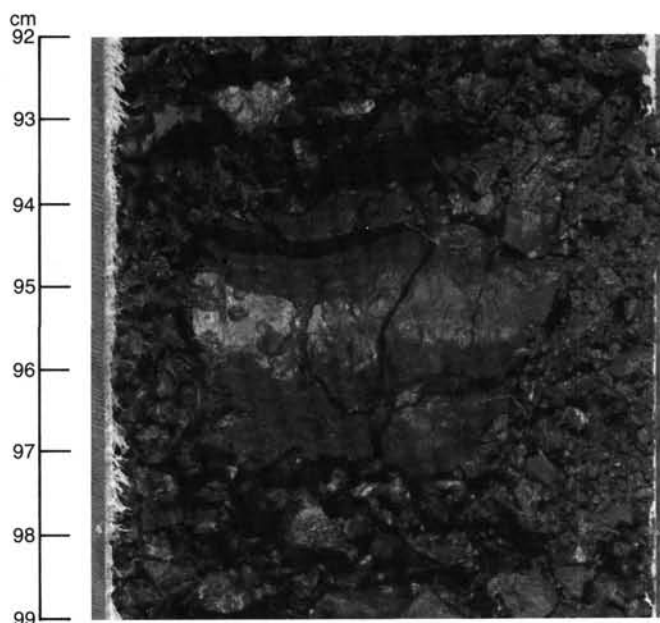


Figure 35. Conjugate, polished fracture surfaces evidencing compression normal to the core axis in Subunit IIA, Sample 112-685A-48X-1, 92–99 cm.

and *D. antepenultimus* were found in the same samples (112-684A-22X, CC and 112-685A-23X, CC). This assemblage indicates the *Didymocyrtis antepenultimus* Zone, which represents the lower part of the upper Miocene. Therefore, either a contamination (mixture of two levels during sample preparation or downhole contamination) or a reworked Miocene fauna occurs at the Quaternary level. Some radiolarians are poorly preserved and could represent some older reworked radiolarians that were unidentifiable.

Sections 112-685A-24X, CC (213.1 mbsf) and 112-685A-26X, CC (232.1 mbsf) were unavailable for paleontological investigation.

Didymocyrtis hughesi, *D. antepenultimus*, *D. laticonus*, and some *Stichocorys delmontensis* were found in Section 112-685A-25X, CC to 112-685A-51X, CC (223–459.1 mbsf). This assemblage indicates the *D. antepenultimus* Zone, which represents the lower part of the upper Miocene.

Some traces of reworked radiolarians were suspected in Sections 112-685A-34X, CC (310 mbsf) and 112-685A-38X, CC (338.6 mbsf), but these forms are unidentifiable. In Section 112-685A-43X, CC (386.3 mbsf) *Lithocyclus aristotelis*, *L. ocellus*, and “*Dictyoprora* aff. *amphora*” (Nigrini, 1977) were found. These indicate the upper Eocene. These species may have been reworked in the upper Miocene or belong to a reworked fragment of Eocene rock.

Besides the lower upper Miocene assemblages, we found various species indicating different levels in Section 112-685A-44X, CC (396.1 mbsf). These include the following: *Dorcadospyrus simplex* (or *D. forcipata*), which indicates the early Miocene; *Dorcadospyrus ateuchus*, which indicates the Oligocene to latest Eocene; and *Calocyclus hispida* and *Eusyringium fistuligerum*, which date in the middle Eocene.

Planktonic Foraminifers

Core-catcher samples from Hole 685A were examined for planktonic foraminifers. Above Section 112-685A-19X, CC (166.3 mbsf), planktonic foraminifers are few or rare and well preserved. Below Section 112-685A-20X, CC (185.6 mbsf), core-catcher samples are barren of planktonic foraminifers, except in

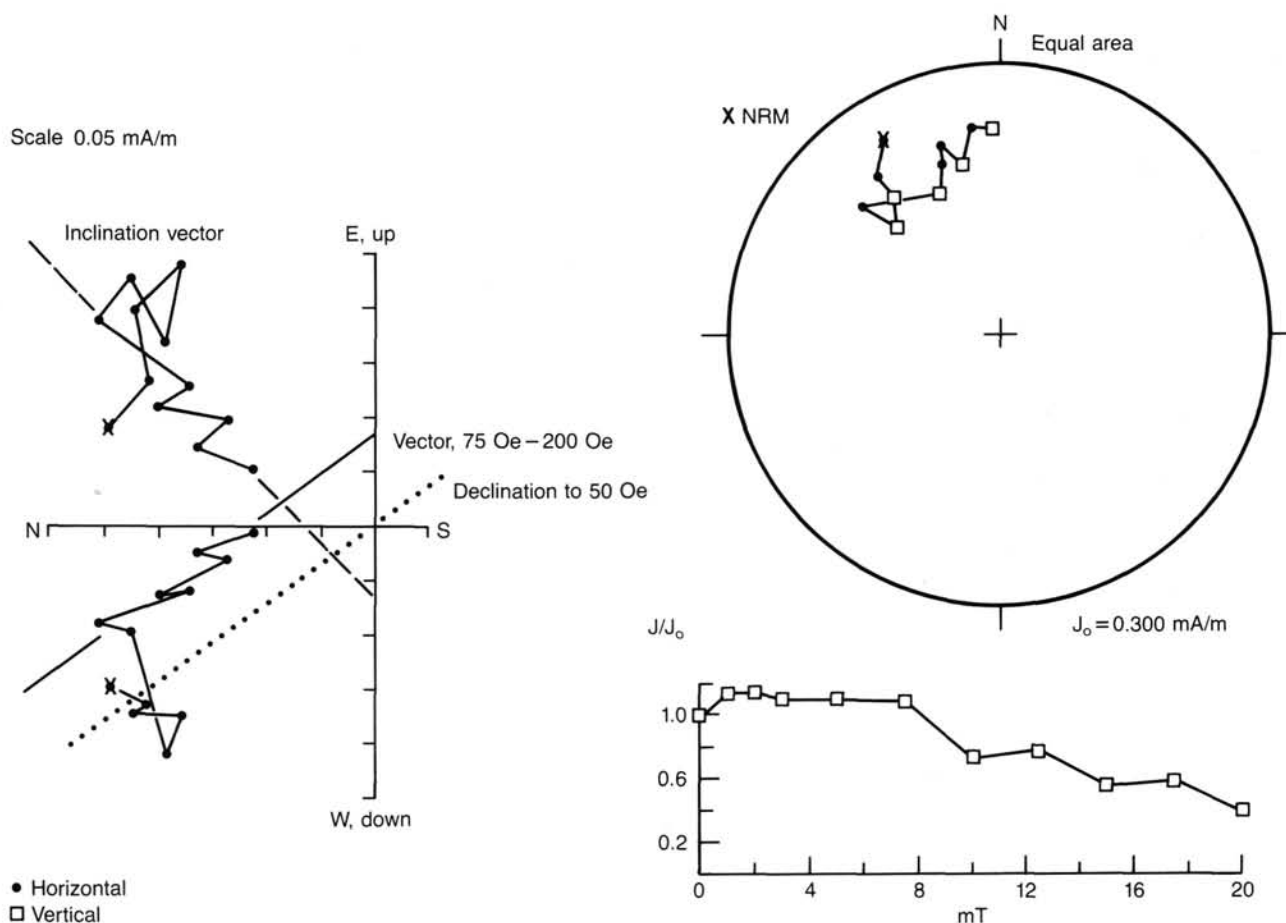


Figure 36. Orientation of faults in Sample 112-685A-48X-1, 91-99 cm by paleomagnetic methods. The paleomagnetic measurements performed on a sample retrieved from the biscuit containing two faults shown in Figure 35. The sample is weakly magnetized but shows a declination of 324° and inclination of 43° . The sample appears to have acquired a magnetization during the demagnetization process, probably during the 75-Oe treatment. The inclination is steep for this locality but is not inconsistent with values obtained throughout this core.

Sections 112-685A-22X, CC (199.8 mbsf), 112-685A-38X, CC (338.6 mbsf), 112-685A-44X, CC (396.1 mbsf), and 112-685A-50X, CC (450.6 mbsf).

Above Section 112-685A-19X, CC (166.3 mbsf), planktonic foraminifers are modern species and mostly the same assemblages. *Globigerina bulloides* and *Neogloboquadrina dutertrei* were commonly found in Section 112-685A-12X, CC (110 mbsf) and *Globorotalia inflata* was observed in Sections 112-685A-18X, CC and 112-685A-19X, CC. These species are known to occur in late Pliocene or Quaternary deposits of temperate regions.

Globoquadrina altispira altispira and *Neogloboquadrina dutertrei* were found in Section 112-685A-22X, CC (199.8 mbsf). The last occurrence of *Globoquadrina altispira altispira* is in Zone N21, 2.9 Ma (Berggren, 1977). The range of *Neogloboquadrina dutertrei* is from Zone N21 to N23 (Poore, 1979). Based on planktonic foraminifers, this sample was placed in Zone N21 and is Pliocene in age.

Catapsydrax dissimilis and *Catapsydrax stainforthi* were found in Section 112-685A-44X, CC (396.1 mbsf). The last appearance of *Catapsydrax dissimilis* is in Zone N6, 17.5 Ma (Bolli and Saunders, 1985); the range of *Catapsydrax stainforthi* is from N4 to N7 (Blow, 1969; Berggren, 1977). This sample was placed in N4 to N6 and is early Miocene in age.

Rare and poorly preserved *Catapsydrax unicava* and *Cassigerinella chipolensis* were recognized in Section 112-685A-50X, CC (450.6 mbsf). The range of *Catapsydrax unicava* is from

Zones P14 to N6 (Poore, 1979). The range of *Cassigerinella chipolensis* is Oligocene to middle Miocene (Bolli and Saunders, 1985). Based on planktonic foraminifers, this sample is Oligocene to early Miocene in age.

Benthic Foraminifers

Except for Sections 112-685A-1H, CC (4 mbsf) and 112-685A-20X, CC (185.6 mbsf), which are barren of foraminifers, benthic foraminifers were observed throughout samples of Quaternary age in Hole 685A from Sections 112-685A-2H, CC through 112-685A-22X, CC (13.7-199.8 mbsf). These were common to abundant in Sections 112-685A-4H, CC (33 mbsf), 112-685A-6X, CC through 112-685A-12X, CC (51.4-110 mbsf), 112-685A-14X, CC through 112-685A-17X, CC (123.1-158 mbsf), and 112-685A-21X, CC (195.3 mbsf). The species register a mixture of environments: the outer-shelf/upper-bathyal species *Bolivina costata* makes up from 50% to 90% of the benthic foraminifers in all but two samples (in which foraminifers are rare); lower-bathyal species such as *Astrononion schwageri*, *Melonis pompilioides*, *M. affinis*, *Pullenia bulloides*, *Stainforthia complanata*, and *Uvigerina senticososa* are less common but consistently present; middle-bathyal species, such as *Cassidulina cushmani* and *Bulimina exilis tenuata*, are present occasionally. The water depth at Site 685 is below the CCD, and this mixture of species with its fluctuating, but mostly high abundance, can be attributed to the downslope transportation of foraminifers along with fine sediment, which resulted in the great thickness of Quaternary

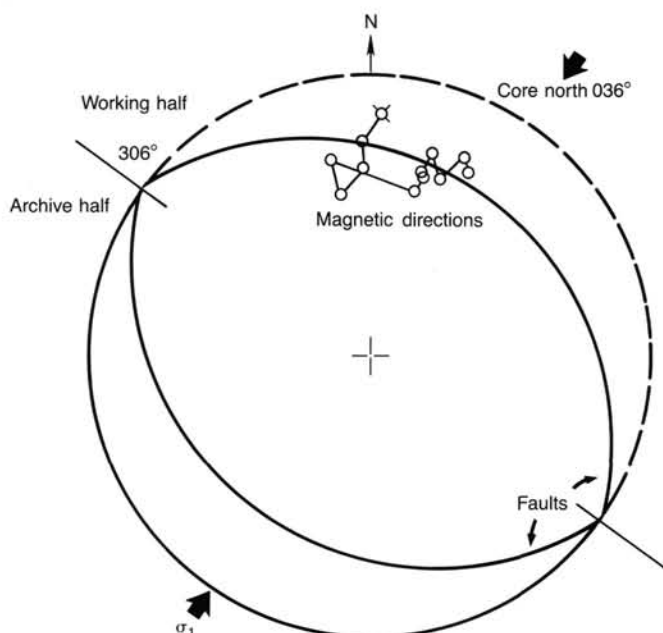


Figure 37. Using the paleomagnetic data from a sample at 94 cm (Fig. 36), the biscuit containing two faults in Section 112-685A-48X-1 was oriented. The faults are found to strike at 36° . The principal stress direction indicated by the faults is horizontal and strikes northeast-southwest (036° with an error of roughly $\pm 15^\circ$). See "Paleomagnetism" section, Site 688 chapter, for a further discussion of the orientation method.

sediments at this site. *Bolivina costata*, the principal benthic foraminifer component of these samples, was selectively transported downslope from the shelf edge because of its small size and thin-walled test.

The upper Miocene samples from Sections 112-685A-23X, CC through 112-685A-51X, CC (203.6–459.1 mbsf) are barren of benthic foraminifers, except for rare specimens of mostly long-ranging lower-bathyal to abyssal species in Sections 112-685A-23X, CC (203.6 mbsf), 112-685A-25X, CC (222.6 mbsf), 112-685A-38X, CC (338.6 mbsf), 112-685A-44X, CC (396.1 mbsf), 112-685A-50X, CC (450.6 mbsf), and 112-685A-51X, CC (459.1 mbsf). *Melonis affinis* and *M. pompilioides* are generally present in these samples. *Bolivina* cf. *vaughani*, present in Sections 112-685A-23X, CC (203.6 mbsf), 112-685A-38X, CC (338.6 mbsf), and 112-685A-50X, CC (450.6 mbsf), and *Gyroidina zealandica*, present in Sections 112-685A-38X, CC (338.6 mbsf), 112-685A-44X, CC (396.1 mbsf), and 112-685A-50X, CC (450.6 mbsf) were recovered in Miocene strata at Site 683. The scarcity

and poor condition of the specimens of benthic foraminifers in the Miocene section suggests that they were transported below the CCD; however, deposition at lower-bathyal to abyssal depths cannot be entirely discounted. Three robust specimens of *Robulus*, *Glandulina*, and *Gyroidina*, recovered from Section 112-685A-50X, CC (459.1 mbsf), were not encountered previously and may be reworked from older strata, as reworking has been shown for the other microfossil groups.

The source of the benthic foraminifers recovered from the Quaternary age sediment of the lower-slope prism at this site is the continental margin, as shown by the abundance and persistent influx of shelf- to upper slope-dwelling *Bolivina costata*. *Bolivina* cf. *vaughani*, present in three samples of the Miocene section down to Section 112-685A-50X, CC (450.6 mbsf), was also derived from the continental shelf or upper slope, as shown by its abundance at Site 679.

Percentage Distribution of the Biogenic Groups in the Coarse Fraction

The percentage distribution of the sand-sized biogenic groups (benthic and planktonic foraminifers, diatoms, radiolarians, and others) was determined by assessing component abundance in washed residues greater than 0.063 mm in size; the total of all biogenic groups was fixed at 100% (Fig. 39). Benthic and planktonic foraminifer tests are persistently present from Sections 112-685A-1H, CC through 112-685A-22X, CC (4–199.8 mbsf); both groups suddenly disappear at this break, which coincides with the boundary between the Quaternary and the Miocene. Diatoms are continuously present from Sections 112-685A-1H, CC through 112-685A-9X, CC (4–81.9 mbsf) and reappear downward from Section 112-685A-24X, CC (213.1 mbsf). Radiolarians are present without interruption from top to bottom of the cored section. Other groups consist of sponge spicules, echinoid spines, and fish remains, which are present throughout the section.

In addition to the biogenic components, high abundances of glauconite and pyrite were observed in Sections 112-685A-1H, CC to 112-685A-7X, CC (4–56.1 mbsf). In Sections 112-685A-5X, CC to 112-685A-7X, CC, we estimated pyrite as 65% of the total abiogenic grains. In these samples, pyrite replaces worm tubes, radiolarians, and diatoms.

ORGANIC GEOCHEMISTRY

Hole 685A was drilled into lower-slope deposits of the Peru Outer Continental Margin. This was the third site to be located in deep water (5070 m); the others are Site 682 (water depth of 3790 m) and Site 683 (water depth of 3072 m). The same organic geochemical approaches were taken at Site 685 as at these previous deep-water sites. Details of methods and procedures are given in the "Organic Geochemistry" sections, Site 679 and 682

Table 5. Deformational style zones at Site 685.

Lith. unit	Core-section	Depth (mbsf)	Deformational features	Tectonic significance
IA	112-685A-1H–9X-3	0–74	Localized, gentle oceanward tilting of beds; oceanward-facing normal faults.	Gravity-related down-slope extension.
IB	112-685A-9X-4–22X	80–203.6	Pervasive high-angle, planar, dewatering fabric and folding.	?down-slope slumping and dewatering ?with a component of tectonic kneading.
II	112-685A-22X–51X	203.6–468.6	Scaly cleavage and localized compression-related fracturing. Rotation of bedding to moderate dips.	Thrusting during accretion.

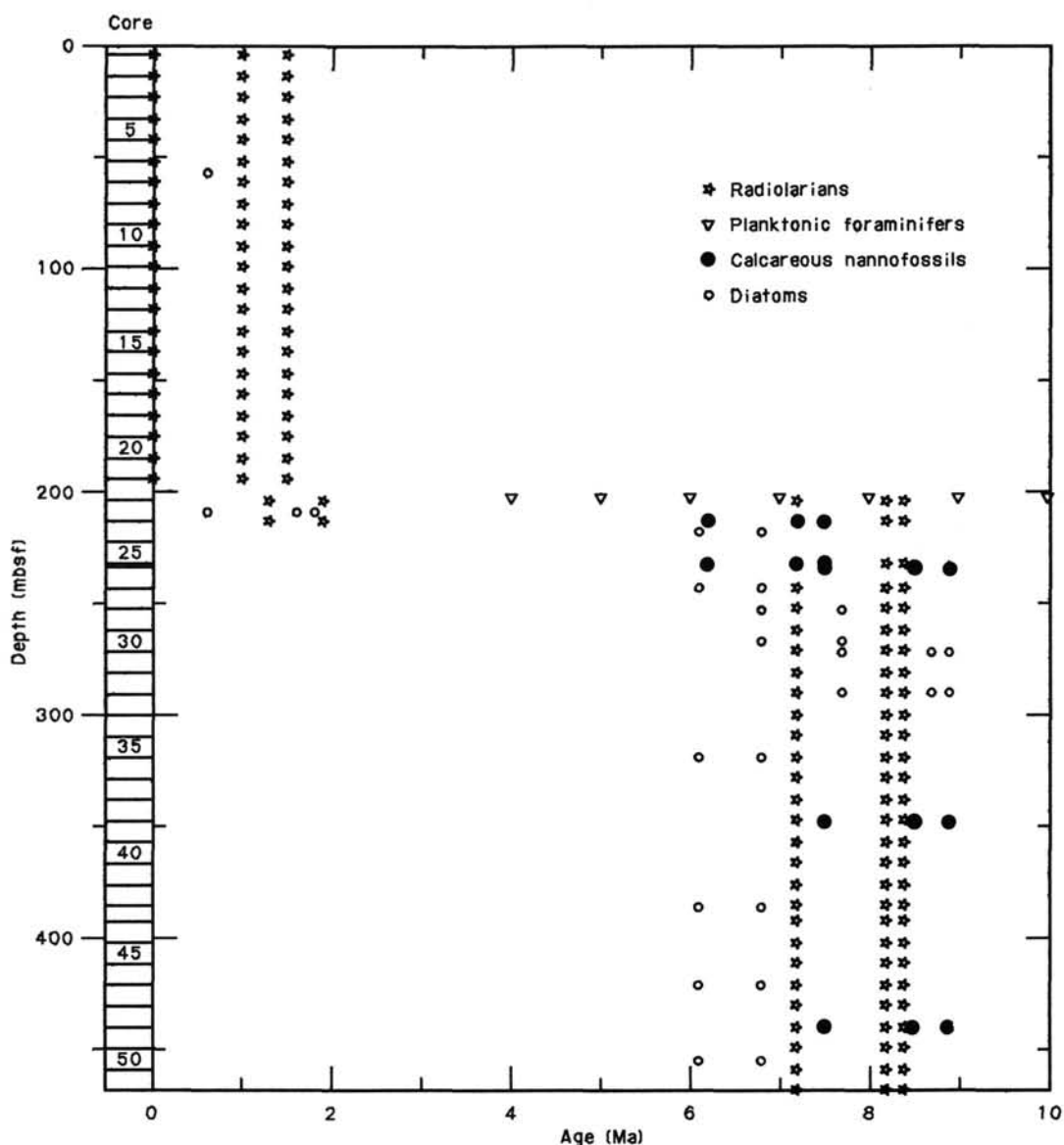


Figure 38. Occurrences and ranges of microfossil data at Hole 685A.

chapters (this volume). Instruments are described in the "Explanatory Notes" (this volume).

Hydrocarbon Gases

Vacutainer Gases

Gas pockets were initially noted in Core 112-685A-4H (30.3 mbsf) and were present in most other cores to the bottom of the hole. This visible manifestation of high amounts of gas duplicates what was observed at Site 683, where gas pockets also were seen and were sampled by vacutainers, starting with the fourth core. The concentrations of C_1 in vacutainer samples from Hole 685A range from 22.0% (probably badly contaminated with air) to 93.4% (Table 6). The main balance gases are probably CO_2 from the sample itself and air from procedural contamination. The shallow occurrence of C_1 at this site results from the rapid depletion of sulfate. Sulfate values decrease to zero in Core 112-685A-3H (see "Inorganic Geochemistry," this chapter), thus allowing methanogenesis to proceed without competition from the sulfate reducers (Claypool and Kaplan, 1974).

Accompanying the relatively pure C_1 are C_2 and C_3 at parts per million (ppm) concentrations (Table 6). For example, the amounts of C_2 range from 5.8 to 610 ppm, with the higher concentrations usually found in the deeper sediments. C_3 concentrations range from 1.4 to 87 ppm, and as with C_2 , the higher amounts occur in the deeper sediments. In fact, the concentrations of these two hydrocarbons abruptly increase near 195.5 mbsf, at the hiatus between lower Pleistocene and upper Miocene sediments (see "Biostratigraphy," this chapter). This correspondence between changes in concentrations of C_2 and C_3 and lithologic boundaries was noted previously (see "Organic Geochemistry," Site 683 chapter).

C_1/C_2 ratios in the vacutainer gases decrease irregularly but exponentially with depth (Table 6 and Fig. 40). Between 30 and 177 mbsf, the ratios are very large (ranging between 10,000 and 110,000). Below 177 mbsf, this ratio is smaller and ranges between 1300 and 6700. This ratio changes at the Pleistocene-Miocene hiatus, as discussed previously. The overall exponential decrease in the C_1/C_2 ratios at this site follows the expected trend, based on a compilation of data from oceanic sediments

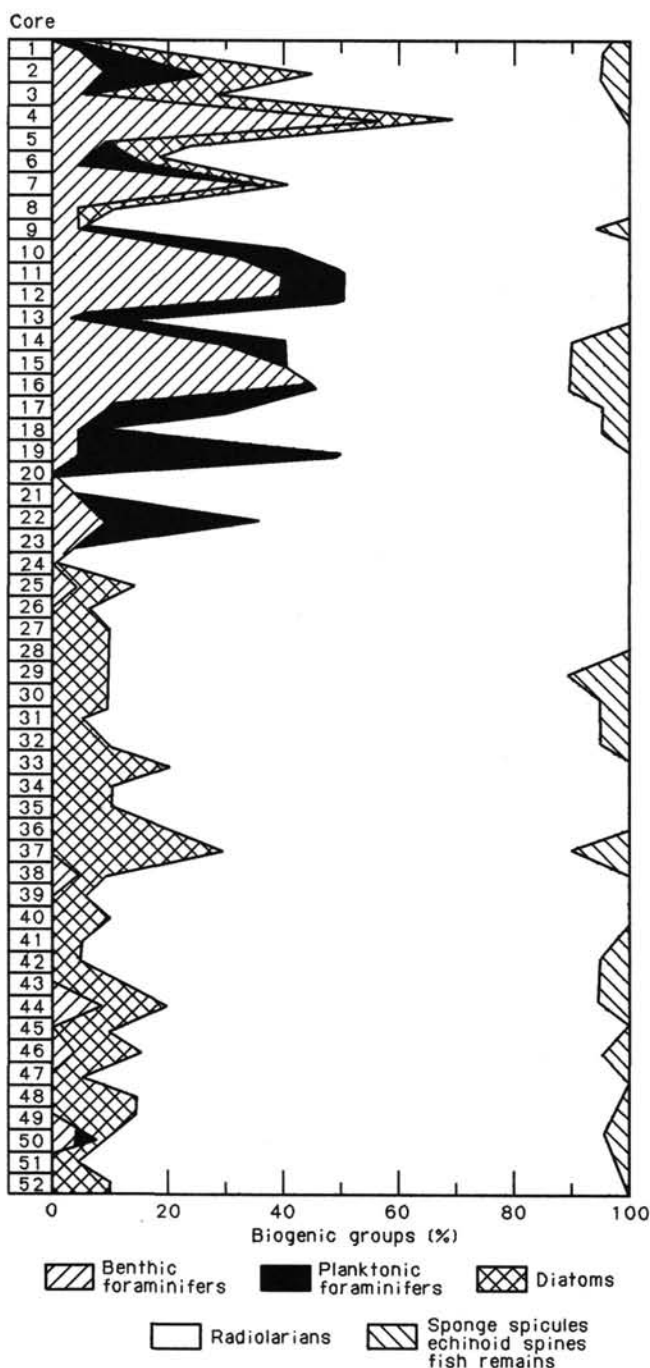


Figure 39. Biogenic groups in the coarse fraction of core-catcher samples.

worldwide (Claypool and Kvenvolden, 1983). This decrease reflects the early diagenesis of organic matter leading to increasing amounts of C_2 with depth. The rate of decrease of this ratio is apparently controlled by many factors, including temperature, time, lithology, and type of organic matter. The primary factors influencing the C_1/C_2 ratios at this site are not known.

Extracted Gases

Besides the gases collected by means of vacutainers, hydrocarbon gases were also extracted from sediment samples by the headspace and can procedures (Tables 7 and 8). The amount of samples used in these two procedures differs by a factor of

Table 6. Vacutainer gases at Site 685.

Core-section interval (cm)	Depth (mbsf)	C_1 (%)	C_2 (ppm)	C_3 (ppm)	C_1/C_2
112-685A-4H-5, 115	30.0	91.0	15	2.4	61,000
5X-2, 145	35.6	67.0	12	2.2	58,000
6X-5, 93	49.1	93.4	20	3.8	47,000
7X-2, 46	53.6	77.7	18	4.1	44,000
8X-6, 93	69.5	89.6	20	5.4	44,000
9X-7, 91	79.4	78.6	11	3.6	73,000
10X-5, 50	86.6	86.5	9.1	5.0	95,000
11X-6, 13	97.3	92.5	25	1.4	37,000
12X-6, 132	107.9	87.5	7.9	6.4	110,000
13X-2, 142	111.5	72.9	6.8	7.0	110,000
14X-3, 60	121.7	80.1	22	7.7	37,000
15X-5, 30	132.7	88.5	13	11	68,000
16X-3, 110	141.2	74.8	26	7.8	29,000
17X-6, 20	153.8	76.6	14	11	59,000
18X-7, 77	164.5	22.0	5.8	5.5	38,000
20X-6, 74	177.0	86.6	84	11	10,000
22X-1, 141	195.5	81.3	120	24	6,700
27X-2, 25	235.2	65.3	170	36	3,900
28X-8, 50	252.6	83.3	400	23	2,100
29X-3, 22	255.8	82.6	330	44	2,500
30X-1, 133	264.9	74.7	230	83	3,300
32X-2, 94	283.5	83.5	290	32	2,900
34X-8, 140	309.6	81.2	350	59	2,300
35X-3, 130	315.6	68.9	290	80	2,400
36X-7, 85	327.9	80.3	530	61	1,500
37X-3, 7	331.7	88.2	510	86	1,700
39X-3, 74	351.3	81.9	490	87	1,700
43X-1, 40	386.0	66.2	22	7.3	3,000
44X-2, 150	395.6	88.9	510	80	1,800
47X-1, 68	421.8	75.6	610	82	1,300
48X-1, 65	431.3	78.5	370	68	2,100

Note: units of (%) and (ppm) are in volume of gas component per volume of gas mixture. All measurements were performed on the Hach-Carle Gas Chromatograph.

about 40, with the headspace procedure using about 4 cm³ and the can procedure about 170 cm³ of sediment. The results from the two procedures, when calculated on the common basis of volume of gas per volume of wet sediment are not the same but are similar. Certainly, the overall trends are comparable.

Figure 41 compares the concentrations of extracted C_1 obtained from the can and headspace procedures; the headspace procedure gives more detail because of closer sample spacing. Data from the can procedure appear to yield minimum values. The C_1 content increases rapidly with depth, and by Core 112-685A-2H the extracted C_1 concentrations reach more than 100,000 $\mu\text{L/L}$ of wet sediment. The sulfate content of the pore water of this core was not measured, but in the next lower core (112-685A-3H) the sulfate concentration was 0 mmol/L. These observations show that the zone of C_1 generation, as indicated by vacutainer sampling to include Core 112-685A-4H, actually extends into Core 112-685A-2H. Thus, the zone of sulfate reduction is quite thin at this site (< 11.6 m), whereas the zone of C_1 generation apparently extends downward from about this depth to the bottom of the hole and certainly to the last analyzed sample from 432.3 mbsf. The concentrations of extracted C_2 and C_3 show the same abrupt changes near 200 mbsf as do C_2 and C_3 concentrations from vacutainer gases.

Ethane ($C_{2:1}$) was monitored at this site (Table 7) as it was at one previous deep-water site (see "Organic Geochemistry," Site 683 chapter). $C_{2:1}$ was encountered only when using the headspace procedure. In the can procedure, small amounts of $C_{2:1}$ may dissolve in the water and not be detectable. The amount detected in the headspace procedure is uniform (ranging from 3.6 to 12.6 $\mu\text{L/L}$); we believe that the $C_{2:1}$ is desorbed from the sediment by heating at 70°C in the headspace procedure. The amount of $C_{2:1}$ released may depend mainly on the temperature of heating, which would account for the uniform results observed downhole.

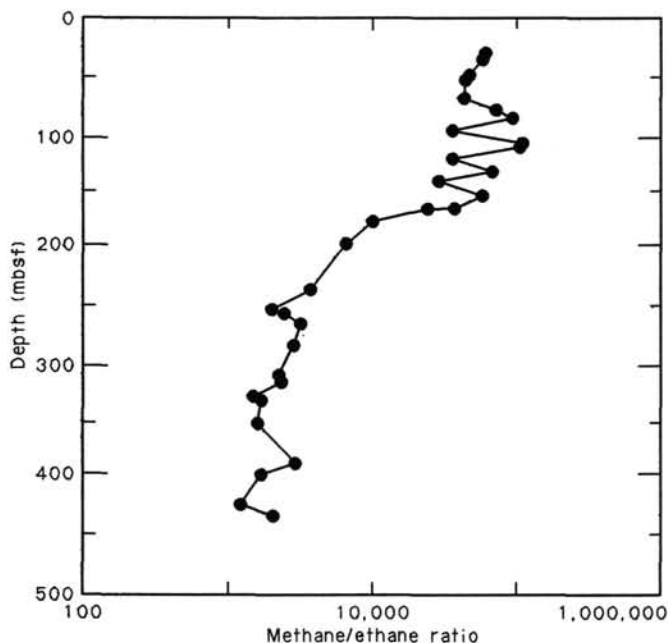


Figure 40. Methane/ethane ratios in gas collected by means of vacuainers from Hole 685A.

Gas Hydrates

After anticipating gas hydrates at the two previous deep-water sites, based on gas and pore-water chemistries (see "Organic Geochemistry" and "Inorganic Geochemistry" sections, Site 682 and 683 chapters, this volume), we finally observed these

clathrates in Sections 112-685A-12X-1 (about 99 mbsf) and 112-685A-18X-8 (about 164 mbsf). Core recovery was disturbed by the rapid gas expansion that, in many instances, forcibly ejected core out of the core liners. A few small pieces (1 cm × 1 cm × 1 cm) of dark gray gas hydrate were first noticed in Core 112-685A-12X.

Two pieces of dark gray gas hydrate, measuring about 3 cm × 3 cm × 2 cm and 1 cm × 1 cm × 1 cm, were found in void space at the bottom of Section 112-685A-18X-8. At first, the material looked like partially rounded, lithified sediment, but closer examination showed a rapidly bubbling foam on the edges and coldness to the touch. These samples were placed in special pressure vessels (Kvenvolden et al., 1984). One vessel held pressure when the confined gas hydrate decomposed. The following preliminary information was obtained:

- Equilibrium pressure and temperature: 383 psig, 25°C.
- Composition of gas: C₁ = 95 %, C₂ = 39 ppm, C₃ = 28 ppm; the balance (about 5%) is air and possibly CO₂.
- Volume of C₁: 587 cm³ (STP).
- Volume of H₂O: 5.89 mL.
- Volume C₁/Volume H₂O: 100.
- Weight of sediment: 1.25 g.
- Composition of water: salinity = 4.0 g/kg, alkalinity = 17.93 mmol/L,
- Chloride content = 51.4 mmol/L.
- pH = 7.24.

These results augment those found previously using gas hydrates in sediments of continental margins (for example, Kvenvolden and Barnard, 1983; Kvenvolden and McDonald, 1985).

Fully saturated C₁ hydrate has a composition defined by the formula C₁·5.75 H₂O, which means that upon decomposition

Table 7. Headspace gases at Site 685.

Core-section interval (cm)	Depth (mbsf)	C ₁ (μL/L)	C ₂ (μL/L)	C _{2:1} (μL/L)	C ₃ (μL/L)	C ₁ /C ₂
112-685A-1H-3, 0-1	3.0	5,100				
2H-6, 0-1	11.6	110,000	8.1	5.4		13,000
3H-4, 0-1	18.1	170,000	4.1			41,000
4H-6, 0-1	30.6	30,000				
5X-6, 0-1	40.1	40,000	5.9	4.1	5.0	6,800
6X-5, 0-1	48.1	27,000	5.9	3.6		4,700
8X-6, 0-1	68.6	44,000	7.1	4.4	6.1	6,100
9X-8, 41-42	80.0	30,000		3.7		
10X-5, 0-1	86.1	31,000		3.6		
12X-6, 149-150	108.1	26,000	4.4	7.6		6,000
14X-3, 0-1	121.1	44,000	5.0	5.0	5.7	8,800
15X-5, 0-1	132.4	31,000	6.8	4.5	8.1	4,600
16X-3, 0-1	140.1	24,000	6.3	4.1	1.8	3,900
18X-7, 0-1	163.8	28,000		4.1	9.9	
20X-6, 0-1	182.3	38,000	9.9	6.8	28	3,800
22X-3, 0-1	197.1	31,000	6.3		16	4,900
27X-2, 0-1	234.9	44,000	95	5.0	140	470
28X-9, 0-1	252.0	440,000	200	6.9	37	2,200
30X-2, 0-1	263.6	180,000	63	4.5	160	2,900
32X-4, 0-1	285.5	150,000	91	6.8	72	1,600
33X-1, 0-1	290.6	140,000	63	5.4	59	2,300
34X-8, 0-1	309.5	17,000	24	4.1	33	710
35X-6, 0-1	315.8	43,000	58	10	101	740
36X-7, 0-1	326.6	45,000	38	9.0	140	520
38X-1, 53-54	338.6	170,000	110	5.9	200	1,500
39X-4, 0-1	352.1	57,000	130	7.7	180	440
40X-CC, 0-1	366.5	38,000	72	7.8	73	530
42X-1, 0-1	376.1	230,000	200	6.4	210	1,100
43X-1, 0-1	385.6	110,000	140		140	820
44X-2, 0-1	394.1	33,000	180		190	180
46X-2, 0-1	413.1	150,000	140	6.8	110	1,100
48X-2, 0-1	432.1	270,000	240	12.6	180	1,100

Note: units are in microliters (μL) of gas component per liter (L) of wet sediment. All measurements were performed on the Hach-Carle Gas Chromatograph.

Table 8. Canned gases at Site 685.

Core-section interval (cm)	Depth (mbsf)	C ₁ (μL/L)	C ₂ (μL/L)	C ₃ (μL/L)	C ₁ /C ₂
112-685A-1H-2, 140-145	1.5	410	0.6		710
3H-3, 140-145	18.1	83,000	2.4		34,000
6X-4, 140-145	48.1	25,000	1.3		19,000
9X-7, 145-150	79.9	14,000	0.9	0.6	15,000
15X-4, 135-140	132.3	25,000	1.6	6.7	15,000
22X-2, 135-140	197.0	26,000	5.8	13	4,200
28X-8, 20-25	252.5	50,000	49	24	1,000
35X-5, 135-140	315.7	36,000	26	47	1,400
39X-3, 135-140	351.9	31,000	97	95	320
46X-1, 145-150	413.1	41,000	130	70	310

Note: units are in microliters (μL) of gas component per liter (L) of wet sediment. All measurements were performed on the Hach-Carle Gas Chromatograph.

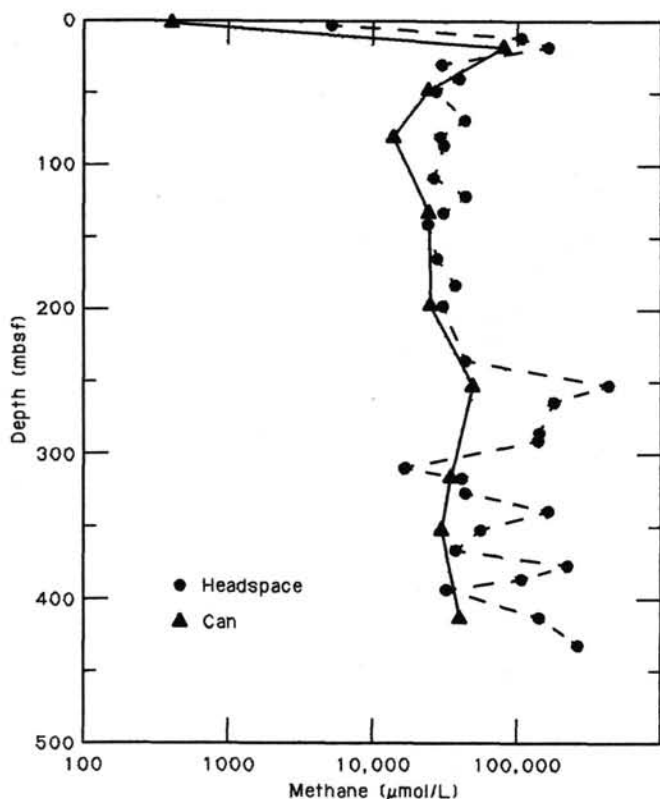


Figure 41. Comparison of extracted methane concentrations with depth obtained with the headspace procedure with those concentrations obtained by the can procedure.

one can expect a volumetric ratio of C₁ to H₂O of about 164. The gas hydrate at Site 685 has a volumetric ratio of 100, indicating partial decomposition and/or undersaturation. The water of the gas hydrate is fresh and has a salinity about 11% of seawater and a chloride content about 9% of seawater. The chloride content contrasts with that of nearby pore water obtained from sediments of Core 112-685A-18X, which has a value of 541 mmol/L. This value is 96.8% of seawater (559 mmol/L). The freshwater composition of the gas hydrate explains the lowered salinity and chlorinity that was measured in pore waters from sediments that contained gas hydrates (see "Inorganic Geochemistry," this chapter). Well logs run in this hole clearly show the occurrences of gas hydrates as discrete layers in the sediment column by high resistivity and sonic velocity and by low density (see "Logging," this chapter).

A bottom-simulating reflector (BSR) occurs on a marine seismic record about 4.6 km seaward of Site 685. This BSR was inferred to represent the base of the zone of gas hydrates. Finding gas hydrates at this site was evidence that our inference was probably correct. The BSR is located at a depth of 0.68 s or, if we assume a velocity of 1800 m/s, at 612 mbsf. Using the pressure-temperature phase relations applicable to C₁ hydrate and a bottom-water temperature of 1.5°C, and following the work of Shipley et al. (1979) and Yamano et al. (1982), we calculated that the temperature at the base of the zone of inferred gas hydrates was 27.6°C, and thus the geothermal gradient at this site is approximately 43°C/km. The gradients estimated at the other deep-water sites, calculated by the same methods, were 49°C/km at Site 682 and 57°C/km at Site 683. For further discussion of geothermal gradients, see "Geophysics" sections; Sites 682 and 683 chapters and this chapter. These geothermal gradients appear high compared with the range of gradients of 22 to 35°C/km calculated for slope sediments of the Middle America Trench offshore Mexico and Central America (Shipley et al., 1979), but are comparable to the gradients of 42 to 66°C/km calculated for slope sediments of the Nankai Trough (Yamano et al., 1982).

Carbon

Total-carbon, carbonate-carbon, and organic-carbon contents were determined on 15 sediment "squeeze-cakes" from the pore-water geochemistry studies. The results are listed in Table 9. Organic carbon (OC), an important parameter in organic geochemistry, ranges from 1.61% to 4.30%. These values are high for oceanic sediments but are generally lower than at the other deep-water sites (see "Organic Geochemistry" sections, Sites 682 and 683 chapters). There is no obvious break in the OC profile with depth (Fig. 42) at the major hiatus between lower Pleistocene and upper Miocene sediments at about 200 mbsf. OC values are greater than 2.5% above 250 mbsf, and less than 2.5% below this depth, with the exception of one sample at 326.9 mbsf (3.2%). This low-resolution OC profile does not appear to correlate with any of the lithologic or biostratigraphic units. The total organic carbon (TOC), as measured by Rock-Eval pyrolysis, also is given in Table 9 and plotted in Figure 42. The profiles with depth are comparable, but the TOC values are consistently lower than the OC values. These results contrast with those from the other deep-water sites, where there was usually close agreement between measurements performed on the same samples (see "Organic Geochemistry" section, Sites 682 and 683 chapters.)

Rock-Eval pyrolysis results are given in Table 10 and Figure 43. The results show that the sediments at this site are organic-rich (TOC greater than 1%) and that the organic matter is immature (all T_{max} values less than 420°C). These sediments are not as rich in organic matter as those at the previous deep-water sites; the hydrogen indices (HI) are generally lower, and oxygen indices (OI) are usually higher. Figure 44 shows the wide distribution of these parameters, plotted between type II and type III organic matter. We concluded that the organic matter in these sediments was probably of marine origin but underwent some oxidation during its sedimentation history.

INORGANIC GEOCHEMISTRY

Introduction and Operation

A total of 17 samples from 15 whole-round samples (six 5-cm, six 10-cm) and two *in-situ* deployments were obtained for inorganic-geochemical analyses from Hole 685A. Only results of 12 samples are presented in Table 11, however. The reason for this is that the large volume of gas, particularly methane, (see "Organic Geochemistry" section, this chapter) encountered at this site severely disrupted the sediments within the cores. Below

Table 9. Organic carbon and carbonate carbon at Hole 685A.

Core-section interval (cm)	Depth (mbsf)	Total carbon (%)	Inorganic carbon (%)	Organic carbon (%)	TOC (%)
112-685A-1H-2, 145-150	3.0	2.84	0.04	2.80	2.52
3H-3, 145-150	18.1	2.95	0.14	2.81	2.55
6X-4, 145-150	48.1	3.05	0.03	3.02	2.74
9X-7, 145-150	79.9	3.77	0.95	2.82	2.69
12X-5, 145-150	106.6	3.64	0.71	2.93	2.50
15X-4, 140-150	132.3	4.32	0.49	3.83	3.40
18X-6, 145-150	163.7	3.13	0.45	2.68	2.37
27X-1, 120-130	234.8	4.47	0.17	4.30	3.98
30X-2, 127-137	264.9	2.20	0.15	2.03	1.89
35X-5, 140-150	315.7	1.86	0.04	1.82	1.53
36X-6, 140-150	326.9	3.31	0.11	3.20	2.90
39X-3, 140-150	352.0	1.75	0.03	1.72	1.56
44X-3, 40-50	396.0	2.36	0.75	1.61	1.41
47X-1, 123-138	422.4	2.23	0.37	1.86	1.59
50X-1, 92-102	450.5	2.72	0.39	2.33	1.27

TOC = total organic carbon from Rock-Eval pyrolysis.

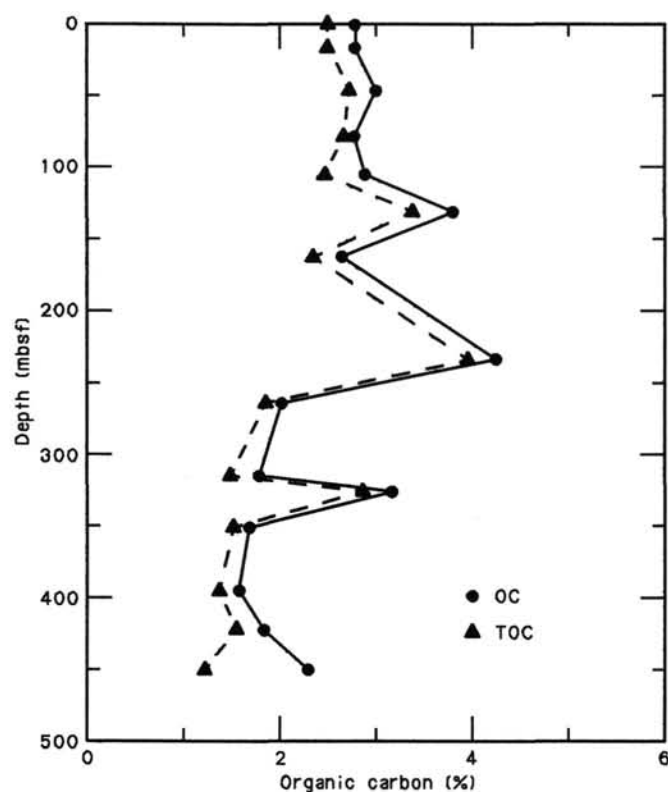


Figure 42. Comparison of organic carbon (OC) with total organic carbon (TOC) from Rock-Eval pyrolysis with depth at Site 685.

a depth of ~300 m, sediment condition was frequently so poor that additional steps in sample preparation before squeezing interstitial waters were necessary. In "shattered" sediments, composed of various mixtures of drilling slurry and small- to medium-sized, angular, indurated sediment pieces, the two components were physically separated from each other. The indurated sediment pieces, which were wettened externally by drill-hole water, were immediately dried with paper tissues and only then introduced into the squeezers.

Even after these precautions, three samples (i.e., 112-685A-35X-6, 140-150 cm, 112-685A-39X-3, 140-150 cm, and 112-685A-47X-1, 128-138 cm) still contained some admixed drill-

hole water, as indicated by their SO_4^{2-} concentrations. These samples were recovered from the thick, continuous, zero sulfate zone. On the basis of sulfate analyses of 1.4, 3.5, and 2.0 mmol/L, respectively, the three samples were discarded because of contamination. The two *in-situ* water samples also were contaminated by drill-hole water, which amounted to 15.5% and 53.6%, respectively (Table 12). For discussion of *in-situ* water contamination problems, see "Inorganic Geochemistry Appendix," Site 682 chapter (this volume).

Another source of contamination was from freshwater used in core splitting. Use of such samples exposed to the saw should be avoided whenever possible. A case study indicates the unfavorable effects of freshwater dilution of pore fluids. Table 13 compares chemical data obtained from a squeezed 50-cm³ core-catcher sample used for physical-properties measurements with two bracketing whole-round sediment samples squeezed without exposure to freshwater. Clearly, the core-catcher sample is diluted by 2.5% to 6.0% freshwater used while cutting the core.

As at Sites 682 and 683, where we found gas hydrates, interstitial-water profiles at Site 685 show systematic downhole variations with well-developed, extreme concentration minima and maxima (Figs. 45 to 53). Because of the very high sedimentation rates at this site (more than ~100 m/m.y. in the first 200 m and considerably faster below), these concentration gradients were significantly more extreme than at Sites 682 and 683.

The maxima in alkalinity (156.4 mmol/L) and in phosphate (826.2 $\mu\text{mol/L}$) by far exceed the highest alkalinity and phosphate values previously reported during the Ocean Drilling Program. The ammonia value of 32.32 mmol/L may also be the highest concentration ever encountered in marine environments. The previous record of 120.8 mmol/L in alkalinity was recorded in the Middle America Trench, DSDP Leg 67, Site 496 (Harrison et al., 1982).

The most significant downhole concentration gradients are decreases in SO_4^{2-} and pH, first increases and sequentially decreases in salinity, alkalinity, NH_4^+ , Mg^{2+} , $\text{Mg}^{2+}/\text{Ca}^{2+}$, an increase in Ca^{2+} , and an unusually irregular profile of decreasing Cl^- concentrations downhole, followed by a weak trend of increasing concentrations toward the bottom of the hole (Figs. 45 to 53). Although these profiles were generally similar to those obtained at Sites 682 and 683, the concentration increases, which in several of the profiles preceded the systematic downhole decreasing profiles, were intense and strongly compressed toward the sediment/water interface.

The hiatus of about 4.3 m.y. duration between Cores 112-685A-22X and 112-685A-23X (~200 mbsf) (see "Biostratigraphy" section, this chapter) can be seen clearly in most of the chemical profiles at this site.

Chloride and Salinity

At this site, the Cl^- concentration profile is not as smooth and continuous as the Cl^- profiles at Sites 682 and 683 (Fig. 45 and Table 11). A small but distinct maximum is evident at ~18 mbsf, as well as the main trend of continuous downhole decreases in chloride to ~200 mbsf, the depth of the hiatus. Between ~200 to 400 mbsf, Cl^- concentrations do not vary significantly; however, these do remain below the values of seawater throughout. Near the bottom of the hole, the Cl^- concentration increases, which suggests the approach of the lower boundary of the gas-hydrates zone. As at Sites 682 and 683, most of the sediments cored at this site were within the stability field for gas hydrates (Kvenvolden and McMenamin, 1980). On the basis of the Cl^- profile, one can infer that at 40 m below the sediment/water interface, disseminated gas hydrates "dilute" the pore water of the sediments recovered (e.g., Sample 112-685A-9X-7, 145-150 cm). The distinct Cl^- maximum at ~18 mbsf may represent the anticipated maximum above the stability field of ma-

Table 10. Summary of data obtained from Rock-Eval pyrolysis at Site 685.

Core-section interval (cm)	Depth (mbsf)	Weight (mg)	T _{max}	S ₁	S ₂	S ₃	PI	S ₂ /S ₃	PC	TOC (%)	HI	OI
112-685A-1H-2, 145-150	2.95	92.4	413	0.79	6.19	2.93	0.11	2.11	0.58	2.52	245	116
3H-3, 145-150	18.05	96.8	408	1.02	7.32	2.83	0.12	2.58	0.69	2.55	287	110
6X-4, 145-150	48.05	93.2	412	0.89	7.54	2.99	0.11	2.52	0.70	2.74	275	109
9X-7, 145-150	79.92	95.1	409	0.90	6.50	4.31	0.12	1.50	0.61	2.69	241	160
12X-5, 145-150	106.55	93.5	410	0.81	7.45	4.19	0.10	1.77	0.68	2.50	298	167
15X-4, 140-150	132.30	87.6	409	1.50	12.02	4.36	0.11	2.75	1.12	3.40	353	128
18X-6, 145-150	163.72	91.1	405	0.82	6.47	4.28	0.11	1.51	0.60	2.37	272	180
27X-1, 120-130	234.80	96.0	409	1.27	16.93	2.63	0.07	6.43	1.51	3.98	425	66
30X-2, 127-137	264.87	95.6	405	1.18	7.47	1.68	0.14	4.44	0.72	1.89	395	88
35X-5, 140-150	315.74	89.5	408	0.60	5.94	1.47	0.09	4.04	0.54	1.53	388	96
36X-6, 140-150	326.90	83.9	410	0.95	11.64	2.46	0.08	4.73	1.04	2.90	401	84
39X-3, 140-150	352.00	99.1	415	0.40	5.00	0.99	0.07	5.05	0.45	1.56	320	63
44X-3, 40-50	396.00	98.8	418	0.29	3.23	1.32	0.08	2.44	0.29	1.41	229	93
47X-1, 128-138	422.38	95.4	406	0.53	4.84	1.92	0.10	2.52	0.44	1.59	304	120
50X-1, 92-102	450.52	93.9	415	0.42	6.60	2.14	0.06	3.08	0.58	1.27	519	168

Rock-Eval parameters are defined in "Inorganic Geochemistry" section, Site 679 chapter.

rine gas hydrates, which depends on pressure, temperature, and pCH₄.

Superimposed on this general trend within the clathrate zone are two equal but weaker chloride maxima at about 107 and 165 mbsf (Samples 112-685A-12X-5, 145-150 cm, and 112-685A-18X-6, 145-150 cm, respectively), depicted in Figure 45. Gas hydrates were recovered from these two cores, and a small sample of gas hydrate from Core 112-685A-18X was analyzed for salinity, Cl⁻, alkalinity, and pH (Table 11). The determined low salinity and Cl⁻ concentrations of 4.0 g/kg and 51.42 mmol/L, respectively, support the dilution "artifact" suggested by Harrison et al. (1982) and discussed in "Inorganic Geochemistry" section of the Site 683 chapter (this volume).

The downhole extent of these two more massive gas-hydrate zones are easily recognized on the resistivity, velocity, and to

some extent, on density logs (see "Logging" section, this chapter). The gas-hydrate zones from these logs are designated in Figure 45. The massive nature of these zones probably protected the gas hydrates from complete destruction and dissociation before recovery. Partial preservation of the gas hydrate, instead of complete dissociation and thus higher Cl⁻ concentrations, may have been responsible for a lower dilution "artifact" observed at these two depth intervals than was the case above or below the interval.

The effect of alkalinity on salinity is clearly demonstrated in Figures 45 and 46. The salinity maximum of 40.3 g/kg corresponds to the record alkalinity maximum. Despite the presence of gas hydrates, salinity increases at rather shallow depths. It decreases to less than seawater salinity only below the hiatus at ~200 mbsf.

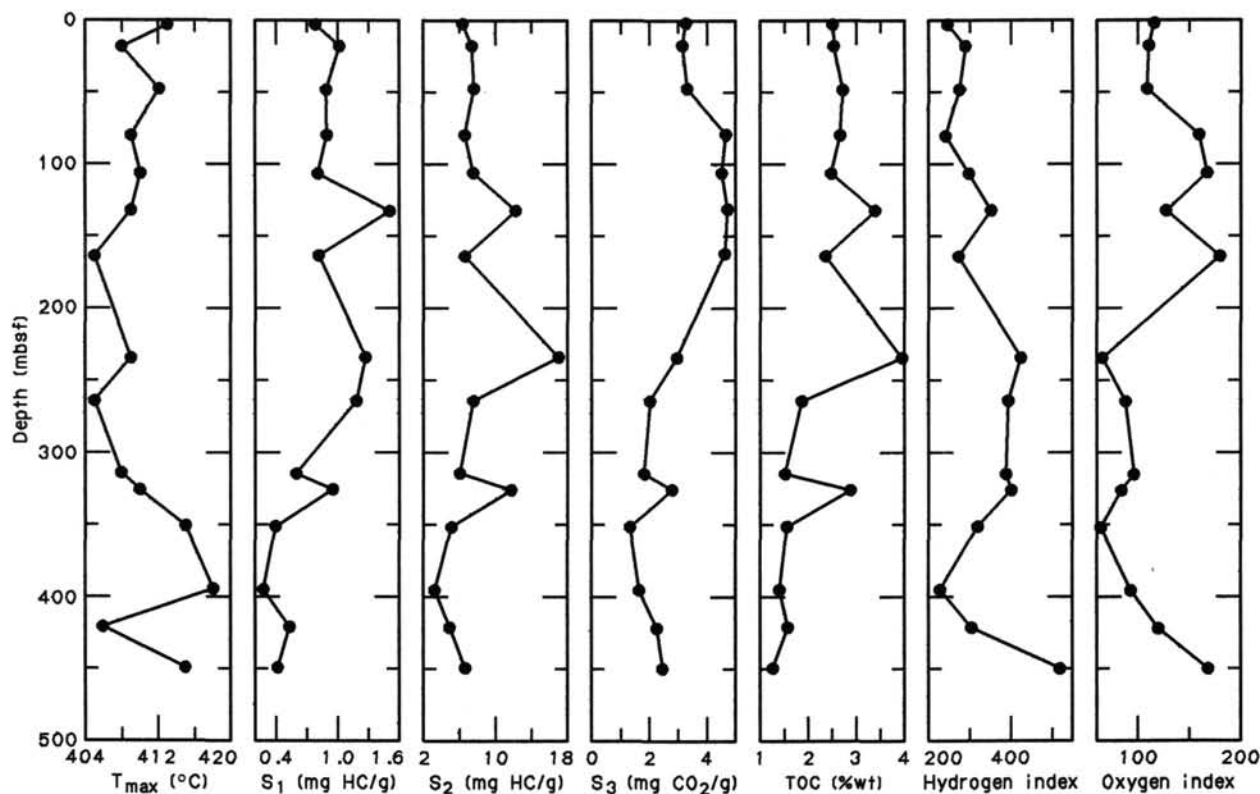


Figure 43. Comparison of Rock-Eval parameters T_{max}, S₁, S₂, S₃, TOC, HI, and OI in sediments from Hole 685A.

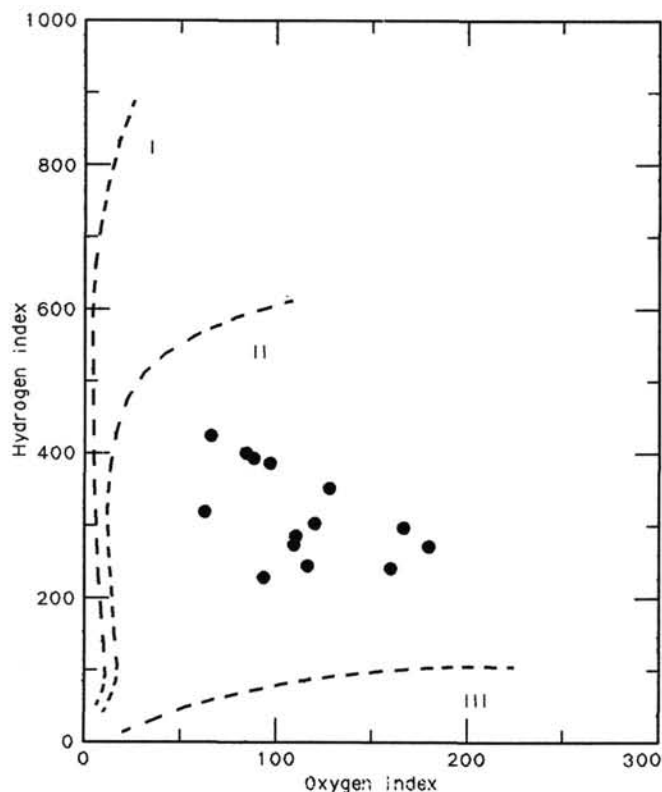


Figure 44. Hydrogen and oxygen indices (HI and OI) obtained from Rock-Eval pyrolysis of sediments from Hole 685A and plotted on a van Krevelen-type diagram (Tissot and Welte, 1984).

Alkalinity and Sulfate

Alkalinities reach extreme values at this site (Fig. 47 and Table 11). These increase rapidly and, as at Site 683, reach the maximum value at >100 m deeper than the sulfate minimum, which at this site occurs near the sediment/water interface. At 18 mbsf, sulfate is already completely exhausted. The methane concentration profile (see "Organic Geochemistry" section, this chapter) indicates that sulfate reduction is already complete in Core 112-685A-2H, which was not available for interstitial-water analyses (Fig. 48).

Calcite precipitation within the top 20 to 30 m (Fig. 51) consumes some of the alkalinity. The reduction of CO_2 to CH_4 also reduces alkalinity. Conversely, high ammonia concentrations (Fig. 49) contribute to the extremely high alkalinity zone, measured

between ~40 and almost 200 mbsf. Below the hiatus, alkalinity values decrease sharply.

Sulfate concentrations remain at 0 mmol/L from 18 mbsf to the bottom of the hole.

Ammonia and Phosphate

Ammonia concentrations are generally high and reach a maximum value of 32.32 mmol/L at 165 mbsf. At Site 683, the ammonia maximum is >10 mmol/L lower (21.45 mmol/L), and at Site 682 it reaches only about 50% (16.01 mmol/L) of the NH_4^+ maximum at Site 685. Sedimentation rates at Sites 683 and 682 were considerably lower than at Site 685.

Already at 18 mbsf, phosphate concentrations of 368.0 $\mu\text{mol/L}$ are close or equal to the maximum concentration reported previously. Concentrations reach a new record high at ~107 mbsf, about 60 m above the ammonia maximum. At greater depths, especially below the hiatus, phosphate concentrations decrease rapidly, but remain high (i.e., ~70 $\mu\text{mol/L}$ in the deepest sample analyzed). The phosphate profile above and below the depth of maximum concentration is a diffusion-production-reaction profile, above the maximum, a diffusion-production profile, and below it, a diffusion-reaction (consumption) profile. The reacting parts in both segments of the profile are controlled by biological activity (i.e., decomposition of sedimentary organic matter).

Silica

As at all other sites of Leg 112, the diatomaceous sediments control the silica concentration profiles. The low geothermal gradients typical to this tectonic setting do not promote extensive early silica diagenetic reactions.

pH

pH values decrease with depth by >1 pH unit, from pH 7.9 to ~6.6. This decrease was observed before in gas-rich sediments. During sample handling, considerable gas losses occur, which may affect the measured pH values.

Calcium and Magnesium

The general reaction scheme in a depositional environment where gas hydrates are stable was discussed extensively in the "Inorganic Geochemistry" sections of Sites 682 and 683 chapters (this volume). We thus emphasize only the few observations characteristic of this site (Figs. 51 through 53 and Table 11).

Already at 3 mbsf, the $\text{Mg}^{2+}/\text{Ca}^{2+}$ ratio of 6.02 is greater than that of seawater ratio (5.4). At 40.05 mbsf, the $\text{Mg}^{2+}/\text{Ca}^{2+}$ ratio attains a new record maximum of 16.66 for nonevaporite environments. Below the hiatus depth, the $\text{Mg}^{2+}/\text{Ca}^{2+}$ ratios promptly decrease below 5.4, and the deepest sample analyzed had a ratio of just 1.53.

Table 11. Interstitial-water geochemical data for Site 685.

Core-section interval (cm)	Depth (mbsf)	pH	Salinity (g/kg)	Cl^- (mmol/L)	Alkalinity (mmol/L)	SO_4^{2-} (mmol/L)	PO_4^{3-} ($\mu\text{mol/L}$)	NH_4^+ (mmol/L)	SiO_2 ($\mu\text{mol/L}$)	Ca^{2+} (mmol/L)	Mg^{2+} (mmol/L)	$\text{Mg}^{2+}/\text{Ca}^{2+}$
112-685A-1H-2, 145-150	3.0	7.9	34.0	548.15	15.17	21.06	92.0	1.15	919	8.56	51.56	6.02
3H-3, 145-150	18.1	7.8	35.8	555.16	71.42	0	368.0	7.40	995	4.57	60.05	13.14
6X-4, 145-150	40.1	7.2	38.2	541.86	118.52	0	409.2	16.17	1078	4.01	66.80	16.66
9X-7, 145-150	79.6	7.1	39.8	530.43	142.91	0	597.1	27.19	1069	4.42	67.43	15.26
12X-5, 145-150	106.6	7.1	40.0	540.91	155.62	0	826.2	31.52	1058	4.35	66.95	15.39
15X-4, 140-150	133.5	6.8	40.3	530.43	156.37	0	755.7	31.76	1104	5.51	68.25	12.39
18X-6, 145-150	165.1	6.6	39.8	540.91	146.61	0	526.6	32.32	1169	5.35	61.49	11.49
27X-1, 120-130	234.8	6.8	34.5	525.33	78.53	0.03	146.6	23.98	1050	6.77	40.15	5.93
30X-2, 127-137	264.9	6.6	35.0	535.91	75.91	0.06	121.7	20.17	1165	9.34	41.20	4.41
36X-6, 140-150	328.0	6.9	34.2	534.95	64.98	0	92.9	17.29	1162	11.85	37.07	3.18
44X-3, 40-50	396.0	6.6	33.5	533.98	36.76	0	94.0	11.14	1225	14.90	32.02	2.15
50X-1, 92-102	450.5	6.8	33.8	542.64	18.73	0.03	69.6	10.57	997	18.39	28.04	1.53
Gas-hydrate sample of 3.5 cm^3												
18X-8, 150	165.6	7.2	4.0	51.42	17.93							

Table 12. Comparison of interstitial-water chemical data from squeezed sediment samples with interstitial-water chemical data from *in-situ* samples contaminated with drill-hole water, Hole 685A.

Core-section interval (cm)	Depth (mbsf)	Salinity (g/kg)	Alkalinity (mmol/L)	SO ₄ ²⁻ (mmol/L)	SiO ₂ (μmol/L)	Contamination (based on SO ₄ ²⁻) (%)
112-685A-30X-2, 127-137	264.9	35.0	75.91	0.06	1165	
<i>In-situ</i> #2	290.6	35.5	63.29	4.49	1095	15.5
112-685A-36X-6, 140-150	328.0	34.2	64.98	0	1162	
<i>In-situ</i> #3	347.6	34.5	29.32	15.50	800	53.6
112-685A-44X-3, 40-50	396.0	33.5	36.76	0	1225	
Seawater (IAPSO)		~35	2.5	28.9		

Table 13. Interstitial-water geochemical data of squeezed whole-round samples vs. a 50-cm³ split core sample, Site 685.

Core-section interval (cm)	Depth (mbsf)	Type	Salinity (g/kg)	Cl ⁻ (mmol/L)	SO ₄ ²⁻ (mmol/L)	NH ₄ ⁺ (mmol/L)	SiO ₂ (μmol/L)
112-685A-44X-3, 40-50	396.0	Squeezed whole round	33.5	533.98	0	11.14	1225
^a 112-685A-48X, CC (7-11)	440.1	50 cm ³ split core	31.8	528.21	0	8.92	819
112-685A-50X-1, 92-102	450.5	Squeezed whole round	33.8	542.64	0	10.57	997

^a On the basis of Cl⁻ and salinity, percentage of contamination with freshwater ranges between 2.5 and 6.0%.

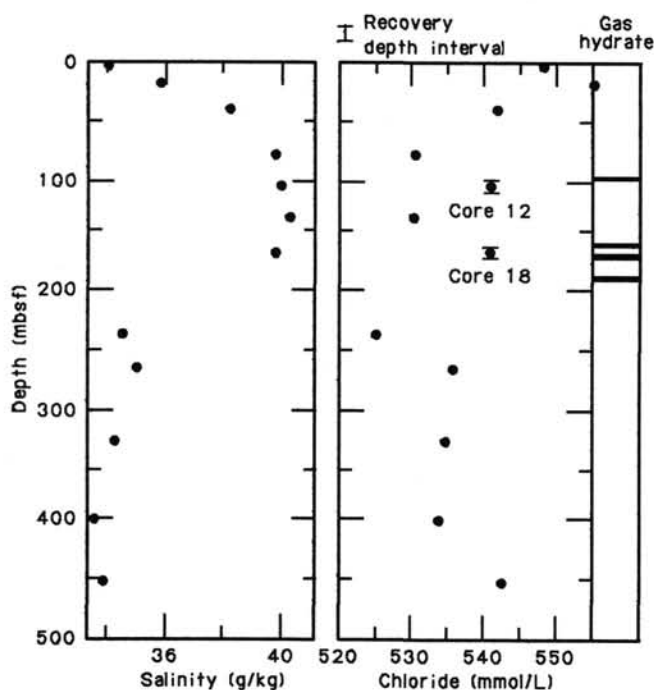


Figure 45. Interstitial salinity and chloride at Site 685.

On the basis of these observations and the profiles of Ca²⁺, Mg²⁺, and alkalinity concentration, the formation of small amounts of diagenetic carbonates, mainly calcite plus dolomite (and most likely also some ankerite, rhodochrosite, or siderite) was expected. Although forming at different times or simultaneously at different depths, these were superimposed in the sediment record. These diagenetic carbonates appear as coexisting assemblages, which may be (and has been) interpreted as paragenetic assemblages.

Figure 53 strongly supports Gieskes et al.'s suggestion (1982) that the ion exchange reaction between NH₄⁺ and Mg²⁺ may be responsible for pronounced Mg²⁺ maxima (shown in Figs. 52 and 53).

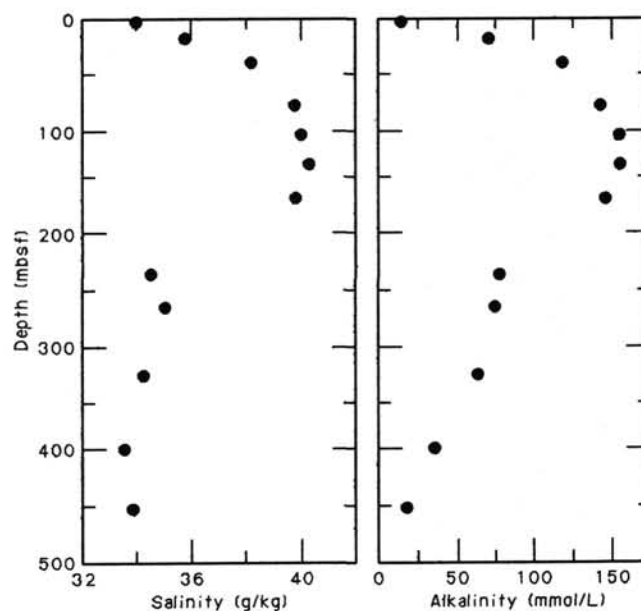


Figure 46. Interstitial salinity and alkalinity at Site 685.

Concluding Remarks

Despite extreme concentration profiles observed at this site, especially those of alkalinity, phosphate, Ca²⁺ and Mg²⁺, the amounts of diagenetic minerals, in particular of carbonates and phosphates, that form per unit volume of sediment was not large. At such high sedimentation rates and without convective flow, the system rapidly closes; the available amounts of the essential components needed for various diagenetic reactions are depleted rapidly and cannot be replenished.

Condensed sections and/or hiatuses represent time intervals of great importance for diagenesis, particularly in rapidly accumulating sediments. During these time intervals, a previously closed system is reopened and becomes recharged by diffusion from seawater; a new generation of diagenetic products will be superimposed on the earlier ones.

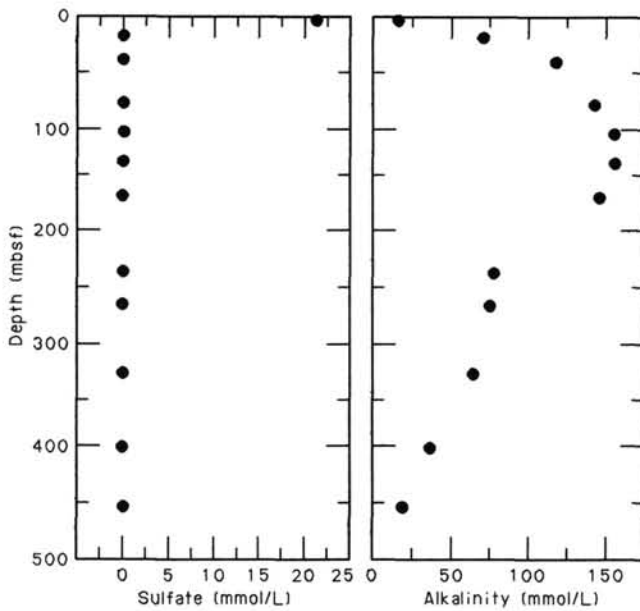


Figure 47. Interstitial sulfate and alkalinity at Site 685.

PALEOMAGNETISM

Introduction

The first 14 cores retrieved had a strong magnetic signal that was easy to measure with the shipboard spinner magnetometer. The directions isolated appeared to be stable, and the inclination value was consistent throughout all 14 cores. However, not

all samples were characterized by a single direction of magnetization (as defined by vector plots). We abandoned the sampling of Hole 685A for two reasons: (1) the sediments collected from lower cores were characterized by weak magnetic moments (<0.05 mA/m) and (2) the presence of dipping strata in Cores 112-685A-4H, 112-685A-9X, and lower. Not knowing the true geographic strike and dips of these zones meant that we could not make structural corrections on these samples.

Results

Figure 54 shows the declination, inclination, and intensity values vs. depth below seafloor for the samples measured. The value selected and reported in the plots is the 150-Oe demagnetization value. At this level of demagnetization, each sample was characterized by a low value for the circular standard deviation. A study of the inclinations collected shows that the entire measured section of the hole was characterized by normal polarities. These data suggest that the entire measured section was deposited during the Brunhes Chron. However, an examination of the declination values in Figure 54 suggests that many of the samples show anomalous declinations that may be related to the dipping strata observed in this hole. This statement is supported by the widely scattered declination values observed from samples within an individual core.

With one exception, which will be discussed next, the samples collected from Hole 685A were all normal (negative inclination in the Southern Hemisphere) down to 122.5 mbsf. The Brunhes/Matuyama boundary was not located. Similar to the results reported from Sites 680 and 683, a cyclicity of intensity of magnetization vs. depth was observed. Five distinct maxima and associated minima were noted. If these data were similar to data from Site 683A and if the sedimentation rate below 122 m was similar to the sedimentation rate observed in the upper 122 m,

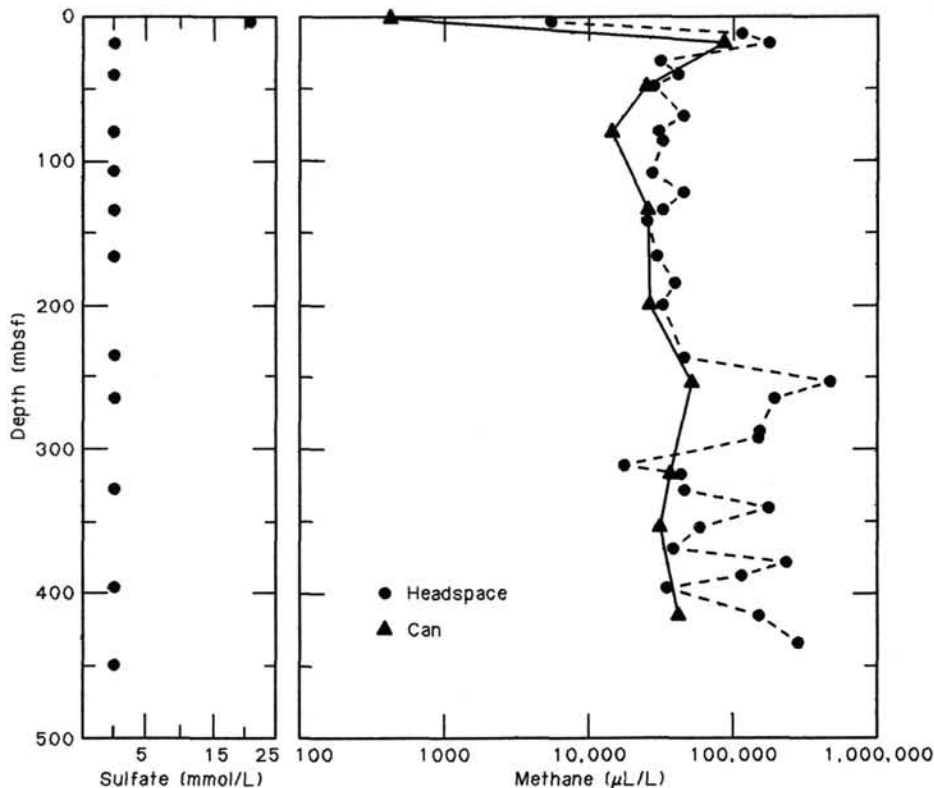


Figure 48. Interstitial sulfate and extracted methane for Site 685. Extracted methane from "Organic Geochemistry" section, this chapter and Figure 41.

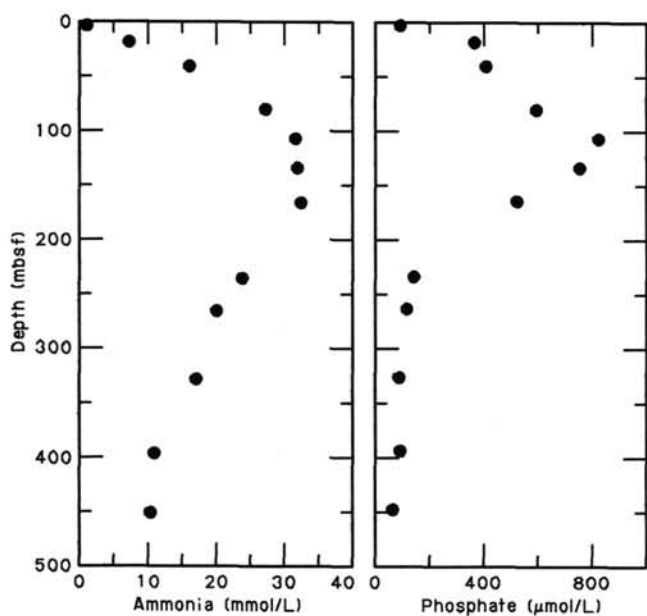


Figure 49. Interstitial phosphate and ammonia at Site 685.

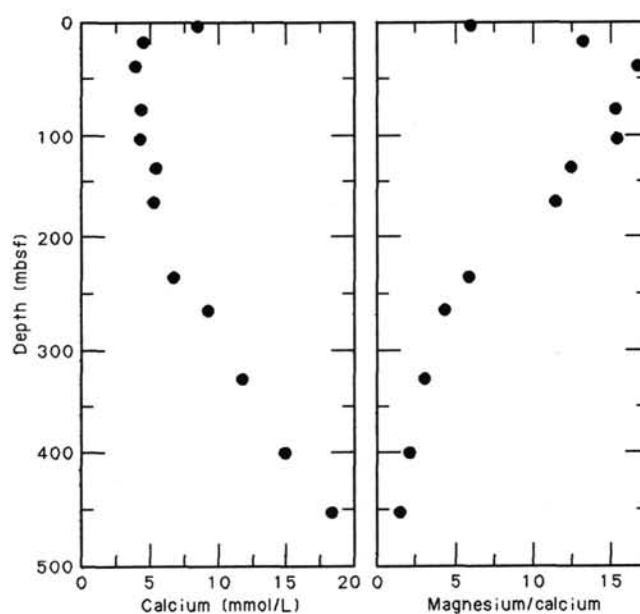
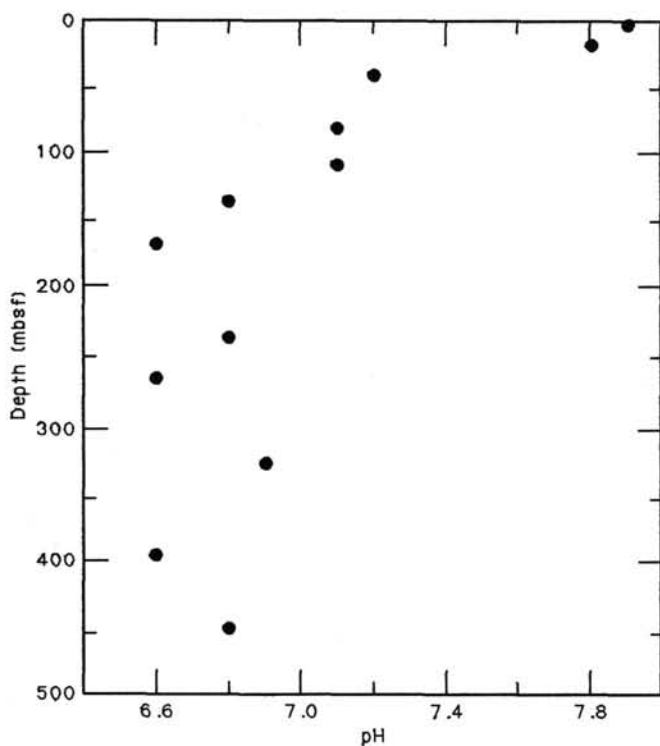
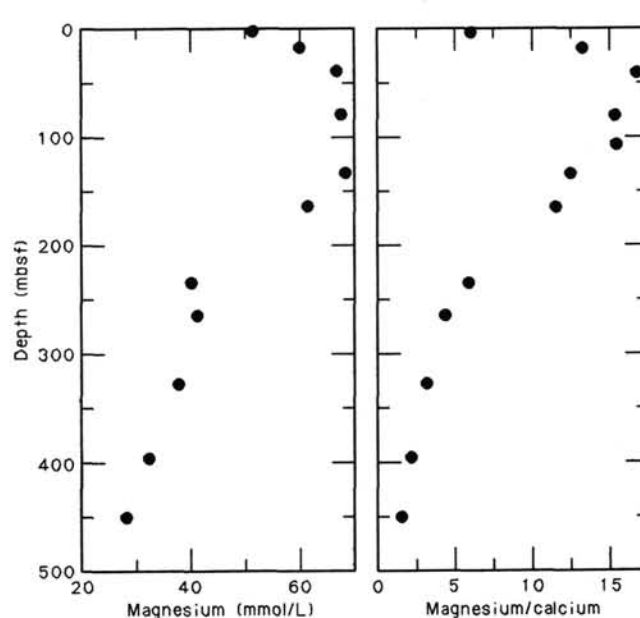
Figure 51. Interstitial calcium and Mg^{2+}/Ca^{2+} ratios at Site 685.

Figure 50. Interstitial pH at Site 685.

these five maxima would suggest that the Brunhes/Matuyama boundary occurred within the next few cores (Cores 112-685A-15X or 112-685A-16X). One exception to the normal polarity in Site 685A was noted from one section of Core 112-685A-4H. Until we can better examine this core at land-based laboratories, we cannot say if this anomalous result is related to a reversed event (Blake event?) or caused by a misorientation of this sample during collection.

Figure 52. Interstitial magnesium and Mg^{2+}/Ca^{2+} ratios at Site 685.

Orientation of Cores

When inclined bedding or structural fabric elements are encountered in a core, their *in-situ* orientation is always of interest, and it is often possible to obtain orientation information of reasonable quality from paleomagnetic data. This was done on previous legs with reasonable results. During Leg 108, results obtained using a multishot tool were compared with those obtained from the paleomagnetic data. Agreement between the two was generally excellent, except in instances where the cores had been strongly remagnetized during coring or handling (Rudiman, Sarnthein, et al., 1988). This kind of disturbance will be

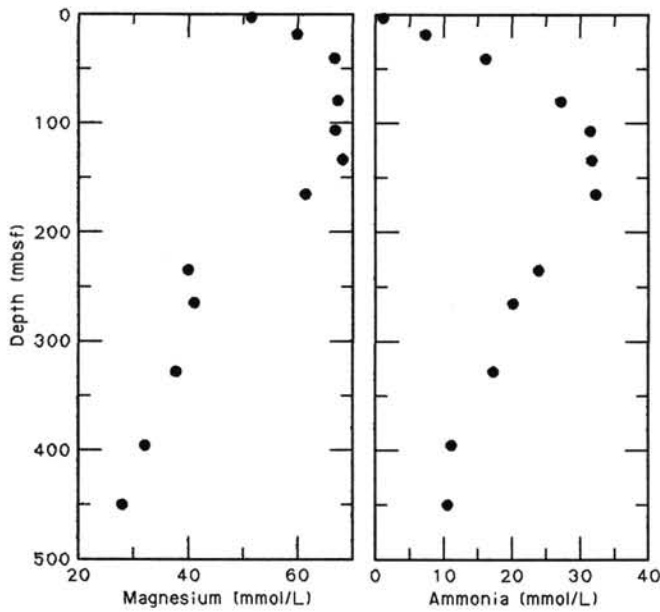


Figure 53. Interstitial magnesium and ammonia at Site 685.

indicated by its presence in either the measured declinations and inclinations or in the measured intensity values.

Orienting cores based on paleomagnetic data is fairly straightforward where the core is relatively undisturbed by drilling and the structure present is simple. The data needed for this orienta-

tion consisted of the declinations relative to the core liner (Fig. 55) and of inclinations obtained from measurements on discrete samples or on the whole core. Our procedures were as follows:

1. An average apparent declination, relative to the standard ODP core-liner orientation (Fig. 55), was calculated for a coherent segment of core.
2. The polarity of the magnetization, normal or reversed, was determined from the inclinations. The true declination should be 0° for normally magnetized cores or 180° for cores with a reverse magnetization, assuming that for cores of the Brunhes Chron no significant tectonic event, i.e., rotations and slumps, has occurred.
3. The core and any structures of interest that it featured were then properly oriented when their orientation was given with respect to the direction indicated by the inclination.

The orientation obtained is probably good to $\pm 15^\circ$ when care is taken in splitting and handling the cores, where cores are reasonably coherent, and where any structures present are fairly simple. The first two factors also apply to cores oriented with the multishot tool. However, as noted at Site 683, significant declination anomalies (up to 45°) can occur within a single core. This may result from rotation of the core parts or the entire core within the core barrel. If such anomalous declinations are noted, this procedure should not be attempted.

Site 685

The paleomagnetic data obtained from APC cores of Hole 685A are shown in Figure 56. The declinations obtained (rela-

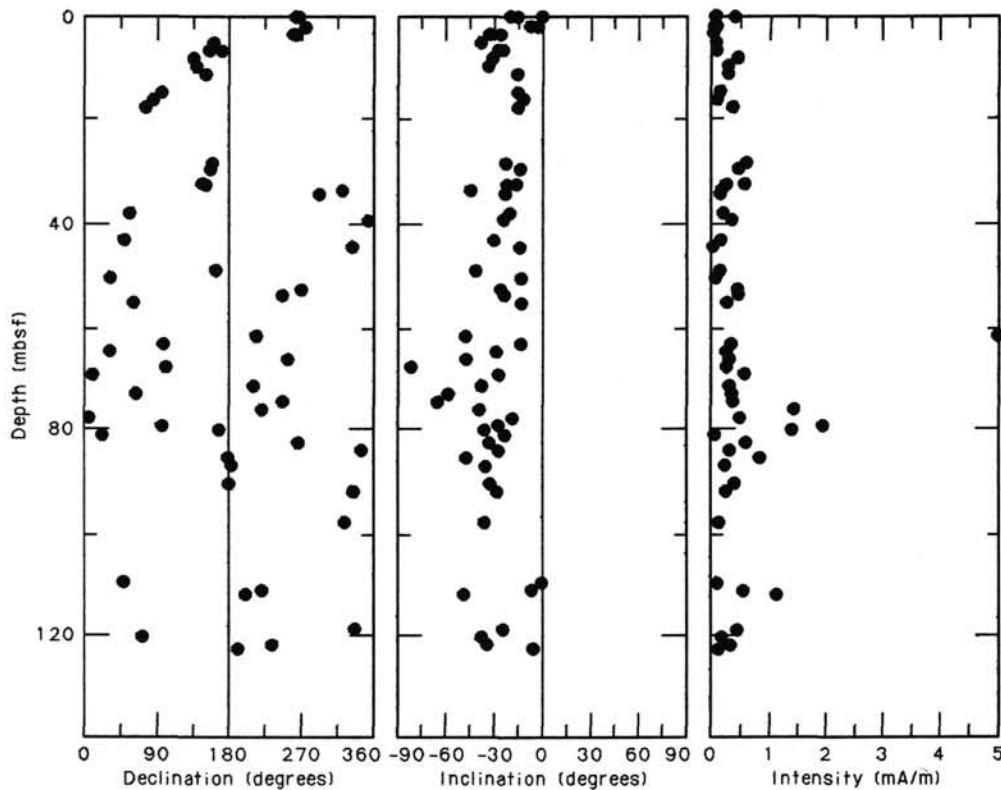


Figure 54. Declination, inclination, and magnetic-intensity plots vs. depth below seafloor of Site 685A. The entire measured section of core appears to represent the Brunhes Chron. A small possible magnetic reversed event is seen at 22 mbsf. Five distinct maxima are noted in the plot of intensities vs. depth.

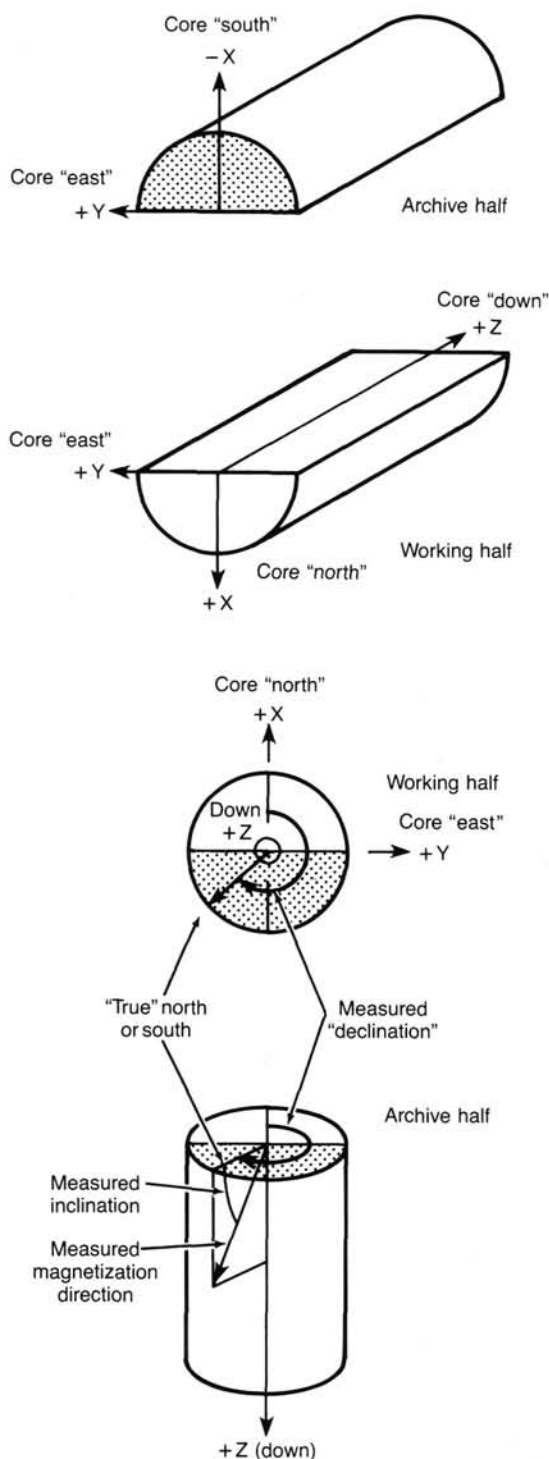


Figure 55. Standard ODP core orientation is shown, along with a magnetization direction. The declination of the magnetization gives the actual orientation of the core; the inclination determines whether the magnetization is normal or reversed.

tive to core north) are reasonably consistent in individual cores. Except for a measurement in Section 112-685A-3 (the sample having the lowest intensity of magnetization of those shown), declination values fall within 15° of the average value for the respective core. Interestingly, the bedding in Section 112-685A- H-

4 is inclined at 20° to the core-east, striking roughly core-north (Fig. 55). The average declination for this section is 155° . The simple interpretation of this is that the beds actually strike roughly 205° , dipping to the west-northwest or roughly seaward (Fig. 57). This feature was discussed further in the "Lithostratigraphy" section (this chapter).

The above interpretation assumes that magnetization was acquired diagenetically and after the beds were tilted. The interpretation would not change greatly if one were to assume that the magnetization was original. Figure 57 also shows where the magnetizations would fall if a structural correction were applied: roughly around 163° and with a slightly increased inclination. This would give the beds a strike of 197° , not significantly different from 205° . The expected inclination for this site was 18° , closer to the uncorrected inclinations but certainly not ruling out the corrected values. In this instance, we could not distinguish between the two possibilities without further study.

PHYSICAL PROPERTIES

Physical-properties measurements at Site 685 were performed on split cores, generally at an interval of one every two sections (3 m) in good quality APC cores and, where quality of recovery permitted, in XCB cores. In the bottom 200 m of Hole 685A, the sediment recovered was heavily fractured. Subsequent disturbance imposed by drilling and splitting the cores caused these fractured sediments to break up. The resulting mixture of drilling slurry, water from the saw, and chunks of sediment were unsuitable for physical-properties measurements. However, the core-catcher samples were in much better condition, probably because they were drilled last and experienced the least amount of drilling disturbance. Therefore, much of the data from this interval was obtained from intact biscuits of sediment in the core-catcher samples. Data presented here include index properties, compressional-wave velocity, undrained vane shear strength, and thermal conductivity.

Use of Core-Catcher Samples

During sampling at Site 685, we were concerned that the sediment in the core catcher was not representative of the material being cored. The cores consisted of a mixture of hard chunks of sediment, drill-hole water, and water from the saw used in splitting the cores. It would have been impossible to obtain meaningful index-property data from this material. The biscuits of sediment in the core catcher appeared to be the most intact material available.

A sample of the sediment from the split core-catcher sample of Core 112-685A-48X was obtained for interstitial-water analyses. The results showed no seawater contamination, indicating that the biscuits of sediment were intact and were not contaminated by drill-hole water. Thus, we assumed that the core-catcher samples represented the true state of the sediment.

However, interstitial-water analysis did indicate approximately 2.5% to 6.0% contamination by freshwater from splitting with the saw (see Table 13, "Inorganic Geochemistry" section, this chapter). Therefore, we scraped off approximately 0.5 cm of the split core surface before obtaining an index-properties sample. Thus, we thought that contamination would be lower and would only be significant when the amplitude of the variations was low.

Index Properties

The index properties measured at Site 685 include water content (presented as a percentage of dry sample weight), porosity, bulk density, and grain density (Table 14). The methods specified in "Explanatory Notes" (this volume) were used to measure

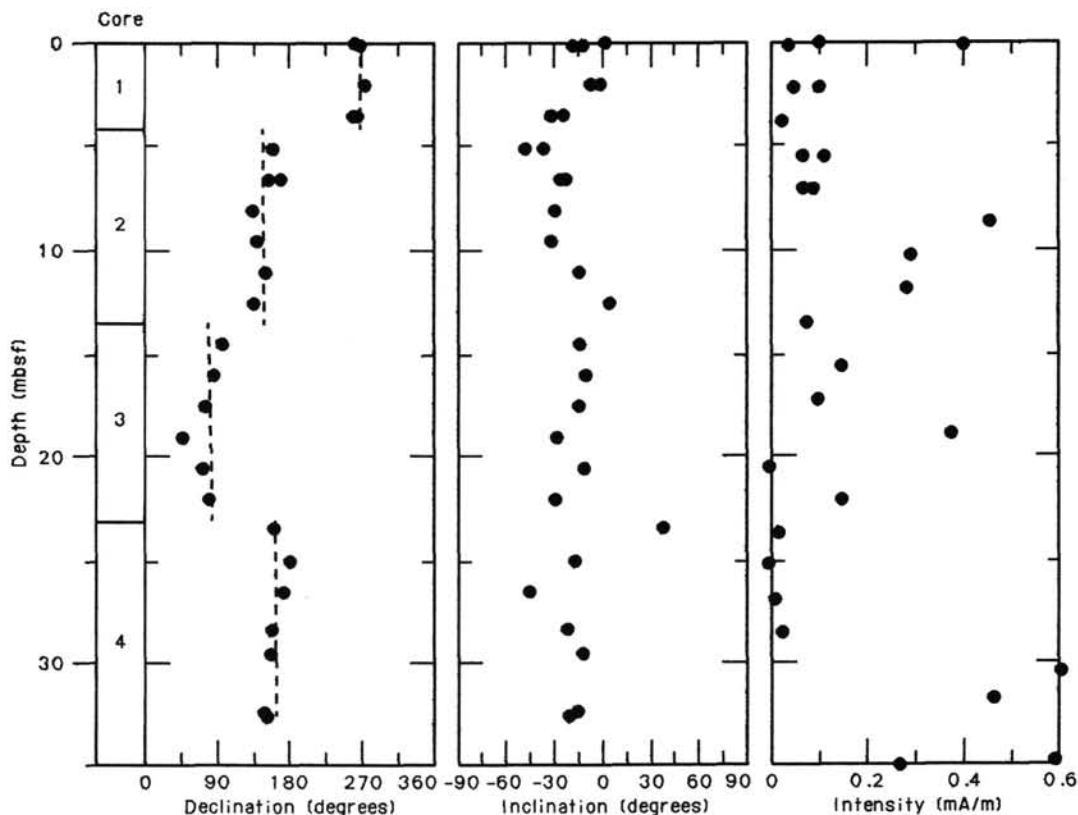


Figure 56. Magnetic declination, inclination, and intensity for APC cores from Hole 685A. Declinations within individual cores are within $\pm 15^\circ$ of average values, indicating that little relative rotation of the core occurred during coring.

the index properties at Site 685. In our calculations we assumed that the salinity of the pore water was 35‰.

Figure 58 illustrates the downhole trends in water content and porosity with depth and the lithology for this site. Figure 59 shows the bulk-density data obtained from samples of the split cores and from the GRAPE profiles. The chart on the left of Figure 59 shows data obtained from the samples, while the chart on the right shows the GRAPE data (small dots), with the data from the samples superimposed as the larger open circles. All APC core sections were run through the GRAPE. Index-properties sample data show generally good correlation with the GRAPE profile. In most cases, the XCB cores were too disturbed to provide meaningful GRAPE data; however, we did run the core-catcher samples through the GRAPE. As a result of the drilling slurry and sample disturbance, GRAPE bulk densities are consistently lower than the bulk densities of samples from XCB cores.

In general, the water contents and porosities decrease linearly with depth through the upper 400 m at Site 685. The water contents are at a maximum of 135% near the mud line and a minimum of 38% at 412 mbsf, and the porosities range from 79% near the mud line to a minimum of 51% at 412 mbsf. The bulk densities at this site generally increase fairly linearly, with a minimum of 1.40 g/cm^3 near the mud line and a maximum of 1.93 g/cm^3 at 393 mbsf.

There is some moderate fluctuation in the index-properties profiles (Fig. 60) caused by the moderately variable lithology. However, the range of these fluctuations is not as significant as it has been in previous holes. Poor recovery at the Subunit IB/Unit II boundary impeded index-properties sampling at this level, but apparently no significant change occurred in the profiles across this boundary (Fig. 58).

The sediment consists of 10% authigenic carbonate below 410 mbsf, but despite cementation, we noted a decrease in the water content to 51% and in the porosity to 59%–60%. The sparse water-content and porosity measurements below this depth remain constant at these values. The bulk-density values decrease to 1.8 g/cm^3 at the same depth, and the few measurements obtained below this depth gave the same values.

Compressional-Wave Velocity

The *P*-wave logger, which is run in conjunction with the GRAPE, was used to measure velocities through the sediments in the APC cores before the cores were split. Velocity data from the *P*-wave logger were reduced manually by selecting reasonable values of velocity from the shipboard printouts. However, few data were obtained. The cores were very gassy, which may be the cause of the poor data. Reliable velocity profiles were obtained for the first few cores only. The velocities ranged between 1490 and 1530 m/s; these values were probably low because of the high water content of the sediments.

We tried several times to take Hamilton Frame samples. However, we found it difficult to obtain samples of sufficient quality to give a clear signal. Fractures in the sediment made it impossible to cut parallel faces needed by the frame. One sample having a velocity of 1.8 m/s was obtained at approximately 412 mbsf. This sample was one of the harder, unfractured chunks of sediment that had remained reasonably intact during drilling and splitting, and thus provided an indication of the velocity through the deeper sediments at this site.

Vane Shear Strength

The undrained vane shear strength measurements for Site 685 were performed with the Wykham Farrance vane apparatus.

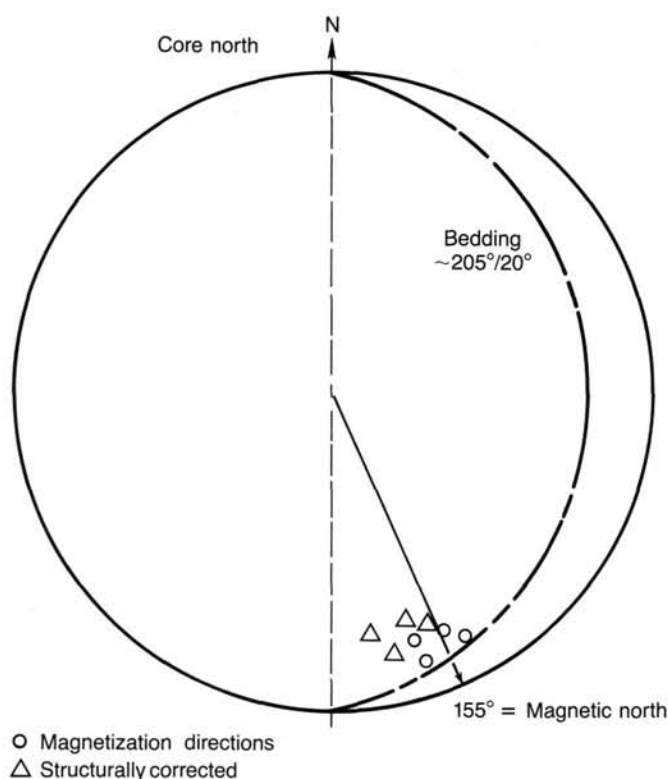


Figure 57. Stereo projection showing the directions of magnetization for samples from Core 112-685A-4H, with and without structural corrections, and the orientation of the bedding plane in this core. The bedding plane strikes roughly 205°.

The XCB cores were either of insufficient quality or too hard for measuring vane shear strength. Thus, measurements were obtained only in lithologic Subunit IA. Values obtained for peak undrained shear strength are presented in Table 15 and are shown vs. depth below seafloor in Figure 61.

The vane shear strengths at Site 685 range from 20 to 40 kPa near the mud line and then increase over several cycles to values around 100 kPa at approximately 80 mbsf. The high peaks in the vane-shear-strength profile correspond to low water-content values, and the low shear strengths correspond to high water-content values. These variations probably result from subtle lithology changes.

Total overburden stress was calculated using bulk-density determinations and assuming hydrostatic pore-pressure conditions. Profiles of total stress and assumed hydrostatic conditions are shown vs. depth below seafloor in Figure 62. Changes in the slope of the total-stress curve occur at approximately 100 and 220 mbsf. The change at 100 mbsf is caused by the slight increase in bulk density that occurs at this depth. The change at 220 mbsf is the result of the change in the slope of the bulk-density profile that occurs across the boundary between lithologic Subunit IB and Unit II. This depth is slightly lower than the actual boundary depth because the first sample obtained for Unit II was at 232 mbsf.

The ratio of peak undrained vane shear strength to effective overburden pressure (C_u/P') is plotted vs. depth below seafloor in Figure 63. Theoretically, the ratio of C_u/P' should be very high near the mud line and should decrease quickly to a constant value with depth. C_u/P' obtained from data at Site 685 never deviates significantly from the theoretical profile. The deviation at only one location (i.e., at 12 mbsf) is caused by the low vane shear strength combined with the relatively high bulk density at this depth.

Thermal Conductivity

Thermal conductivity was measured by the needle-probe method. Measurements were performed on whole-round samples to Core 112-685A-7X by inserting the probes perpendicular to the core axis. After Core 112-685A-8X, split samples were used, and probes were inserted from the ends of the sections parallel to the core axis. There were many voids and cracks in the samples caused by expansion of gas present in the sediment. Testing points were selected so as to avoid the cracks as much as possible, but most likely the values obtained from samples in Cores 112-685A-10X and 112-685A-11X were affected by gas cracks. No continuous undisturbed intervals for measurements were found after Core 112-685A-11X. Although we attempted to measure Cores 112-685A-18X, 112-685A-20X, and 112-685A-37X, the results are questionable.

The values obtained are presented in Table 16 and Figure 64. The thermal conductivity is 0.85 to 1.0 W/m·K between the seafloor and 30 mbsf, while most of the values below 30 mbsf are 0.8 to 0.9 W/m·K. The water content decreases slightly with depth in the same depth range, and no significant change in lithology occurs at 30 mbsf. Therefore, we found it difficult to explain the decreased thermal conductivity as results of changes in the water content and/or the grain thermal conductivity. One possible cause may be that the samples below 30 mbsf were somewhat disturbed by drilling or gas expansion. A slight decrease in the GRAPE bulk density at about the same depth might support this inference.

Summary and Discussion

The water contents at Site 685 decreased fairly linearly from values of 134% near the mud line to values of 38% at 412 mbsf. In the top 200 m of the water-content profile, varied lithology results in fluctuating values, but these fluctuations were not as significant as those that occurred at other sites. We did not expect coherent cyclicity at this site because of the rapid, hemipelagic sedimentation, which was not as greatly affected by sea-level changes as at other sites. The porosities at this site decrease fairly linearly from near 80% at the mud line to 51% at 412 mbsf. The bulk densities show slightly more variation with depth than do the other index properties. The bulk densities in lithologic Subunits IA and IB show some slight variability, but generally these densities increase slightly with depth throughout these units. A slight increase occurs in the slope of the profile across the Subunit IB/Unit II boundary (at 203 mbsf) to a depth of 393 mbsf.

An increase in water contents to 48% was noted at 412 mbsf, while the values remain constant in the range of 52% for the last three samples of the hole to a depth of 440 mbsf. These sediments are more intensely fractured than those above (see "Lithostratigraphy" section, this chapter), and the constant values may indicate fluid movement through the fractures that equilibrate the water contents with depth. The porosity profile also indicates a slight change in behavior at this depth, with an increase to 57%–60% for the bottom 30 m of the hole. Below 400 mbsf, the bulk densities appear to decrease slightly with increasing depth. This decrease would indicate that the increase in carbonate content may not be the cause of the change in index properties, as bulk density should increase with an increase in carbonate content. This may provide further evidence for a process such as fluid movement at this depth.

Perhaps the most significant characteristic of the physical-properties data gathered thus far for Site 685 is their minimal correlation with major lithological boundaries. The trend in index properties and vane shear strength indicates a normally consolidating sequence, with water contents and porosities decreasing and bulk densities and shear strengths increasing with increasing depth. Although the slope of the index-property profiles

Table 14. Summary of index properties at Site 685.

Core/section interval (cm)	Depth (mbsf)	Water content (% dry wt)	Porosity (%)	Bulk density (g/cm ³)	Grain density (g/cm ³)
112-685A-1H-1, 103	1.03	133.97	78.38	1.40	2.39
1H-2, 52	2.02	134.12	78.45	1.40	2.48
1H-3, 66	3.66	135.26	79.38	1.41	2.60
2H-2, 96	6.56	92.17	73.68	1.57	2.60
2H-4, 51	9.11	130.08	78.46	1.42	2.61
2H-6, 42	12.02	95.33	73.69	1.55	2.71
3H-1, 73	14.33	88.76	71.58	1.56	2.48
3H-3, 73	17.33	107.22	75.81	1.50	2.48
3H-5, 53	20.13	115.68	78.36	1.50	2.50
4H-2, 80	25.40	99.93	75.44	1.55	2.47
4H-4, 35	27.95	102.84	75.64	1.53	2.58
4H-6, 118	31.78	103.65	76.71	1.54	2.63
5X-2, 80	34.90	97.82	75.51	1.56	2.56
5X-3, 71	36.31	99.71	76.16	1.56	2.59
5X-5, 69	39.29	93.20	73.97	1.57	2.50
6X-2, 109	44.69	116.93	77.22	1.47	2.47
6X-4, 38	46.98	91.98	73.16	1.56	2.50
6X-6, 96	50.56	84.42	68.70	1.54	2.35
7X-2, 18	53.28	99.56	73.00	1.50	2.42
7X-3, 65	55.25	102.09	74.12	1.50	2.45
8X-2, 94	63.54	86.63	71.05	1.57	2.54
8X-3, 121	65.31	93.28	71.82	1.52	2.46
8X-5, 120	68.30	107.21	75.27	1.49	2.51
9X-2, 118	72.15	95.15	73.01	1.53	2.38
9X-4, 58	74.55	93.93	73.10	1.55	2.51
9X-7, 89	79.36	96.62	72.22	1.51	2.44
10X-2, 63	82.23	79.89	71.05	1.64	2.65
10X-3, 56	83.66	88.67	72.65	1.58	2.64
10X-5, 141	87.51	97.71	72.74	1.51	2.26
11X-1, 110	90.70	104.15	75.43	1.51	2.51
11X-2, 96	92.06	107.21	75.33	1.49	2.38
11X-6, 54	97.64	95.78	73.58	1.54	2.50
12X-5, 45	105.55	93.55	72.46	1.54	2.48
13X-2, 112	111.22	80.85	73.60	1.69	2.53
14X-3, 46	121.56	73.55	68.43	1.65	2.49
15X-3, 114	130.54	96.37	75.11	1.57	2.35
16X-2, 13	138.73	103.13	74.97	1.51	2.38
16X-3, 87	140.97	97.54	75.96	1.58	2.38
18X-7, 35	164.12	75.27	67.82	1.62	2.50
20X-4, 111	180.43	90.58	71.58	1.54	2.36
25X, CC (12)	232.12	70.16	64.48	1.60	2.36
27X, CC (10)	243.10	57.93	62.97	1.76	2.48
30X, CC (12)	271.60	53.72	59.15	1.73	2.41
31X, CC (16)	281.10	45.32	54.65	1.80	2.35
32X, CC (6)	290.60	51.64	59.73	1.80	2.47
33X, CC (6)	300.10	68.76	64.96	1.63	2.32
34X, CC (10)	309.62	43.84	55.38	1.86	2.61
35X, CC (29)	319.10	62.88	63.22	1.68	2.37
37X, CC (6)	338.10	53.54	59.88	1.76	2.57
40X-1, 15	357.25	55.75	61.69	1.77	2.51
42X, CC (9)	385.60	43.11	53.97	1.84	2.49
44X-1, 37	392.97	39.98	53.85	1.93	2.60
45X, CC (24)	411.60	38.00	51.09	1.90	2.45
46X-1, 75	412.35	47.77	56.82	1.80	2.43
46X, CC (12)	421.10	51.20	58.71	1.78	2.56
47X, CC (9)	430.60	51.64	60.34	1.82	2.52
48X, CC (14)	440.10	51.22	59.59	1.80	2.40

presented remains essentially the same throughout the hole, there is a noticeable shift in water content and porosity below the lithologic boundary. The lower values in Unit II support the evidence for a hiatus at this boundary.

GEOPHYSICS

Seismic Records

Site 685, located on the lower slope of the Peru Continental Margin, is one of two sites that straddle the transition from continental crust to the accretionary complex. This transition occurs beneath the mid-slope terrace, and Site 685 is seaward on the lower slope in the area of accreted sediment. The accretionary complex was imaged best on seismic record CDP-2. These data were recorded in 1973 by Seiscom-Delta under exclusive

contract to the Nazca Plate Project using a DFS-3 system having a nontapered rectangular array of two 300-in.³ and two 1000-in.³ air guns with wave-shaped kits. The returning signal was detected on a 1600-m hydrophone streamer having 24 groups. The processing performed for the Nazca Plate Project was also conducted in 1973 with a 1200% CDP stack but no migration. The data were first reprocessed in 1984 at the U.S. Geological Survey DISCO facility in Denver (von Huene et al., 1985) and were reprocessed again for Leg 112 drilling to improve imaging where some significant structures were unclear (Kulm et al., 1986). Both reprocessing efforts included migration before stacking of all 24 channels and were applied in a manner developed for deep-water data (Miller and von Huene, 1986).

Additional cross-lines were shot from the French research vessel, *Jean Charcot*, to satisfy the requirements of the Safety

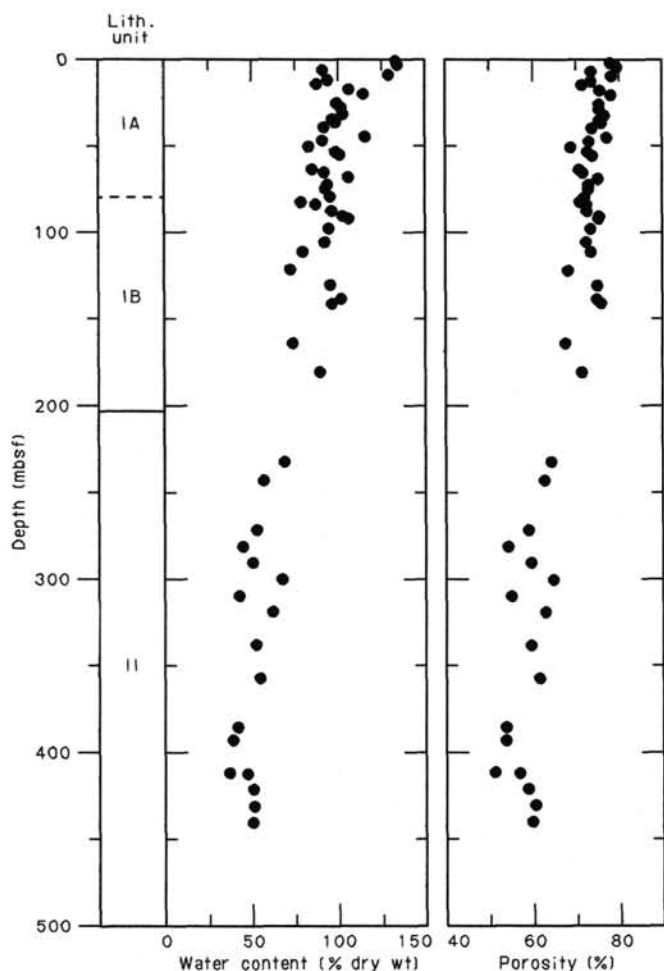


Figure 58. Water content and porosity profiles for Site 685. Schematic of lithologic units is also shown.

Panel for approval of a JOIDES drill site. These lines were recorded using a "portable" U.S. Geological Survey DFS-5 system, a single 540-in.³ air gun, and a 1200-m 24-channel streamer. The limited volume of air required 50-m shot-point intervals, and thus the data could only be stacked at 1200%. The first processing included post-stacking migration. Because there was only one week for processing between the end of the cruise and the Safety Panel meeting, not much was possible to enhance the quality of the records. Further processing of these data is planned as a post-cruise project.

After drilling, a downhole acoustic velocity log was obtained from 70 m to a depth of 270 m, where the hole had bridged. These data are combined with the generalized velocity function developed previously (see "Geophysics" section, Site 683 chapter) to correlate the seismic reflections with the lithologies recovered (Fig. 65).

An interpretation of CDP-2 performed by von Huene et al. (1985) was refined by Kulm et al. (1986) on the basis of this reprocessing. The line-drawing interpretation of the depth section shows a classical accretionary structure at the front of the margin (Fig. 66). The first three thrust packets landward of the trench axis are clearly delineated. Farther landward, as the structure becomes more complex and covered by slope deposits, the accretion complex is more difficult to interpret. The seismic imaging is obscured by out-of-plane features that do not respond well to the processing algorithms, which only collapse

ideal diffractions. Despite the loss of clearly defined thrust packets progressively landward, the general landward-dipping fabric of the lower slope is not lost.

Site 685 was selected for sampling landward-dipping reflections that are not deeply buried by slope deposits. CDP-2 passes across the side of a small knoll on the lower slope, and the corresponding seismic reflections indicated the nose of a fold at the forward part of a thrust packet (Fig. 67). No indication of an adjacent scarp from slumping upslope occurs, based on studies of detailed Seabeam data, and thus the knoll is not a slump block. The slope cover appears no thicker than 0.25 s (about 220 m), which is about half of the intercept time displayed clearly elsewhere. The seismic cross-lines indicate a general slope cover in the area of from 0.5 to 0.8 s thick (about 420–800 mbsf). Drilling through slope deposits of this thickness would not only have required added time to achieve target depth, but also placed the top of the accreted material near the depth of the base of gas hydrate and thus risked abandonment of the hole because of excessive hydrate.

About 3 km upslope lies another series of landward-dipping reflections that are not deeply buried by slope material. A proposed site was located to sample this reflective series but could not be drilled with Site 685 because of insufficient time. Our reasons for not choosing to drill here involved the continuation of the reflections across most of the record to the base of the accretionary complex (Fig. 67), which differs from the generally shorter reflective sequences of the accretion complex. Because of their continuity across the upper plate, these reflections may be part of the bounding structure between continental-crust and accreted sediments. Therefore, drilling here might have involved a more complex geology because of conditions across a major thrust boundary. The distinction between continental and accreted sediments on a lithologic basis was difficult because of the high rates of Neogene sedimentation that not only flooded the slope but also dumped sediment into the trench only to be accreted a short time later. The distinctive oceanic lithologies such as pelagic clays or igneous crust are subducted (Fig. 67).

The major lithological boundary at Site 685 is the division between the slope deposits above and the accreted thrust packet below. At 200 m, this contact was partially hidden in the lowest reverberation of the outgoing signal at the seafloor. Thus, it was difficult to detect the deformation of the slope deposits as observed in the cores. However, some adjacent areas of thicker slope deposits revealed irregular short reflections, suggesting tectonic deformation of the slope material. The landward-dipping beds appear as relatively coherent reflections in the upper part of the section penetrated but are more irregular or broken in the lower part. The irregularity is accompanied by higher-amplitude reflections that may be related to changes in velocity as the carbonate content of the mudstones varies. Variations in carbonate at corresponding depths were noted in the cored lithology (see "Lithostratigraphy" section, this chapter).

The geophysical data at Site 685 illustrate a typical expression of an accretionary complex in a well-processed seismic record. The site is located only 3 km seaward of the suspected boundary between the continental crust and the accretionary prism. Thus, at Site 685 we should have been able to sample some of the oldest accreted sediment. The lithologies drilled are consistent with the seismic character observed beneath the site on seismic record CDP-2, as are the boundaries between the slope material and the underlying thrust packet.

Heat Flow

Temperature Measurements Using the APC Tool

At Site 685, APC coring was possible only to Core 112-685A-4H because of very stiff sediment. As a result, we did not

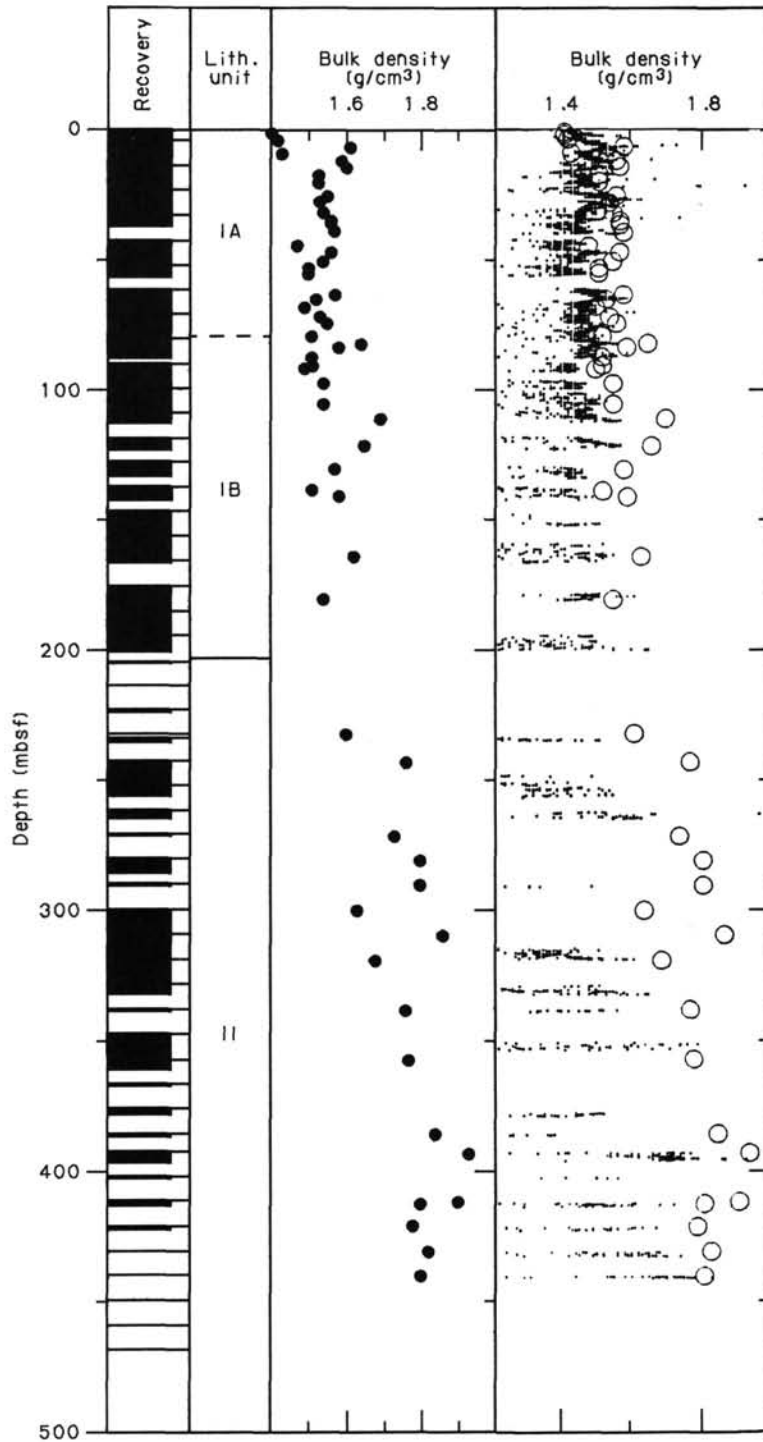


Figure 59. Sample bulk-density measurements and GRAPE bulk-density profile for Site 685. The chart on the left shows the data from the index-property samples, while the chart on the right shows the GRAPE data (small dots) and the data from the samples (larger open circles). Schematics of recovery and lithologic units are also shown.

try to measure temperatures during APC coring. The APC tool was deployed four times with the pore-water sampler (after Cores 112-685A-13X, 112-685A-19X, 112-685A-32X, and 112-685A-38X). On the second run, the instrument produced no temperature record. From the temperature records on the other runs, the lower limits of the true formation temperatures were determined to be 2.6, 5.6, and 4.7°C at 118.1, 290.6, and 347.6 mbsf, respectively.

Formation Temperature From Logging

Two logging temperatures were taken in Hole 685A. The values are presented in Figure 68 (as crosses and dots). Note the following observations:

1. First logged temperature curve: a) useful data start at about 68 mbsf; b) temperatures have a gradient of $16.6 \cdot 10^{-3} \text{ K/m}$ between 75 and 180 mbsf; below 180 mbsf, temperature val-

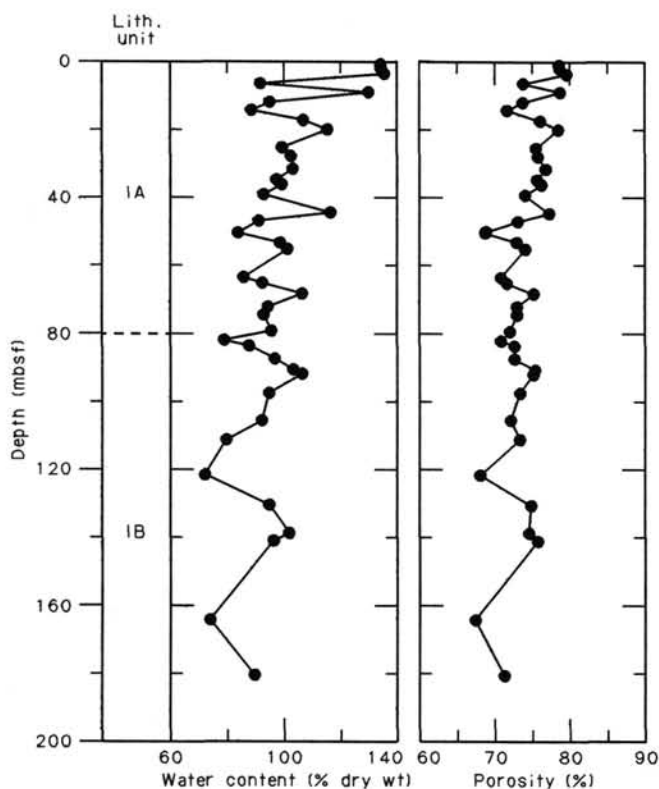


Figure 60. Expanded profile of water content and porosity for the upper 200 m of Site 685, showing slight cyclic variation with depth below sea-floor.

ues depart significantly from this gradient; and c) the thermal gradient for the depth range of 200 to 260 mbsf is $15.4 \cdot 10^{-3}$ K/m, which is not much different from the $16.6 \cdot 10^{-3}$ K/m gradient above 200 mbsf.

2. Second logged temperature curve: a) temperature values between 75 and 160 mbsf have a gradient of $19.1 \cdot 10^{-3}$ K/m; the gradient increased, as compared with the first temperature curve; b) the thermal gradient below 214 mbsf is $14.3 \cdot 10^{-3}$ K/m; this gradient is lower than that of the first temperature log.

The formation temperature was calculated using the procedure described in the "Explanatory Notes" (this volume), Fig. 68. The following observations are of particular interest for these results:

1. The extrapolated temperature has an irregular gradient below 160 mbsf, which is the depth interval with very low thermal gradients.

2. The temperature gradient between 75 and 150 mbsf is $31.0 \cdot 10^{-3}$ K/m. The bottom-water temperature estimated from this gradient is 2.7°C , which is higher than that measured during the final logging run, 1.4°C ("Logging" section, this chapter).

3. The least-squares line fit constrained by the bottom-water temperature gives a gradient of $42.0 \cdot 10^{-3}$ K/m for the depth range of 0-150 mbsf.

The anomalous behavior of the formation temperature below 150 mbsf may be explained by fluid ascent toward the sea-floor because of a relatively higher pore-fluid than hydrostatic pressure below 200 mbsf. The depth below which the temperature gradient is lower decreased from 180 mbsf on the first logging run to 160 mbsf on the second logging run, which suggests

Table 15. Summary of vane shear strength at Site 685.

Core/section interval (cm)	Depth (mbsf)	Peak (kPa)
112-685A-1H-1, 103	1.03	18.93
1H-1, 127	1.27	41.06
1H-2, 52	2.02	21.43
1H-3, 66	3.66	30.79
2H-2, 96	6.56	54.93
2H-4, 51	9.11	49.73
2H-6, 42	12.02	42.86
3H-1, 73	14.33	70.92
3H-3, 73	17.33	71.67
3H-5, 53	20.13	73.16
4H-2, 80	25.40	97.05
4H-4, 35	27.95	106.76
4H-6, 118	31.78	74.66
5X-2, 79	34.89	62.71
5X-3, 71	36.31	59.72
5X-5, 72	39.32	68.68
6X-2, 108	44.68	52.26
6X-4, 37	46.97	74.66
6X-6, 99	50.59	92.57
7X-2, 21	53.31	61.96
7X-3, 68	55.28	65.70
8X-2, 93	63.53	93.32
8X-3, 120	65.30	108.25
8X-5, 120	68.30	86.60
9X-2, 120	72.17	79.88
9X-4, 57	74.54	97.80
9X-7, 112	79.59	73.91

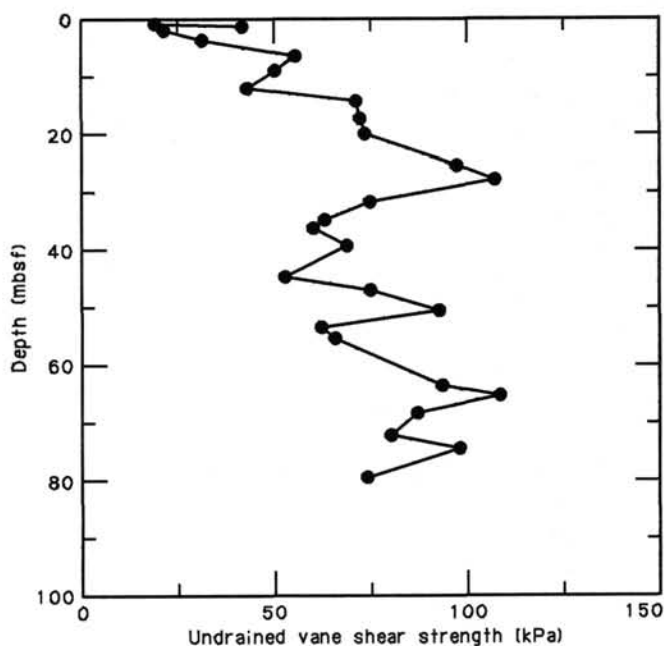


Figure 61. Profile of peak undrained vane shear strength for Site 685.

ascent of a cooler fluid. Hence, the depth range where the logged temperature can be used to estimate a general thermal gradient is 75 to 150 mbsf. Extrapolated temperatures may be highly perturbed by fluid movement below 150 mbsf.

Thermal Conductivity from Logging

Thermal conductivity can also be estimated from logging data by the method described in the "Explanatory Notes" (this volume). Neutron porosity, temperatures, and resistivity data were read from the wireline logging records every 10 m, except

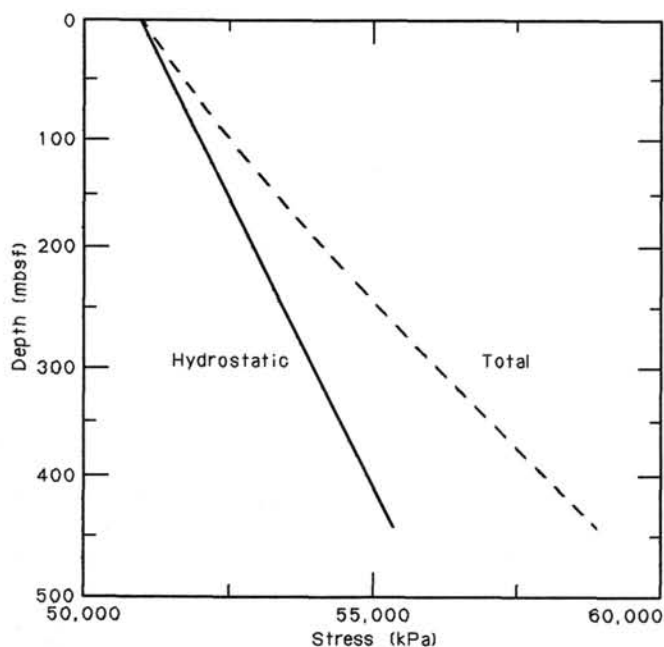


Figure 62. Profiles of assumed hydrostatic stress and calculated total stress for Site 685.

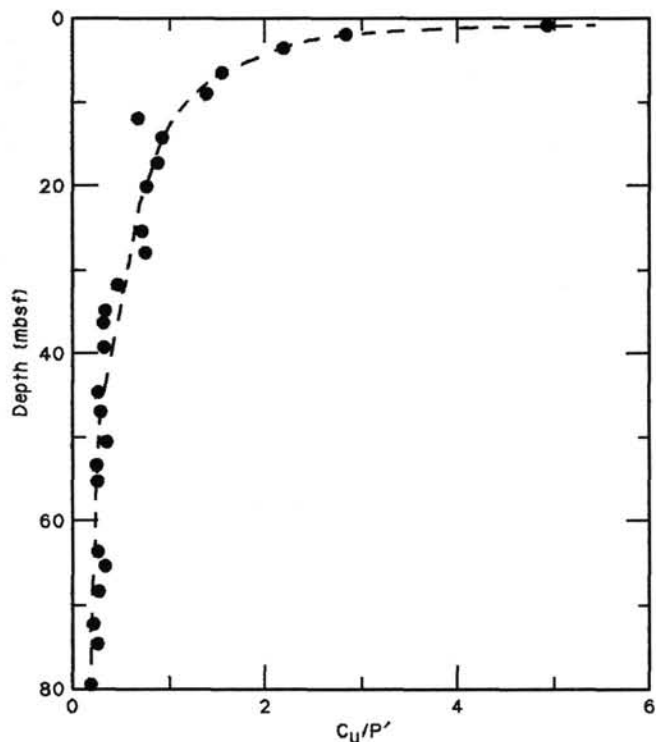


Figure 63. Profile of the ratio of peak undrained vane shear strength to effective overburden pressure at Site 685.

where the log traces changed rapidly with depth. In such cases, the sampling interval was doubled. The averaging depth window was about 4 m, i.e., 2 m on either side of the central reading depth. Only logging data above 214 mbsf were considered to be reliable for this study. Below 214 mbsf, the caliper reached its maximum extension and probably stopped making contact with

Table 16. Thermal conductivity measurements at Site 685.

Core-section interval (cm)	Depth (mbsf)	Thermal conductivity (W/m·K)
112-685A-1H-2, 74	2.24	0.900
1H-2, 54	3.54	0.876
2H-2, 83	6.43	1.039
2H-3, 90	8.00	0.990
2H-4, 70	9.30	0.951
2H-6, 70	12.30	0.995
3H-1, 60	14.20	0.922
3H-2, 70	15.80	0.868
3H-4, 90	19.00	0.858
3H-5, 80	20.40	0.897
3H-6, 84	21.94	0.921
4H-2, 80	25.13	0.898
4H-3, 93	26.76	0.969
4H-4, 68	28.01	0.931
4H-6, 108	31.41	0.872
5X-1, 120	33.91	0.873
5X-2, 58	34.79	0.841
5X-3, 74	36.53	0.873
5X-4, 112	38.33	0.795
5X-5, 78	39.45	0.823
6X-2, 100	44.60	0.800
6X-4, 77	47.37	0.911
6X-5, 139	49.49	0.897
6X-6, 106	50.66	0.878
7X-1, 121	52.81	0.788
7X-2, 67	53.77	0.792
8X-3, 3	64.13	0.978
8X-3, 147	65.57	0.967
8X-4, 147	67.07	0.828
8X-7, 31	70.41	0.911
9X-3, 3	73.63	0.925
9X-4, 3	75.05	0.832
9X-7, 137	80.26	0.931
9X-8, 3	80.42	0.891
10X-1, 147	81.57	0.933
10X-2, 147	83.07	0.887
10X-5, 147	87.57	0.827
10X-6, 3	87.63	0.834
11X-1, 147	90.98	0.833
11X-2, 3	91.04	0.770
11X-6, 3	93.98	0.819
11X-6, 67	94.62	0.843
18X-1, 8	156.18	0.955
20X-4, 100	179.14	0.841
20X-5, 116	180.04	0.812
20X-6, 147	181.35	0.885
20X-7, 3	181.41	0.915
37X, CC, 13	337.98	0.976

the hole wall. Salinity information, as determined from interstitial water, is given in the "Inorganic Geochemistry" section (this chapter).

Thermal-conductivity values computed from these data are presented in Table 17 and Figure 69. Although these computations were conducted for depths ranging from 75 to 260 mbsf, only data above 214 mbsf should be considered reliable. Thermal conductivity was almost constant with depth from 75 to 200 mbsf, with an average of 0.89 W/m·K and a standard deviation of 0.01 W/m·K. Thermal conductivity data, measured by the needle-probe method, corrected for temperature and pressure effects, also are plotted in Figure 69. Between 75 and 95 mbsf, conductivity measured by logging was slightly higher than conductivity measured by the needle probe. This may result from gas expansion in the samples measured for conductivity using the needle probe (see "Physical Properties" section, this chapter).

Heat-Flow Estimation

Using the formation temperature and thermal conductivity computed from the wireline logging data, heat flow from 75 to 150 mbsf in Hole 685A was estimated to be 28 mW/m². If we

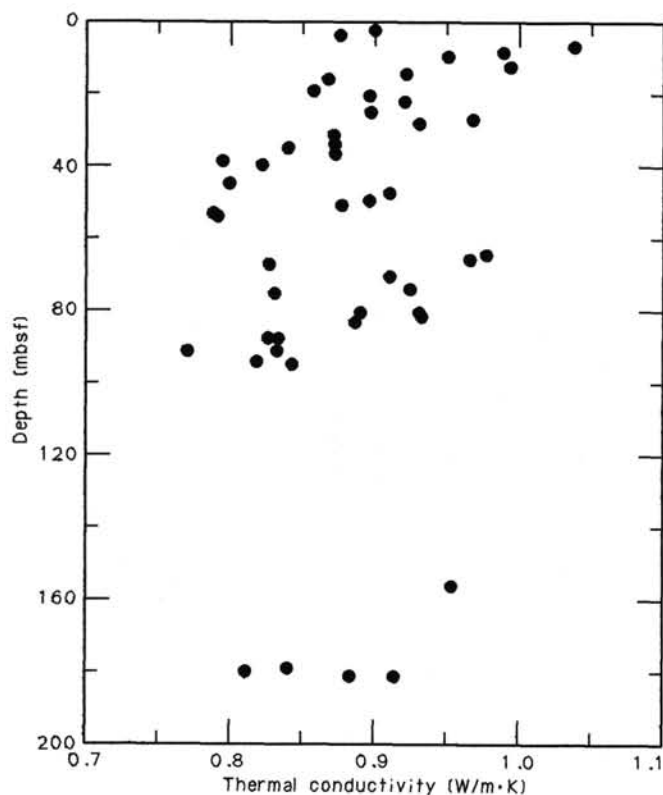


Figure 64. Thermal conductivity vs. depth below seafloor at Site 685.

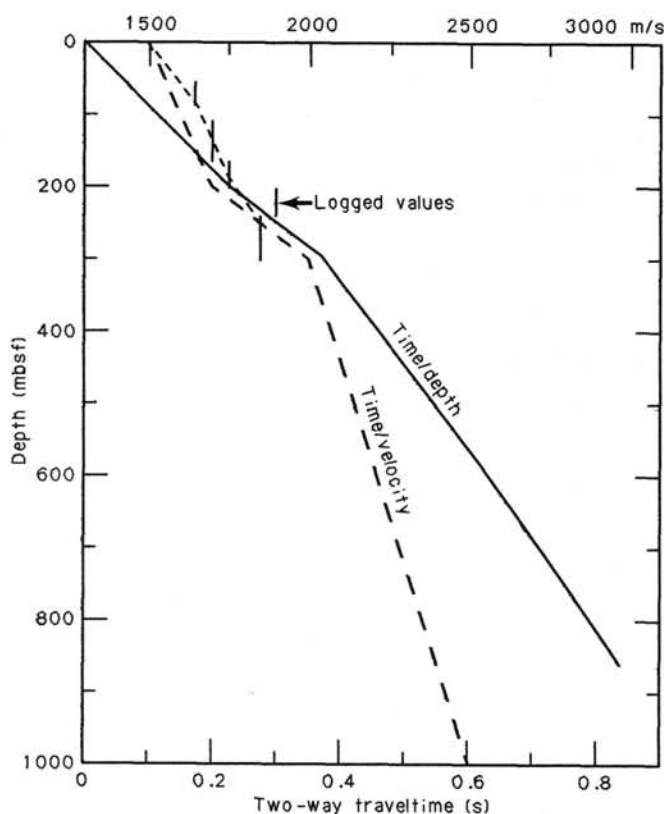


Figure 65. A generalized velocity/depth function for the Leg 112 area on which are plotted the velocities logged at Site 685, shown as vertical bars of averaged values.

use the thermal-conductivity value measured by the needle probe, the heat flow is 27 mW/m^2 . Since thermal conductivity measured by the needle probe method was probably lowered by gas expansion, the heat flow values may be slightly higher.

Heat flow between the seafloor and 75 mbsf was calculated to be 41 mW/m^2 from the bottom-water temperature, the extrapolated temperature, and the thermal-conductivity data measured by the needle probe. The difference in heat-flow results could result from errors in the extrapolated temperatures. If these differences are correct, then conductive heat flow decreases with depth, which may be caused by fluid flowing upward in the sediment (e.g., Anderson and Skilbeck, 1981). Possibly the pore waters extruded during the subduction process flow upward. Fluid venting on the landward slope of the Peru Trench is indicated by living giant white clams (Kulm et al., 1986).

Site 685 is located on the multichannel seismic reflection line CDP-2. On this record, a gas hydrate BSR can be seen about 5 km seaward of Site 685. The depth of the reflector from the seafloor is about 0.7 s in two-way traveltime. Using the generalized velocity/depth function for Leg 112 (Fig. 65), the heat flow was estimated as about 45 mW/m^2 (Yamano et al., 1982).

Some surface heat-flow data were measured near Site 685. The nearest station was about 10 km north-northwest of Site 685, and the heat-flow value was 37 mW/m^2 (Yamano, 1986). Considering all these data, we believe that heat-flow values are between 30 and 50 mW/m^2 in this area.

LOGGING

Hole 685A was logged continuously from 79 to 264 mbsf on 29 November 1986. Log measurements were obtained from the Long Spaced Sonic (LSS), Caliper, Dual Induction (DIT), Gamma Ray (GR), Gamma Spectrometry (GST), Aluminum Clay (ACT), Natural Gamma Spectrometry (NGT), Temperature (AMS), Lithodensity (LDT), and Compensated Neutron (CNL) tools. All of these logging tools were provided by Schlumberger Well Services.

Operations

Hole 685A was cored to 468.6 mbsf. The hole was drilled with seawater and conditioned with a polymer before logging. During the first logging run (LSS/DIT/GR), an obstruction was encountered at 289 mbsf. This obstruction, which we suspected was solid filling in the hole, prevented acquisition of logging data at greater depths. The GST/ACT/NGT suite was logged next and reached 281 mbsf. The final logging run (LDT/CNL/NGT) reached 279 mbsf.

A bottom-hole temperature of 7.5°C was measured at 1153 hr during the second run (19 hr, 53 min after circulation stopped). A second bottom-hole temperature measurement of 7.8°C was taken at 1842 hr, at the start of the final logging run. A temperature of 1.4°C was measured inside the drill pipe, 10 m above the mud line. We believed that this last measurement was the equilibrium ocean bottom-water temperature at Site 685, where the water depth was 5085.5 m.

Logging Measurements

The Schlumberger logging tools have been thoroughly described in the literature (Serra, 1984; Anderson and Pezard, 1986) and are not reviewed here. Logging data, referenced to zero depth at the seafloor, are presented in the logging summary. A discussion of the GST presentation is given in the "Logging" section of the Site 679 chapter. Photoelectric effect (PEF) responses (measured by the LDT) to some characteristic minerals also are given.

Because of an electrical leak on the wireline cable, the Dual Induction deep (ILD) and medium (ILM) logs show erroneous data and thus are not presented here. The shallow, spherically focused log (SFL) indicated a normal compaction trend with the exception of one interval (discussed below).

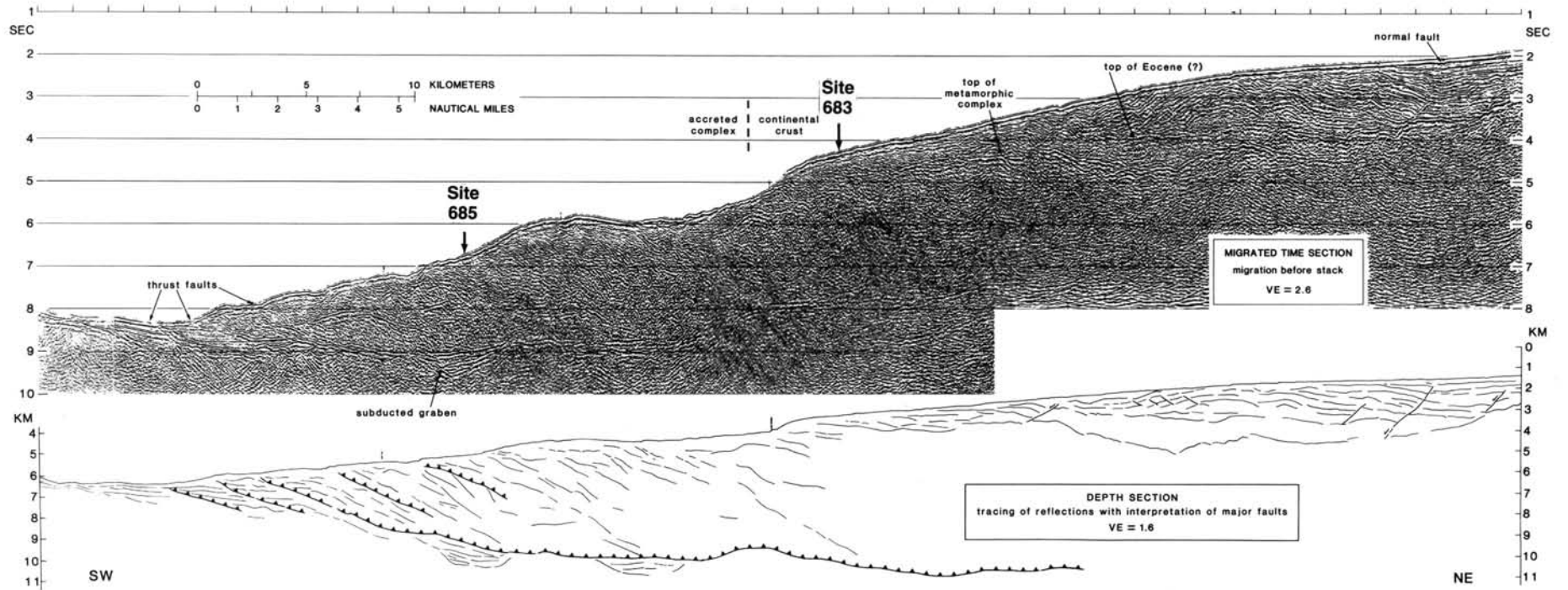


Figure 66. The seaward part of seismic-reflection record CDP-2. The upper display is a time section at a vertical exaggeration of about 2.5. The lower display is an interpreted depth section using velocities determined before drilling (from Kulm et al., 1986).

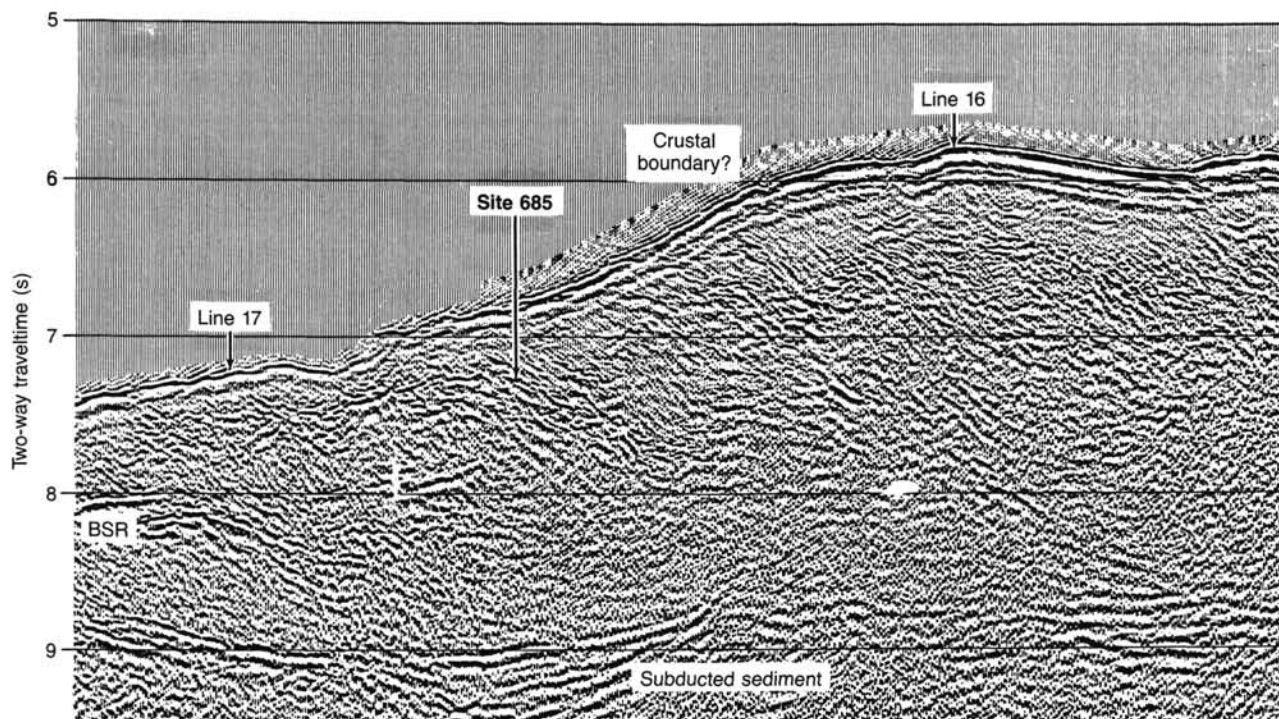


Figure 67. A large-scale display of the part of CDP-2 around Site 685, showing the location of the cross-lines, the site, and the suspected boundary between crustal types. The display is a time section, with horizontal lines at 1-s intervals.

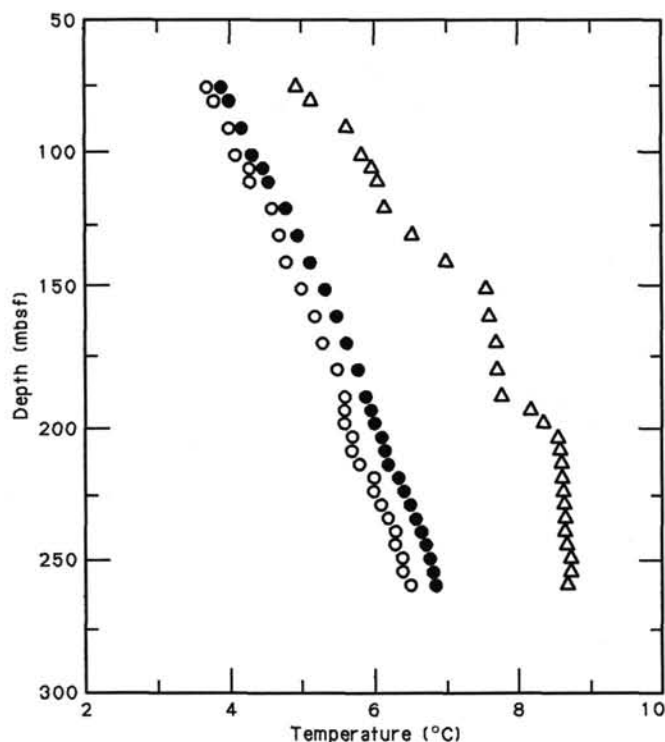


Figure 68. Estimation of the formation temperatures from the logged temperatures in Hole 685A. Open and closed circle indicate the first and second logged temperatures, respectively. Triangles depict the formation temperatures.

The ACT aluminum yield log was calibrated to seven core samples obtained from Holes 685A and 683A in the following intervals:

Hole	Section
112-683A	3H-3
112-683A	5H-2
112-683A	7H-4
112-683A	9H-5
112-683A	40X-4
112-685A	18X-6
112-685A	28X-2

A gain and offset to the raw ACT aluminum count rate was determined from this calibration data set. Although a number of lithologies were encountered during Leg 112, we thought that a small set of core samples would reasonably allow for an adequate shipboard calibration. The uncalibrated aluminum log is presented in the logging summary (Table 17).

Acoustic-velocity measurements also indicated normal compaction above 207 mbsf. An average value of 1.2 g/cm³ was the measured density below 246 mbsf, which is considered to be (uncorrected) borehole fluid density. The caliper log, which was fully open (reading its maximum value) below 223 mbsf, together with suppression of the SGR log support our conclusion that the hole was enlarged. Bulk-density measurements in the core and GRAPE density data indicate sediment densities in excess of 1.5 g/cm³ below 223 mbsf (see "Physical Properties" section, this chapter). These physical-property measurements support the claim that log bulk density did not respond to the formation. Note, however, that the acoustic velocity and resistivity continued to respond to the formation below 246 mbsf. The GST ratios also seemed to be affected by the enlarged borehole.

Table 17. Thermal conductivity values from logging data in Hole 685A.

Depth (mbsf)	Thermal conductivity (W/m·K)
75.0	0.86
80.0	0.89
90.0	0.88
100.0	0.89
105.0	0.89
110.0	0.91
120.0	0.88
130.0	0.89
140.0	0.88
150.0	0.88
160.0	0.90
170.0	0.89
180.0	0.89
190.0	0.90
195.0	0.90
200.0	0.89
205.0	0.88
210.0	0.89
215.0	0.87
220.0	0.82
225.0	0.86
230.0	0.89
235.0	0.85
240.0	0.85
245.0	0.82
250.0	0.82
255.0	0.86
260.0	0.84

The stratigraphic units that were logged (see "Lithostratigraphy" section, this chapter) included the base of Subunit IA, all of Subunit IB, and the upper part of lithologic Unit II. There was no clear change in the logs to indicate the lithologic boundary of Subunits IA/IB, while the Subunit IB/Unit II interface can be clearly seen at 207 mbsf.

Description of Subunit IB (and the Base of Subunit IA)

The shallowest depth logged, 79 mbsf, is 5 m above the base of Subunit IA, as determined from the core (see "Lithostratigraphy" section, this chapter). The base of Subunit IB, at 207 mbsf, corresponds to an increase in density, velocity, and resistivity. Subunit IB contains numerous shows of gas hydrate (discussed next).

The natural radioactivity in Subunit IB was observed to be fairly constant. Slight increases in uranium content near 124 and 184 mbsf were interpreted as phosphate-bearing intervals. The bulk density (RHOB), PEF, and neutron porosity (NPPI, recorded using a limestone porosity transform) also showed little variation, indicating a uniform, quartz-dominated lithology. Deposition rate was approximately 100 m/m.y. (see "Biostratigraphy" section, this chapter).

Acoustic velocity, which does increase with depth in Subunit IB (normal compaction), indicated that significant horizontal heterogeneity occurs in the interval at 79–116 mbsf, based on separation of the long and short velocity logs. This separation probably results from drilling disturbance. The base of the disturbed zone correlates with a slight increase in natural radioactivity. No change in lithology or porosity was otherwise indicated by the logs at 116 mbsf.

The salinity indicator ratio (SIR), measured by the GST, qualitatively indicated a constant salinity in Subunit IB. Much of the activity of the other yield ratios was the result of the very low calcium-yield measurements (often zero). Therefore, quantitative interpretation will be required before we can reach any significant conclusions from the GST data.

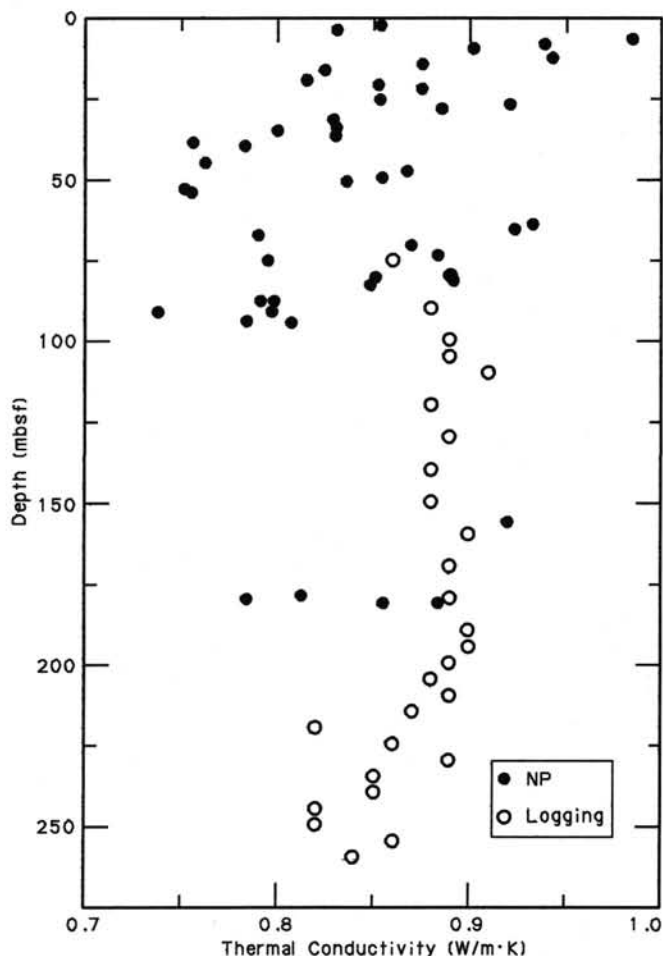


Figure 69. Thermal conductivity estimated from wireline logging data and thermal conductivity found using the needle-probe method, corrected for *in-situ* temperature and pressure conditions.

Gas-hydrate shows (within the logged interval) were indicated by expansion of Cores 112-685A-9X, 112-685A-12X, 112-685A-17X, 112-685A-18X, 112-685A-20X, and 112-685A-21X (see "Organic Geochemistry" section, this chapter). A sample of gas hydrate was found in Section 112-685A-17X, CC (see "Lithostratigraphy" section, this chapter). Core 112-685A-9X (70.6–80.1 mbsf) spans the topmost logged interval. The bulk density appears anomalously low above 84 mbsf; however, there was no obvious indication of gas hydrates from the other logs.

Log responses to gas hydrates were determined during DSDP Leg 84 (Mathews and von Huene, 1985), when a pure hydrate zone was logged at DSDP Site 570. There, methane hydrate was characterized by a density of 0.92 to 0.93 g/cm³, a velocity of 3.73 km/s, and infinite resistivity.

Although pure gas-hydrate zones were not indicated by the logs at Hole 685A, intervals containing gas hydrates corresponded to increases in velocity and resistivity with a corresponding decrease in density. Natural radioactivity may only decrease when the percentage by volume of gas hydrate is higher than was observed at this site. Similarly, salinity, as indicated by SIR (measured by the GST), may not show a noticeable decrease when the hydrate volume is low.

Gas hydrates were indicated by the logs at 103, 105, 160, 164, 169, 171, 173, 187, and 191 mbsf. Acoustic velocity showed significant increases at these depths, while the variation in density and resistivity was more subtle. Although quantitative analysis

will be required, we observed that the gas hydrates encountered in Hole 685A were disseminated or found in small masses mixed with the sediment. Horizontal heterogeneity based on the LSS was also observed to correspond with most of the gas-hydrate zones; this may indicate dissolution of gas hydrate near the borehole caused by the presence of borehole fluid.

Structurally, Subunit IB is characterized by highly dipping beds (see "Lithostratigraphy" section, this chapter). Thus, one must exercise caution in attempts to assess the thicknesses of the gas-hydrate zones. As Subunit IB was found from the logs to be fairly uniform otherwise, there is no evidence of dipping beds from the logging data.

Description of Unit II

The top of lithologic Unit II (placed at 207 mbsf from logs) is an unconformity along which a hiatus of 4.3 Ma occurs (see "Biostratigraphy" section). The upper 28 m of Unit II consists of two thick, acoustically fast beds (207–218 mbsf and 226–235 mbsf) separated by three porous stringers. Below 235 mbsf, the borehole is greatly enlarged, preventing a lithologic analysis from the LDT log.

The two faster beds were seen to have an average density of 1.55 g/cm^3 . The associated increase in PEF was considered indicative of calcite cementation, which was observed (along with dolomite rhombs) in the sediment recovered (see "Lithostratigraphy" section, this chapter). The increase in resistivity and the significant velocity peak in these beds support the conclusion that calcite cementation, rather than dolomitization, is the dominant feature of the two beds considered.

Below 235 mbsf, the acoustic and resistivity logs evidently continued to respond to the formation. Between 235 and 247 mbsf, both logs recorded values greater than their respective compaction trend lines (straight lines drawn to best fit the data trend over the entire logged interval). This apparent deviation from normal compaction may be evidence of excessive pore pressure. However, calcite cementation could result in the same effect. The GST measurement of the lithology indicator ratio (LIR) in this interval was observed to read as low as 0.2 (pure mineral responses are quartz = 1.0; dolomite = 0.18; calcite = 0.0). Thus, the LIR measurement indicated the presence of carbonates. Our preliminary conclusion then was that the interval was cemented rather than overpressured.

The enlarged borehole below 246 mbsf correlates with a lithologic transition from mudstone above to mud below ("Lithostratigraphy" section, this chapter). The undercompacted interval below 246 mbsf (which is capped by the thick, calcite cemented beds) is, in fact, a good candidate for overpressure. Although the NPHI log did not indicate a porosity constriction in the cap rock, the resistivity increase may indicate a permeability constriction. Interpretation of the sedimentary column below 207 mbsf as an accreted section (see "Summary and Conclusions," this chapter) was supported by the logging data, which do not show clear evidence of overpressure and yet indicate undercompaction.

Comparison of the SGR log through lithologic Unit II in Hole 685A with the SGR data observed in lithologic Units II and III of Hole 679E (see "Logging" section, Site 679 chapter, this volume) revealed that cyclicity may be present in Hole 685A. The ages of these sections are comparable ("Biostratigraphy" section, this chapter; "Biostratigraphy" section, Site 679 chapter, this volume). We consider an exemplary cycle in Hole 685A, which exhibits the same SGR features as those discussed for Hole 679E, to be the interval at 240 to 256 mbsf. The longer wavelength at Site 685A is consistent with the greater sedimentation rate ("Biostratigraphy" section, this chapter) when compared to observed cyclicity at Hole 679E.

Our attempt to determine the tops of shallower cycles was problematic as lithologic Unit II was faulted. The interval of

220–240 mbsf may correspond to a shallower cycle. Above the hiatus, the interval of 182–207 mbsf also was seen to have the same cyclic SGR features (sediment of comparable age to Subunit IB in Hole 685A was not logged in Hole 679E).

The higher uranium concentration observed between the hiatus (207 mbsf) and 220 mbsf and again within the next lower cycle, may be evidence of fluid flow. A combination of cyclic deposition, faulting (during accretion), and post-depositional fluid flow (carrying dissolved uranium) accounts for the essential features of the lithologic Unit II logging data from Hole 685A.

A significant decrease in pore-water salinity was observed to occur near the Subunit IB/Unit II interface ("Inorganic Geochemistry" section, this chapter). The GST measurement of SIR does decrease below 207 mbsf, which indicates pore-water freshening, but returns to the average reading of Subunit IB below 219 mbsf. This increase in SIR with depth is consistent with the previously discussed enlarged borehole, which results in a SIR that approaches the value appropriate to the borehole fluid (seawater).

Quantitative Analysis of Logging Data

A synthetic seismogram (Fig. 70) was calculated from the log-derived density and velocity data for comparison with the seismic section. Further analysis of the log data will be accomplished onshore at the Lamont-Doherty Borehole Geophysics offices.

SUMMARY AND CONCLUSIONS

A major tectonic boundary at the front of the Peruvian convergent margin abruptly juxtaposes the seaward end of the continental crust against the landward end of the accretionary complex. Sites 683 and 685 were placed on either side of this boundary to establish its nature and to date the beginning of accretion. This required identifying a good accretionary structure in seismic records that could be verified by coring and examining the earliest sediment accreted against the boundary with the continental crust. From all indications, cores from Site 685 contain accreted sediment that is of late Miocene age and that is separated from its cover of slope deposits by a 4.3-m.y. hiatus.

Site 685, on the lower slope of the Peru Trench at a water depth of 5070 m, is about 1200 m above the floor of the trench and about 1000 m below the level of a mid-slope terrace. The terrace is a topographic feature associated with the transitional contact between continental crust and the complex of imbricated sediment accreted against it at the front of the margin. The frontmost part of the continental crust probably occurs just seaward of the edge of the mid-slope terrace, as indicated in a reprocessed seismic-reflection record, CDP-2 (Kulm et al., 1986), which shows a landward-dipping structure that cuts the entire upper plate and merges with the subduction zone. Therefore, the site was located in the first packet of landward-dipping reflections about 1 km downslope from the inferred boundary, where the cover of slope deposits was thin enough to allow ample drilling into the thrust packet. This location coincided with a small knoll on the slope detailed by the Seabeam survey of the *Jean Charcot* (Bourgeois et al., 1986) and thus is bypassed by much of the sediment transported downslope.

The two main lithologies represented in the 468 m cored were a slope cover and the accreted complex. The slope deposits (0–200 m) consist of an 80-m-thick diatomaceous mud with small oceanward-dipping normal faults, overlying a diatomaceous mud with variable bedding, folding, locally developed fissility, and a fabric that cuts these beds at high angles. Microfossil assemblages are of Pleistocene age, and most were transported from shallow-water environments on the shelf, with fewer transported from upper and intermediate slope areas. The age range is well constrained and yields a surprisingly high sedimentation rate (100 m/m.y.). In seismic records across the site the correspond-

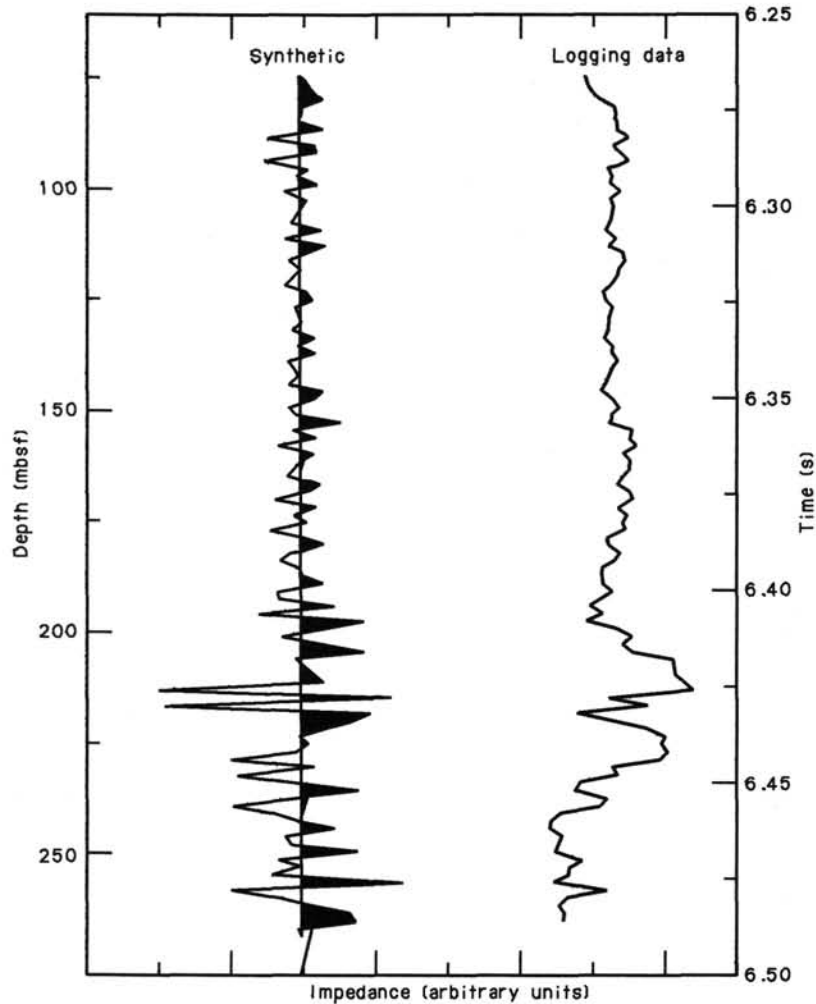


Figure 70. Synthetic seismogram using a Ricker wavelet with a 35-Hz center frequency and assuming that the velocity between the seafloor and 75 mbsf is 1608 m/s. Analysis based on LSS and LDT data.

ing reflections are hidden in the outgoing signal, but in adjacent areas the slope reflections are short irregular events of variable dip.

A hiatus having a minimum duration of 4.3 m.y. separates the lower Pleistocene from the lower upper Miocene. The Miocene rocks are dominantly diatomaceous mudstones that are variably calcareous. In the upper part relatively constant dips were observed, and the rocks showed a moderate-to-strong, scaly fabric parallel to the bedding. Toward the bottom of the cored section, the well-lithified parts are intensely fractured and show a strong scaly cleavage and structure that can be related to compressional deformation. The apparent bedding dips cluster between 45° and 60° , whereas those of the reflections in the seismic record are from 10° to 20° . Sedimentary breccias and sand occur near the bottom of the hole. The breccia clasts have various ages from Eocene to late Miocene, and some show two generations of consolidation and erosion. The lower unit has the same characteristic transported fauna observed in the slope cover. Diatom assemblages in the recovered section are characteristic of a single zone that lasted from 6.1 to 6.8 m.y. Therefore, a minimum rate of sedimentation (not corrected for tectonic thickening) is about 250 m/m.y., but only about one-half of the thrust packet seen in the seismic record was penetrated.

Unusually steep gradients of chemical species dissolved in pore waters were characteristic of this site. The sulfate-reduction zone is very thin; thus methane generation begins at <11.6 mbsf. Methane gas hydrate was first recovered at about 99 mbsf and was observed visually to about 165 mbsf. The depth of recovery is unusually shallow in this environment and may be linked with the early generation of the methane. TOC contents are lower at this site than at the other sites drilled during Leg 112, perhaps because of dilution by rapid sedimentation. This rapid rate of sedimentation is responsible for some extreme concentration gradients. The maxima in alkalinity (156 mmol/L), phosphate (0.826 mmol/L), and ammonia (31.76 mmol/L) are the highest ever reported from deep ocean drilling. Despite the extreme concentration gradients at this site, the amounts of diagenetic minerals (particularly carbonates and phosphates) that form per unit volume of sediment is small. When sedimentation rates are high and convective flow is impeded, the system rapidly closes, thereby reducing the replenishment of the essential components needed for various diagenetic reactions.

The stratigraphy and structure observed in cores from this site are consistent with the interpretations of the landward-dipping seismic reflections at the front of the Peru Continental Margin as an accreted complex. This confirmation from the

cores is evidenced by the differing structural styles in sediment of the upper part of the slope cover and in sediment of the landward-dipping beds. The lower part of the slope cover appears to have been involved in tectonic deformation of the slope. Today's deformation is indicated in the Seamark images, where numerous anastomosing low ridges, inferred to be thrust faults, parallel the lower slope. The high rates of slope sedimentation at the site probably prevail on the slope in general. Thus, the rate of deformation required to maintain the ridges is probably high as well. The implied high rates of Miocene sedimentation in the accreted unit are consistent with deposition in a lower-slope basin or the trench axis. Abundant microfossils transported down-slope from the shelf are typical of lower-slope basins and trench deposits. Therefore, all indications from the section drilled at Site 685 are consistent with the geophysical evidence for an accreted thrust packet. Its late Miocene age (6.1 to 6.8 m.y.) indicated the time at which accretion began to prevail over other tectonic processes at the front of the margin.

The plate reconstruction of Cande (1985) indicates that the crest of the Nazca Ridge, because of its trend at an angle to the direction of plate convergence, has progressively intercepted the Peru margin in a southward path as the ridge migrated to its present position south of the latitude of Pisco. The Nazca Ridge was subducted at the latitude of the Leg 112 northern transect about 7.5 m.y. ago and was completely subducted within 1 Ma. Thus, the accreted sediment was deposited shortly after a major topographic feature on the oceanic plate was subducted. In addition, the rates of sedimentation at other sites on the slope (Sites 682 and 683) were relatively vigorous during the middle and late Miocene. Thus, the change from nonaccretionary to accretionary may have involved the subduction of the Nazca Ridge and an increase in sediment supply relative to the Oligocene and early Miocene.

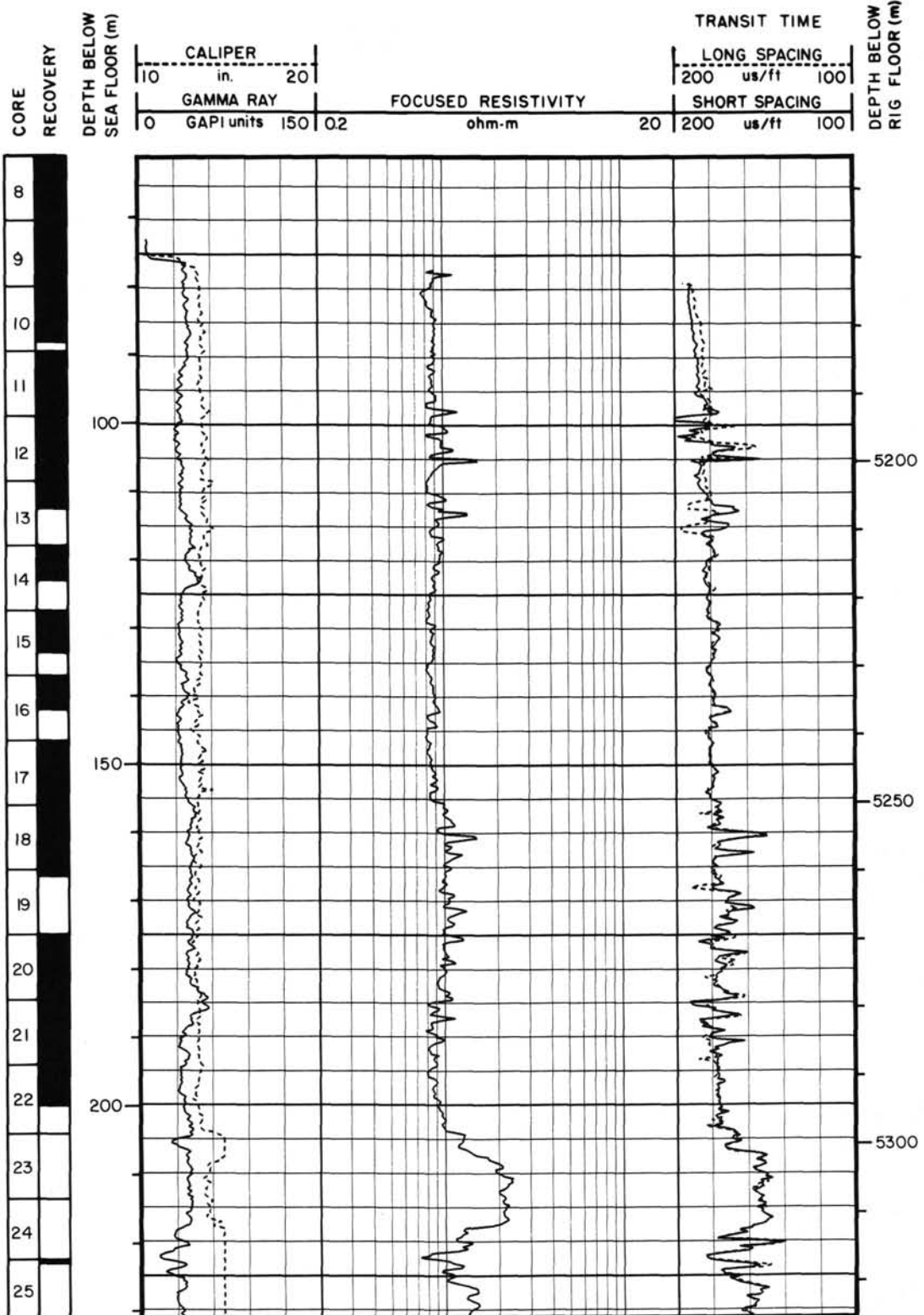
REFERENCES

- Anderson, R. N., and Pezard, P., 1986. *Nuclear Logs, Section L, Leg 111 Shipboard Hole Summaries*: College Station (Ocean Drilling Program).
- Anderson, R. N., and Skilbeck, J. N., 1981. Oceanic heat flow. In Emiliani, C. (Ed.), *The Sea* (Vol. 7): New York (Wiley), 489-523.
- Barron, J. A., 1980. Miocene to Quaternary diatom biostratigraphy of DSDP Leg 57, off northeast Japan. In Scientific Party, *Init. Repts. DSDP*, 56, 57 (Pt. 2): Washington (U.S. Govt. Printing Office), 641-685.
- , 1985. Late Eocene to Holocene diatom biostratigraphy of the equatorial Pacific Ocean, Deep Sea Drilling Project Leg 85. In Mayer, L., Thayer, F., Thomas, E., et al., *Init. Repts. DSDP*, 85: Washington (U.S. Govt. Printing Office), 413-456.
- Berggren, W. A., 1977. Late Neogene planktonic foraminiferal biostratigraphy of Site 357 (Rio Grande Rise). In Supko, P. R., Perch-Nielsen, K., et al., *Init. Repts. DSDP*, 39: Washington (U.S. Govt. Printing Office), 591-614.
- Blow, W. H., 1969. Late middle Eocene to Recent planktonic foraminiferal biostratigraphy. In Bronnimann, R., and Renz, H. H. (Eds.), *Proc. 1st Internat. Conf. Planktonic Microfossils*, Geneva, 1967, 1: 199-421.
- Bolli, H. M., and Saunders, J. B., 1985. Oligocene to Holocene low latitude planktic foraminifera. *Planktic*, 155-256.
- Burckle, L. H., 1978. Marine diatoms. In Haq, B. U., and Boersma, A. (Eds.), *Introduction to Marine Micropaleontology*: New York, Amsterdam, Oxford (Elsevier Biomedical), 245-266.
- Cande, S. C., 1985. Nazca-South America plate interactions since 50 m.y.b.p. to present. In Hussong, D. M., et al. (Eds.), *Atlas of the Ocean Margin Drilling Program, Peru Continental Margin, Region VI*: Woods Hole (Marine Science International), 14.
- Claypool, G. E., and Kaplan, I. R., 1974. The origin and distribution of methane in marine sediments. In Kaplan, I. R. (Ed.), *Natural Gases in Marine Sediments*: New York (Plenum Press), 94-129.
- Claypool, G. E., and Kvenvolden, K. A., 1983. Methane and other hydrocarbon gases in marine sediment. *Ann. Rev. Earth Planet. Sci.* 1983, 11:299-327.
- DeVries, T., and Schrader, H., 1981. Variation of upwelling/oceanic conditions during the latest Pleistocene through Holocene off the central Peruvian coast: A diatom record. *Mar. Micropaleontol.*, 6: 157-167.
- De Wever, P., 1982. Radiolaires du Trias et du Lias de la Téthys (taxonomie, stratigraphie). *Ann. Soc. Géol. Nord*, 7:599.
- De Wever, P., Riedel, W. R., et al., 1979. Recherches actuelles sur les Radiolaires en Europe. *Ann. Soc. Géol. Nord*, 98, 205-222.
- Fenner, J., 1984. Eocene-Oligocene planktic diatom stratigraphy in the low latitudes and the high southern oceans. *Micropaleontology*, 30: 319-342.
- , 1985. Late Cretaceous to Oligocene planktic diatoms. In Bolli, H., Saunders, J. B., and Perch-Nielsen, K. (Eds.) *Plankton Stratigraphy*: Cambridge (Cambridge University Press), 713-762.
- Fenner, J., Schrader, H., and Wienigk, H., 1976. Diatom phytoplankton studies in the Southern Ocean, composition and correlation to the Antarctic convergence and its paleoecological significance. In Hollister, C. D., Craddock, C., et al., *Init. Repts. DSDP*, 35: Washington (U.S. Govt. Printing Office), 757-813.
- Garrison, R. E., and Kenedy, W. J., 1977. Origin of solution seams flaser structure in Upper Cretaceous chalks of southern England. *Sed. Geol.*, 19:107-137.
- Gieskes, J. M., Elderfield, H., Lawrence, J. R., Johnson, J., Meyers, B., and Campbell, A., 1982. Geochemistry of interstitial waters and sediments, Leg 64, Gulf of California. In Curray, J. R., Moore, D. G., et al., *Init. Repts. DSDP*, 64: Washington (U.S. Govt. Printing Office), 675-694.
- Goldhaber, M. B., and Kaplan, I. R., 1974. The sulfur cycle. In Goldberg, E. D. (Ed.), *The Sea*, Vol. 7: New York (J. Wiley and Sons), 569-655.
- Harrison, W. E., Hesse, R., and Gieskes, J. M., 1982. Relationship between sedimentary facies and interstitial water chemistry of slope, trench and Cocos Plate sites from the Middle America Trench transect, active margin off Guatemala, Deep Sea Drilling Project, Leg 67. In Aubouin, J., von Huene, R., et al., *Init. Repts. DSDP*, 67: Washington (U.S. Govt. Printing Office), 603-613.
- Johns, D. R., 1978. Mesozoic carbonate rudites, megabreccias and associated deposits from Central Greece. *Sedimentology*, 25:561-574.
- Koizumi, I., 1973. The late Cenozoic diatoms of Sites 183-193, Leg 19. In Creager, J. S., Scholl, D. W., et al., *Init. Repts. DSDP*, 19: Washington (U.S. Govt. Printing Office), 805-855.
- , 1986. Pliocene and Pleistocene diatom datum levels related with paleoceanography in the northwest Pacific. *Mar. Micropaleontol.*, 10:309-325.
- Kulm, L. D., Suess, E., Thornburg, T. M., Embley, W. M., Hussong, D. M., and Resig, J. M., 1986. Fluid venting processes and their relation to tectonic styles in subduction zones of the eastern Pacific. *Intl. Kaiko Conf. Subduction Zones*, 28-29. (Abstract)
- Kulm, L. D., Miller, J., and von Huene, R., 1986. The Peru Continental Margin Record Section 2. In von Huene, R. (Ed.), *Seismic Images of Modern Convergent Margins*: Tulsa (AAPG), Spec. Studies in Geology, 26.
- Kvenvolden, K. A., and McMenamin, M. K., 1980. Hydrates of natural gas: a review of their geologic occurrence. *U.S. Geol. Survey Circ.*, 815.
- Kvenvolden, K. A., and Barnard, L. A., 1983. Gas hydrates of the Blake Outer Ridge, Site 533, Deep Sea Drilling Project Leg 76. In Sheridan, R. E., Gradstein, F. M., et al., *Init. Repts. DSDP*, 76: Washington (U.S. Govt. Printing Office), 353-365.
- Kvenvolden, K. A., Claypool, G. E., Threlkeld, C. N., and Sloan, E. D., 1984. Geochemistry of a naturally occurring massive marine gas hydrate. *Org. Geochem.*, 6: 703-713.
- Kvenvolden, K. A., and McDonald, T. J., 1985. Gas hydrates of the Middle America Trench-Deep Sea Drilling Project Leg 84. In von Huene, R., Aubouin, J., et al., *Init. Repts. DSDP*, 84: Washington (U.S. Govt. Printing Office), 667-682.
- Locker, S., and Martini, E., 1986. Silicoflagellates and some sponge spicules from the southwest Pacific, Deep Sea Drilling Project, Leg 90. In Kennett, J. P., von der Borch, C. C., et al., *Init. Repts. DSDP*, 90: Washington (U.S. Govt. Printing Office), 887-924.
- Mathews, M. A., and von Huene, R., 1985. Site 570 methane hydrate zone. In von Huene, R., Aubouin, J., et al., *Init. Repts. DSDP*, 84: Washington (U.S. Govt. Printing Office), 773-790.
- Miller, J., and von Huene, R., 1986. Processing techniques for multi-channel seismic data in deep water. In von Huene, R. (Ed.), *Seismic*

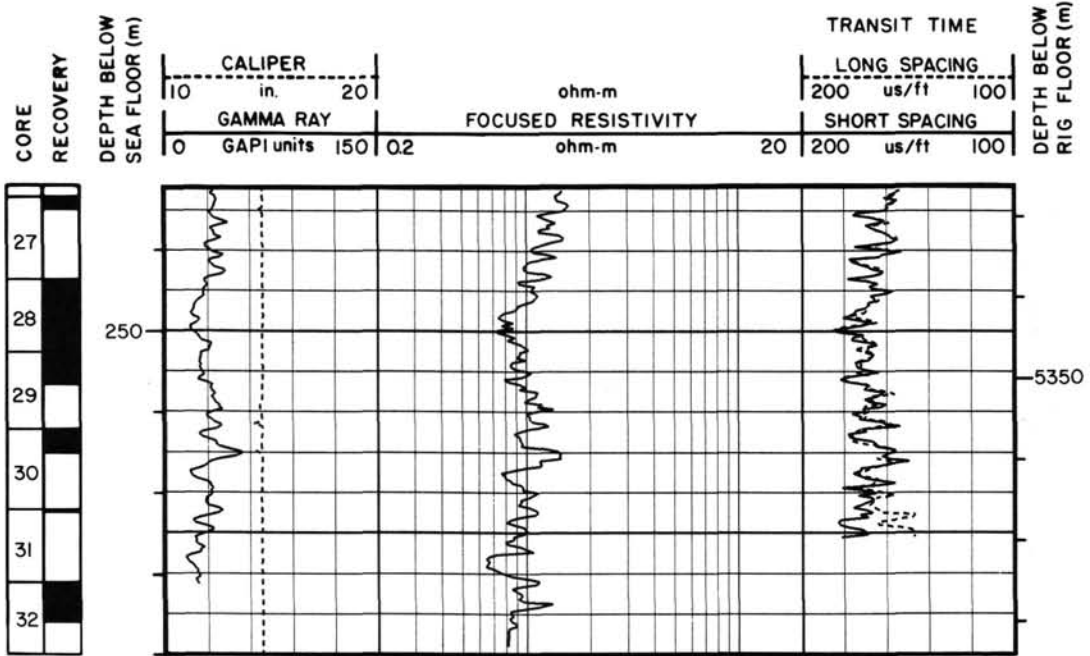
- Images of Modern Convergent Margins*: Tulsa (AAPG), Spec. Studies in Geology, 26.
- Naylor, M. A., 1982. The Casanova Complex of the Northern Apennines: a melange formed on a distal passive continental margin. *J. Struct. Geol.*, 4:1-18.
- Nigrini, C., 1977. Tropical Cenozoic Artostrobiidae (Radiolaria). *Micropaleontology*, 23(3):241-269.
- Poore, R. Z., 1979. Oligocene through Quaternary planktonic foraminiferal biostratigraphy of the north Atlantic: DSDP Leg 49. In Luyendyk, B. P., Cann, J. R., et al., *Init. Repts. DSDP*, 49: Washington (U.S. Govt. Printing Office), 447-517.
- Ruddiman, W., Sarnthein, M., et al., 1988. *Proc. ODP, Init. Repts.*, 108: College Station, TX (Ocean Drilling Program).
- Schrader, H., 1973. Cenozoic diatoms from the northeast Pacific, Leg 18. In Kulm, L. D., von Huene, R., et al., *Init. Repts. DSDP*, 18: Washington (U.S. Govt. Printing Office), 673-797.
- _____, 1976. Cenozoic planktonic diatom biostratigraphy of the southern Pacific Ocean. In Hollister, C. D., Craddock, C., et al., *Init. Repts. DSDP*, 35: Washington (U.S. Govt. Printing Office), 605-671.
- Schuette, G., and Schrader, H., 1979. Diatom taphocoenoses in the coastal upwelling area off western South America. *Nova Hedwigia, Beihefte*, 64:359-378.
- _____, 1981. Diatoms in surface sediments: A reflection of coastal upwelling. In Richards, F. A. (Ed.), *Coastal Upwelling*: Washington (Am. Geophys. Union), 372-380.
- Serra, O., 1984. *Fundamentals of Well Log Interpretation*: Amsterdam (Elsevier).
- Shiple, T. H., Houston, M. H., Buffler, R. T., Shaub, F. J., McMillan, K. J., Ladd, J. W., and Worzel, J. L., 1979. Seismic evidence for widespread possible gas hydrate horizons on continental slopes and rises. *AAPG Bull.*, 63:2204-2213.
- Stow, D.A.V., 1984. Turbidite facies, associations, and sequences in the Southeastern Angola Basin. In Hay, W. W., Sibuet, J.-C., et al., *Init. Repts. DSDP*, 75: Washington (U.S. Govt. Printing Office), 785-800.
- Tissot, B. P., and Welte, D. H., 1984. *Petroleum Formation and Occurrence* (2nd Ed.): Berlin-Heidelberg (Springer-Verlag).
- von Huene, R., Kulm, L. D., and Miller, J., 1985. Structure of the frontal part of the Andean convergent margin. *J. Geophys. Res.*, 90: 5429-5442.
- Ward, J. C., 1970. The structure and properties of some iron sulfides. *Rev. Pure Appl. Chem.*, 20:175-206.
- Yamano, M., 1986. Heat flow studies of the circum-Pacific subduction zones [D.Sc. dissert.]. University of Tokyo, Tokyo.
- Yamano, M., Uyeda, S., Aoki, Y., and Shipley, T. H., 1982. Estimates of heat flow derived from gas hydrates. *Geology*, 10:339-343.

Ms 112A-116

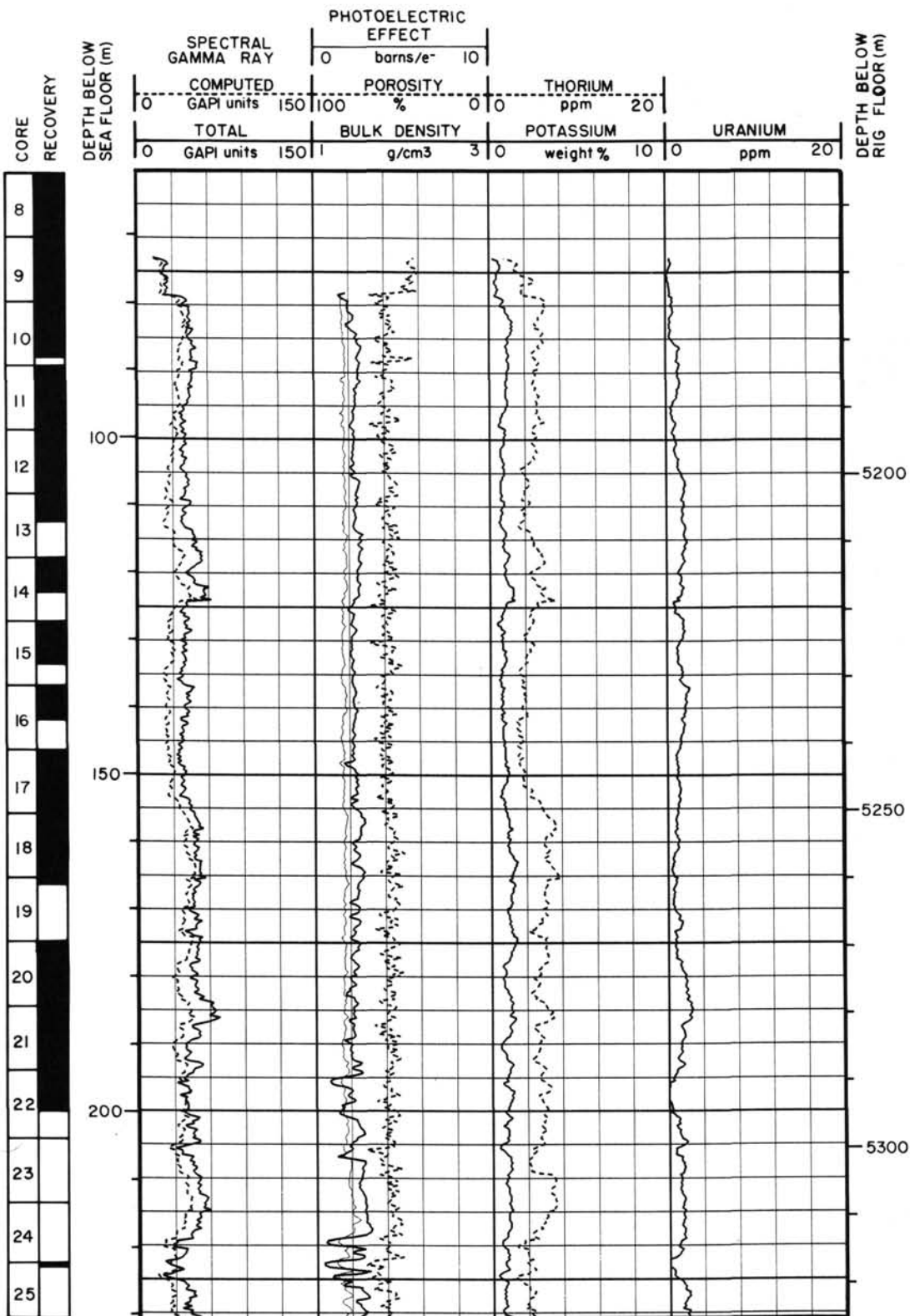
Summary logs for Site 685.



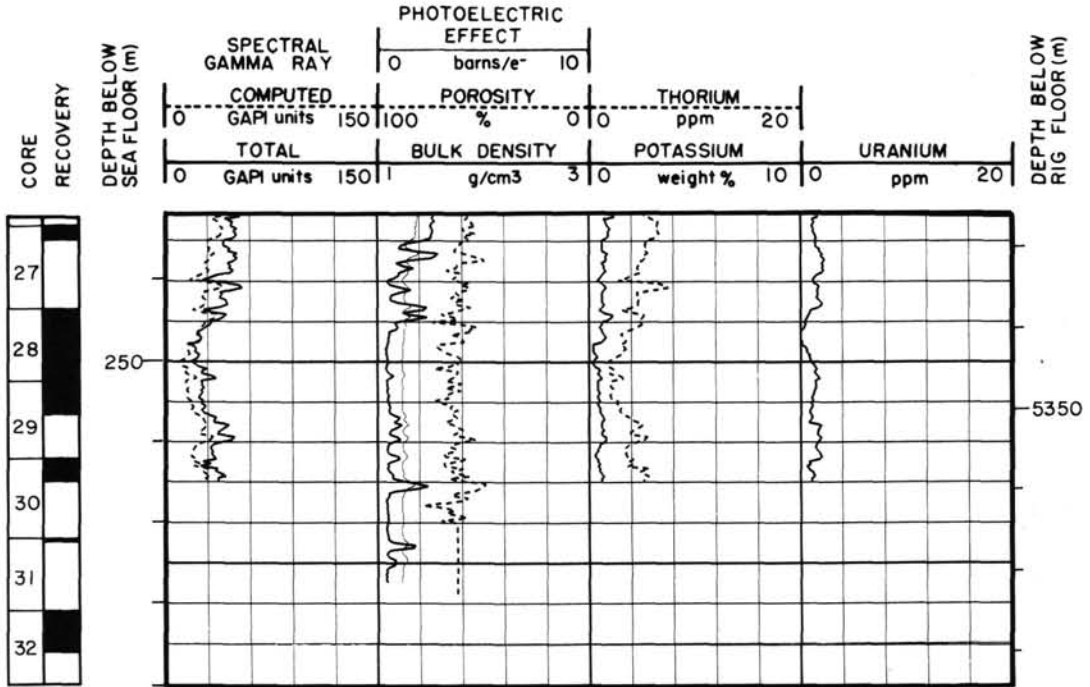
Summary logs for Site 685 (continued).



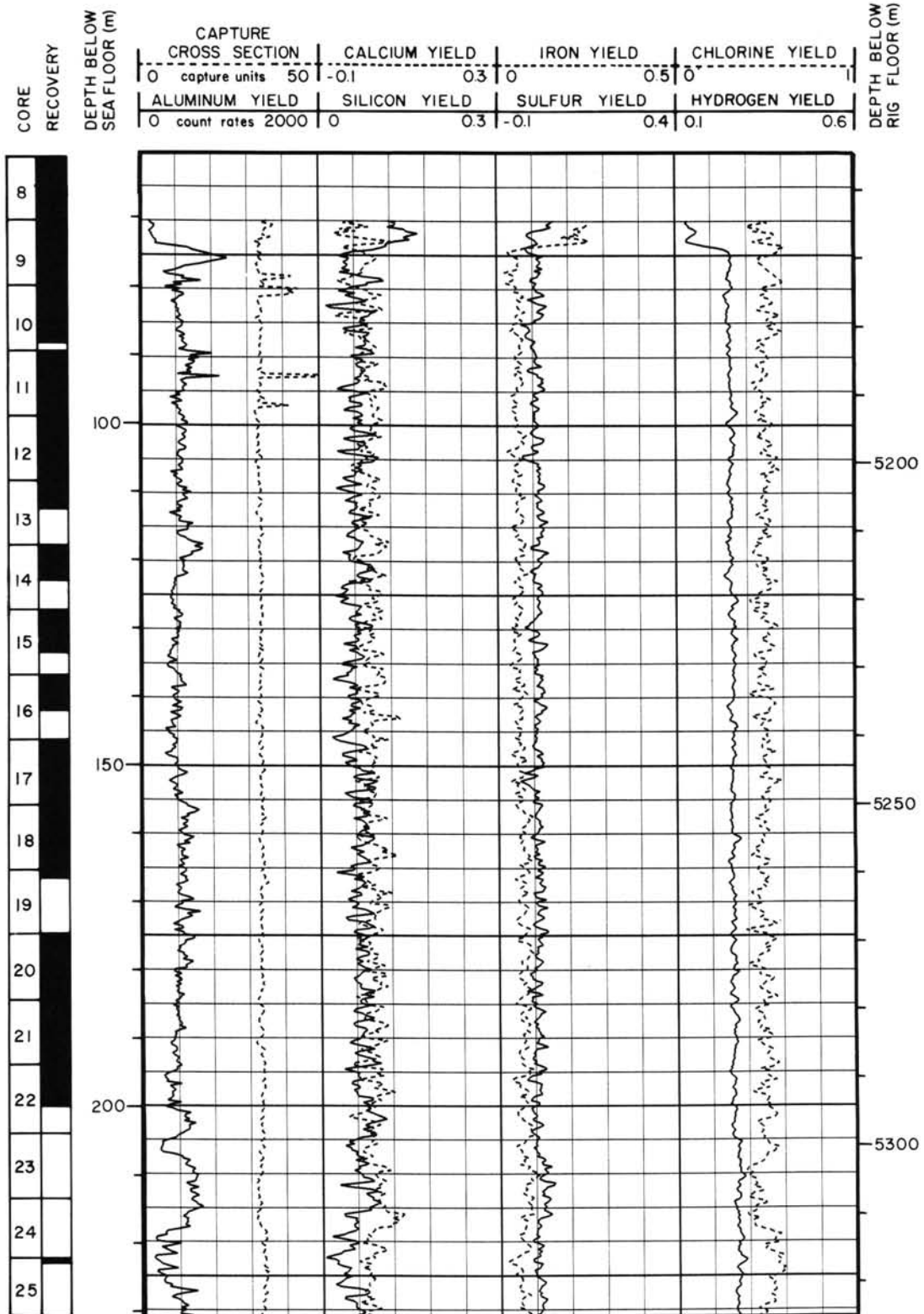
Summary logs for Site 685 (continued).



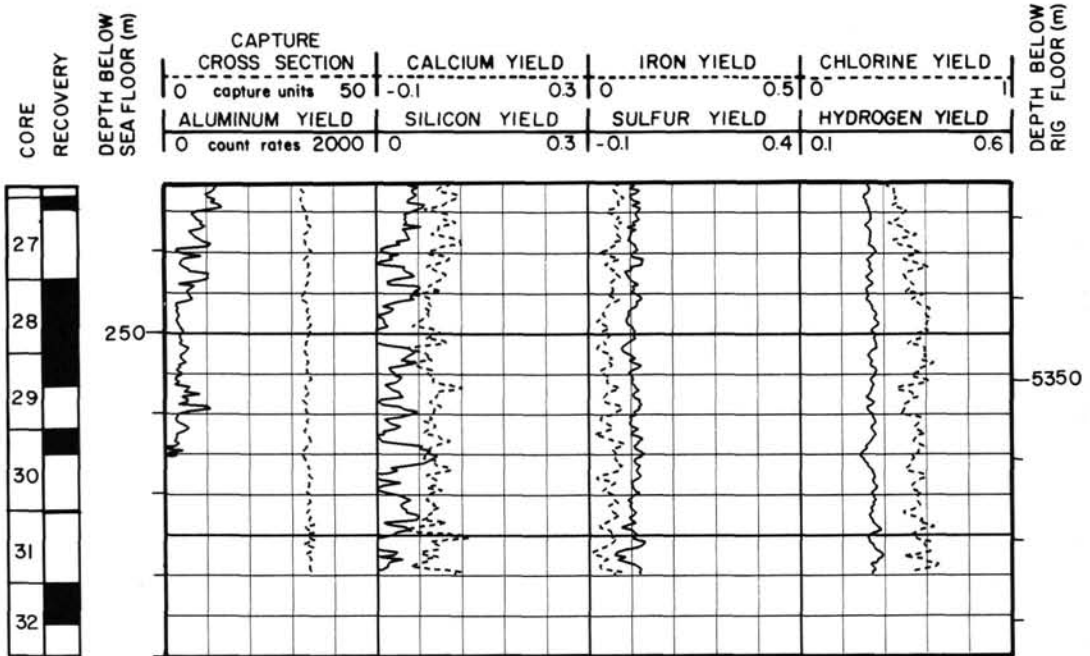
Summary logs for Site 685 (continued).



Summary logs for Site 685 (continued).

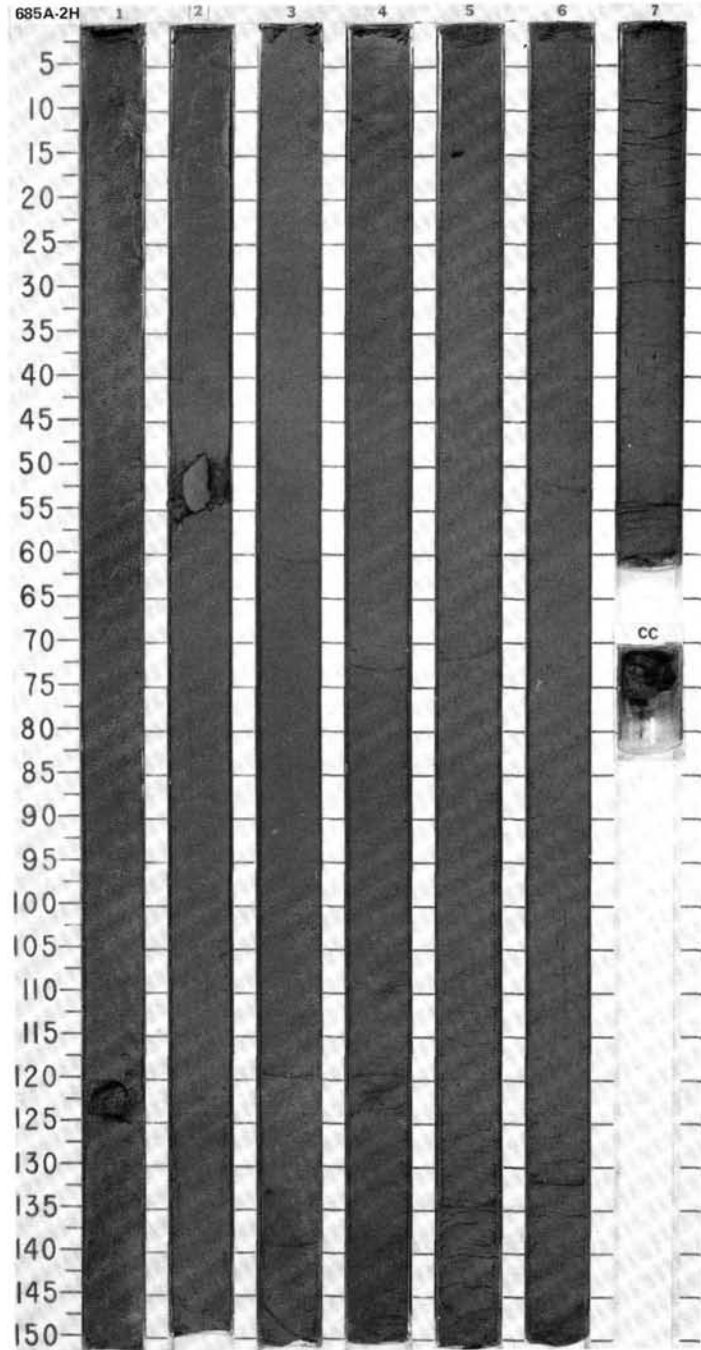


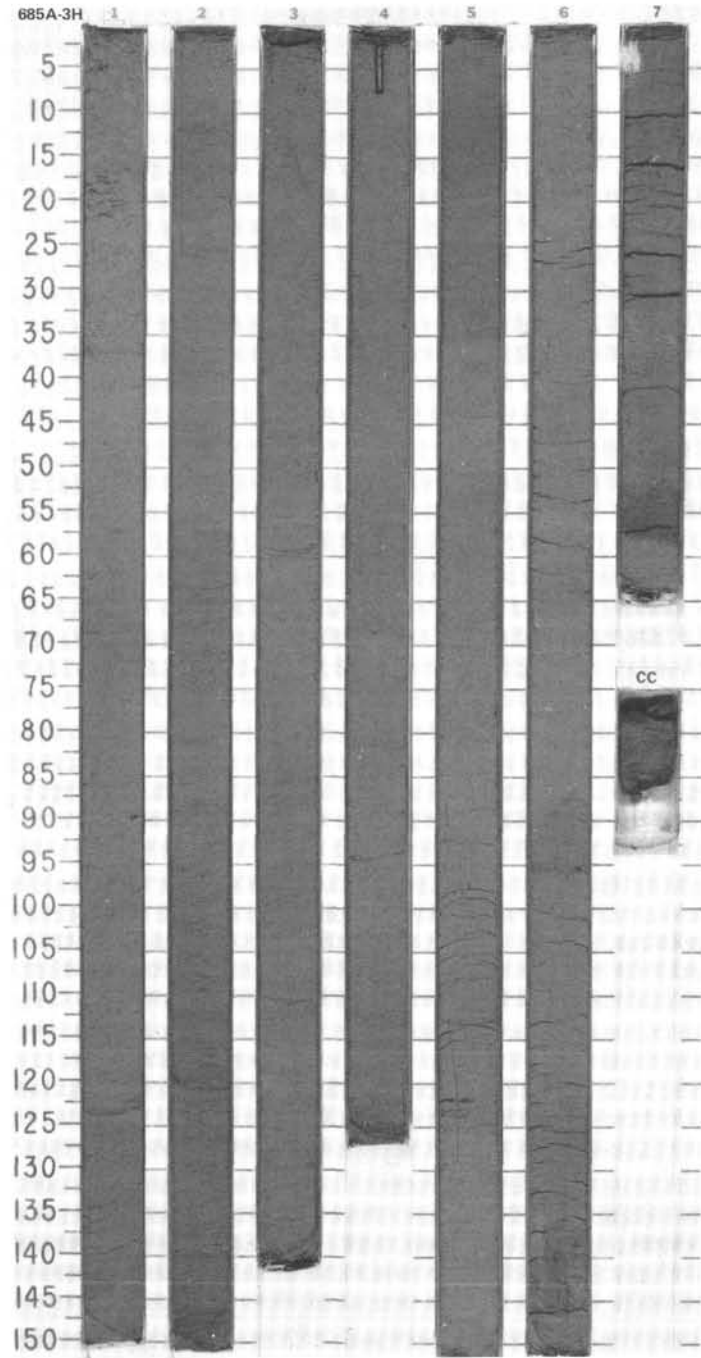
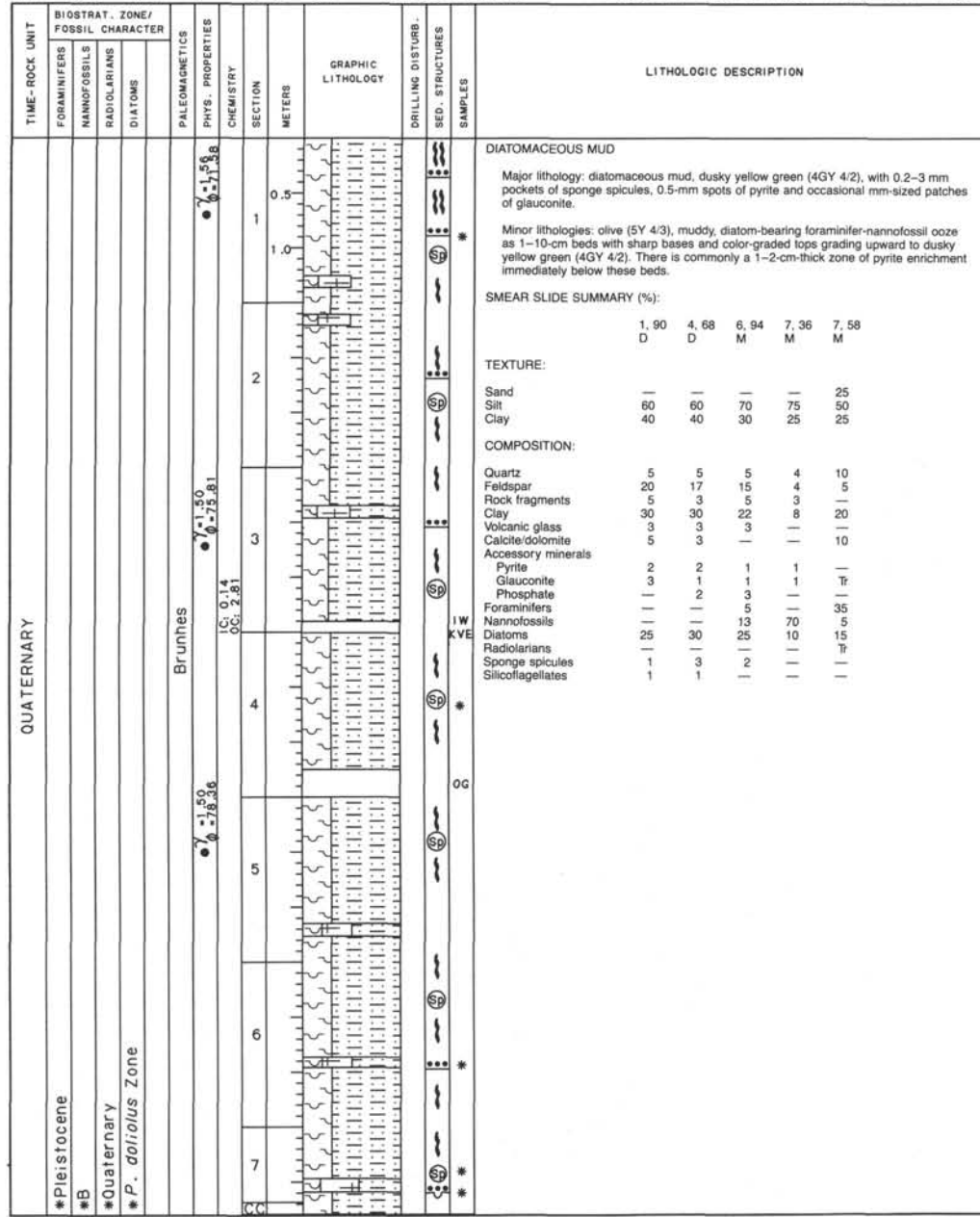
Summary logs for Site 685 (continued).



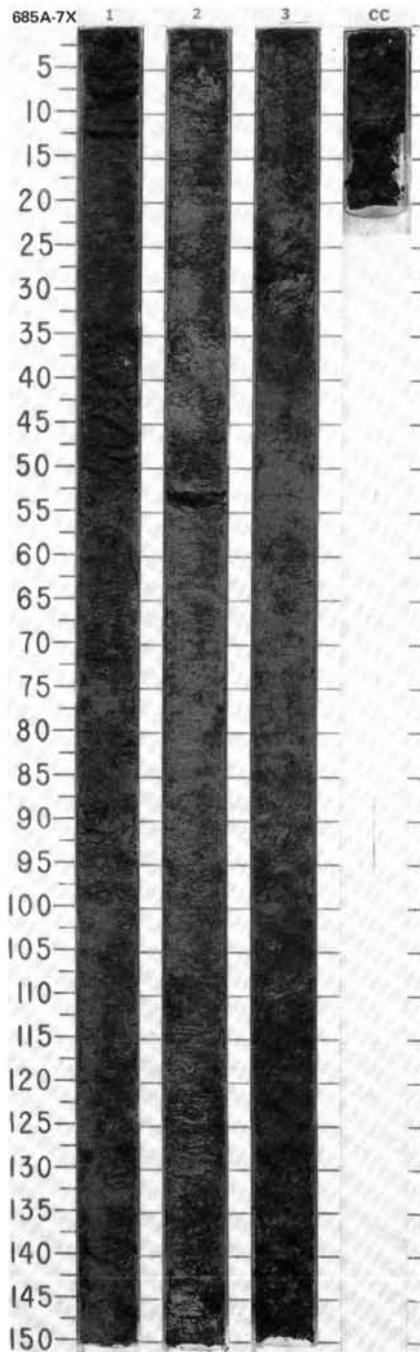
SITE 685 HOLE A CORE 2H CORED INTERVAL 5074.9-5084.4 mbsl; 4.1-13.6 mbsf

TIME-ROCK UNIT	BIOSTRAT. ZONE/ FOSSIL CHARACTER				PALEOMAGNETICS	PHYS. PROPERTIES	CHEMISTRY	SECTION	METERS	GRAPHIC LITHOLOGY	DRILLING DISTURB.	SEC. STRUCTURES	SAMPLES	LITHOLOGIC DESCRIPTION																																																																																																																																																																	
	FORAMINIFERS	NANNOFOSSILS	RADIOLARIANS	DIATOMS																																																																																																																																																																											
QUATERNARY	* Quaternary				Brunnhes	• $\gamma^1_{1.57}$ $\theta = 73.68$			0.5 1.0					<p>DIATOMACEOUS MUD</p> <p>Major lithology: diatomaceous mud, dusky yellow green (4GY 4/2), with 0.2-3 mm pockets of sponge spicules, 0.5-mm spots of pyrite and occasional mm-sized patches of glauconite.</p> <p>Minor lithologies: olive (5Y 4/3), muddy, diatom-bearing foraminifer-nannofossil ooze as 1-10 cm beds with sharp bases and color-graded tops grading upward to dusky yellow green (4GY 4/2).</p> <p>SMEAR SLIDE SUMMARY (%):</p> <table border="1"> <thead> <tr> <th></th> <th>1, 74</th> <th>1, 124</th> <th>4, 90</th> <th>4, 123</th> <th>6, 80</th> <th>7, 25</th> </tr> <tr> <th></th> <th>D</th> <th>M</th> <th>D</th> <th>M</th> <th>M</th> <th>D</th> </tr> </thead> <tbody> <tr> <td>Sand</td> <td>-</td> <td>-</td> <td>-</td> <td>5</td> <td>25</td> <td>-</td> </tr> <tr> <td>Silt</td> <td>60</td> <td>80</td> <td>40</td> <td>40</td> <td>50</td> <td>45</td> </tr> <tr> <td>Clay</td> <td>40</td> <td>20</td> <td>60</td> <td>55</td> <td>25</td> <td>55</td> </tr> </tbody> </table> <p>TEXTURE:</p> <p>Sand - - - 5 25 - Silt 60 80 40 40 50 45 Clay 40 20 60 55 25 55</p> <p>COMPOSITION:</p> <table border="1"> <thead> <tr> <th></th> <th>5</th> <th>3</th> <th>4</th> <th>3</th> <th>5</th> <th>10</th> </tr> </thead> <tbody> <tr> <td>Quartz</td> <td>5</td> <td>3</td> <td>4</td> <td>3</td> <td>5</td> <td>10</td> </tr> <tr> <td>Feldspar</td> <td>15</td> <td>3</td> <td>3</td> <td>10</td> <td>5</td> <td>10</td> </tr> <tr> <td>Rock fragments</td> <td>2</td> <td>2</td> <td>3</td> <td>2</td> <td>-</td> <td>-</td> </tr> <tr> <td>Mica</td> <td>-</td> <td>-</td> <td>-</td> <td>-</td> <td>-</td> <td>Tr</td> </tr> <tr> <td>Clay</td> <td>36</td> <td>17</td> <td>55</td> <td>10</td> <td>25</td> <td>55</td> </tr> <tr> <td>Volcanic glass</td> <td>5</td> <td>-</td> <td>-</td> <td>-</td> <td>-</td> <td>Tr</td> </tr> <tr> <td>Calcite/dolomite</td> <td>Tr</td> <td>60</td> <td>3</td> <td>5</td> <td>-</td> <td>Tr</td> </tr> </tbody> </table> <p>Accessory minerals</p> <table border="1"> <thead> <tr> <th></th> <th>3</th> <th>-</th> <th>1</th> <th>1</th> <th>60</th> <th>-</th> </tr> </thead> <tbody> <tr> <td>Pyrite</td> <td>3</td> <td>-</td> <td>1</td> <td>1</td> <td>60</td> <td>-</td> </tr> <tr> <td>Glauconite</td> <td>2</td> <td>-</td> <td>2</td> <td>1</td> <td>Tr</td> <td>-</td> </tr> <tr> <td>Phosphate</td> <td>2</td> <td>3</td> <td>-</td> <td>35</td> <td>-</td> <td>-</td> </tr> <tr> <td>Foraminifers</td> <td>-</td> <td>-</td> <td>-</td> <td>20</td> <td>-</td> <td>-</td> </tr> <tr> <td>Nannofossils</td> <td>-</td> <td>2</td> <td>-</td> <td>-</td> <td>-</td> <td>-</td> </tr> <tr> <td>Diatoms</td> <td>25</td> <td>7</td> <td>25</td> <td>15</td> <td>5</td> <td>25</td> </tr> <tr> <td>Sponge spicules</td> <td>-</td> <td>3</td> <td>4</td> <td>2</td> <td>-</td> <td>Tr</td> </tr> <tr> <td>Silicoflagellates</td> <td>-</td> <td>-</td> <td>-</td> <td>-</td> <td>-</td> <td>Tr</td> </tr> <tr> <td>Fish remains</td> <td>-</td> <td>-</td> <td>1</td> <td>-</td> <td>-</td> <td>-</td> </tr> </tbody> </table>		1, 74	1, 124	4, 90	4, 123	6, 80	7, 25		D	M	D	M	M	D	Sand	-	-	-	5	25	-	Silt	60	80	40	40	50	45	Clay	40	20	60	55	25	55		5	3	4	3	5	10	Quartz	5	3	4	3	5	10	Feldspar	15	3	3	10	5	10	Rock fragments	2	2	3	2	-	-	Mica	-	-	-	-	-	Tr	Clay	36	17	55	10	25	55	Volcanic glass	5	-	-	-	-	Tr	Calcite/dolomite	Tr	60	3	5	-	Tr		3	-	1	1	60	-	Pyrite	3	-	1	1	60	-	Glauconite	2	-	2	1	Tr	-	Phosphate	2	3	-	35	-	-	Foraminifers	-	-	-	20	-	-	Nannofossils	-	2	-	-	-	-	Diatoms	25	7	25	15	5	25	Sponge spicules	-	3	4	2	-	Tr	Silicoflagellates	-	-	-	-	-	Tr	Fish remains	-	-	1	-	-	-
		1, 74	1, 124	4, 90											4, 123	6, 80	7, 25																																																																																																																																																														
		D	M	D											M	M	D																																																																																																																																																														
	Sand	-	-	-											5	25	-																																																																																																																																																														
	Silt	60	80	40											40	50	45																																																																																																																																																														
	Clay	40	20	60											55	25	55																																																																																																																																																														
		5	3	4											3	5	10																																																																																																																																																														
Quartz	5	3	4	3	5	10																																																																																																																																																																									
Feldspar	15	3	3	10	5	10																																																																																																																																																																									
Rock fragments	2	2	3	2	-	-																																																																																																																																																																									
Mica	-	-	-	-	-	Tr																																																																																																																																																																									
Clay	36	17	55	10	25	55																																																																																																																																																																									
Volcanic glass	5	-	-	-	-	Tr																																																																																																																																																																									
Calcite/dolomite	Tr	60	3	5	-	Tr																																																																																																																																																																									
	3	-	1	1	60	-																																																																																																																																																																									
Pyrite	3	-	1	1	60	-																																																																																																																																																																									
Glauconite	2	-	2	1	Tr	-																																																																																																																																																																									
Phosphate	2	3	-	35	-	-																																																																																																																																																																									
Foraminifers	-	-	-	20	-	-																																																																																																																																																																									
Nannofossils	-	2	-	-	-	-																																																																																																																																																																									
Diatoms	25	7	25	15	5	25																																																																																																																																																																									
Sponge spicules	-	3	4	2	-	Tr																																																																																																																																																																									
Silicoflagellates	-	-	-	-	-	Tr																																																																																																																																																																									
Fish remains	-	-	1	-	-	-																																																																																																																																																																									
	* non diagnostic							VOID	CC																																																																																																																																																																						
	* insignificant																																																																																																																																																																														
	* Quaternary																																																																																																																																																																														
	* P. dolioolus Zone																																																																																																																																																																														
	• $\gamma^1_{1.55}$ $\theta = 73.69$																																																																																																																																																																														
	• $\gamma^1_{1.52}$ $\theta = 73.66$																																																																																																																																																																														
	* Quaternary																																																																																																																																																																														

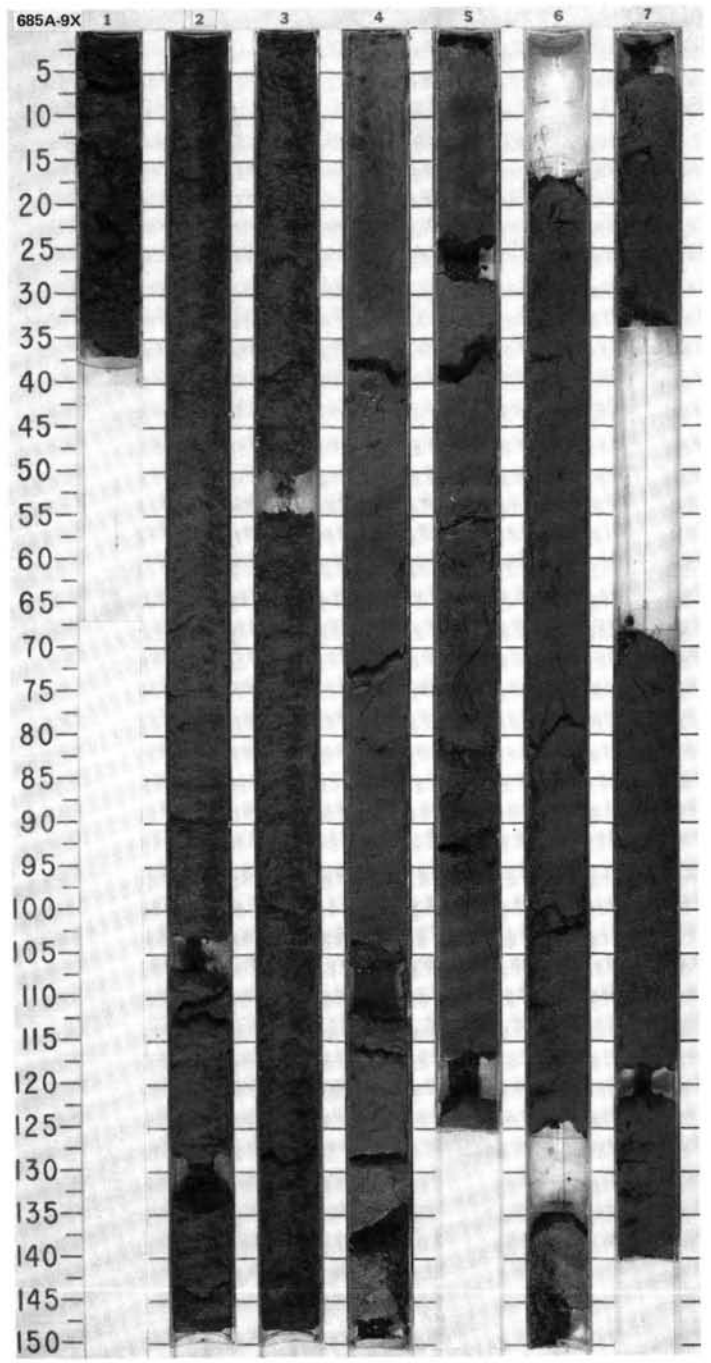




TIME - ROCK UNIT	BIOSTRAT. ZONE/ FOSSIL CHARACTER				PALEOMAGNETICS	PHYS. PROPERTIES	CHEMISTRY	SECTION	METERS	GRAPHIC LITHOLOGY	DRILLING DISTURB.	SED. STRUCTURES	SAMPLES	LITHOLOGIC DESCRIPTION																																																																																																									
	FORAMINIFERS	NANNOFOSSILS	RADIOLARIANS	DIATOMS																																																																																																																			
QUATERNARY	* Pleistocene	* insignificant	* Quaternary	* <i>N. reinholdii</i> Zone	Brunhes	• $\gamma = 1.50$ • $\delta = 73.00$		1	0.5 1.0					DIATOMACEOUS MUD Major lithology: diatomaceous mud, dark greenish gray to dark olive gray (5GY 4/1 to 5Y 3/2), heavily mottled with very dark gray (N 4) pyrite-rich mud with 0.2-3-mm pockets of sponge spicules. Predominantly black to very dark gray (N 2 and N 4) from Section 3, 70 cm, to base. But N.B., black color fades to greenish gray and dark olive gray quickly on oxidation. Minor lithologies: olive (5Y 4/3), muddy, diatom-bearing foraminifer-nannofossil ooze as occasional 5-8-cm beds. SMEAR SLIDE SUMMARY (%): <table border="1"> <tr> <td></td> <td>1, 100</td> <td>2, 77</td> <td>3, 37</td> <td>3, 116</td> </tr> <tr> <td></td> <td>D</td> <td>D</td> <td>M</td> <td>M</td> </tr> </table> TEXTURE: <table border="1"> <tr> <td>Sand</td> <td>10</td> <td>5</td> <td>50</td> <td>10</td> </tr> <tr> <td>Silt</td> <td>20</td> <td>60</td> <td>15</td> <td>40</td> </tr> <tr> <td>Clay</td> <td>70</td> <td>35</td> <td>35</td> <td>50</td> </tr> </table> COMPOSITION: <table border="1"> <tr> <td>Quartz</td> <td>5</td> <td>4</td> <td>10</td> <td>5</td> </tr> <tr> <td>Feldspar</td> <td>2</td> <td>3</td> <td>10</td> <td>2</td> </tr> <tr> <td>Rock fragments</td> <td>5</td> <td>3</td> <td>5</td> <td>5</td> </tr> <tr> <td>Clay</td> <td>45</td> <td>25</td> <td>10</td> <td>40</td> </tr> <tr> <td>Volcanic glass</td> <td>Tr</td> <td>—</td> <td>—</td> <td>5</td> </tr> <tr> <td>Calcite/dolomite</td> <td>—</td> <td>1</td> <td>3</td> <td>—</td> </tr> <tr> <td>Accessory minerals</td> <td>—</td> <td>—</td> <td>2</td> <td>—</td> </tr> <tr> <td>Pyrite</td> <td>2</td> <td>2</td> <td>5</td> <td>8</td> </tr> <tr> <td>Glauconite</td> <td>Tr</td> <td>Tr</td> <td>—</td> <td>—</td> </tr> <tr> <td>Micrite</td> <td>5</td> <td>—</td> <td>—</td> <td>5</td> </tr> <tr> <td>Foraminifers</td> <td>—</td> <td>Tr</td> <td>20</td> <td>Tr</td> </tr> <tr> <td>Nannofossils</td> <td>3</td> <td>—</td> <td>25</td> <td>Tr</td> </tr> <tr> <td>Diatoms</td> <td>33</td> <td>55</td> <td>10</td> <td>25</td> </tr> <tr> <td>Radiolarians</td> <td>Tr</td> <td>3</td> <td>—</td> <td>Tr</td> </tr> <tr> <td>Sponge spicules</td> <td>Tr</td> <td>2</td> <td>—</td> <td>5</td> </tr> <tr> <td>Silicoflagellates</td> <td>—</td> <td>2</td> <td>—</td> <td>—</td> </tr> </table>		1, 100	2, 77	3, 37	3, 116		D	D	M	M	Sand	10	5	50	10	Silt	20	60	15	40	Clay	70	35	35	50	Quartz	5	4	10	5	Feldspar	2	3	10	2	Rock fragments	5	3	5	5	Clay	45	25	10	40	Volcanic glass	Tr	—	—	5	Calcite/dolomite	—	1	3	—	Accessory minerals	—	—	2	—	Pyrite	2	2	5	8	Glauconite	Tr	Tr	—	—	Micrite	5	—	—	5	Foraminifers	—	Tr	20	Tr	Nannofossils	3	—	25	Tr	Diatoms	33	55	10	25	Radiolarians	Tr	3	—	Tr	Sponge spicules	Tr	2	—	5	Silicoflagellates	—	2	—	—
	1, 100	2, 77	3, 37	3, 116																																																																																																																			
	D	D	M	M																																																																																																																			
Sand	10	5	50	10																																																																																																																			
Silt	20	60	15	40																																																																																																																			
Clay	70	35	35	50																																																																																																																			
Quartz	5	4	10	5																																																																																																																			
Feldspar	2	3	10	2																																																																																																																			
Rock fragments	5	3	5	5																																																																																																																			
Clay	45	25	10	40																																																																																																																			
Volcanic glass	Tr	—	—	5																																																																																																																			
Calcite/dolomite	—	1	3	—																																																																																																																			
Accessory minerals	—	—	2	—																																																																																																																			
Pyrite	2	2	5	8																																																																																																																			
Glauconite	Tr	Tr	—	—																																																																																																																			
Micrite	5	—	—	5																																																																																																																			
Foraminifers	—	Tr	20	Tr																																																																																																																			
Nannofossils	3	—	25	Tr																																																																																																																			
Diatoms	33	55	10	25																																																																																																																			
Radiolarians	Tr	3	—	Tr																																																																																																																			
Sponge spicules	Tr	2	—	5																																																																																																																			
Silicoflagellates	—	2	—	—																																																																																																																			
						• $\gamma = 1.50$ • $\delta = 74.12$		2																																																																																																															
								3																																																																																																															
								CC																																																																																																															

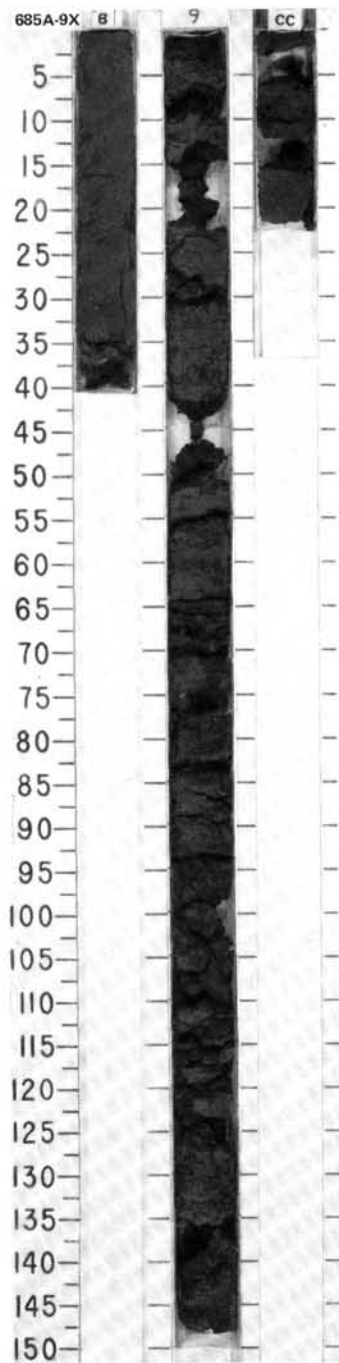


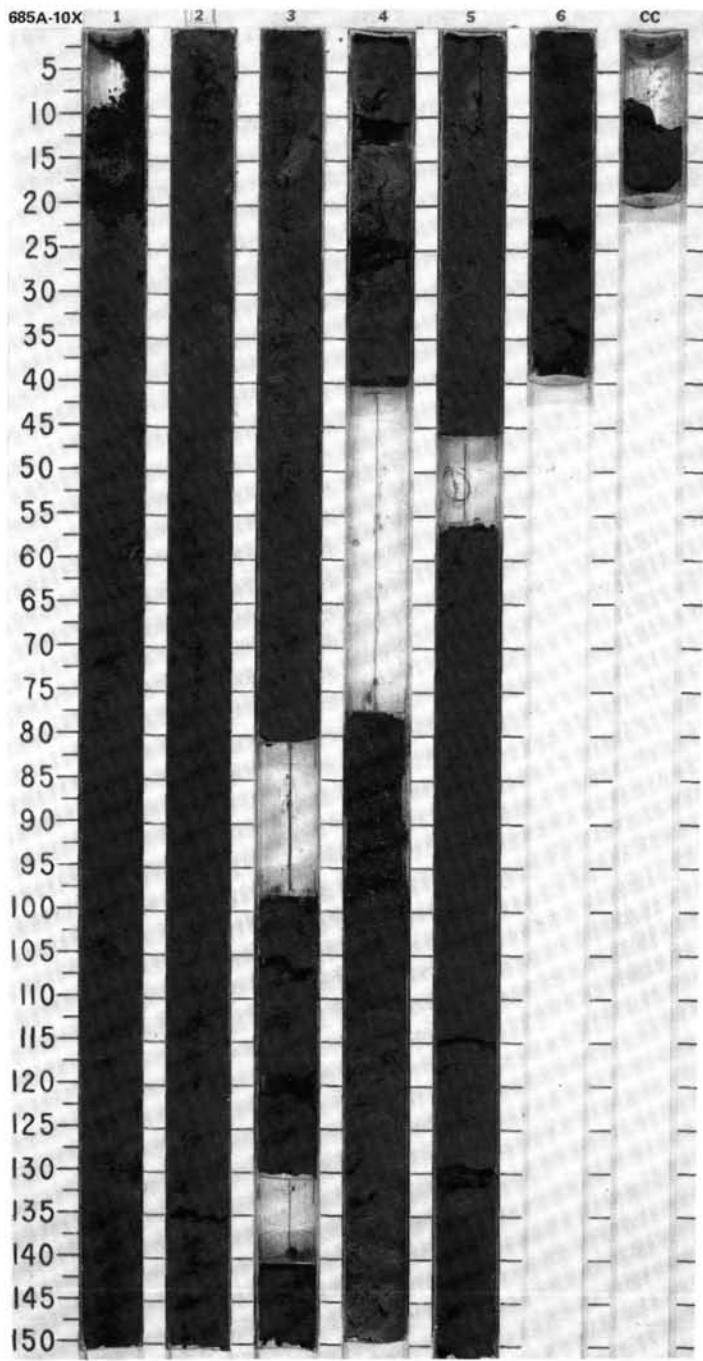
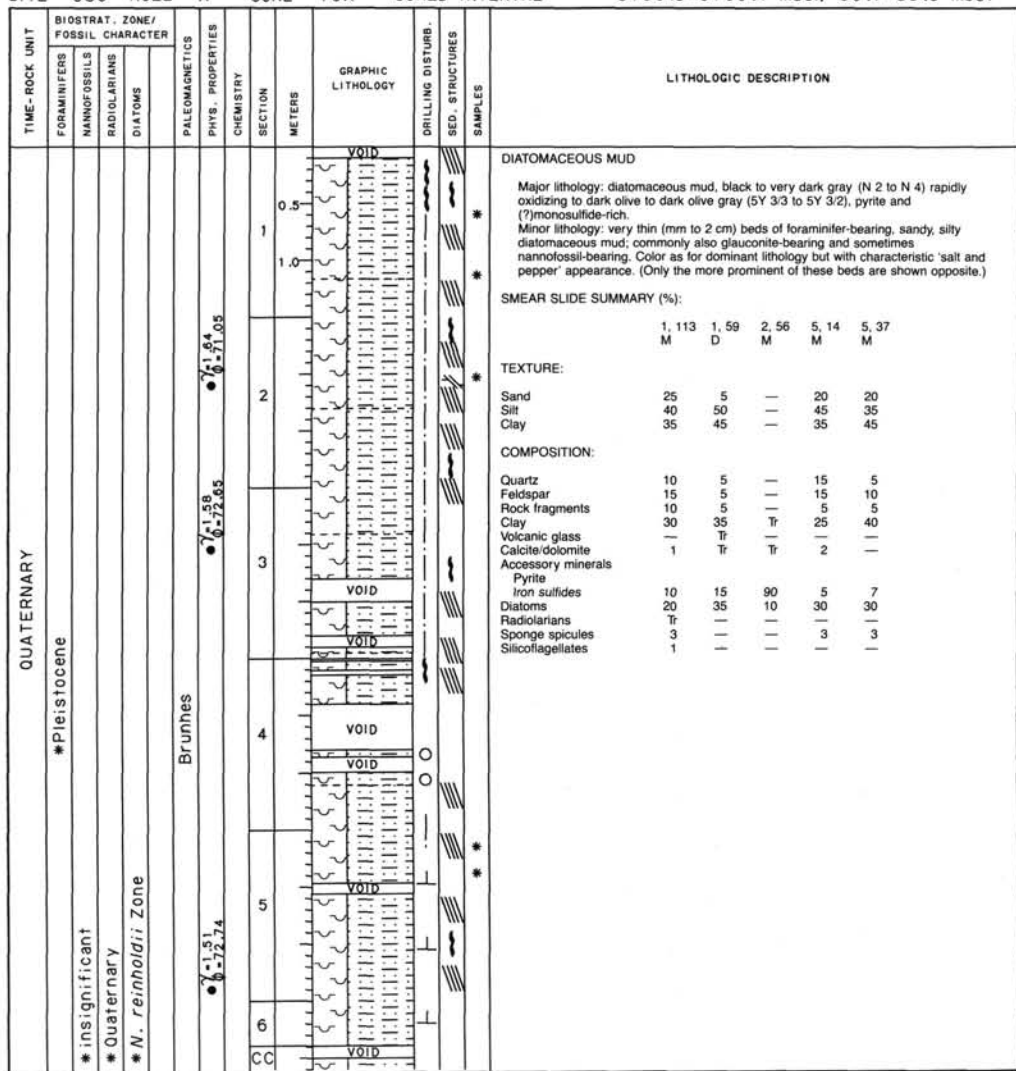
TIME-ROCK UNIT	BIOSTRAT. ZONE/ FOSSIL CHARACTER			PALEOMAGNETICS	PHYS. PROPERTIES	CHEMISTRY	SECTION	METERS	GRAPHIC LITHOLOGY	DRILLING DISTURB.	SED. STRUCTURES	SAMPLES	LITHOLOGIC DESCRIPTION																																																																																																																		
	FORAMINIFERS	NANNOFOSSILS	RADIOLARIANS											DIATOMS																																																																																																																	
QUATERNARY								0.5					<p>DIATOMACEOUS MUD</p> <p>Major lithology: Section 1, 0 cm, to Section 3, 100 cm: diatomaceous mud, predominantly black (N 2), pyrite-bearing, with subordinate dark greenish gray to dark olive gray (5GY 4/1, 5Y 3/2), with 0.2-3-mm pockets of sponge spicules. Section 3, 100 cm, to CC: diatomaceous mud, black to very dark gray (N 2 to N 4) rapidly oxidizing to dark olive to dark olive gray (5Y 3/3 to 5Y 3/2), pyrite- and ?monosulfide-rich.</p> <p>Minor lithologies: 1. olive (5Y 4/3), muddy, diatom-bearing nannofossil-foraminifer ooze as occasional thin beds in Section 1, 0 cm, to Section 3, 100 cm. 2. very thin (mm to 2 cm) beds of foraminifer-bearing, sandy, silty diatomaceous mud; commonly also glauconite-bearing and sometimes nannofossil-bearing. Color as for dominant lithology but with characteristic 'salt and pepper' appearance. (Only the more prominent of these beds are shown opposite.)</p> <p>* SMEAR SLIDE SUMMARY (%):</p> <table border="1"> <tr> <td></td> <td>2, 72</td> <td>4, 22</td> <td>4, 77</td> <td>6, 94</td> <td>6, 47</td> </tr> <tr> <td></td> <td>D</td> <td>M</td> <td>D</td> <td>D</td> <td>M</td> </tr> </table> <p>TEXTURE:</p> <table border="1"> <tr> <td>Sand</td> <td>15</td> <td>40</td> <td>5</td> <td>5</td> <td>—</td> </tr> <tr> <td>Silt</td> <td>25</td> <td>30</td> <td>35</td> <td>40</td> <td>40</td> </tr> <tr> <td>Clay</td> <td>60</td> <td>30</td> <td>60</td> <td>55</td> <td>60</td> </tr> </table> <p>COMPOSITION:</p> <table border="1"> <tr> <td>Quartz</td> <td>5</td> <td>10</td> <td>Tr</td> <td>5</td> <td>5</td> </tr> <tr> <td>Feldspar</td> <td>5</td> <td>15</td> <td>5</td> <td>5</td> <td>5</td> </tr> <tr> <td>Rock fragments</td> <td>5</td> <td>5</td> <td>—</td> <td>—</td> <td>—</td> </tr> <tr> <td>Mica</td> <td>—</td> <td>—</td> <td>—</td> <td>—</td> <td>10</td> </tr> <tr> <td>Clay</td> <td>40</td> <td>20</td> <td>50</td> <td>40</td> <td>60</td> </tr> <tr> <td>Calcite/dolomite</td> <td>Tr</td> <td>Tr</td> <td>2</td> <td>—</td> <td>5</td> </tr> </table> <p>Accessory minerals</p> <table border="1"> <tr> <td>Pyrite</td> <td>—</td> <td>—</td> <td>—</td> <td>—</td> <td>—</td> </tr> <tr> <td>Iron sulfides</td> <td>10</td> <td>5</td> <td>3</td> <td>20</td> <td>—</td> </tr> <tr> <td>Foraminifers</td> <td>—</td> <td>25</td> <td>Tr</td> <td>—</td> <td>5</td> </tr> <tr> <td>Nannofossils</td> <td>—</td> <td>5</td> <td>—</td> <td>—</td> <td>—</td> </tr> <tr> <td>Diatoms</td> <td>35</td> <td>15</td> <td>35</td> <td>25</td> <td>10</td> </tr> <tr> <td>Radiolarians</td> <td>—</td> <td>—</td> <td>—</td> <td>Tr</td> <td>Tr</td> </tr> <tr> <td>Sponge spicules</td> <td>—</td> <td>—</td> <td>—</td> <td>Tr</td> <td>Tr</td> </tr> <tr> <td>Silicoflagellates</td> <td>—</td> <td>—</td> <td>—</td> <td>Tr</td> <td>Tr</td> </tr> </table>		2, 72	4, 22	4, 77	6, 94	6, 47		D	M	D	D	M	Sand	15	40	5	5	—	Silt	25	30	35	40	40	Clay	60	30	60	55	60	Quartz	5	10	Tr	5	5	Feldspar	5	15	5	5	5	Rock fragments	5	5	—	—	—	Mica	—	—	—	—	10	Clay	40	20	50	40	60	Calcite/dolomite	Tr	Tr	2	—	5	Pyrite	—	—	—	—	—	Iron sulfides	10	5	3	20	—	Foraminifers	—	25	Tr	—	5	Nannofossils	—	5	—	—	—	Diatoms	35	15	35	25	10	Radiolarians	—	—	—	Tr	Tr	Sponge spicules	—	—	—	Tr	Tr	Silicoflagellates	—	—	—	Tr	Tr
		2, 72	4, 22	4, 77	6, 94	6, 47																																																																																																																									
		D	M	D	D	M																																																																																																																									
	Sand	15	40	5	5	—																																																																																																																									
	Silt	25	30	35	40	40																																																																																																																									
	Clay	60	30	60	55	60																																																																																																																									
	Quartz	5	10	Tr	5	5																																																																																																																									
Feldspar	5	15	5	5	5																																																																																																																										
Rock fragments	5	5	—	—	—																																																																																																																										
Mica	—	—	—	—	10																																																																																																																										
Clay	40	20	50	40	60																																																																																																																										
Calcite/dolomite	Tr	Tr	2	—	5																																																																																																																										
Pyrite	—	—	—	—	—																																																																																																																										
Iron sulfides	10	5	3	20	—																																																																																																																										
Foraminifers	—	25	Tr	—	5																																																																																																																										
Nannofossils	—	5	—	—	—																																																																																																																										
Diatoms	35	15	35	25	10																																																																																																																										
Radiolarians	—	—	—	Tr	Tr																																																																																																																										
Sponge spicules	—	—	—	Tr	Tr																																																																																																																										
Silicoflagellates	—	—	—	Tr	Tr																																																																																																																										
				7-1.53 6-73.01			1	VOID																																																																																																																							
							2																																																																																																																								
							3	VOID																																																																																																																							
							4																																																																																																																								
				7-1.53 6-73.10			5	VOID																																																																																																																							
							6	VOID																																																																																																																							
							7	VOID																																																																																																																							

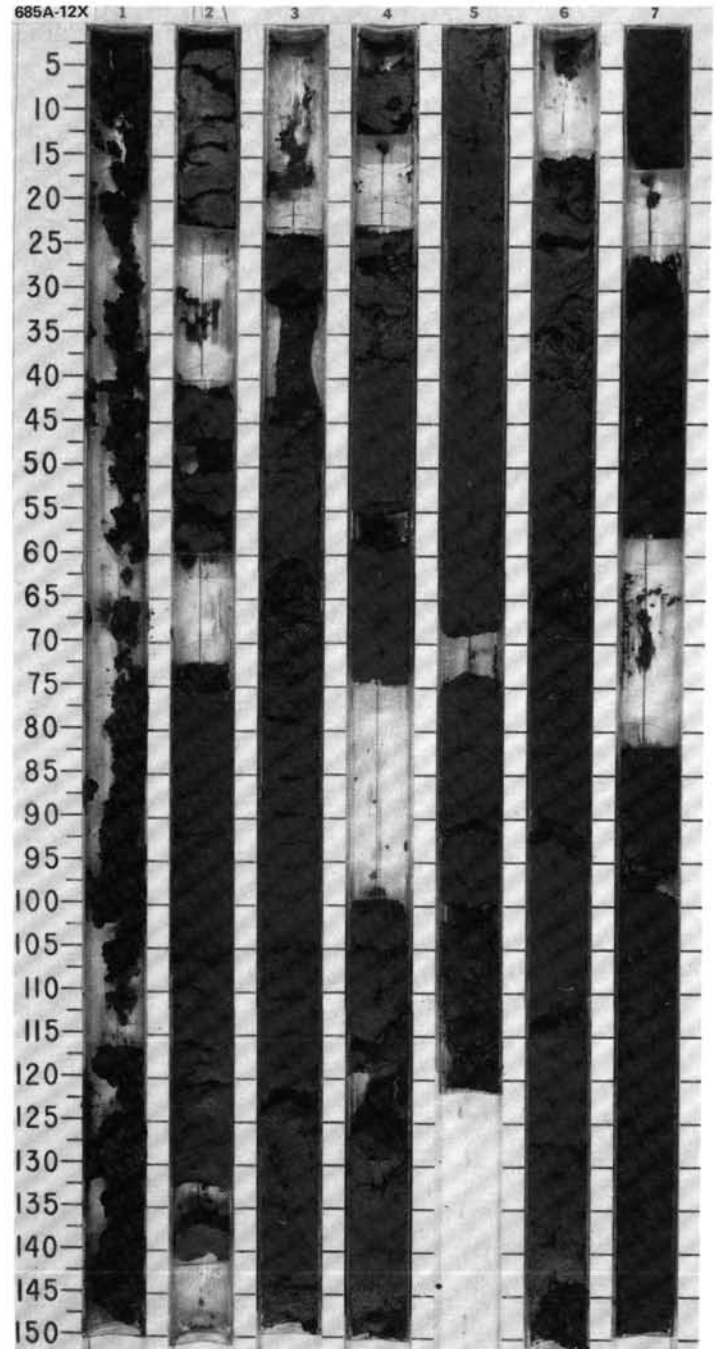
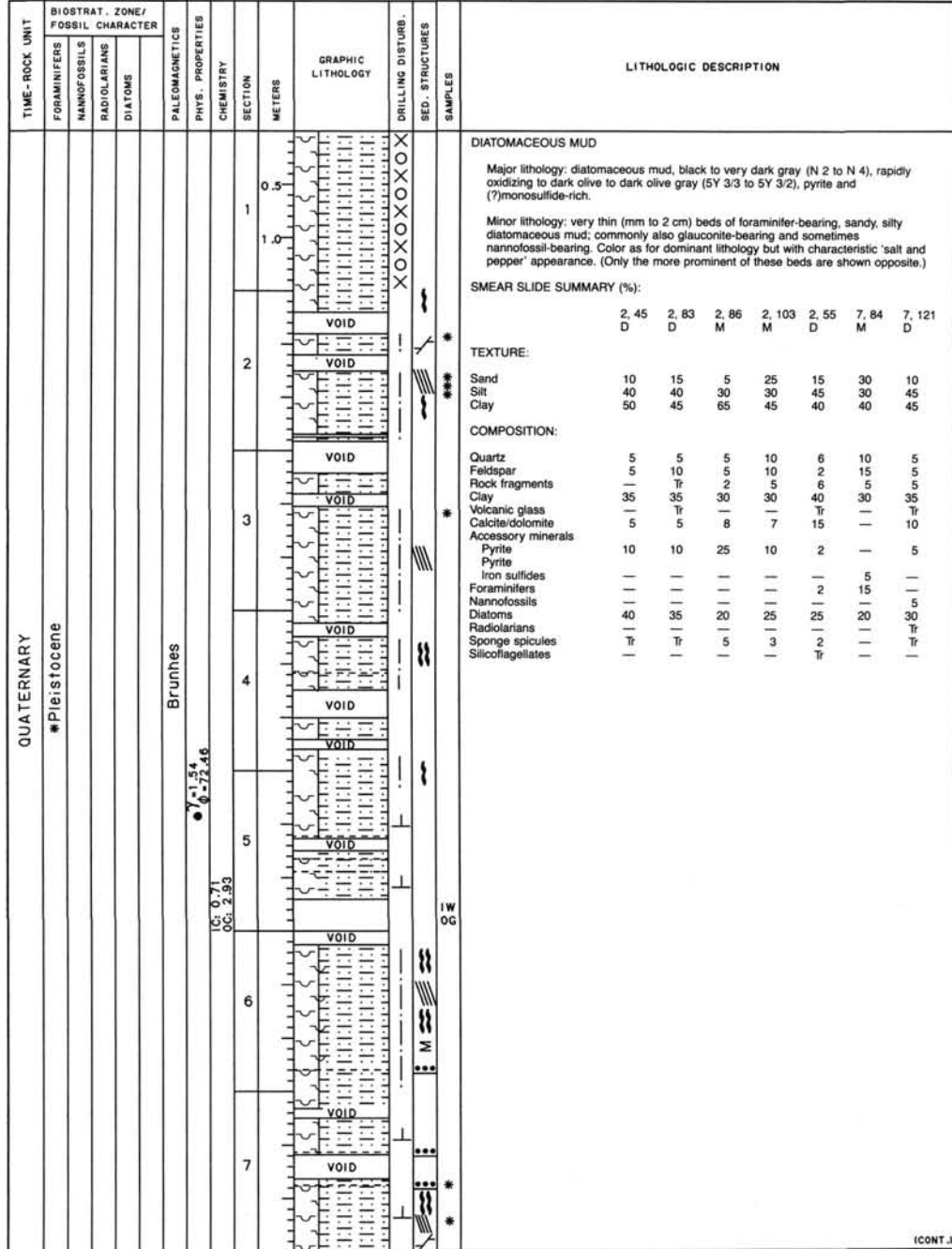


SITE 685 HOLE A CORE 9X CORED INTERVAL 5141.4-5150.9 mbsl; 70.6-80.1 mbsf

TIME-ROCK UNIT	BIOSTRAT. ZONE/ FOSSIL CHARACTER				PALEOMAGNETICS	PHYS. PROPERTIES	CHEMISTRY	SECTION	METERS	GRAPHIC LITHOLOGY	DRILLING DISTURB. SED. STRUCTURES	SAMPLES	LITHOLOGIC DESCRIPTION
	FORAMINIFERS	NANNOFOSSILS	RADIOLARIANS	DIAZONS									
QUATERNARY	* Pleistocene * insignificant * Quaternary * <i>N. reinholdii</i> Zone												(cont.)

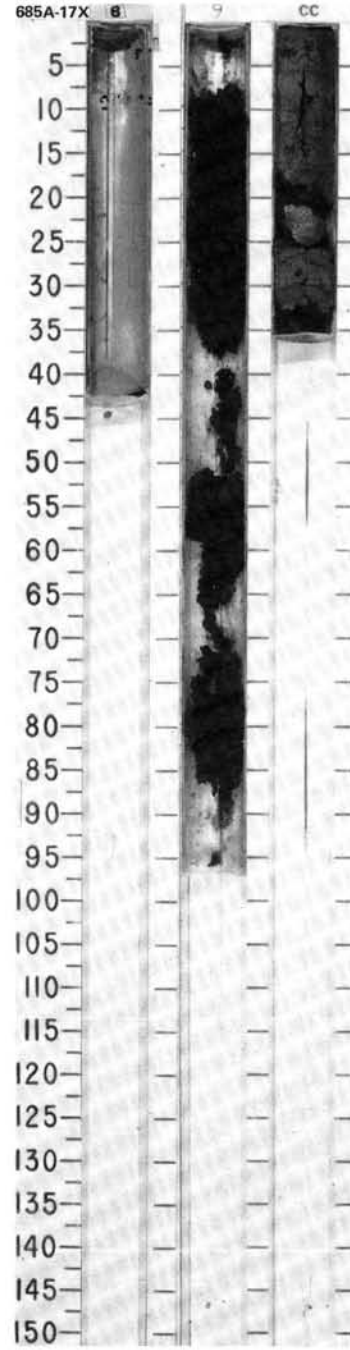






SITE 685 HOLE A CORE 17X CORED INTERVAL 5217.4-5226.9 mbsl; 146.6-156.1 mbsf

TIME-ROCK UNIT	BIOSTRAT. ZONE/ FOSSIL CHARACTER				PALEOMAGNETICS	PHYS. PROPERTIES	CHEMISTRY	SECTION	METERS	GRAPHIC LITHOLOGY	DRILLING DISTURB.	SED. STRUCTURES	SAMPLES	LITHOLOGIC DESCRIPTION
	FORAMINIFERS	NANNOFOSSILS	RADIOLARIANS	DIATOMS										
QUATERNARY	*Pleistocene ?	*B	*Quaternary	* <i>N. reinholdii</i> Zone					0.5 1.0	VOID				(CONT.)

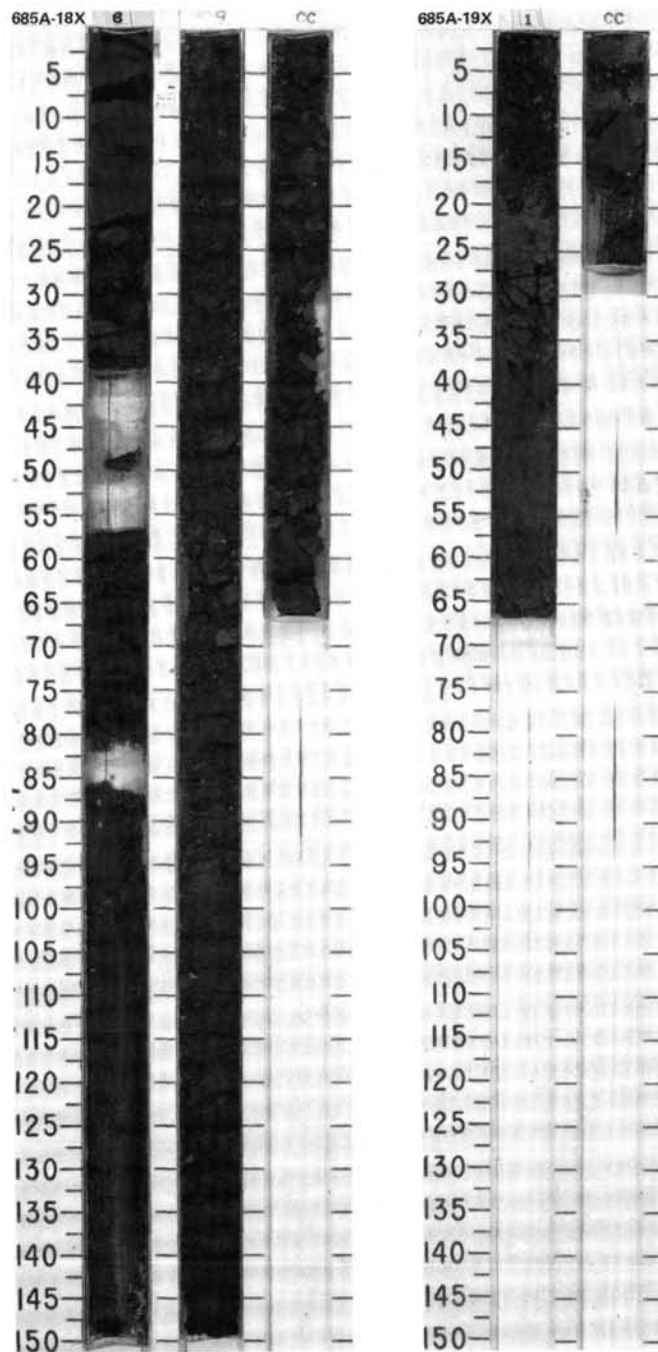


SITE 685 HOLE A CORE 18X CORED INTERVAL 5226.9-5236.4 mbsl; 156.1-165.6 mbsf

TIME-ROCK UNIT	BIOSTRAT. ZONE/ FOSSIL CHARACTER				PALEOMAGNETICS	PHYS. PROPERTIES	CHEMISTRY	SECTION	METERS	GRAPHIC LITHOLOGY	DRILLING DISTURB. SED. STRUCTURES	SAMPLES	LITHOLOGIC DESCRIPTION
	FORAMINIFERS	NANNOFOSSILS	RADIOLARIANS	DIATOMS									
QUATERNARY	*N21 to N22	*B	*Quaternary	* <i>N. reinholdii</i> Zone					0.5 VOID 1.0 VOID			*	(CONT.)

SITE 685 HOLE A CORE 19X CORED INTERVAL 5236.4-5245.9 mbsl; 165.6-175.1 mbsf

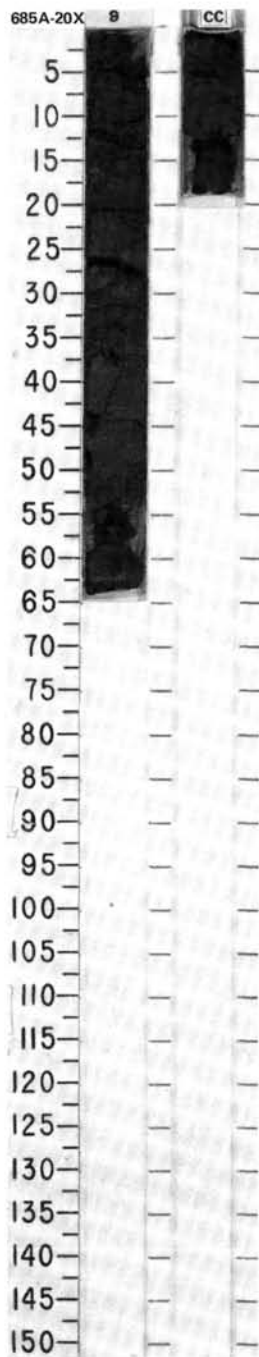
TIME-ROCK UNIT	BIOSTRAT. ZONE/ FOSSIL CHARACTER				PALEOMAGNETICS	PHYS. PROPERTIES	CHEMISTRY	SECTION	METERS	GRAPHIC LITHOLOGY	DRILLING DISTURB. SED. STRUCTURES	SAMPLES	LITHOLOGIC DESCRIPTION																																																																		
	FORAMINIFERS	NANNOFOSSILS	RADIOLARIANS	DIATOMS																																																																											
QUATERNARY	N21 to N22 *	Quaternary *	<i>N. reinholdii</i> Zone *					1 0.5				**	<p>DIATOMACEOUS MUD</p> <p>Major lithology: diatomaceous mud, black to very dark gray (5Y 2.5/1, 5Y 3/1), rapidly changing to dark olive to dark olive gray (5Y 3/3 to 5Y 3/2). Relatively micrite-rich and pyritic.</p> <p>Minor lithology: very thin (mm to 2 cm) beds of foraminifer-bearing, sandy, silty diatomaceous mud; commonly also glauconite-bearing and sometimes nannofossil-bearing. Color as for dominant lithology but with characteristic 'salt and pepper' appearance. (Only the more prominent of these beds are shown opposite.)</p> <p>SMEAR SLIDE SUMMARY (%):</p> <table border="1"> <tr> <td></td> <td>1, 43</td> <td>1, 48</td> </tr> <tr> <td></td> <td>D</td> <td>D</td> </tr> </table> <p>TEXTURE:</p> <table border="1"> <tr> <td>Sand</td> <td>5</td> <td>5</td> </tr> <tr> <td>Silt</td> <td>30</td> <td>45</td> </tr> <tr> <td>Clay</td> <td>65</td> <td>50</td> </tr> </table> <p>COMPOSITION:</p> <table border="1"> <tr> <td>Quartz</td> <td>5</td> <td>7</td> </tr> <tr> <td>Feldspar</td> <td>3</td> <td>5</td> </tr> <tr> <td>Rock fragments</td> <td>2</td> <td>3</td> </tr> <tr> <td>Clay</td> <td>30</td> <td>35</td> </tr> <tr> <td>Volcanic glass</td> <td>5</td> <td>—</td> </tr> <tr> <td>Calcite/dolomite</td> <td>2</td> <td>—</td> </tr> <tr> <td>Accessory minerals</td> <td></td> <td></td> </tr> <tr> <td> Pyrite</td> <td>5</td> <td>3</td> </tr> <tr> <td> Glauconite</td> <td>—</td> <td>2</td> </tr> <tr> <td> Micrite</td> <td>15</td> <td>5</td> </tr> <tr> <td>Foraminifers</td> <td>3</td> <td>5</td> </tr> <tr> <td>Nannofossils</td> <td>Tr</td> <td>Tr</td> </tr> <tr> <td>Diatoms</td> <td>30</td> <td>35</td> </tr> <tr> <td>Radiolarians</td> <td>Tr</td> <td>Tr</td> </tr> <tr> <td>Sponge spicules</td> <td>Tr</td> <td>Tr</td> </tr> <tr> <td>Silicoflagellates</td> <td>Tr</td> <td>—</td> </tr> <tr> <td>Pellets</td> <td>Tr</td> <td>—</td> </tr> </table>		1, 43	1, 48		D	D	Sand	5	5	Silt	30	45	Clay	65	50	Quartz	5	7	Feldspar	3	5	Rock fragments	2	3	Clay	30	35	Volcanic glass	5	—	Calcite/dolomite	2	—	Accessory minerals			Pyrite	5	3	Glauconite	—	2	Micrite	15	5	Foraminifers	3	5	Nannofossils	Tr	Tr	Diatoms	30	35	Radiolarians	Tr	Tr	Sponge spicules	Tr	Tr	Silicoflagellates	Tr	—	Pellets	Tr	—
	1, 43	1, 48																																																																													
	D	D																																																																													
Sand	5	5																																																																													
Silt	30	45																																																																													
Clay	65	50																																																																													
Quartz	5	7																																																																													
Feldspar	3	5																																																																													
Rock fragments	2	3																																																																													
Clay	30	35																																																																													
Volcanic glass	5	—																																																																													
Calcite/dolomite	2	—																																																																													
Accessory minerals																																																																															
Pyrite	5	3																																																																													
Glauconite	—	2																																																																													
Micrite	15	5																																																																													
Foraminifers	3	5																																																																													
Nannofossils	Tr	Tr																																																																													
Diatoms	30	35																																																																													
Radiolarians	Tr	Tr																																																																													
Sponge spicules	Tr	Tr																																																																													
Silicoflagellates	Tr	—																																																																													
Pellets	Tr	—																																																																													



SITE 685

SITE 685 HOLE A CORE 20X CORED INTERVAL 5245.9-5255.4 mbsl; 175.1-184.6 mbsf

TIME-ROCK UNIT	BIOSTRAT. ZONE/ FOSSIL CHARACTER	PALEOMAGNETICS	PHYS. PROPERTIES	CHEMISTRY	SECTION	METERS	GRAPHIC LITHOLOGY	DRILLING DISTURB. SED. STRUCTURES	SAMPLES	LITHOLOGIC DESCRIPTION
B *										(CONT.)
B *	Quaternary* <i>N. reinholdii</i> Zone*					0.5				



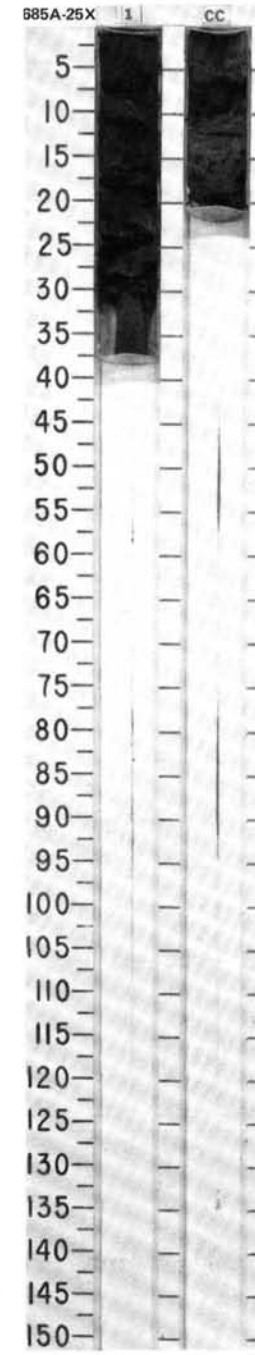
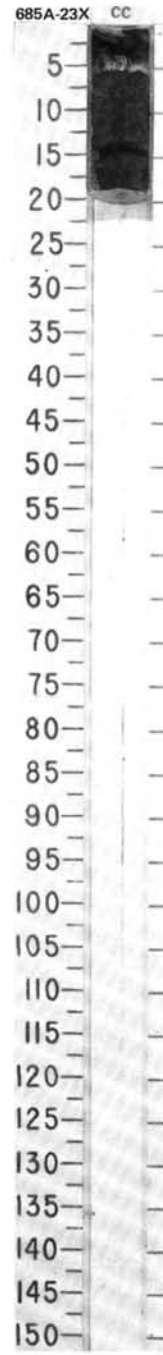
SITE 685 HOLE A CORE 23X CORED INTERVAL 5274.4-5283.9 mbsl; 203.6-213.1 mbsf

TIME-ROCK UNIT	BIOSTRAT. ZONE/ FOSSIL CHARACTER				PALEOMAGNETICS	PHYS. PROPERTIES	CHEMISTRY	SECTION	METERS	GRAPHIC LITHOLOGY	DRILLING DISTURB.	SED. STRUCTURES	SAMPLES	LITHOLOGIC DESCRIPTION
	FORAMINIFERS	NANNOFOSSILS	RADIOLARIANS	DIATOMS										
UPPER MIOCENE	N16 to N19 *	NN11 *	Quaternary and Miocene *	<i>N. miocenica</i> Zone *										DIATOMACEOUS MUDSTONE Major lithology: diatomaceous mudstone, dark olive gray to black (5Y 3/1, 5Y 2.5/1). SMEAR SLIDE SUMMARY (%): CC D TEXTURE: Sand 5 Silt 35 Clay 60 COMPOSITION: Quartz 5 Feldspar 5 Rock fragments Tr Clay 50 Calcite/dolomite 5 Accessory minerals Pyrite 3 Foraminifers Tr Diatoms 32

CORE 112-685A-24X NO RECOVERY

SITE 685 HOLE A CORE 25X CORED INTERVAL 5293.4-5302.9 mbsl; 222.6-232.1 mbsf

TIME-ROCK UNIT	BIOSTRAT. ZONE/ FOSSIL CHARACTER				PALEOMAGNETICS	PHYS. PROPERTIES	CHEMISTRY	SECTION	METERS	GRAPHIC LITHOLOGY	DRILLING DISTURB.	SED. STRUCTURES	SAMPLES	LITHOLOGIC DESCRIPTION
	FORAMINIFERS	NANNOFOSSILS	RADIOLARIANS	DIATOMS										
UPPER MIOCENE	B *	NN11 *	<i>D. antepenultimus</i> Zone *	<i>N. miocenica</i> Zone *	1.40 0.54, 48			1 0.5						DIATOMACEOUS TO DIATOM-BEARING MUDSTONE Major lithology: diatomaceous to diatom-bearing mudstone, black (5Y 2.5/1, 5Y 2.5/2). SMEAR SLIDE SUMMARY (%): CC, 4 D, 4 CC, 15 D, 15 CC, 16 D, 16 TEXTURE: Silt 40 35 30 Clay 60 65 70 COMPOSITION: Quartz 5 5 5 Feldspar 5 5 5 Mica, BT Tr Tr Tr Clay 50 62 67 Volcanic glass Tr Tr Tr Calcite/dolomite 5 Tr Tr Accessory minerals Glauconite Tr 5 Tr Pyrite 1 3 3 Foraminifers Tr - - Diatoms 20 15 15 Radiolarians Tr Tr Tr Sponge spicules 5 5 5 Silicoflagellates Tr - -



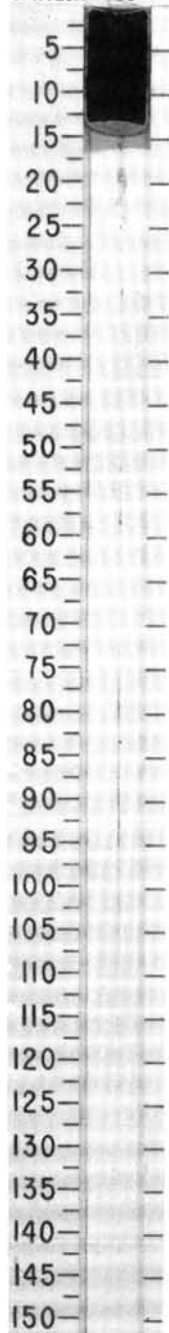
SITE 685 HOLE A CORE 26X CORED INTERVAL 5302.9-5304.4 mbsl; 232.1-233.6 mbsf

TIME-ROCK UNIT	BIOSTRAT. ZONE/ FOSSIL CHARACTER				PALEOMAGNETICS	PHYS. PROPERTIES	CHEMISTRY	SECTION	METERS	GRAPHIC LITHOLOGY	DRILLING DISTURB.	SED. STRUCTURES	SAMPLES	LITHOLOGIC DESCRIPTION																																								
	FORAMINIFERS	NANOFOSSELS	RADIOLARIANS	DIATOMS																																																		
UPPER MIOCENE		NN TO *												DIATOMACEOUS MUDSTONE Major lithology: diatomaceous mudstone, black(5Y 2.5/2). Silt-rich. SMEAR SLIDE SUMMARY (%): <table style="margin-left: 20px;"> <tr><td>CC</td><td>CC</td></tr> <tr><td>D</td><td>M</td></tr> </table> COMPOSITION: <table style="margin-left: 20px;"> <tr><td>Quartz</td><td>5</td><td>18</td></tr> <tr><td>Feldspar</td><td>8</td><td>7</td></tr> <tr><td>Rock fragments</td><td>2</td><td>15</td></tr> <tr><td>Clay</td><td>50</td><td>22</td></tr> <tr><td>Volcanic glass</td><td>2</td><td>—</td></tr> <tr><td>Calcite/dolomite</td><td>3</td><td>15</td></tr> <tr><td>Pyrite</td><td>2</td><td>8</td></tr> <tr><td>Glaucanite</td><td>1</td><td>—</td></tr> <tr><td>Phosphate</td><td>Tr</td><td>—</td></tr> <tr><td>Diatoms</td><td>25</td><td>15</td></tr> <tr><td>Radiolarians</td><td>Tr</td><td>Tr</td></tr> <tr><td>Sponge spicules</td><td>2</td><td>Tr</td></tr> </table>	CC	CC	D	M	Quartz	5	18	Feldspar	8	7	Rock fragments	2	15	Clay	50	22	Volcanic glass	2	—	Calcite/dolomite	3	15	Pyrite	2	8	Glaucanite	1	—	Phosphate	Tr	—	Diatoms	25	15	Radiolarians	Tr	Tr	Sponge spicules	2	Tr
CC	CC																																																					
D	M																																																					
Quartz	5	18																																																				
Feldspar	8	7																																																				
Rock fragments	2	15																																																				
Clay	50	22																																																				
Volcanic glass	2	—																																																				
Calcite/dolomite	3	15																																																				
Pyrite	2	8																																																				
Glaucanite	1	—																																																				
Phosphate	Tr	—																																																				
Diatoms	25	15																																																				
Radiolarians	Tr	Tr																																																				
Sponge spicules	2	Tr																																																				

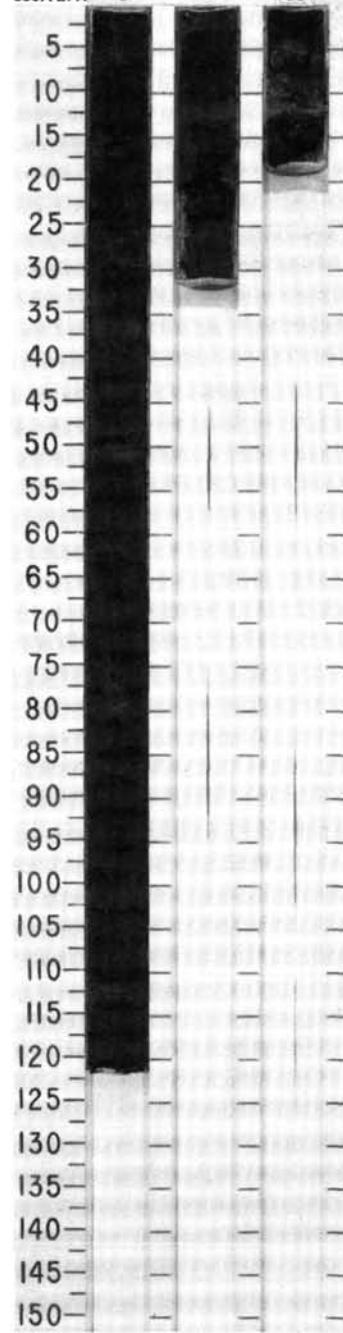
SITE 685 HOLE A CORE 27X CORED INTERVAL 5304.4-5313.9 mbsl; 233.6-243.1 mbsf

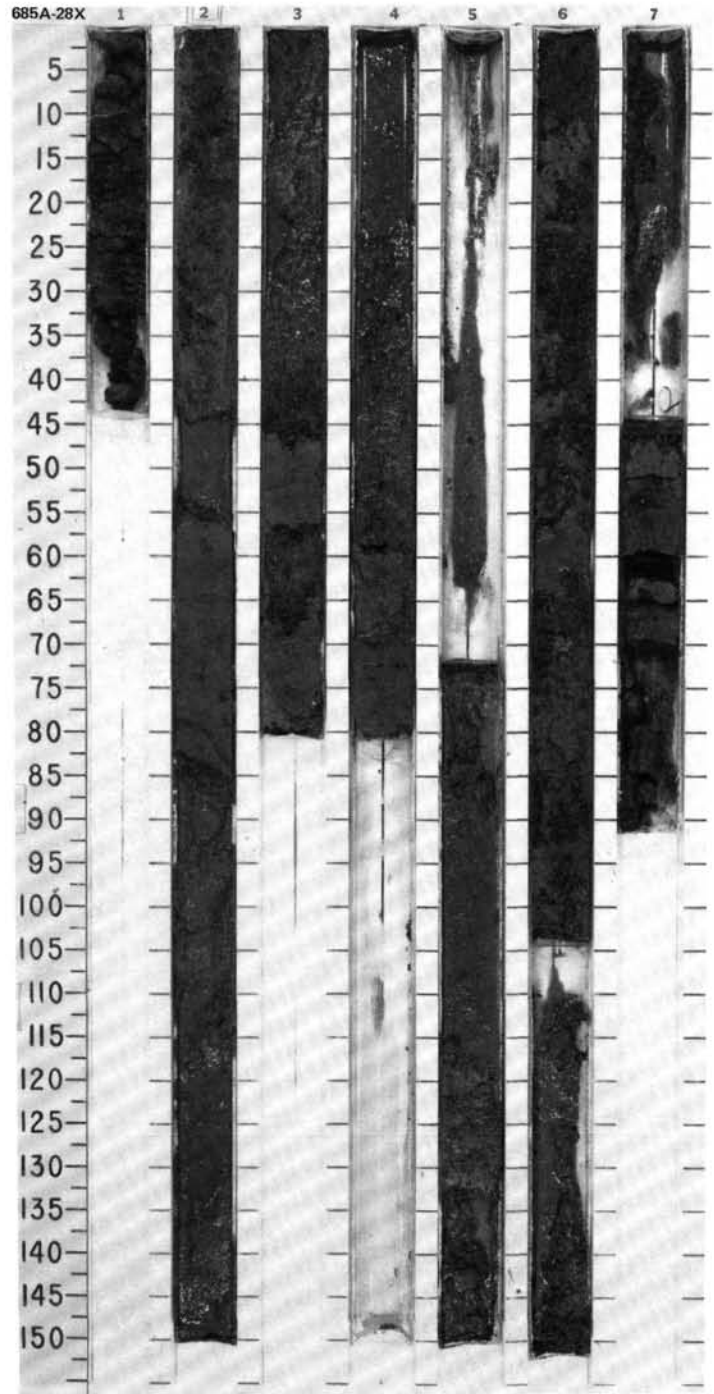
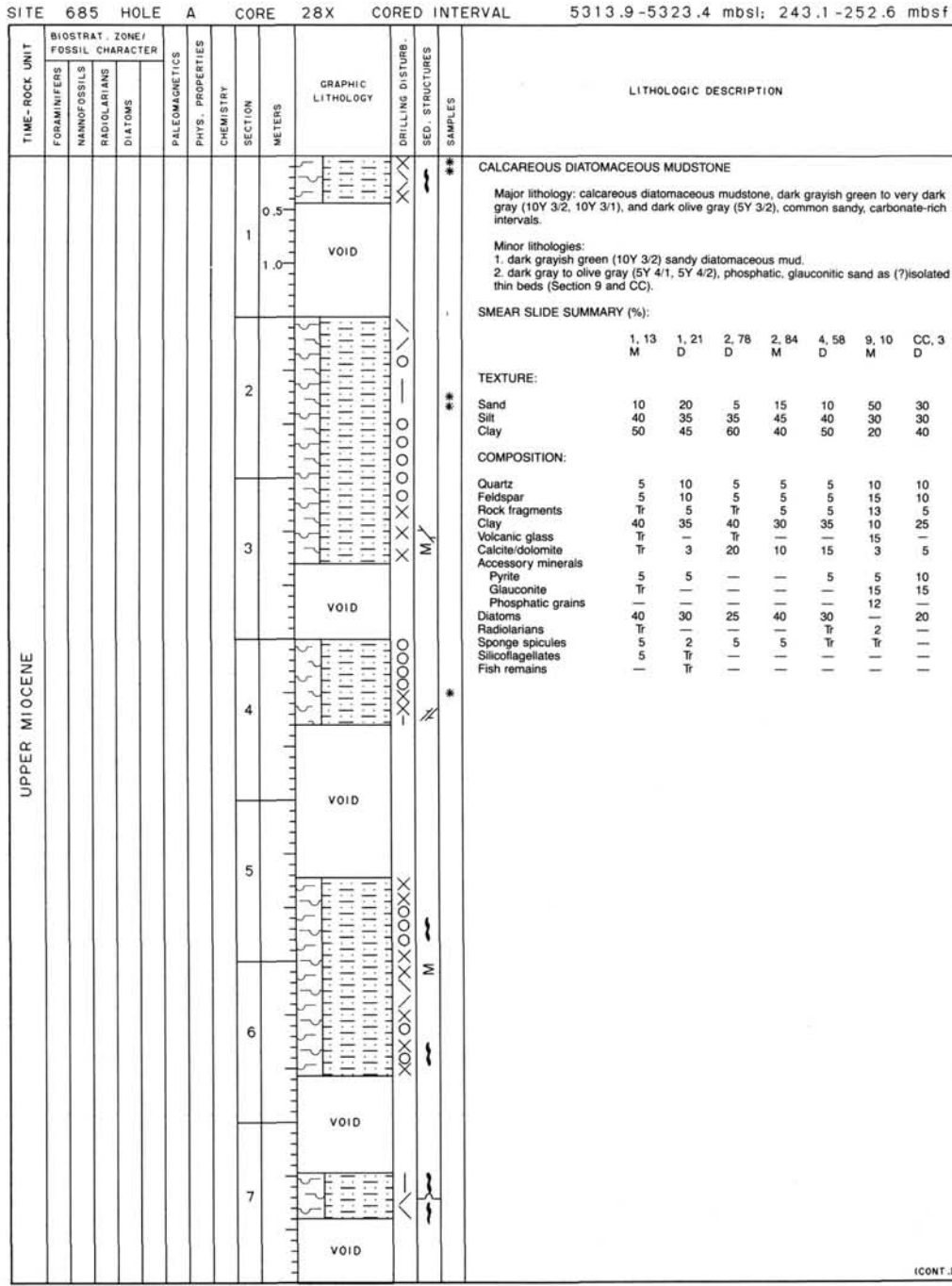
TIME-ROCK UNIT	BIOSTRAT. ZONE/ FOSSIL CHARACTER				PALEOMAGNETICS	PHYS. PROPERTIES	CHEMISTRY	SECTION	METERS	GRAPHIC LITHOLOGY	DRILLING DISTURB.	SED. STRUCTURES	SAMPLES	LITHOLOGIC DESCRIPTION																																																							
	FORAMINIFERS	NANOFOSSELS	RADIOLARIANS	DIATOMS																																																																	
UPPER MIOCENE	B *	B *												DIATOM-BEARING MUDSTONE Major lithology: diatom-bearing mudstone, dark olive gray (5Y 3/2). SMEAR SLIDE SUMMARY (%): <table style="margin-left: 20px;"> <tr><td>1, 68</td><td>CC, 14</td></tr> <tr><td>M</td><td>D</td></tr> </table> TEXTURE: <table style="margin-left: 20px;"> <tr><td>Silt</td><td>30</td><td>35</td></tr> <tr><td>Clay</td><td>70</td><td>65</td></tr> </table> COMPOSITION: <table style="margin-left: 20px;"> <tr><td>Quartz</td><td>3</td><td>5</td></tr> <tr><td>Feldspar</td><td>3</td><td>10</td></tr> <tr><td>Rock fragments</td><td>2</td><td>2</td></tr> <tr><td>Mica</td><td>1</td><td>—</td></tr> <tr><td>Clay</td><td>65</td><td>55</td></tr> <tr><td>Volcanic glass</td><td>3</td><td>3</td></tr> <tr><td>Calcite/dolomite</td><td>3</td><td>3</td></tr> <tr><td>Accessory minerals</td><td></td><td></td></tr> <tr><td>Pyrite</td><td>1</td><td>2</td></tr> <tr><td>Glaucanite</td><td>2</td><td>2</td></tr> <tr><td>Micrite</td><td>—</td><td>3</td></tr> <tr><td>Foraminifers</td><td>1</td><td>—</td></tr> <tr><td>Diatoms</td><td>15</td><td>10</td></tr> <tr><td>Radiolarians</td><td>Tr</td><td>Tr</td></tr> <tr><td>Sponge spicules</td><td>1</td><td>5</td></tr> </table>	1, 68	CC, 14	M	D	Silt	30	35	Clay	70	65	Quartz	3	5	Feldspar	3	10	Rock fragments	2	2	Mica	1	—	Clay	65	55	Volcanic glass	3	3	Calcite/dolomite	3	3	Accessory minerals			Pyrite	1	2	Glaucanite	2	2	Micrite	—	3	Foraminifers	1	—	Diatoms	15	10	Radiolarians	Tr	Tr	Sponge spicules	1	5
1, 68	CC, 14																																																																				
M	D																																																																				
Silt	30	35																																																																			
Clay	70	65																																																																			
Quartz	3	5																																																																			
Feldspar	3	10																																																																			
Rock fragments	2	2																																																																			
Mica	1	—																																																																			
Clay	65	55																																																																			
Volcanic glass	3	3																																																																			
Calcite/dolomite	3	3																																																																			
Accessory minerals																																																																					
Pyrite	1	2																																																																			
Glaucanite	2	2																																																																			
Micrite	—	3																																																																			
Foraminifers	1	—																																																																			
Diatoms	15	10																																																																			
Radiolarians	Tr	Tr																																																																			
Sponge spicules	1	5																																																																			

685A-26X CC



685A-27X 1 2 CC



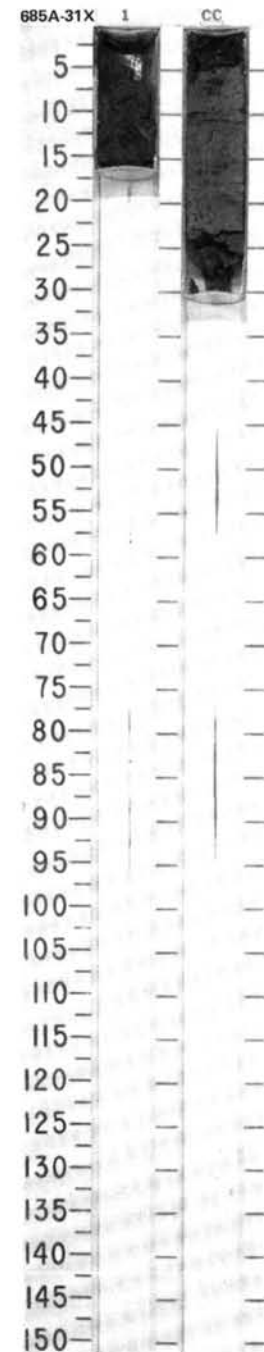
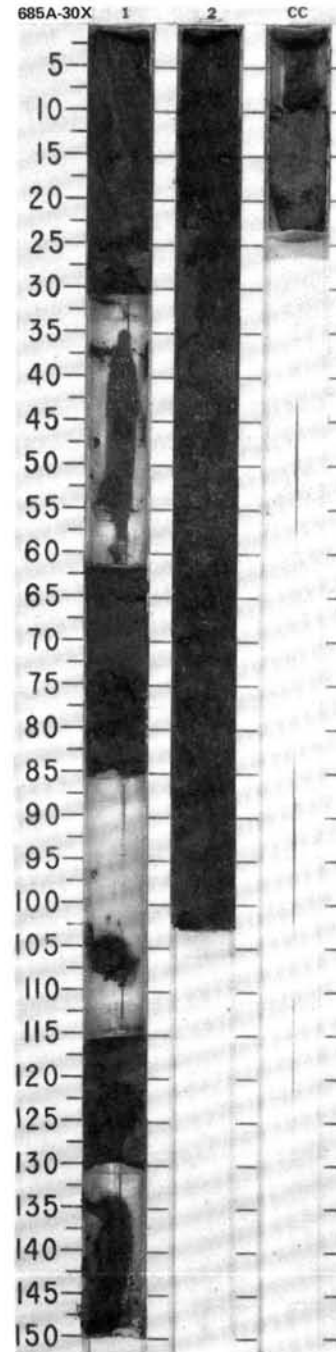


SITE 685 HOLE A CORE 30X CORED INTERVAL 5332.9-5342.4 mbsl; 262.1-271.6 mbsf

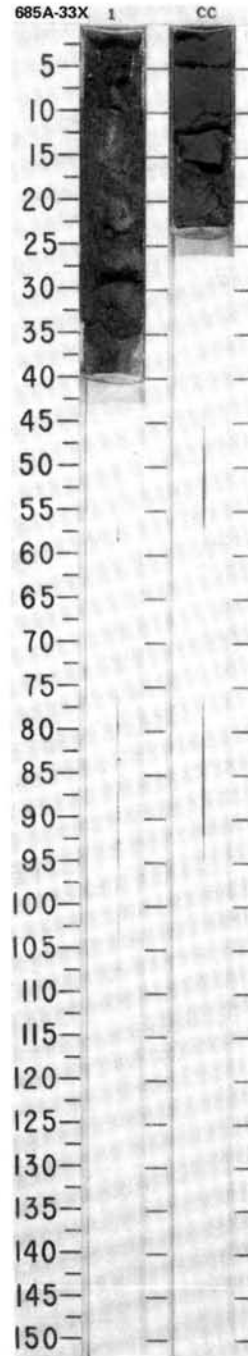
TIME-ROCK UNIT	BIOSTRAT. ZONE/ FOSSIL CHARACTER				PALEOMAGNETICS	PHYS. PROPERTIES	SECTION	METERS	GRAPHIC LITHOLOGY	DRILLING DISTURB.	SED. STRUCTURES	SAMPLES	LITHOLOGIC DESCRIPTION																																																			
	FORAMINIFERS	NANNOFOSSILS	RADIOLARIANS	DIATOMS																																																												
UPPER MIOCENE	* B	* B	* <i>Didymocyrtis antepenultimus</i> Zone	* <i>C. yabei</i> Zone			0.5 1.0 1.5 2.0						<p>DIATOMACEOUS MUD</p> <p>Major lithology: diatomaceous mud, dusky grayish green to dark olive gray 5GY 4/2, 5Y 3/2. Frequent locally glauconitic sandy mud patches.</p> <p>SMEAR SLIDE SUMMARY (%):</p> <table border="1"> <tr> <td></td> <td>1, 67</td> <td>CC, 15</td> </tr> <tr> <td>D</td> <td>D</td> <td>D</td> </tr> </table> <p>TEXTURE:</p> <table border="1"> <tr> <td>Sand</td> <td>20</td> <td>5</td> </tr> <tr> <td>Silt</td> <td>35</td> <td>45</td> </tr> <tr> <td>Clay</td> <td>45</td> <td>55</td> </tr> </table> <p>COMPOSITION:</p> <table border="1"> <tr> <td>Quartz</td> <td>5</td> <td>5</td> </tr> <tr> <td>Feldspar</td> <td>10</td> <td>5</td> </tr> <tr> <td>Rock fragments</td> <td>5</td> <td>5</td> </tr> <tr> <td>Clay</td> <td>30</td> <td>40</td> </tr> <tr> <td>Calcite/dolomite</td> <td>10</td> <td>Tr</td> </tr> <tr> <td>Accessory minerals</td> <td></td> <td></td> </tr> <tr> <td> Glauconite</td> <td>3</td> <td>—</td> </tr> <tr> <td> Pyrite</td> <td>7</td> <td>5</td> </tr> <tr> <td> Diatoms</td> <td>23</td> <td>38</td> </tr> <tr> <td> Radiolarians</td> <td>2</td> <td>2</td> </tr> <tr> <td> Sponge spicules</td> <td>5</td> <td>Tr</td> </tr> <tr> <td> Fish remains</td> <td>Tr</td> <td>—</td> </tr> </table>		1, 67	CC, 15	D	D	D	Sand	20	5	Silt	35	45	Clay	45	55	Quartz	5	5	Feldspar	10	5	Rock fragments	5	5	Clay	30	40	Calcite/dolomite	10	Tr	Accessory minerals			Glauconite	3	—	Pyrite	7	5	Diatoms	23	38	Radiolarians	2	2	Sponge spicules	5	Tr	Fish remains	Tr	—
	1, 67	CC, 15																																																														
D	D	D																																																														
Sand	20	5																																																														
Silt	35	45																																																														
Clay	45	55																																																														
Quartz	5	5																																																														
Feldspar	10	5																																																														
Rock fragments	5	5																																																														
Clay	30	40																																																														
Calcite/dolomite	10	Tr																																																														
Accessory minerals																																																																
Glauconite	3	—																																																														
Pyrite	7	5																																																														
Diatoms	23	38																																																														
Radiolarians	2	2																																																														
Sponge spicules	5	Tr																																																														
Fish remains	Tr	—																																																														

SITE 685 HOLE A CORE 31X CORED INTERVAL 5342.4-5351.9 mbsl; 271.6-281.1 mbsf

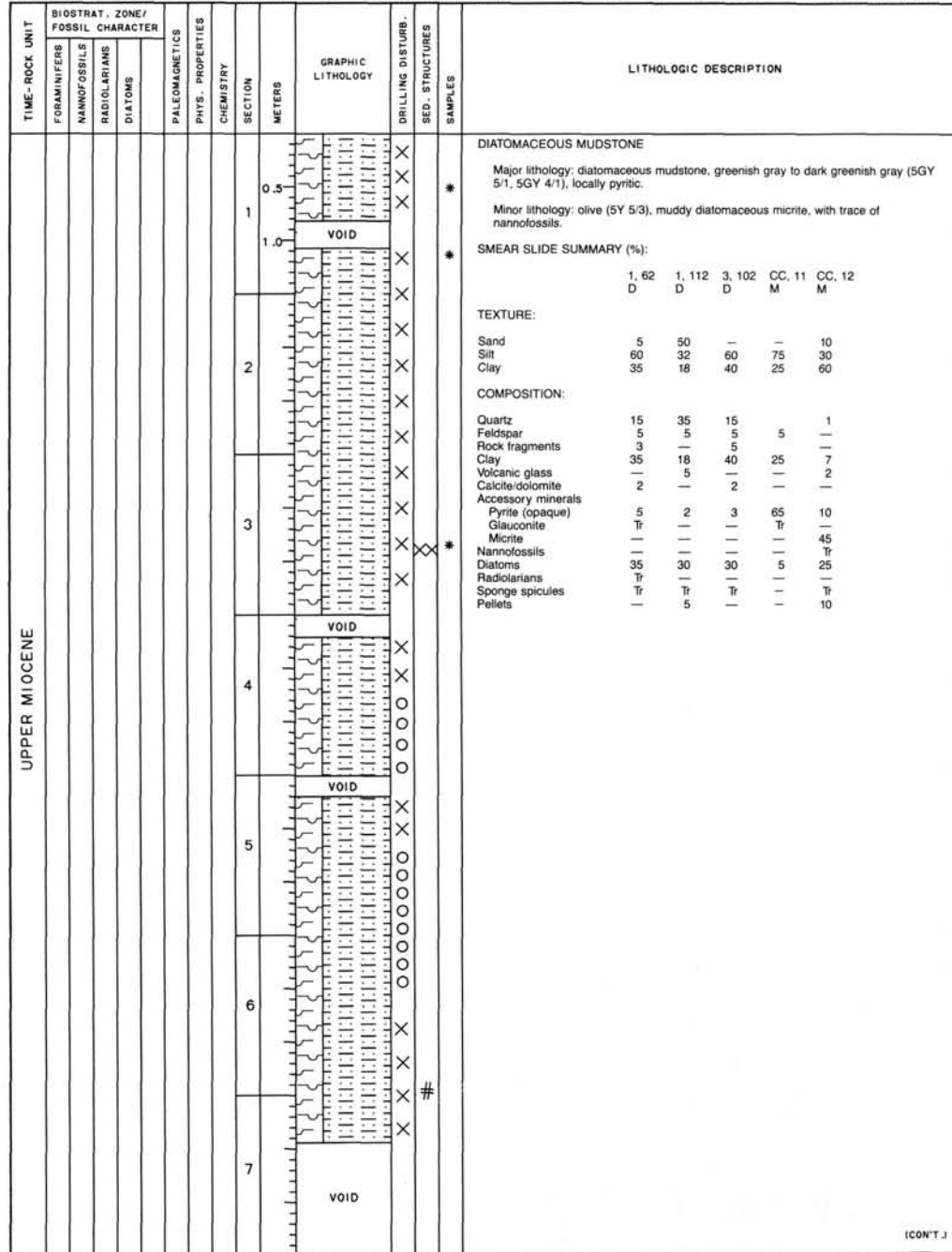
TIME-ROCK UNIT	BIOSTRAT. ZONE/ FOSSIL CHARACTER				PALEOMAGNETICS	PHYS. PROPERTIES	SECTION	METERS	GRAPHIC LITHOLOGY	DRILLING DISTURB.	SED. STRUCTURES	SAMPLES	LITHOLOGIC DESCRIPTION																																																												
	FORAMINIFERS	NANNOFOSSILS	RADIOLARIANS	DIATOMS																																																																					
UPPER MIOCENE	B *	B *	* <i>Didymocyrtis antepenultimus</i> Zone *	* <i>C. yabei</i> Zone *			1.80 0-5.85						<p>DIATOMACEOUS MUDSTONE</p> <p>Major lithology: diatomaceous mudstone, greenish gray to dark greenish gray (5Y 5/1 to 5Y 4/1), carbonate-bearing.</p> <p>SMEAR SLIDE SUMMARY (%):</p> <table border="1"> <tr> <td></td> <td>1, 11</td> <td>CC, 15</td> </tr> <tr> <td>D</td> <td>D</td> <td>D</td> </tr> </table> <p>TEXTURE:</p> <table border="1"> <tr> <td>Sand</td> <td>10</td> <td>10</td> </tr> <tr> <td>Silt</td> <td>50</td> <td>30</td> </tr> <tr> <td>Clay</td> <td>40</td> <td>60</td> </tr> </table> <p>COMPOSITION:</p> <table border="1"> <tr> <td>Quartz</td> <td>Tr</td> <td>Tr</td> </tr> <tr> <td>Feldspar</td> <td>10</td> <td>15</td> </tr> <tr> <td>Rock fragments</td> <td>5</td> <td>5</td> </tr> <tr> <td>Clay</td> <td>30</td> <td>47</td> </tr> <tr> <td>Volcanic glass</td> <td>3</td> <td>6</td> </tr> <tr> <td>Calcite/dolomite</td> <td>10</td> <td>10</td> </tr> <tr> <td>Accessory minerals</td> <td></td> <td></td> </tr> <tr> <td> Pyrite</td> <td>5</td> <td>2</td> </tr> <tr> <td> Glauconite</td> <td>3</td> <td>3</td> </tr> <tr> <td> Nannofossils</td> <td>Tr</td> <td>—</td> </tr> <tr> <td> Diatoms</td> <td>29</td> <td>10</td> </tr> <tr> <td> Radiolarians</td> <td>Tr</td> <td>—</td> </tr> <tr> <td> Sponge spicules</td> <td>5</td> <td>2</td> </tr> <tr> <td> Silicoflagellates</td> <td>Tr</td> <td>Tr</td> </tr> <tr> <td> Plant debris</td> <td>Tr</td> <td>—</td> </tr> </table>		1, 11	CC, 15	D	D	D	Sand	10	10	Silt	50	30	Clay	40	60	Quartz	Tr	Tr	Feldspar	10	15	Rock fragments	5	5	Clay	30	47	Volcanic glass	3	6	Calcite/dolomite	10	10	Accessory minerals			Pyrite	5	2	Glauconite	3	3	Nannofossils	Tr	—	Diatoms	29	10	Radiolarians	Tr	—	Sponge spicules	5	2	Silicoflagellates	Tr	Tr	Plant debris	Tr	—
	1, 11	CC, 15																																																																							
D	D	D																																																																							
Sand	10	10																																																																							
Silt	50	30																																																																							
Clay	40	60																																																																							
Quartz	Tr	Tr																																																																							
Feldspar	10	15																																																																							
Rock fragments	5	5																																																																							
Clay	30	47																																																																							
Volcanic glass	3	6																																																																							
Calcite/dolomite	10	10																																																																							
Accessory minerals																																																																									
Pyrite	5	2																																																																							
Glauconite	3	3																																																																							
Nannofossils	Tr	—																																																																							
Diatoms	29	10																																																																							
Radiolarians	Tr	—																																																																							
Sponge spicules	5	2																																																																							
Silicoflagellates	Tr	Tr																																																																							
Plant debris	Tr	—																																																																							



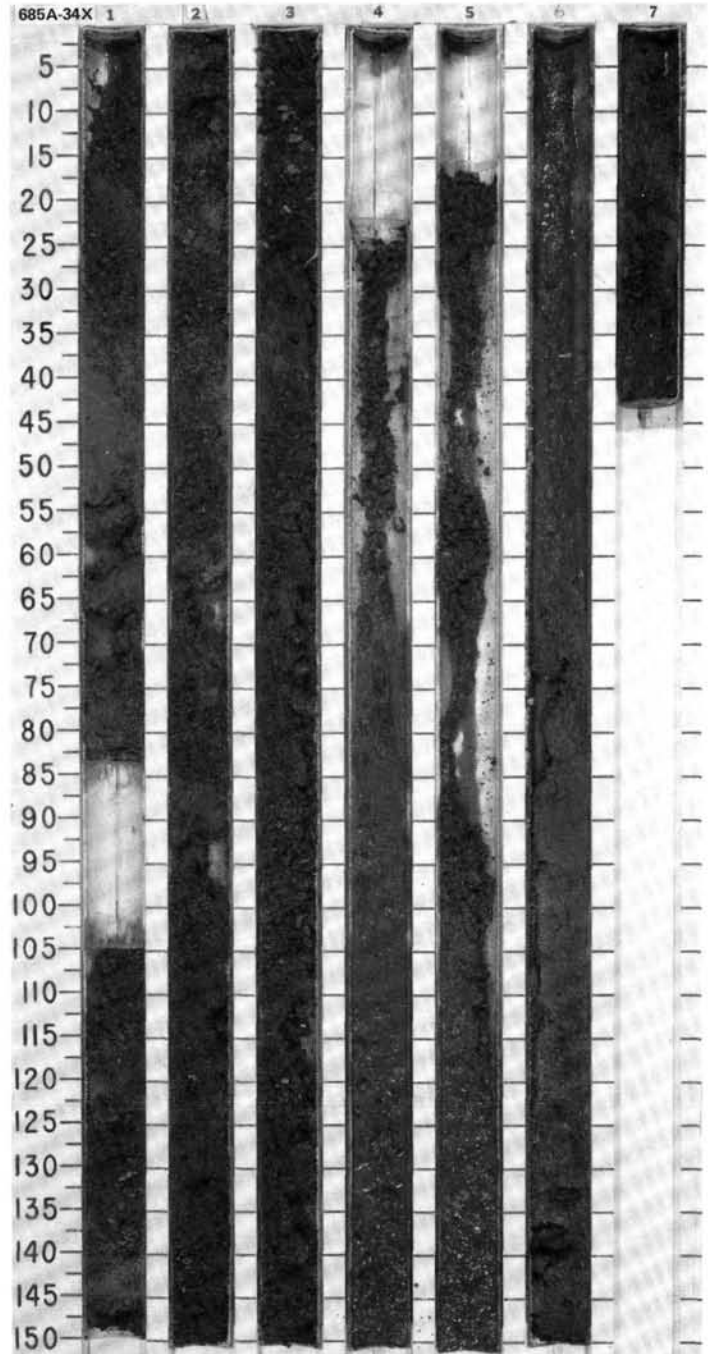
TIME-ROCK UNIT	BIOSTRAT. ZONE/ FOSSIL CHARACTER			PALEOMAGNETICS	PHYS. PROPERTIES	CHEMISTRY	SECTION	METERS	GRAPHIC LITHOLOGY	DRILLING DISTURB.	SED. STRUCTURES	SAMPLES	LITHOLOGIC DESCRIPTION																																										
	FORAMINIFERS	NANNOFOSSILS	RADIOLARIANS																																																				
UPPER MIOCENE	B *	B *	<i>Didymocyrtis antepenultimus</i> Zone *		γ ₁ -63 δ ₁ -54.96 *		1	0.5				X	<p>DIATOMACEOUS AND DIATOM-BEARING MUDSTONE</p> <p>Major lithology: diatomaceous and diatom-bearing mudstone, greenish gray (5GY 5/1).</p> <p>Minor lithology: dark greenish gray (5GY 4/1), pyritic mudstone in thin seams along microfaults.</p> <p>SMEAR SLIDE SUMMARY (%):</p> <table border="1"> <thead> <tr> <th></th> <th>CC, 2 M</th> <th>CC, 11 D</th> </tr> </thead> <tbody> <tr> <td>Silt</td> <td>45</td> <td>30</td> </tr> <tr> <td>Clay</td> <td>55</td> <td>70</td> </tr> </tbody> </table> <p>TEXTURE:</p> <p>COMPOSITION:</p> <table border="1"> <tbody> <tr><td>Quartz</td><td>5</td><td>5</td></tr> <tr><td>Feldspar</td><td>5</td><td>5</td></tr> <tr><td>Mica</td><td>—</td><td>Tr</td></tr> <tr><td>Clay</td><td>55</td><td>70</td></tr> <tr><td>Calcite/dolomite</td><td>—</td><td>Tr</td></tr> <tr><td>Accessory minerals</td><td>—</td><td>—</td></tr> <tr><td> Glauconite</td><td>—</td><td>Tr</td></tr> <tr><td> Pyrite</td><td>10</td><td>—</td></tr> <tr><td> Diatoms</td><td>25</td><td>15</td></tr> <tr><td> Radiolarians</td><td>Tr</td><td>Tr</td></tr> <tr><td> Sponge spicules</td><td>Tr</td><td>5</td></tr> </tbody> </table>		CC, 2 M	CC, 11 D	Silt	45	30	Clay	55	70	Quartz	5	5	Feldspar	5	5	Mica	—	Tr	Clay	55	70	Calcite/dolomite	—	Tr	Accessory minerals	—	—	Glauconite	—	Tr	Pyrite	10	—	Diatoms	25	15	Radiolarians	Tr	Tr	Sponge spicules	Tr	5
	CC, 2 M	CC, 11 D																																																					
Silt	45	30																																																					
Clay	55	70																																																					
Quartz	5	5																																																					
Feldspar	5	5																																																					
Mica	—	Tr																																																					
Clay	55	70																																																					
Calcite/dolomite	—	Tr																																																					
Accessory minerals	—	—																																																					
Glauconite	—	Tr																																																					
Pyrite	10	—																																																					
Diatoms	25	15																																																					
Radiolarians	Tr	Tr																																																					
Sponge spicules	Tr	5																																																					



SITE 685 HOLE A CORE 34X CORED INTERVAL 5370.9-5380.4 mbsl; 300.1-309.6 mbsf



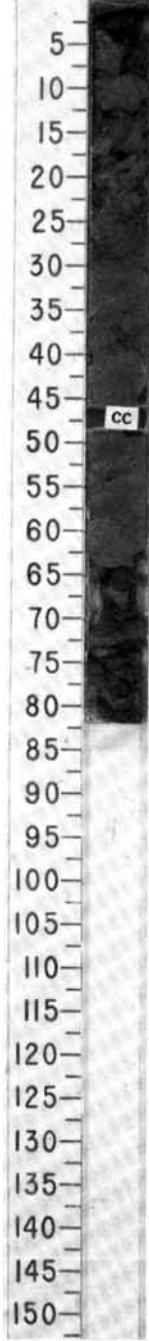
(CONT.)



SITE 685 HOLE A CORE 34X CORED INTERVAL 5370.9-5380.4 mbsl; 300.1-309.6 mbsf

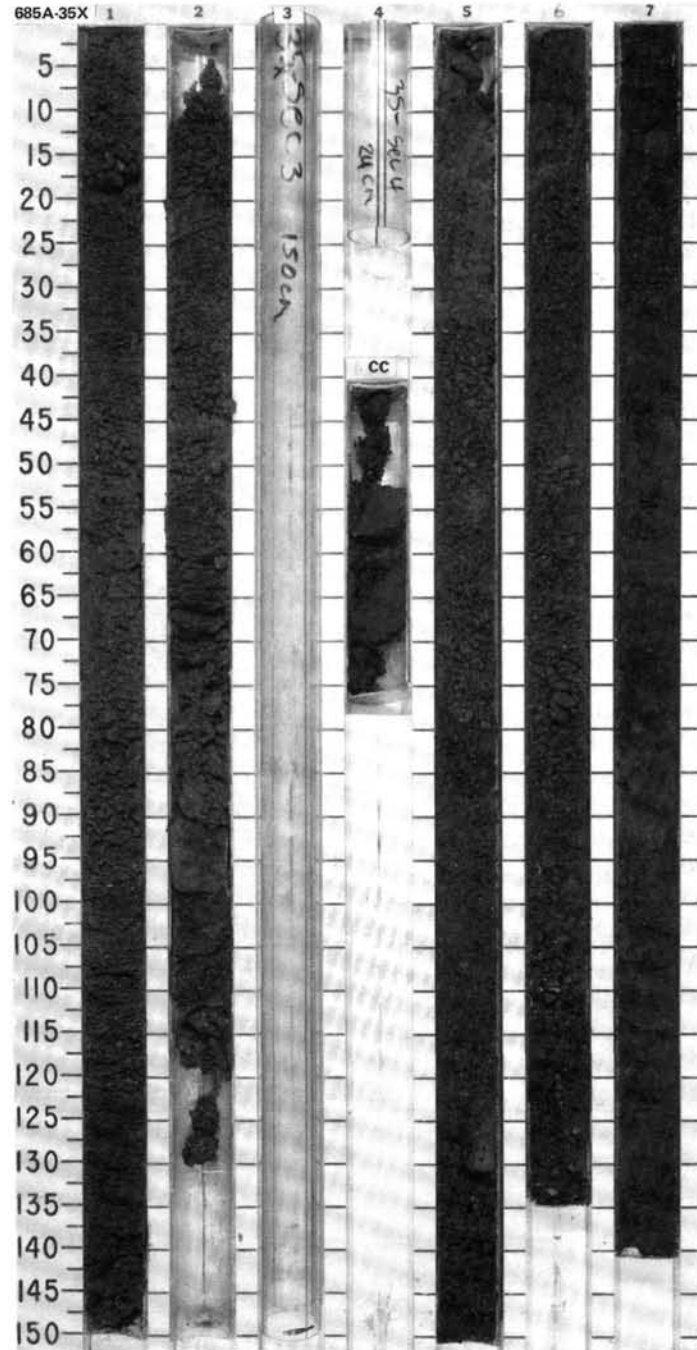
TIME-ROCK UNIT	BIOSTRAT. ZONE/ FOSSIL CHARACTER			PALEOMAGNETICS	PHYS. PROPERTIES	CHEMISTRY	SECTION	METERS	GRAPHIC LITHOLOGY	DRILLING DISTURB. SED. STRUCTURES	SAMPLES	LITHOLOGIC DESCRIPTION
	FORAMINIFERS	NANNOFOSSILS	RADIOLARIANS									
	B *							0.5				(CONT.)
	B *							1.0	VOID			
	<i>Didymocyrtis antepenultimus</i> (Lower Upper Miocene) * non diagnostic *											
					1.05 0.15-0.8							
							CC				**	

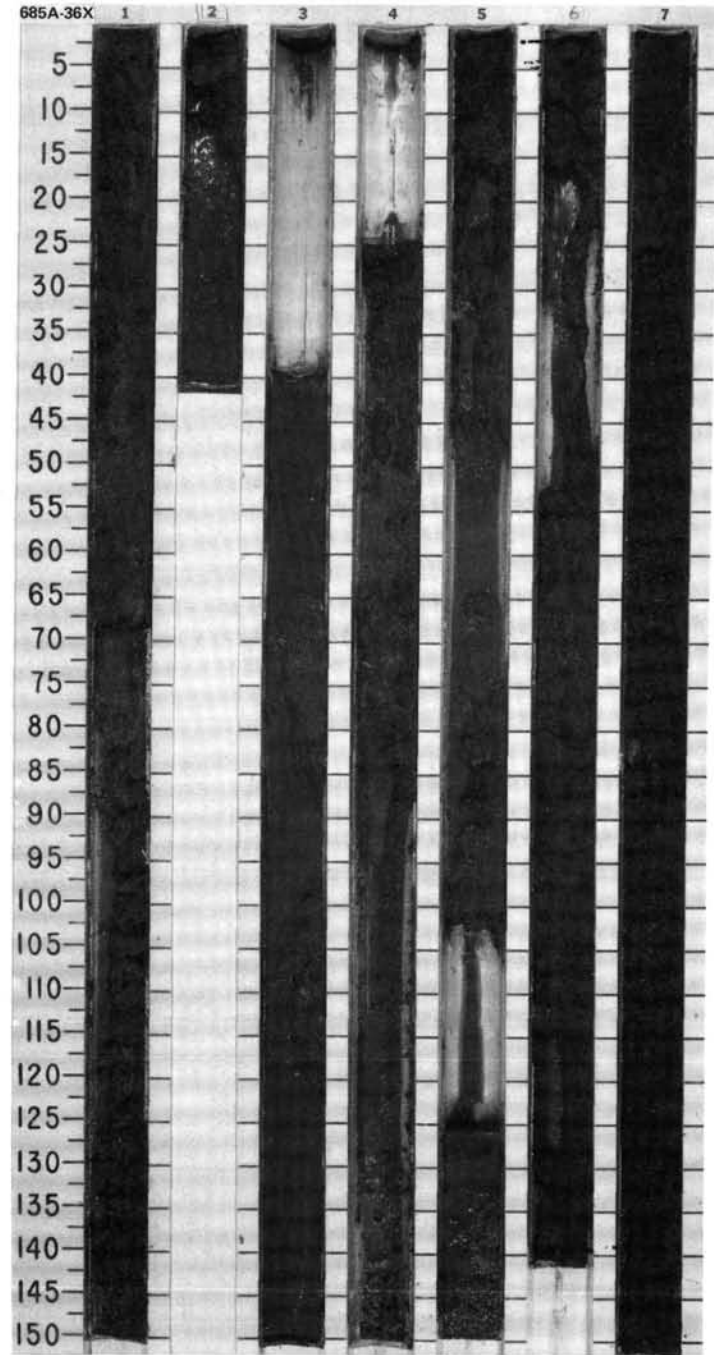
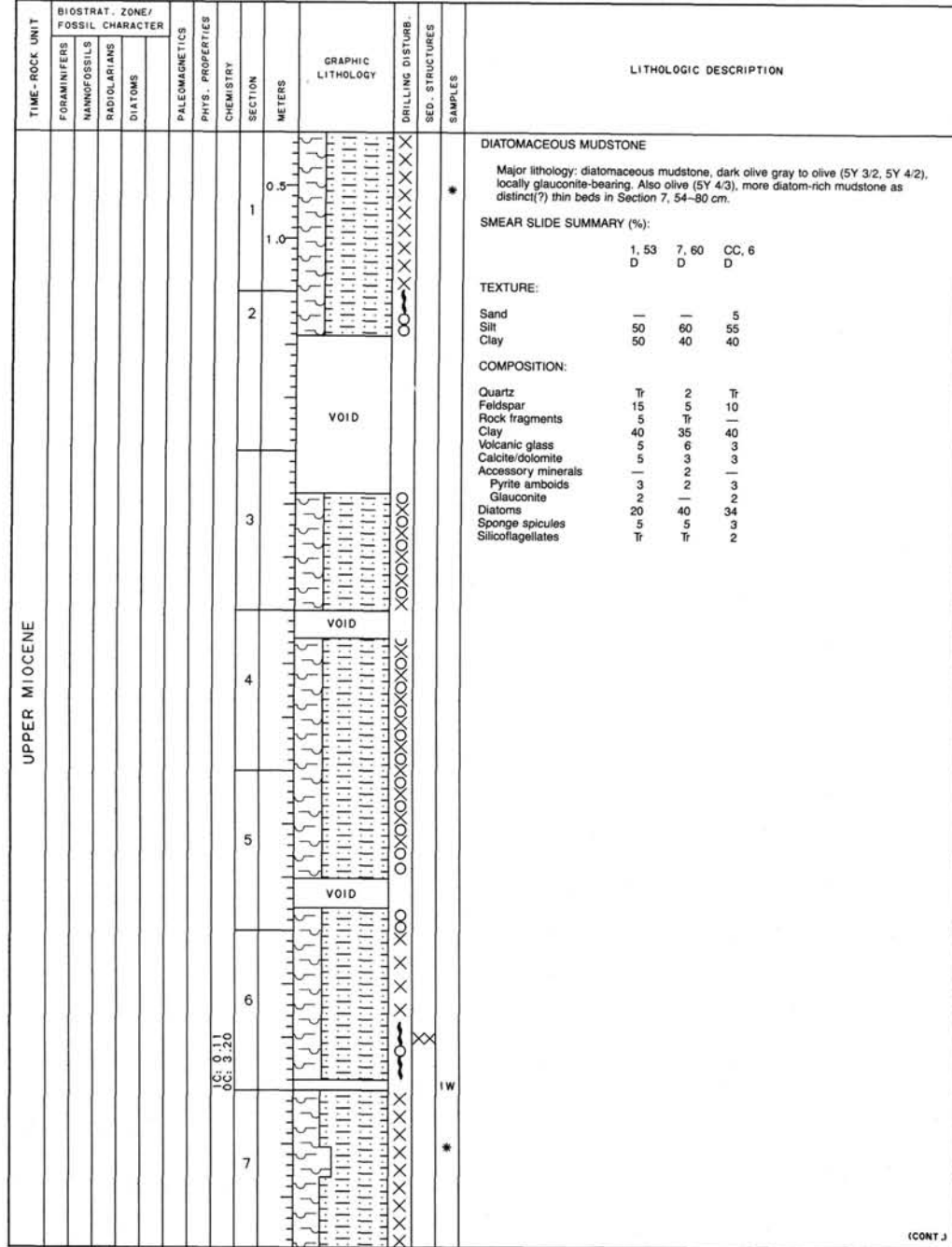
685A-34X 8



SITE 685 HOLE A CORE 35X CORED INTERVAL 5380.4 - 5389.9 mbsl; 309.6 - 319.1 mbsf

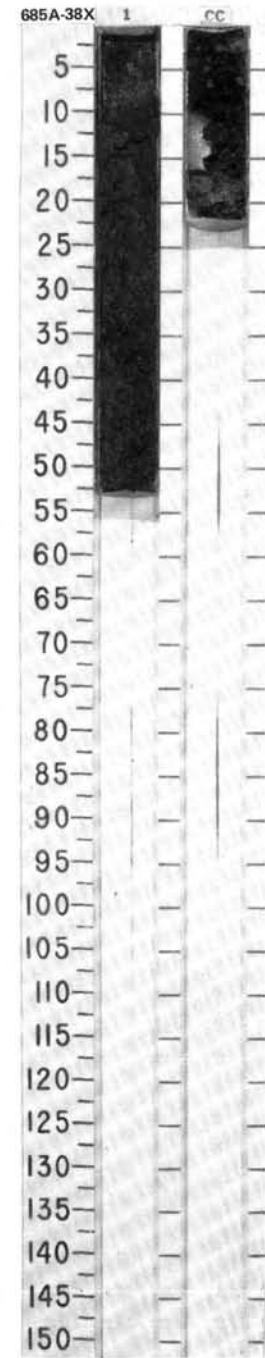
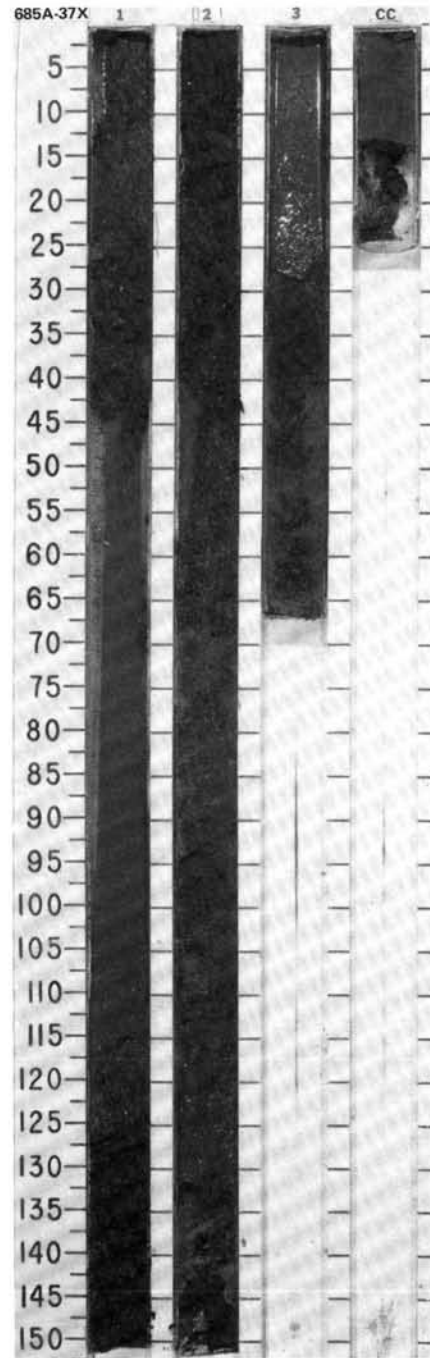
TIME-ROCK UNIT	BIOSTRAT. ZONE/ FOSSIL CHARACTER				PALEOMAGNETICS	PHYS. PROPERTIES	CHEMISTRY	SECTION	METERS	GRAPHIC LITHOLOGY	DRILLING DISTURB. SED. STRUCTURES	SAMPLES	LITHOLOGIC DESCRIPTION																												
	FORAMINIFERS	NAKNOFOSSILS	RADIOLARIANS	DIATOMS																																					
UPPER MIOCENE	* B								0.5 1.0				DIATOM-BEARING MUDSTONE and DIATOMACEOUS MUDSTONE Major lithology: Section 1, 0 cm, to Section 3, 90 cm: diatom-bearing mudstone, greenish gray to dark greenish gray (5GY 5/1, 5GY 4/1), locally micritic; and Section 3, 90 cm, to CC: diatomaceous mudstone, dark olive gray to olive gray (5Y 3/2, 5Y 4/2). Minor lithology: black (5Y 2.5/2), muddy, diatom-bearing dolomite as 8-cm bed in CC. SMEAR SLIDE SUMMARY (%): <table border="1"> <thead> <tr> <th></th> <th>1, 30 M</th> <th>1, 126 D</th> <th>5, 77 D</th> <th>5, 79 M</th> <th>7, 85 D</th> <th>7, 88 M</th> </tr> </thead> <tbody> <tr> <td>Sand</td> <td>—</td> <td>—</td> <td>5</td> <td>5</td> <td>5</td> <td>5</td> </tr> <tr> <td>Silt</td> <td>35</td> <td>30</td> <td>35</td> <td>40</td> <td>35</td> <td>35</td> </tr> <tr> <td>Clay</td> <td>65</td> <td>70</td> <td>60</td> <td>55</td> <td>60</td> <td>60</td> </tr> </tbody> </table> TEXTURE: Sand — — 5 5 5 5 Silt 35 30 35 40 35 35 Clay 65 70 60 55 60 60 COMPOSITION: Quartz 5 4 17 5 5 20 Feldspar 5 6 — — 5 — Rock fragments 3 3 — — 5 — Mica, biotite 1 — 5 3 — Tr Clay 64 50 30 20 50 20 Volcanic glass 3 3 5 2 Tr 5 Calcite/dolomite — 2 Tr 60 5 5 Accessory minerals Pyrite 1 5 3 Tr 2 — Glauconite 1 — — Tr — 5 Phosphate — 2 — — — — Micrite 2 10 — — — — Pyroxene — — Tr — — — Opaques — — — — 3 — Diatoms 10 12 40 10 25 45 Radiolarians — Tr — — — — Sponge spicules 5 3 — Tr — — Silicoflagellates — — Tr — — — Fish remains — — — Tr — —		1, 30 M	1, 126 D	5, 77 D	5, 79 M	7, 85 D	7, 88 M	Sand	—	—	5	5	5	5	Silt	35	30	35	40	35	35	Clay	65	70	60	55	60	60
		1, 30 M	1, 126 D	5, 77 D	5, 79 M	7, 85 D	7, 88 M																																		
	Sand	—	—	5	5	5	5																																		
	Silt	35	30	35	40	35	35																																		
	Clay	65	70	60	55	60	60																																		
	* B																																								
	* <i>Didymocyrtis antepenultimus</i> Zone																																								
* <i>N. miocenica</i> Zone																																									
* 7-1, 68 8-5, 3, 22									0.84 0.82																																
CC																																									





SITE 685 HOLE A CORE 37X CORED INTERVAL 5399.4-5408.9 mbsl; 328.6-338.1 mbsf

TIME-ROCK UNIT	BIOSTRAT. ZONE/ FOSSIL CHARACTER				PALEOMAGNETICS	PHYS. PROPERTIES	CHEMISTRY	SECTION	METERS	GRAPHIC LITHOLOGY	DRILLING DISTURB. SED. STRUCTURES	SAMPLES	LITHOLOGIC DESCRIPTION																																																																																																												
	FORAMINIFERS	NANNOFOSSILS	RADIOLARIANS	DIATOMS																																																																																																																					
UPPER MIOCENE	* B	* B	* <i>Didymocypris antepenultimus</i> Zone	* <i>N. miocenica</i> Zone					0.5 1.0				<p>DIATOMACEOUS MUDSTONE</p> <p>Major lithology: diatomaceous mudstone, greenish gray and dark greenish gray with beds of dark olive gray, (5Y 3/20) at Section 2, 0-45 cm, and Section 3, 55-67 cm.</p> <p>SMEAR SLIDE SUMMARY (%):</p> <table border="1"> <tr> <td></td> <td>1, 140</td> <td>2, 140</td> <td>3, 44</td> <td>CC, 13</td> <td>CC, 14</td> </tr> <tr> <td></td> <td>D</td> <td>D</td> <td>D</td> <td>D</td> <td>D</td> </tr> </table> <p>TEXTURE:</p> <table border="1"> <tr> <td>Sand</td> <td>5</td> <td>2</td> <td>1</td> <td>5</td> <td>3</td> </tr> <tr> <td>Silt</td> <td>55</td> <td>48</td> <td>49</td> <td>45</td> <td>52</td> </tr> <tr> <td>Clay</td> <td>40</td> <td>50</td> <td>50</td> <td>50</td> <td>45</td> </tr> </table> <p>COMPOSITION:</p> <table border="1"> <tr> <td>Quartz</td> <td>5</td> <td>3</td> <td>3</td> <td>Tr</td> <td>2</td> </tr> <tr> <td>Feldspar</td> <td>10</td> <td>8</td> <td>10</td> <td>10</td> <td>8</td> </tr> <tr> <td>Rock fragments</td> <td>—</td> <td>Tr</td> <td>Tr</td> <td>2</td> <td>2</td> </tr> <tr> <td>Clay</td> <td>35</td> <td>35</td> <td>40</td> <td>45</td> <td>38</td> </tr> <tr> <td>Volcanic glass</td> <td>3</td> <td>5</td> <td>3</td> <td>3</td> <td>3</td> </tr> <tr> <td>Calcite/dolomite</td> <td>10</td> <td>10</td> <td>4</td> <td>3</td> <td>3</td> </tr> <tr> <td>Accessory minerals</td> <td></td> <td></td> <td></td> <td></td> <td></td> </tr> <tr> <td>Pyrite</td> <td>3</td> <td>3</td> <td>4</td> <td>2</td> <td>5</td> </tr> <tr> <td>Glauconite</td> <td>2</td> <td>1</td> <td>1</td> <td>2</td> <td>—</td> </tr> <tr> <td>Diatoms</td> <td>27</td> <td>33</td> <td>32</td> <td>29</td> <td>36</td> </tr> <tr> <td>Radiolarians</td> <td>2</td> <td>2</td> <td>2</td> <td>2</td> <td>1</td> </tr> <tr> <td>Sponge spicules</td> <td>2</td> <td>2</td> <td>1</td> <td>2</td> <td>2</td> </tr> <tr> <td>Silicoflagellates</td> <td>1</td> <td>Tr</td> <td>Tr</td> <td>—</td> <td>Tr</td> </tr> </table>		1, 140	2, 140	3, 44	CC, 13	CC, 14		D	D	D	D	D	Sand	5	2	1	5	3	Silt	55	48	49	45	52	Clay	40	50	50	50	45	Quartz	5	3	3	Tr	2	Feldspar	10	8	10	10	8	Rock fragments	—	Tr	Tr	2	2	Clay	35	35	40	45	38	Volcanic glass	3	5	3	3	3	Calcite/dolomite	10	10	4	3	3	Accessory minerals						Pyrite	3	3	4	2	5	Glauconite	2	1	1	2	—	Diatoms	27	33	32	29	36	Radiolarians	2	2	2	2	1	Sponge spicules	2	2	1	2	2	Silicoflagellates	1	Tr	Tr	—	Tr
	1, 140	2, 140	3, 44	CC, 13	CC, 14																																																																																																																				
	D	D	D	D	D																																																																																																																				
Sand	5	2	1	5	3																																																																																																																				
Silt	55	48	49	45	52																																																																																																																				
Clay	40	50	50	50	45																																																																																																																				
Quartz	5	3	3	Tr	2																																																																																																																				
Feldspar	10	8	10	10	8																																																																																																																				
Rock fragments	—	Tr	Tr	2	2																																																																																																																				
Clay	35	35	40	45	38																																																																																																																				
Volcanic glass	3	5	3	3	3																																																																																																																				
Calcite/dolomite	10	10	4	3	3																																																																																																																				
Accessory minerals																																																																																																																									
Pyrite	3	3	4	2	5																																																																																																																				
Glauconite	2	1	1	2	—																																																																																																																				
Diatoms	27	33	32	29	36																																																																																																																				
Radiolarians	2	2	2	2	1																																																																																																																				
Sponge spicules	2	2	1	2	2																																																																																																																				
Silicoflagellates	1	Tr	Tr	—	Tr																																																																																																																				



SITE 685 HOLE A CORE 38X CORED INTERVAL 5408.9-5418.4 mbsl; 338.1-347.6 mbsf

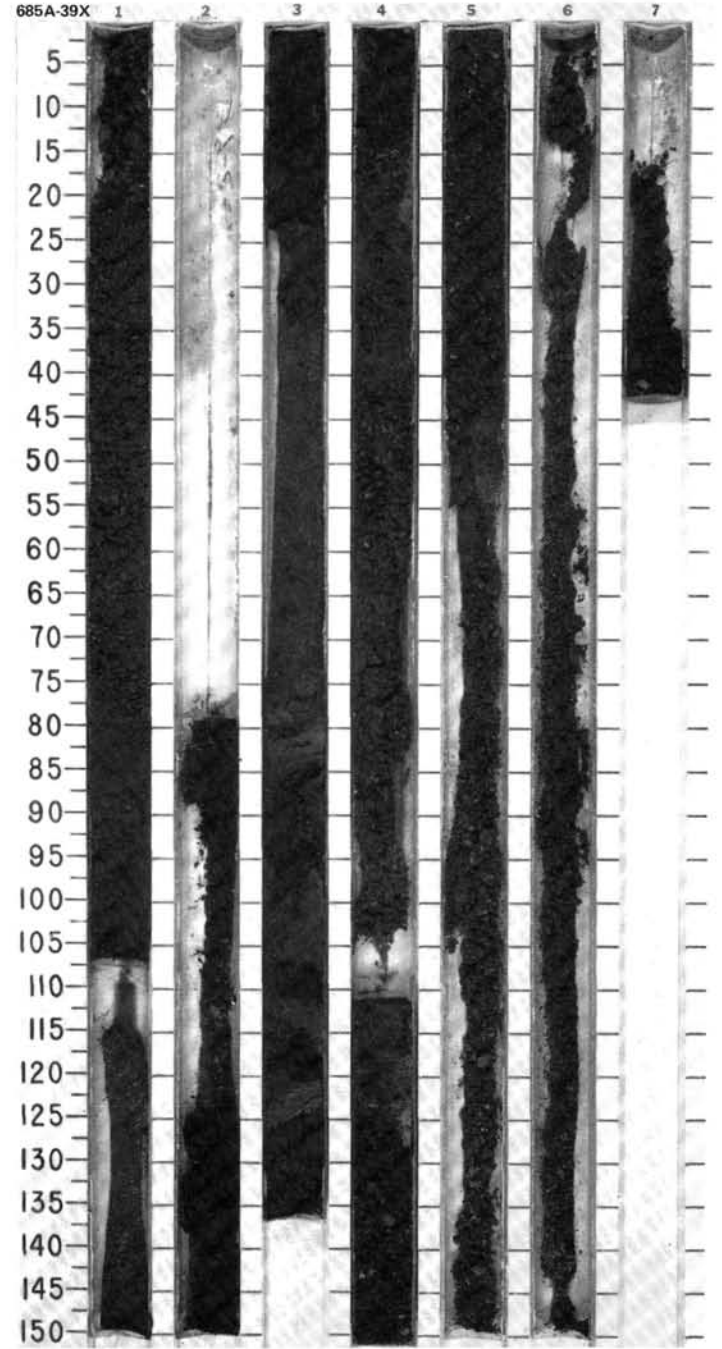
TIME-ROCK UNIT	BIOSTRAT. ZONE/ FOSSIL CHARACTER				PALEOMAGNETICS	PHYS. PROPERTIES	CHEMISTRY	SECTION	METERS	GRAPHIC LITHOLOGY	DRILLING DISTURB. SED. STRUCTURES	SAMPLES	LITHOLOGIC DESCRIPTION																																																																																																																														
	FORAMINIFERS	NANNOFOSSILS	RADIOLARIANS	DIATOMS																																																																																																																																							
UPPER MIOCENE	N16 TO N19*	NN10 ? *	* <i>Didymocypris antepenultimus</i> Zone	* <i>N. miocenica</i> Zone					0.5				<p>DIATOMACEOUS MUDSTONE</p> <p>Major lithology: diatomaceous mudstone, dark greenish gray (5GY 4/1).</p> <p>Minor lithologies: As cm-sized clasts in above from Section 1, 18-30 cm: pale yellow (5Y 7/4), muddy micrite. Greenish gray (5GY 5/1) diatomaceous mudstone. As 6-cm bed at base of CC: pale olive (5Y 6/3) calcareous mudstone.</p> <p>SMEAR SLIDE SUMMARY (%):</p> <table border="1"> <tr> <td></td> <td>1, 18</td> <td>1, 18</td> <td>1, 18</td> <td>CC, 4</td> <td>CC, 18</td> </tr> <tr> <td></td> <td>D</td> <td>(D)</td> <td>M</td> <td>D</td> <td>D</td> </tr> </table> <p>TEXTURE:</p> <table border="1"> <tr> <td>Sand</td> <td>—</td> <td>—</td> <td>—</td> <td>5</td> <td>2</td> </tr> <tr> <td>Silt</td> <td>47</td> <td>60</td> <td>35</td> <td>35</td> <td>20</td> </tr> <tr> <td>Clay</td> <td>53</td> <td>40</td> <td>65</td> <td>60</td> <td>78</td> </tr> </table> <p>COMPOSITION:</p> <table border="1"> <tr> <td>Quartz</td> <td>8</td> <td>15</td> <td>—</td> <td>2</td> <td>5</td> </tr> <tr> <td>Feldspar</td> <td>4</td> <td>5</td> <td>—</td> <td>15</td> <td>2</td> </tr> <tr> <td>Rock fragments</td> <td>3</td> <td>—</td> <td>—</td> <td>—</td> <td>—</td> </tr> <tr> <td>Mica</td> <td>1</td> <td>—</td> <td>—</td> <td>—</td> <td>—</td> </tr> <tr> <td>Clay</td> <td>53</td> <td>40</td> <td>25</td> <td>55</td> <td>20</td> </tr> <tr> <td>Volcanic glass</td> <td>—</td> <td>Tr</td> <td>—</td> <td>3</td> <td>2</td> </tr> <tr> <td>Calcite/dolomite</td> <td>1</td> <td>2</td> <td>27</td> <td>5</td> <td>58</td> </tr> <tr> <td>Accessory minerals</td> <td></td> <td></td> <td></td> <td></td> <td></td> </tr> <tr> <td>Pyrite</td> <td>5</td> <td>3</td> <td>2</td> <td>3</td> <td>3</td> </tr> <tr> <td>Glauconite</td> <td>—</td> <td>—</td> <td>—</td> <td>2</td> <td>2</td> </tr> <tr> <td>Micrite</td> <td>—</td> <td>—</td> <td>40</td> <td>—</td> <td>—</td> </tr> <tr> <td>Nannofossils</td> <td>Tr</td> <td>—</td> <td>1</td> <td>2</td> <td>5</td> </tr> <tr> <td>Diatoms</td> <td>25</td> <td>30</td> <td>5</td> <td>10</td> <td>—</td> </tr> <tr> <td>Radiolarians</td> <td>—</td> <td>—</td> <td>—</td> <td>1</td> <td>1</td> </tr> <tr> <td>Sponge spicules</td> <td>—</td> <td>Tr</td> <td>—</td> <td>2</td> <td>2</td> </tr> <tr> <td>Silicoflagellates</td> <td>—</td> <td>—</td> <td>—</td> <td>Tr</td> <td>Tr</td> </tr> </table>		1, 18	1, 18	1, 18	CC, 4	CC, 18		D	(D)	M	D	D	Sand	—	—	—	5	2	Silt	47	60	35	35	20	Clay	53	40	65	60	78	Quartz	8	15	—	2	5	Feldspar	4	5	—	15	2	Rock fragments	3	—	—	—	—	Mica	1	—	—	—	—	Clay	53	40	25	55	20	Volcanic glass	—	Tr	—	3	2	Calcite/dolomite	1	2	27	5	58	Accessory minerals						Pyrite	5	3	2	3	3	Glauconite	—	—	—	2	2	Micrite	—	—	40	—	—	Nannofossils	Tr	—	1	2	5	Diatoms	25	30	5	10	—	Radiolarians	—	—	—	1	1	Sponge spicules	—	Tr	—	2	2	Silicoflagellates	—	—	—	Tr	Tr
	1, 18	1, 18	1, 18	CC, 4	CC, 18																																																																																																																																						
	D	(D)	M	D	D																																																																																																																																						
Sand	—	—	—	5	2																																																																																																																																						
Silt	47	60	35	35	20																																																																																																																																						
Clay	53	40	65	60	78																																																																																																																																						
Quartz	8	15	—	2	5																																																																																																																																						
Feldspar	4	5	—	15	2																																																																																																																																						
Rock fragments	3	—	—	—	—																																																																																																																																						
Mica	1	—	—	—	—																																																																																																																																						
Clay	53	40	25	55	20																																																																																																																																						
Volcanic glass	—	Tr	—	3	2																																																																																																																																						
Calcite/dolomite	1	2	27	5	58																																																																																																																																						
Accessory minerals																																																																																																																																											
Pyrite	5	3	2	3	3																																																																																																																																						
Glauconite	—	—	—	2	2																																																																																																																																						
Micrite	—	—	40	—	—																																																																																																																																						
Nannofossils	Tr	—	1	2	5																																																																																																																																						
Diatoms	25	30	5	10	—																																																																																																																																						
Radiolarians	—	—	—	1	1																																																																																																																																						
Sponge spicules	—	Tr	—	2	2																																																																																																																																						
Silicoflagellates	—	—	—	Tr	Tr																																																																																																																																						

SITE 685

SITE 685 HOLE A CORE 39X CORED INTERVAL 5418.4-5427.9 mbsl; 347.6-357.1 mbsf

TIME-ROCK UNIT	BIOSTRAT. ZONE/ FOSSIL CHARACTER			PALEOMAGNETICS	PHYS. PROPERTIES	CHEMISTRY	SECTION	METERS	GRAPHIC LITHOLOGY	DRILLING DISTURB.	SEP. STRUCTURES	SAMPLES	LITHOLOGIC DESCRIPTION																																																																																																												
	FORAMINIFERS	NANNOFOSSILS	RADIOLARIANS																																																																																																																						
LATE MIOCENE								0.5					<p>DIATOMACEOUS MUDSTONE</p> <p>Major lithology: diatomaceous mudstone, dark olive green, dark greenish gray (5Y 3/2, 5GY 4/1, 10Y 4/2), locally calcareous.</p> <p>Minor lithology: black (5Y 2.5/2), pyritic diatomaceous mudstone in Section 9 and CC.</p> <p>SMEAR SLIDE SUMMARY (%):</p> <table border="1"> <tr> <td></td> <td>1, 60</td> <td>3, 83</td> <td>6, 40</td> <td>9, 20</td> <td>9, 22</td> </tr> <tr> <td></td> <td>D</td> <td>M</td> <td>D</td> <td>D</td> <td>D</td> </tr> </table> <p>TEXTURE:</p> <table border="1"> <tr> <td>Sand</td> <td>20</td> <td>5</td> <td>5</td> <td>10</td> <td>10</td> </tr> <tr> <td>Silt</td> <td>40</td> <td>25</td> <td>40</td> <td>45</td> <td>45</td> </tr> <tr> <td>Clay</td> <td>40</td> <td>70</td> <td>55</td> <td>45</td> <td>45</td> </tr> </table> <p>COMPOSITION:</p> <table border="1"> <tr> <td>Quartz</td> <td>5</td> <td>5</td> <td>5</td> <td>5</td> <td>10</td> </tr> <tr> <td>Feldspar</td> <td>10</td> <td>5</td> <td>5</td> <td>5</td> <td>5</td> </tr> <tr> <td>Rock fragments</td> <td>5</td> <td>Tr</td> <td>5</td> <td>5</td> <td>5</td> </tr> <tr> <td>Mica</td> <td>—</td> <td>—</td> <td>Tr</td> <td>Tr</td> <td>—</td> </tr> <tr> <td>Clay</td> <td>30</td> <td>60</td> <td>40</td> <td>35</td> <td>30</td> </tr> <tr> <td>Calcite/dolomite</td> <td>5</td> <td>—</td> <td>Tr</td> <td>10</td> <td>Tr</td> </tr> <tr> <td>Accessory minerals</td> <td></td> <td></td> <td></td> <td></td> <td></td> </tr> <tr> <td>Pyrite</td> <td>8</td> <td>5</td> <td>8</td> <td>10</td> <td>10</td> </tr> <tr> <td>Glaucanite</td> <td>2</td> <td>Tr</td> <td>—</td> <td>Tr</td> <td>Tr</td> </tr> <tr> <td>Diatoms</td> <td>30</td> <td>20</td> <td>35</td> <td>30</td> <td>30</td> </tr> <tr> <td>Radiolarians</td> <td>Tr</td> <td>—</td> <td>Tr</td> <td>—</td> <td>5</td> </tr> <tr> <td>Sponge spicules</td> <td>5</td> <td>5</td> <td>2</td> <td>Tr</td> <td>5</td> </tr> <tr> <td>Silicoflagellates</td> <td>Tr</td> <td>—</td> <td>—</td> <td>—</td> <td>—</td> </tr> </table>		1, 60	3, 83	6, 40	9, 20	9, 22		D	M	D	D	D	Sand	20	5	5	10	10	Silt	40	25	40	45	45	Clay	40	70	55	45	45	Quartz	5	5	5	5	10	Feldspar	10	5	5	5	5	Rock fragments	5	Tr	5	5	5	Mica	—	—	Tr	Tr	—	Clay	30	60	40	35	30	Calcite/dolomite	5	—	Tr	10	Tr	Accessory minerals						Pyrite	8	5	8	10	10	Glaucanite	2	Tr	—	Tr	Tr	Diatoms	30	20	35	30	30	Radiolarians	Tr	—	Tr	—	5	Sponge spicules	5	5	2	Tr	5	Silicoflagellates	Tr	—	—	—	—
		1, 60	3, 83	6, 40	9, 20	9, 22																																																																																																																			
		D	M	D	D	D																																																																																																																			
	Sand	20	5	5	10	10																																																																																																																			
	Silt	40	25	40	45	45																																																																																																																			
	Clay	40	70	55	45	45																																																																																																																			
	Quartz	5	5	5	5	10																																																																																																																			
Feldspar	10	5	5	5	5																																																																																																																				
Rock fragments	5	Tr	5	5	5																																																																																																																				
Mica	—	—	Tr	Tr	—																																																																																																																				
Clay	30	60	40	35	30																																																																																																																				
Calcite/dolomite	5	—	Tr	10	Tr																																																																																																																				
Accessory minerals																																																																																																																									
Pyrite	8	5	8	10	10																																																																																																																				
Glaucanite	2	Tr	—	Tr	Tr																																																																																																																				
Diatoms	30	20	35	30	30																																																																																																																				
Radiolarians	Tr	—	Tr	—	5																																																																																																																				
Sponge spicules	5	5	2	Tr	5																																																																																																																				
Silicoflagellates	Tr	—	—	—	—																																																																																																																				
							1.0																																																																																																																		
							2	VOID																																																																																																																	
							3																																																																																																																		
							4																																																																																																																		
							5																																																																																																																		
							6																																																																																																																		
							7	VOID																																																																																																																	

(CONT.)

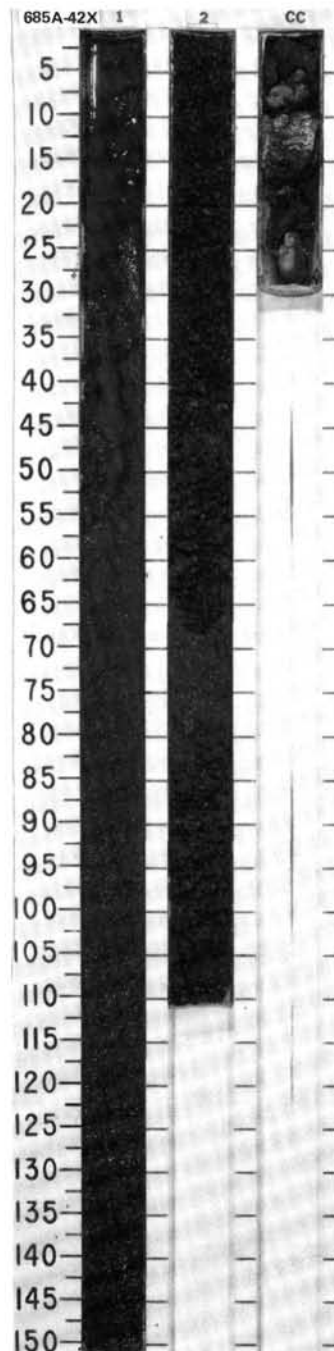
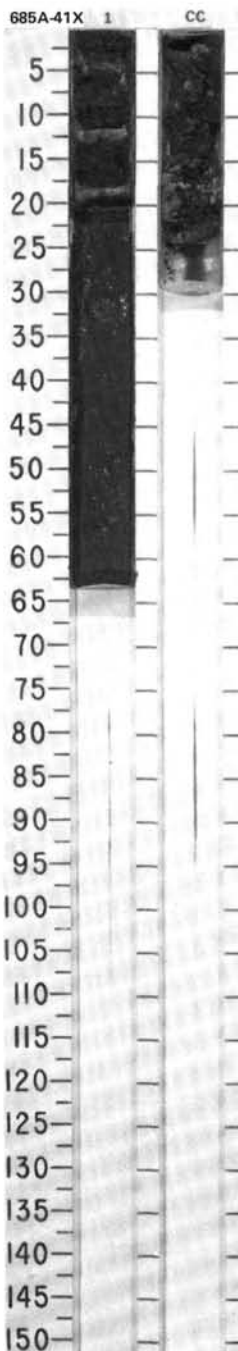


SITE 685 HOLE A CORE 41X CORED INTERVAL 5437.4-5446.9 mbsl; 366.6-376.1 mbsf

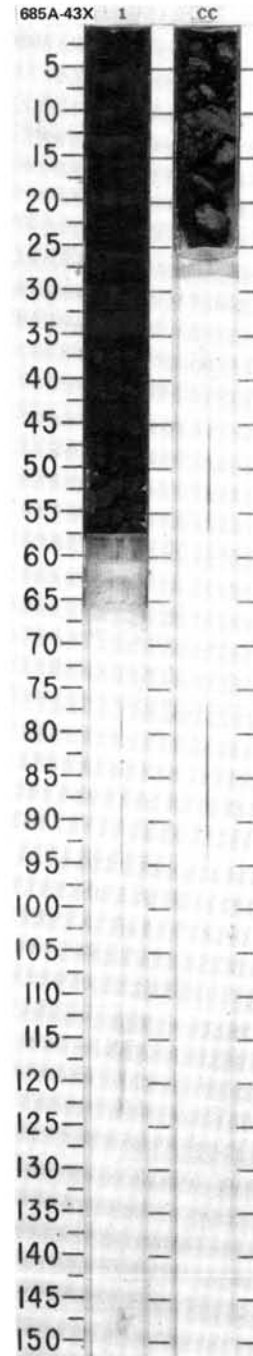
TIME-ROCK UNIT	BIOSTRAT. ZONE/ FOSSIL CHARACTER			PALEOMAGNETICS	PHYS. PROPERTIES	CHEMISTRY	SECTION	METERS	GRAPHIC LITHOLOGY	DRILLING DISTURB. SED. STRUCTURES	SAMPLES	LITHOLOGIC DESCRIPTION				
	FORAMINIFERS	NANNOFOSSILS	RADIOLARIANS										DIATOMS			
UPPER MIOCENE	B*						1	0.5			*	DIATOM-BEARING AND DIATOMACEOUS MUDSTONE				
	B*						CC				**	Major lithology: diatom-bearing and diatomaceous mudstone, dark greenish gray (4GY 4/1), which in CC contains clasts (boudinaged original thin beds?) of: Minor lithology: pale yellow (5Y 7/4) micritic siltstone. Black (N 2/), diatom-bearing pyritic mudstone.				
		* <i>Didymocyrtilis antepenultimus</i> Zone *										SMEAR SLIDE SUMMARY (%):				
												1, 15 D	CC, 16 M	CC, 17 D	CC, 18 M	
												TEXTURE:				
												Sand	5			
												Silt	30	90	40	50
												Clay	65	10	60	50
												COMPOSITION:				
												Quartz	5	3	4	3
												Feldspar	5	1	3	3
												Rock fragments	3	1	3	2
												Mica	Tr	2	2	1
												Clay	46	9	55	44
												Volcanic glass	3	3	3	2
												Accessory minerals				
												Pyrite	1	1	2	25
												Glauconite	2	3	1	1
												Phosphate	2		2	2
												Micrite	5	70	5	2
												Diatoms	25	5	18	13
												Radiolarians	1	1	1	1
												Sponge spicules	2	1	1	1
												Silicoflagellates	Tr			

SITE 685 HOLE A CORE 42X CORED INTERVAL 5446.9-5456.4 mbsl; 376.1-385.6 mbsf

TIME-ROCK UNIT	BIOSTRAT. ZONE/ FOSSIL CHARACTER			PALEOMAGNETICS	PHYS. PROPERTIES	CHEMISTRY	SECTION	METERS	GRAPHIC LITHOLOGY	DRILLING DISTURB. SED. STRUCTURES	SAMPLES	LITHOLOGIC DESCRIPTION	
	FORAMINIFERS	NANNOFOSSILS	RADIOLARIANS										DIATOMS
UPPER MIOCENE	#B						1	0.5				MUDSTONE, MICRITE CHIPS, AND CAVINGS, and DIATOMACEOUS MUD	
	#B						2	1.0				Major lithology: Sections 1 and 2: Drilling chips and cavings comprising olive gray (5Y 4/2) mudstone; pale yellow (5Y 7/4) micrite; black (5Y 2.5/1) mudstone. CC: diatomaceous mud, dark olive gray (5Y 3/2), calcareous. Minor lithology: dark gray (N 4), fractured and veined dolomitic, at base of CC.	
		* <i>Didymocyrtilis antepenultimus</i> Zone *										SMEAR SLIDE SUMMARY (%):	
												CC, 8 D	
												TEXTURE:	
												Silt	45
												Clay	55
												COMPOSITION:	
												Quartz	5
												Feldspar	5
												Rock fragments	Tr
												Clay	55
												Calcite/dolomite	10
												Accessory minerals	
												Glauconite	Tr
												Diatoms	20
												Radiolarians	Tr
												Sponge spicules	5

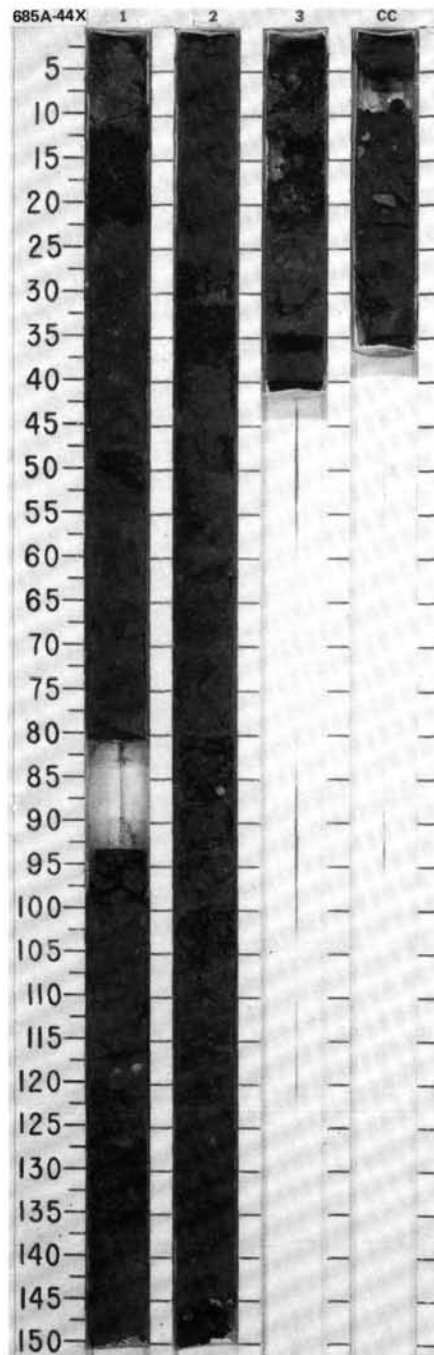


TIME-ROCK UNIT	BIOSTRAT. ZONE/ FOSSIL CHARACTER				PALEOMAGNETICS	PHYS. PROPERTIES	CHEMISTRY	SECTION	METERS	GRAPHIC LITHOLOGY	DRILLING DISTURB.	SED. STRUCTURES	SAMPLES	LITHOLOGIC DESCRIPTION																																																																		
	FORAMINIFERS	NANNOFOSSILS	RADIOLARIANS	DIATOMS																																																																												
UPPER MIOCENE	B*							1	0.5				*	DIATOMACEOUS MUD AND MUDSTONE																																																																		
								CC					**	Major lithology: diatomaceous mud and mudstone, dark olive gray to olive gray (5Y 3/2, 5Y 4/2).																																																																		
													**	Minor lithologies: pale yellow (5Y 7/4) muddy diatom ooze; dark gray (N 4), vitric tuff (.5-cm layer at base of CC and as blebs in Section 1-10 cm).																																																																		
													**	SMEAR SLIDE SUMMARY (%):																																																																		
													**	<table border="1"> <thead> <tr> <th></th> <th>1, 8 M</th> <th>1, 43 D</th> <th>CC, 3 D</th> <th>CC, 11 M</th> <th>CC, 20 M</th> </tr> </thead> <tbody> <tr> <td>Sand</td> <td>55</td> <td>5</td> <td>3</td> <td>3</td> <td>85</td> </tr> <tr> <td>Silt</td> <td>30</td> <td>40</td> <td>42</td> <td>55</td> <td>10</td> </tr> <tr> <td>Clay</td> <td>15</td> <td>55</td> <td>55</td> <td>42</td> <td>5</td> </tr> </tbody> </table>		1, 8 M	1, 43 D	CC, 3 D	CC, 11 M	CC, 20 M	Sand	55	5	3	3	85	Silt	30	40	42	55	10	Clay	15	55	55	42	5																																										
	1, 8 M	1, 43 D	CC, 3 D	CC, 11 M	CC, 20 M																																																																											
Sand	55	5	3	3	85																																																																											
Silt	30	40	42	55	10																																																																											
Clay	15	55	55	42	5																																																																											
													**	TEXTURE:																																																																		
													**	<table border="1"> <tbody> <tr> <td>Sand</td> <td>55</td> <td>5</td> <td>3</td> <td>3</td> <td>85</td> </tr> <tr> <td>Silt</td> <td>30</td> <td>40</td> <td>42</td> <td>55</td> <td>10</td> </tr> <tr> <td>Clay</td> <td>15</td> <td>55</td> <td>55</td> <td>42</td> <td>5</td> </tr> </tbody> </table>	Sand	55	5	3	3	85	Silt	30	40	42	55	10	Clay	15	55	55	42	5																																																
Sand	55	5	3	3	85																																																																											
Silt	30	40	42	55	10																																																																											
Clay	15	55	55	42	5																																																																											
													**	COMPOSITION:																																																																		
													**	<table border="1"> <tbody> <tr> <td>Quartz</td> <td>Tr</td> <td>4</td> <td>5</td> <td>4</td> <td>—</td> </tr> <tr> <td>Feldspar</td> <td>5</td> <td>3</td> <td>5</td> <td>5</td> <td>15</td> </tr> <tr> <td>Rock fragments</td> <td>5</td> <td>3</td> <td>3</td> <td>2</td> <td>—</td> </tr> <tr> <td>Clay</td> <td>10</td> <td>40</td> <td>50</td> <td>40</td> <td>5</td> </tr> <tr> <td>Volcanic glass</td> <td>75</td> <td>—</td> <td>—</td> <td>—</td> <td>80</td> </tr> <tr> <td>Accessory minerals</td> <td></td> <td></td> <td></td> <td></td> <td></td> </tr> <tr> <td> Pyrite</td> <td>5</td> <td>10</td> <td>2</td> <td>2</td> <td>—</td> </tr> <tr> <td>Nannofossils</td> <td>Tr</td> <td>—</td> <td>—</td> <td>—</td> <td>—</td> </tr> <tr> <td>Diatoms</td> <td>Tr</td> <td>40</td> <td>35</td> <td>45</td> <td>—</td> </tr> <tr> <td>Radiolarians</td> <td>—</td> <td>—</td> <td>Tr</td> <td>2</td> <td>—</td> </tr> <tr> <td>Sponge spicules</td> <td>—</td> <td>—</td> <td>Tr</td> <td>—</td> <td>—</td> </tr> </tbody> </table>	Quartz	Tr	4	5	4	—	Feldspar	5	3	5	5	15	Rock fragments	5	3	3	2	—	Clay	10	40	50	40	5	Volcanic glass	75	—	—	—	80	Accessory minerals						Pyrite	5	10	2	2	—	Nannofossils	Tr	—	—	—	—	Diatoms	Tr	40	35	45	—	Radiolarians	—	—	Tr	2	—	Sponge spicules	—	—	Tr	—	—
Quartz	Tr	4	5	4	—																																																																											
Feldspar	5	3	5	5	15																																																																											
Rock fragments	5	3	3	2	—																																																																											
Clay	10	40	50	40	5																																																																											
Volcanic glass	75	—	—	—	80																																																																											
Accessory minerals																																																																																
Pyrite	5	10	2	2	—																																																																											
Nannofossils	Tr	—	—	—	—																																																																											
Diatoms	Tr	40	35	45	—																																																																											
Radiolarians	—	—	Tr	2	—																																																																											
Sponge spicules	—	—	Tr	—	—																																																																											
													*																																																																			



SITE 685 HOLE A CORE 44X CORED INTERVAL 5463.4-5472.9 mbsl; 392.6-402.1 mbsf

TIME-ROCK UNIT	BIOSTRAT. ZONE/ FOSSIL CHARACTER				SECTION	METERS	GRAPHIC LITHOLOGY	DRILLING DISTURB.	SED. STRUCTURES	SAMPLES	LITHOLOGIC DESCRIPTION																																																																																																																																																																																																																																																																																																																																																																																																
	FORAMINIFERS	NANNOFOSSILS	RADIOLARIANS	DIATOMS																																																																																																																																																																																																																																																																																																																																																																																																							
UPPER MIOCENE	N4 to N6 *										<p>POLYMICT BRECCIA/CONGLOMERATE</p> <p>Major lithology: polyimict breccia/conglomerate comprising clasts of:</p> <ol style="list-style-type: none"> 1. dark gray (N 4) sandy pyritic mudstone. 2. black (N 3) mudstone. 3. light gray (5Y 7/1) micritic limestone. 4. light olive brown (5Y 5/3) dolomite. 5. dark greenish gray (5BG 4/1) diatomaceous mudstone. 6. dark grayish green (5G 4/1) chloritic siliceous mudstone. 7. grayish brown medium brown (2.5Y 5/2) diatom foraminifer nannofossil-mudstone. 8. one clast (0.5 cm), feldspathic granitoid. <p>Matrix: dark grayish brown (2.5Y 3.5/2) diatom-bearing mud.</p> <p>SMEAR SLIDE SUMMARY (%):</p> <table border="1"> <thead> <tr> <th></th> <th>1, 113</th> <th>2, 6</th> <th>2, 15</th> <th>2, 72</th> <th>2, 111</th> <th>CC, 6</th> <th>CC, 11</th> </tr> <tr> <th></th> <th>M</th> <th>M</th> <th>M</th> <th>M</th> <th>D</th> <th>M</th> <th>M</th> </tr> </thead> <tbody> <tr> <td>TEXTURE:</td> <td></td> <td></td> <td></td> <td></td> <td></td> <td></td> <td></td> </tr> <tr> <td>Sand</td> <td>15</td> <td>—</td> <td>30</td> <td>—</td> <td>10</td> <td>5</td> <td>—</td> </tr> <tr> <td>Silt</td> <td>25</td> <td>—</td> <td>35</td> <td>53</td> <td>40</td> <td>50</td> <td>2</td> </tr> <tr> <td>Clay</td> <td>60</td> <td>—</td> <td>35</td> <td>47</td> <td>50</td> <td>45</td> <td>98</td> </tr> <tr> <td>COMPOSITION:</td> <td></td> <td></td> <td></td> <td></td> <td></td> <td></td> <td></td> </tr> <tr> <td>Quartz</td> <td>5</td> <td>40</td> <td>10</td> <td>5</td> <td>5</td> <td>5</td> <td>1</td> </tr> <tr> <td>Feldspar</td> <td>5</td> <td>40</td> <td>15</td> <td>5</td> <td>5</td> <td>5</td> <td>—</td> </tr> <tr> <td>Rock fragments</td> <td>5</td> <td>—</td> <td>5</td> <td>2</td> <td>—</td> <td>5</td> <td>—</td> </tr> <tr> <td>Mica</td> <td>Tr</td> <td>—</td> <td>Tr</td> <td>Tr</td> <td>—</td> <td>Tr</td> <td>Tr</td> </tr> <tr> <td>Clay</td> <td>50</td> <td>10</td> <td>30</td> <td>47</td> <td>59</td> <td>68</td> <td>—</td> </tr> <tr> <td>Volcanic glass</td> <td>—</td> <td>—</td> <td>5</td> <td>2</td> <td>Tr</td> <td>Tr</td> <td>—</td> </tr> <tr> <td>Calcite/dolomite</td> <td>—</td> <td>—</td> <td>—</td> <td>Tr</td> <td>5</td> <td>Tr</td> <td>97</td> </tr> <tr> <td>Accessory minerals</td> <td>—</td> <td>2</td> <td>—</td> <td>—</td> <td>—</td> <td>—</td> <td>—</td> </tr> <tr> <td>Pyrite</td> <td>8</td> <td>—</td> <td>20</td> <td>—</td> <td>—</td> <td>5</td> <td>—</td> </tr> <tr> <td>Apatite</td> <td>—</td> <td>—</td> <td>—</td> <td>—</td> <td>1</td> <td>—</td> <td>—</td> </tr> <tr> <td>Glauconite</td> <td>—</td> <td>—</td> <td>—</td> <td>—</td> <td>—</td> <td>Tr</td> <td>—</td> </tr> <tr> <td>Opauques</td> <td>—</td> <td>3</td> <td>—</td> <td>2</td> <td>—</td> <td>—</td> <td>—</td> </tr> <tr> <td>Nannofossils</td> <td>—</td> <td>—</td> <td>—</td> <td>—</td> <td>Tr</td> <td>—</td> <td>—</td> </tr> <tr> <td>Diatoms</td> <td>15</td> <td>5</td> <td>5</td> <td>35</td> <td>15</td> <td>10</td> <td>1</td> </tr> <tr> <td>Radiolarians</td> <td>5</td> <td>—</td> <td>5</td> <td>1</td> <td>—</td> <td>Tr</td> <td>—</td> </tr> <tr> <td>Sponge spicules</td> <td>7</td> <td>—</td> <td>—</td> <td>1</td> <td>5</td> <td>2</td> <td>—</td> </tr> <tr> <td>Silicoflagellates</td> <td>—</td> <td>—</td> <td>—</td> <td>Tr</td> <td>—</td> <td>—</td> <td>—</td> </tr> <tr> <td>Fish remains</td> <td>—</td> <td>—</td> <td>5</td> <td>—</td> <td>—</td> <td>—</td> <td>—</td> </tr> <tr> <td></td> <td>CC, 16</td> <td>CC, 16</td> <td>CC, 18</td> <td>CC, 33</td> <td>CC, 33</td> <td>CC, 33</td> <td></td> </tr> <tr> <td></td> <td>M</td> <td>M</td> <td>M</td> <td>D</td> <td>M</td> <td>M</td> <td></td> </tr> <tr> <td>TEXTURE:</td> <td></td> <td></td> <td></td> <td></td> <td></td> <td></td> <td></td> </tr> <tr> <td>Sand</td> <td>20</td> <td>—</td> <td>—</td> <td>10</td> <td>5</td> <td>—</td> <td>—</td> </tr> <tr> <td>Silt</td> <td>45</td> <td>56</td> <td>70</td> <td>35</td> <td>50</td> <td>—</td> <td>—</td> </tr> <tr> <td>Clay</td> <td>35</td> <td>44</td> <td>30</td> <td>55</td> <td>45</td> <td>—</td> <td>—</td> </tr> <tr> <td>COMPOSITION:</td> <td></td> <td></td> <td></td> <td></td> <td></td> <td></td> <td></td> </tr> <tr> <td>Quartz</td> <td>Tr</td> <td>5</td> <td>—</td> <td>5</td> <td>3</td> <td>—</td> <td>—</td> </tr> <tr> <td>Feldspar</td> <td>Tr</td> <td>3</td> <td>—</td> <td>5</td> <td>5</td> <td>—</td> <td>—</td> </tr> <tr> <td>Rock fragments</td> <td>—</td> <td>—</td> <td>—</td> <td>2</td> <td>—</td> <td>—</td> <td>—</td> </tr> <tr> <td>Mica</td> <td>—</td> <td>2</td> <td>—</td> <td>Tr</td> <td>Tr</td> <td>—</td> <td>—</td> </tr> <tr> <td>Clay</td> <td>22</td> <td>18</td> <td>—</td> <td>55</td> <td>35</td> <td>—</td> <td>—</td> </tr> <tr> <td>Volcanic glass</td> <td>—</td> <td>—</td> <td>—</td> <td>—</td> <td>Tr</td> <td>—</td> <td>—</td> </tr> <tr> <td>Calcite/dolomite</td> <td>10</td> <td>3</td> <td>98</td> <td>—</td> <td>—</td> <td>—</td> <td>—</td> </tr> <tr> <td>Pyrite</td> <td>3</td> <td>—</td> <td>—</td> <td>5</td> <td>7</td> <td>—</td> <td>—</td> </tr> <tr> <td>Glauconite</td> <td>—</td> <td>—</td> <td>—</td> <td>—</td> <td>1</td> <td>—</td> <td>—</td> </tr> <tr> <td>Opauques</td> <td>—</td> <td>8</td> <td>—</td> <td>—</td> <td>—</td> <td>—</td> <td>—</td> </tr> <tr> <td>Phosphate</td> <td>—</td> <td>1</td> <td>—</td> <td>—</td> <td>—</td> <td>—</td> <td>—</td> </tr> <tr> <td>Foraminifers</td> <td>20</td> <td>—</td> <td>—</td> <td>—</td> <td>—</td> <td>—</td> <td>—</td> </tr> <tr> <td>Nannofossils</td> <td>20</td> <td>25</td> <td>—</td> <td>—</td> <td>—</td> <td>—</td> <td>—</td> </tr> <tr> <td>Diatoms</td> <td>25</td> <td>35</td> <td>2</td> <td>20</td> <td>39</td> <td>—</td> <td>—</td> </tr> <tr> <td>Radiolarians</td> <td>—</td> <td>—</td> <td>—</td> <td>5</td> <td>5</td> <td>—</td> <td>—</td> </tr> <tr> <td>Sponge spicules</td> <td>—</td> <td>—</td> <td>—</td> <td>3</td> <td>3</td> <td>—</td> <td>—</td> </tr> </tbody> </table>		1, 113	2, 6	2, 15	2, 72	2, 111	CC, 6	CC, 11		M	M	M	M	D	M	M	TEXTURE:								Sand	15	—	30	—	10	5	—	Silt	25	—	35	53	40	50	2	Clay	60	—	35	47	50	45	98	COMPOSITION:								Quartz	5	40	10	5	5	5	1	Feldspar	5	40	15	5	5	5	—	Rock fragments	5	—	5	2	—	5	—	Mica	Tr	—	Tr	Tr	—	Tr	Tr	Clay	50	10	30	47	59	68	—	Volcanic glass	—	—	5	2	Tr	Tr	—	Calcite/dolomite	—	—	—	Tr	5	Tr	97	Accessory minerals	—	2	—	—	—	—	—	Pyrite	8	—	20	—	—	5	—	Apatite	—	—	—	—	1	—	—	Glauconite	—	—	—	—	—	Tr	—	Opauques	—	3	—	2	—	—	—	Nannofossils	—	—	—	—	Tr	—	—	Diatoms	15	5	5	35	15	10	1	Radiolarians	5	—	5	1	—	Tr	—	Sponge spicules	7	—	—	1	5	2	—	Silicoflagellates	—	—	—	Tr	—	—	—	Fish remains	—	—	5	—	—	—	—		CC, 16	CC, 16	CC, 18	CC, 33	CC, 33	CC, 33			M	M	M	D	M	M		TEXTURE:								Sand	20	—	—	10	5	—	—	Silt	45	56	70	35	50	—	—	Clay	35	44	30	55	45	—	—	COMPOSITION:								Quartz	Tr	5	—	5	3	—	—	Feldspar	Tr	3	—	5	5	—	—	Rock fragments	—	—	—	2	—	—	—	Mica	—	2	—	Tr	Tr	—	—	Clay	22	18	—	55	35	—	—	Volcanic glass	—	—	—	—	Tr	—	—	Calcite/dolomite	10	3	98	—	—	—	—	Pyrite	3	—	—	5	7	—	—	Glauconite	—	—	—	—	1	—	—	Opauques	—	8	—	—	—	—	—	Phosphate	—	1	—	—	—	—	—	Foraminifers	20	—	—	—	—	—	—	Nannofossils	20	25	—	—	—	—	—	Diatoms	25	35	2	20	39	—	—	Radiolarians	—	—	—	5	5	—	—	Sponge spicules	—	—	—	3	3	—	—
	1, 113	2, 6	2, 15	2, 72	2, 111	CC, 6	CC, 11																																																																																																																																																																																																																																																																																																																																																																																																				
	M	M	M	M	D	M	M																																																																																																																																																																																																																																																																																																																																																																																																				
TEXTURE:																																																																																																																																																																																																																																																																																																																																																																																																											
Sand	15	—	30	—	10	5	—																																																																																																																																																																																																																																																																																																																																																																																																				
Silt	25	—	35	53	40	50	2																																																																																																																																																																																																																																																																																																																																																																																																				
Clay	60	—	35	47	50	45	98																																																																																																																																																																																																																																																																																																																																																																																																				
COMPOSITION:																																																																																																																																																																																																																																																																																																																																																																																																											
Quartz	5	40	10	5	5	5	1																																																																																																																																																																																																																																																																																																																																																																																																				
Feldspar	5	40	15	5	5	5	—																																																																																																																																																																																																																																																																																																																																																																																																				
Rock fragments	5	—	5	2	—	5	—																																																																																																																																																																																																																																																																																																																																																																																																				
Mica	Tr	—	Tr	Tr	—	Tr	Tr																																																																																																																																																																																																																																																																																																																																																																																																				
Clay	50	10	30	47	59	68	—																																																																																																																																																																																																																																																																																																																																																																																																				
Volcanic glass	—	—	5	2	Tr	Tr	—																																																																																																																																																																																																																																																																																																																																																																																																				
Calcite/dolomite	—	—	—	Tr	5	Tr	97																																																																																																																																																																																																																																																																																																																																																																																																				
Accessory minerals	—	2	—	—	—	—	—																																																																																																																																																																																																																																																																																																																																																																																																				
Pyrite	8	—	20	—	—	5	—																																																																																																																																																																																																																																																																																																																																																																																																				
Apatite	—	—	—	—	1	—	—																																																																																																																																																																																																																																																																																																																																																																																																				
Glauconite	—	—	—	—	—	Tr	—																																																																																																																																																																																																																																																																																																																																																																																																				
Opauques	—	3	—	2	—	—	—																																																																																																																																																																																																																																																																																																																																																																																																				
Nannofossils	—	—	—	—	Tr	—	—																																																																																																																																																																																																																																																																																																																																																																																																				
Diatoms	15	5	5	35	15	10	1																																																																																																																																																																																																																																																																																																																																																																																																				
Radiolarians	5	—	5	1	—	Tr	—																																																																																																																																																																																																																																																																																																																																																																																																				
Sponge spicules	7	—	—	1	5	2	—																																																																																																																																																																																																																																																																																																																																																																																																				
Silicoflagellates	—	—	—	Tr	—	—	—																																																																																																																																																																																																																																																																																																																																																																																																				
Fish remains	—	—	5	—	—	—	—																																																																																																																																																																																																																																																																																																																																																																																																				
	CC, 16	CC, 16	CC, 18	CC, 33	CC, 33	CC, 33																																																																																																																																																																																																																																																																																																																																																																																																					
	M	M	M	D	M	M																																																																																																																																																																																																																																																																																																																																																																																																					
TEXTURE:																																																																																																																																																																																																																																																																																																																																																																																																											
Sand	20	—	—	10	5	—	—																																																																																																																																																																																																																																																																																																																																																																																																				
Silt	45	56	70	35	50	—	—																																																																																																																																																																																																																																																																																																																																																																																																				
Clay	35	44	30	55	45	—	—																																																																																																																																																																																																																																																																																																																																																																																																				
COMPOSITION:																																																																																																																																																																																																																																																																																																																																																																																																											
Quartz	Tr	5	—	5	3	—	—																																																																																																																																																																																																																																																																																																																																																																																																				
Feldspar	Tr	3	—	5	5	—	—																																																																																																																																																																																																																																																																																																																																																																																																				
Rock fragments	—	—	—	2	—	—	—																																																																																																																																																																																																																																																																																																																																																																																																				
Mica	—	2	—	Tr	Tr	—	—																																																																																																																																																																																																																																																																																																																																																																																																				
Clay	22	18	—	55	35	—	—																																																																																																																																																																																																																																																																																																																																																																																																				
Volcanic glass	—	—	—	—	Tr	—	—																																																																																																																																																																																																																																																																																																																																																																																																				
Calcite/dolomite	10	3	98	—	—	—	—																																																																																																																																																																																																																																																																																																																																																																																																				
Pyrite	3	—	—	5	7	—	—																																																																																																																																																																																																																																																																																																																																																																																																				
Glauconite	—	—	—	—	1	—	—																																																																																																																																																																																																																																																																																																																																																																																																				
Opauques	—	8	—	—	—	—	—																																																																																																																																																																																																																																																																																																																																																																																																				
Phosphate	—	1	—	—	—	—	—																																																																																																																																																																																																																																																																																																																																																																																																				
Foraminifers	20	—	—	—	—	—	—																																																																																																																																																																																																																																																																																																																																																																																																				
Nannofossils	20	25	—	—	—	—	—																																																																																																																																																																																																																																																																																																																																																																																																				
Diatoms	25	35	2	20	39	—	—																																																																																																																																																																																																																																																																																																																																																																																																				
Radiolarians	—	—	—	5	5	—	—																																																																																																																																																																																																																																																																																																																																																																																																				
Sponge spicules	—	—	—	3	3	—	—																																																																																																																																																																																																																																																																																																																																																																																																				
	clasts with Lower Miocene and Eocene nannoplankton *																																																																																																																																																																																																																																																																																																																																																																																																										
	Upper Eocene mixed into N. miocenica Zone *																																																																																																																																																																																																																																																																																																																																																																																																										
	Didymocyrtis antepenultimus Zone plus some Eocene, Oligocene, Lower Miocene species																																																																																																																																																																																																																																																																																																																																																																																																										
	PHYS. PROPERTIES																																																																																																																																																																																																																																																																																																																																																																																																										
	CHEMISTRY																																																																																																																																																																																																																																																																																																																																																																																																										

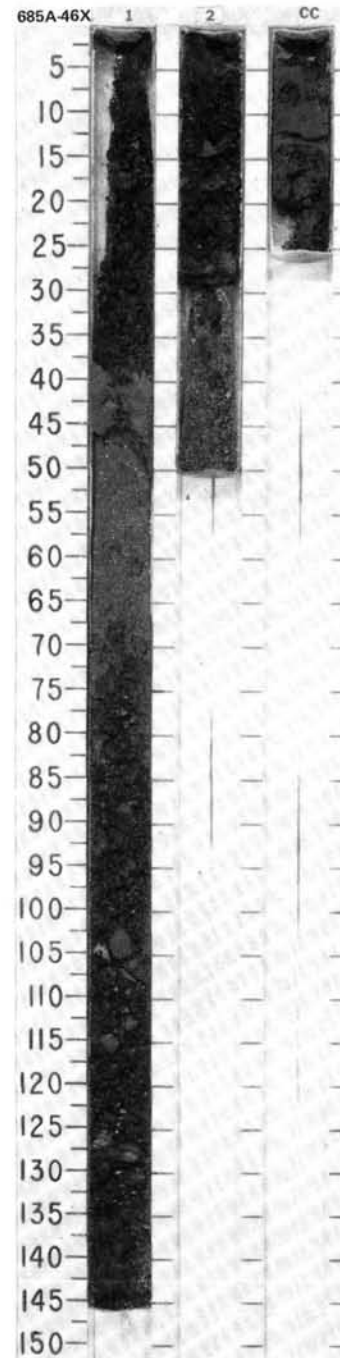
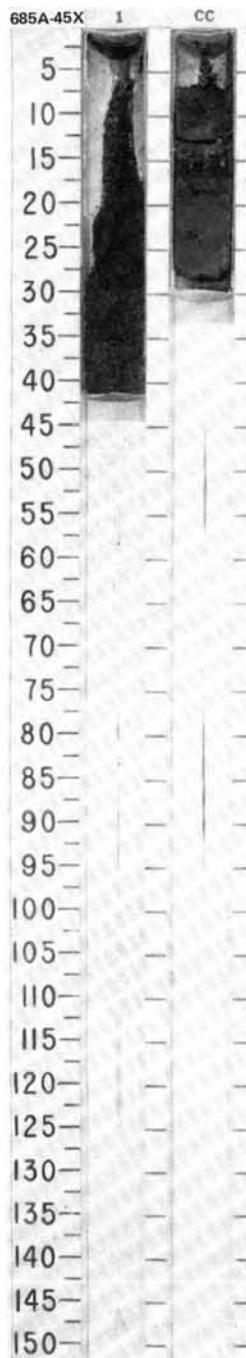


SITE 685 HOLE A CORE 45X CORED INTERVAL 5472.9-5482.4 mbsl; 402.1-411.6 mbsf

TIME-ROCK UNIT	BIOSTRAT. ZONE/ FOSSIL CHARACTER				PALEOMAGNETICS	PHYS. PROPERTIES	CHEMISTRY	SECTION	METERS	GRAPHIC LITHOLOGY	DRILLING DISTURB. SED. STRUCTURES	SAMPLES	LITHOLOGIC DESCRIPTION																																																																												
	FORAMINIFERS	NANNOFOSSILS	RADIOLARIANS	DIATOMS																																																																																					
UPPER MIOCENE	B*	B*	<i>Didymocyrtis antepenultimus</i> Zone*			1.90 0-51.08		1	0.5	VOID	XXX	*	DIATOMACEOUS AND DIATOM-BEARING MUDSTONE Major lithology: diatomaceous and diatom-bearing mudstone, dark greenish gray to very dark greenish gray (5GY 4/1 to 5GY 3/1). SMEAR SLIDE SUMMARY (%): <table border="1"> <tr> <td></td> <td>1, 35</td> <td>CC, 18</td> <td>CC, 26</td> </tr> <tr> <td></td> <td>D</td> <td>M</td> <td>D</td> </tr> </table> TEXTURE: <table border="1"> <tr> <td>Sand</td> <td>5</td> <td>5</td> <td>5</td> </tr> <tr> <td>Silt</td> <td>45</td> <td>35</td> <td>38</td> </tr> <tr> <td>Clay</td> <td>50</td> <td>60</td> <td>60</td> </tr> </table> COMPOSITION: <table border="1"> <tr> <td>Quartz</td> <td>3</td> <td>Tr</td> <td>2</td> </tr> <tr> <td>Feldspar</td> <td>10</td> <td>15</td> <td>10</td> </tr> <tr> <td>Rock fragments</td> <td>5</td> <td>3</td> <td>3</td> </tr> <tr> <td>Mica</td> <td>40</td> <td>50</td> <td>52</td> </tr> <tr> <td>Clay</td> <td>5</td> <td>5</td> <td>8</td> </tr> <tr> <td>Volcanic glass</td> <td>7</td> <td>3</td> <td>Tr</td> </tr> <tr> <td>Accessory minerals</td> <td></td> <td></td> <td></td> </tr> <tr> <td> Pyrite</td> <td>5</td> <td>3</td> <td>2</td> </tr> <tr> <td> Glauconite</td> <td>2</td> <td>3</td> <td>Tr</td> </tr> <tr> <td> ?Apatite</td> <td>—</td> <td>Tr</td> <td>—</td> </tr> <tr> <td>Diatoms</td> <td>20</td> <td>15</td> <td>20</td> </tr> <tr> <td>Radiolarians</td> <td>Tr</td> <td>—</td> <td>—</td> </tr> <tr> <td>Sponge spicules</td> <td>3</td> <td>3</td> <td>3</td> </tr> <tr> <td>Silicoflagellates</td> <td>Tr</td> <td>—</td> <td>—</td> </tr> </table>		1, 35	CC, 18	CC, 26		D	M	D	Sand	5	5	5	Silt	45	35	38	Clay	50	60	60	Quartz	3	Tr	2	Feldspar	10	15	10	Rock fragments	5	3	3	Mica	40	50	52	Clay	5	5	8	Volcanic glass	7	3	Tr	Accessory minerals				Pyrite	5	3	2	Glauconite	2	3	Tr	?Apatite	—	Tr	—	Diatoms	20	15	20	Radiolarians	Tr	—	—	Sponge spicules	3	3	3	Silicoflagellates	Tr	—	—
	1, 35	CC, 18	CC, 26																																																																																						
	D	M	D																																																																																						
Sand	5	5	5																																																																																						
Silt	45	35	38																																																																																						
Clay	50	60	60																																																																																						
Quartz	3	Tr	2																																																																																						
Feldspar	10	15	10																																																																																						
Rock fragments	5	3	3																																																																																						
Mica	40	50	52																																																																																						
Clay	5	5	8																																																																																						
Volcanic glass	7	3	Tr																																																																																						
Accessory minerals																																																																																									
Pyrite	5	3	2																																																																																						
Glauconite	2	3	Tr																																																																																						
?Apatite	—	Tr	—																																																																																						
Diatoms	20	15	20																																																																																						
Radiolarians	Tr	—	—																																																																																						
Sponge spicules	3	3	3																																																																																						
Silicoflagellates	Tr	—	—																																																																																						

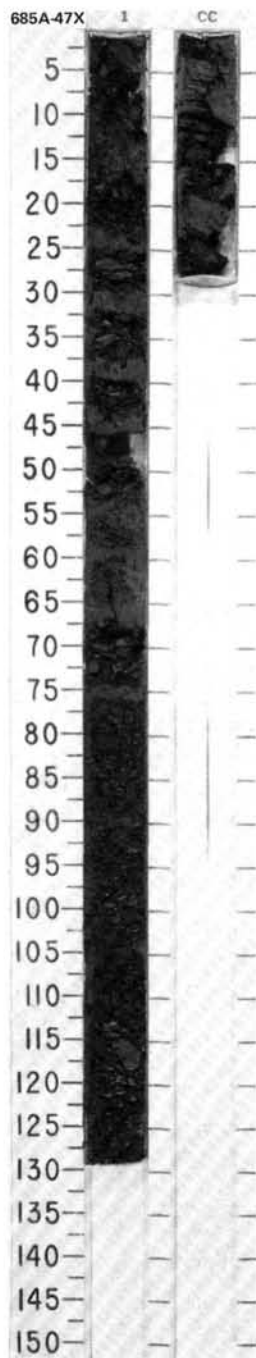
SITE 685 HOLE A CORE 46X CORED INTERVAL 5482.4-5491.9 mbsl; 411.6-421.1 mbsf

TIME-ROCK UNIT	BIOSTRAT. ZONE/ FOSSIL CHARACTER				PALEOMAGNETICS	PHYS. PROPERTIES	CHEMISTRY	SECTION	METERS	GRAPHIC LITHOLOGY	DRILLING DISTURB. SED. STRUCTURES	SAMPLES	LITHOLOGIC DESCRIPTION																																																																																
	FORAMINIFERS	NANNOFOSSILS	RADIOLARIANS	DIATOMS																																																																																									
UPPER MIOCENE	B*	B*	<i>N. miocenica</i> Zone* <i>Didymocyrtis antepenultimus</i> Zone			1.80 0-58.71		1	0.5		XXX	*	DIATOMACEOUS MUDSTONE Major lithology: diatomaceous mudstone, dark olive gray (5Y 3/2). Calcareous. Minor lithology: olive (5Y 5/3) micrite as discrete ca. 0.5-cm blebs. SMEAR SLIDE SUMMARY (%): <table border="1"> <tr> <td></td> <td>1, 44</td> <td>1, 109</td> <td>1, 128</td> </tr> <tr> <td></td> <td>M</td> <td>M</td> <td>D</td> </tr> </table> TEXTURE: <table border="1"> <tr> <td>Sand</td> <td>—</td> <td>—</td> <td>3</td> </tr> <tr> <td>Silt</td> <td>92</td> <td>92</td> <td>37</td> </tr> <tr> <td>Clay</td> <td>98</td> <td>92</td> <td>60</td> </tr> </table> COMPOSITION: <table border="1"> <tr> <td>Quartz</td> <td>2</td> <td>—</td> <td>2</td> </tr> <tr> <td>Feldspar</td> <td>—</td> <td>2</td> <td>6</td> </tr> <tr> <td>Rock fragments</td> <td>—</td> <td>—</td> <td>Tr</td> </tr> <tr> <td>Clay</td> <td>8</td> <td>—</td> <td>45</td> </tr> <tr> <td>Volcanic glass</td> <td>—</td> <td>—</td> <td>3</td> </tr> <tr> <td>Calcite/dolomite</td> <td>—</td> <td>2</td> <td>10</td> </tr> <tr> <td>Accessory minerals</td> <td></td> <td></td> <td></td> </tr> <tr> <td> Pyrite</td> <td>—</td> <td>3</td> <td>2</td> </tr> <tr> <td> Glauconite</td> <td>—</td> <td>—</td> <td>Tr</td> </tr> <tr> <td>Micrite</td> <td>90</td> <td>92</td> <td>—</td> </tr> <tr> <td>Nannofossils</td> <td>Tr</td> <td>Tr</td> <td>2</td> </tr> <tr> <td>Diatoms</td> <td>—</td> <td>Tr</td> <td>28</td> </tr> <tr> <td>Radiolarians</td> <td>—</td> <td>Tr</td> <td>—</td> </tr> <tr> <td>Sponge spicules</td> <td>—</td> <td>1</td> <td>2</td> </tr> <tr> <td>Silicoflagellates</td> <td>—</td> <td>—</td> <td>Tr</td> </tr> </table>		1, 44	1, 109	1, 128		M	M	D	Sand	—	—	3	Silt	92	92	37	Clay	98	92	60	Quartz	2	—	2	Feldspar	—	2	6	Rock fragments	—	—	Tr	Clay	8	—	45	Volcanic glass	—	—	3	Calcite/dolomite	—	2	10	Accessory minerals				Pyrite	—	3	2	Glauconite	—	—	Tr	Micrite	90	92	—	Nannofossils	Tr	Tr	2	Diatoms	—	Tr	28	Radiolarians	—	Tr	—	Sponge spicules	—	1	2	Silicoflagellates	—	—	Tr
	1, 44	1, 109	1, 128																																																																																										
	M	M	D																																																																																										
Sand	—	—	3																																																																																										
Silt	92	92	37																																																																																										
Clay	98	92	60																																																																																										
Quartz	2	—	2																																																																																										
Feldspar	—	2	6																																																																																										
Rock fragments	—	—	Tr																																																																																										
Clay	8	—	45																																																																																										
Volcanic glass	—	—	3																																																																																										
Calcite/dolomite	—	2	10																																																																																										
Accessory minerals																																																																																													
Pyrite	—	3	2																																																																																										
Glauconite	—	—	Tr																																																																																										
Micrite	90	92	—																																																																																										
Nannofossils	Tr	Tr	2																																																																																										
Diatoms	—	Tr	28																																																																																										
Radiolarians	—	Tr	—																																																																																										
Sponge spicules	—	1	2																																																																																										
Silicoflagellates	—	—	Tr																																																																																										



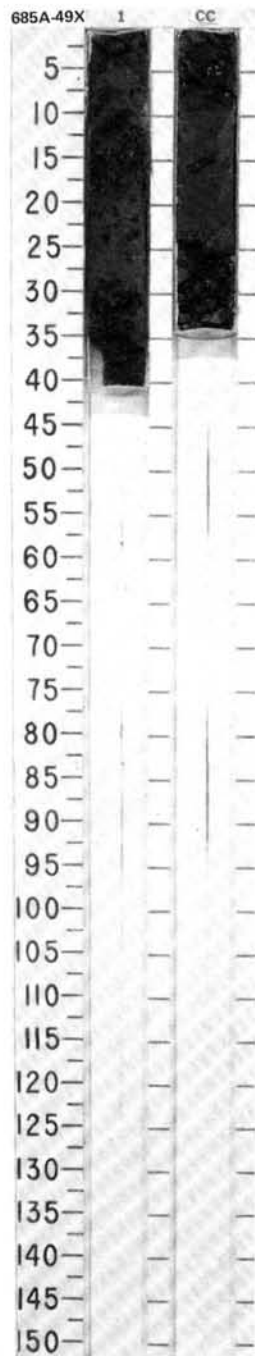
SITE 685 HOLE A CORE 47X CORED INTERVAL 5491.9-5501.4 mbsl; 421.1-430.6 mbsf

TIME-ROCK UNIT	BIOSTRAT. ZONE/ FOSSIL CHARACTER				PALEOMAGNETICS		PHYS. PROPERTIES		CHEMISTRY	SECTION	METERS	GRAPHIC LITHOLOGY	DRILLING DISTURB. SED. STRUCTURES	SAMPLES	LITHOLOGIC DESCRIPTION																																																											
	FORAMINIFERS	NANNOFOSSILS	RADIOLARIANS	DIATOMS																																																																						
UPPER MIOCENE	*B	*B	*100 rare	* <i>N. miocenica</i> Zone					IC: 0.37 OC: 1.86	CC	0.5 1.0		# # # # IW	<p>DIATOMACEOUS MUDSTONE</p> <p>Major lithology: diatomaceous mudstone, dark olive gray (5Y 3/2). Calcareous.</p> <p>Minor lithology: olive gray (5Y 5/2) muddy diatom ooze as a single bed.</p> <p>SMEAR SLIDE SUMMARY (%):</p> <table border="0"> <tr> <td></td> <td>1.27</td> <td>1.60</td> </tr> <tr> <td>D</td> <td></td> <td>M</td> </tr> </table> <p>TEXTURE:</p> <table border="0"> <tr> <td>Sand</td> <td>5</td> <td>5</td> </tr> <tr> <td>Silt</td> <td>45</td> <td>55</td> </tr> <tr> <td>Clay</td> <td>50</td> <td>40</td> </tr> </table> <p>COMPOSITION:</p> <table border="0"> <tr> <td>Quartz</td> <td>7</td> <td>2</td> </tr> <tr> <td>Feldspar</td> <td>12</td> <td>5</td> </tr> <tr> <td>Rock fragments</td> <td>4</td> <td>2</td> </tr> <tr> <td>Clay</td> <td>37</td> <td>32</td> </tr> <tr> <td>Volcanic glass</td> <td>—</td> <td>3</td> </tr> <tr> <td>Calcite/dolomite</td> <td>8</td> <td>Tr</td> </tr> <tr> <td>Accessory minerals</td> <td></td> <td></td> </tr> <tr> <td> Pyrite</td> <td>3</td> <td>2</td> </tr> <tr> <td> Glauconite</td> <td>2</td> <td>2</td> </tr> <tr> <td> Micrite</td> <td>—</td> <td>5</td> </tr> <tr> <td>Nannofossils</td> <td>Tr</td> <td>—</td> </tr> <tr> <td>Diatoms</td> <td>25</td> <td>45</td> </tr> <tr> <td>Radiolarians</td> <td>—</td> <td>Tr</td> </tr> <tr> <td>Sponge spicules</td> <td>2</td> <td>2</td> </tr> <tr> <td>Silicoflagellates</td> <td>—</td> <td>Tr</td> </tr> </table>		1.27	1.60	D		M	Sand	5	5	Silt	45	55	Clay	50	40	Quartz	7	2	Feldspar	12	5	Rock fragments	4	2	Clay	37	32	Volcanic glass	—	3	Calcite/dolomite	8	Tr	Accessory minerals			Pyrite	3	2	Glauconite	2	2	Micrite	—	5	Nannofossils	Tr	—	Diatoms	25	45	Radiolarians	—	Tr	Sponge spicules	2	2	Silicoflagellates	—	Tr
	1.27	1.60																																																																								
D		M																																																																								
Sand	5	5																																																																								
Silt	45	55																																																																								
Clay	50	40																																																																								
Quartz	7	2																																																																								
Feldspar	12	5																																																																								
Rock fragments	4	2																																																																								
Clay	37	32																																																																								
Volcanic glass	—	3																																																																								
Calcite/dolomite	8	Tr																																																																								
Accessory minerals																																																																										
Pyrite	3	2																																																																								
Glauconite	2	2																																																																								
Micrite	—	5																																																																								
Nannofossils	Tr	—																																																																								
Diatoms	25	45																																																																								
Radiolarians	—	Tr																																																																								
Sponge spicules	2	2																																																																								
Silicoflagellates	—	Tr																																																																								

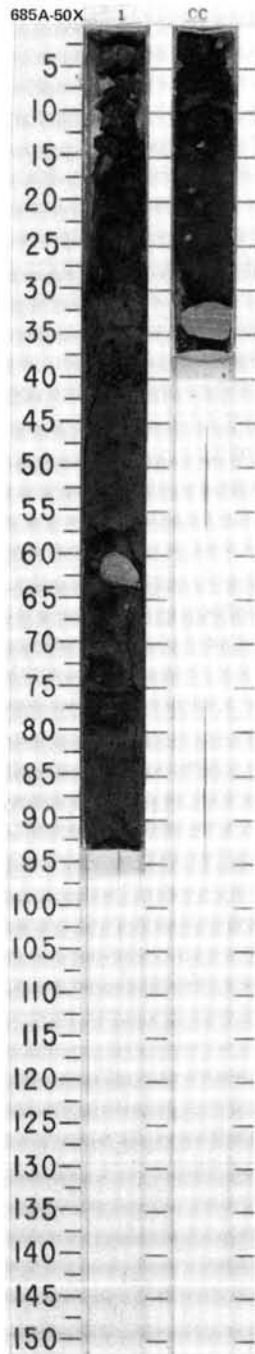


SITE 685 HOLE A CORE 49X CORED INTERVAL 5510.9-5520.4 mbsf; 440.1-449.6 mbsf

TIME-ROCK UNIT	BIOSTRAT. ZONE/ FOSSIL CHARACTER				PALEOMAGNETICS	PHYS. PROPERTIES	CHEMISTRY	SECTION	METERS	GRAPHIC LITHOLOGY	DRILLING DISTURB.	SED. STRUCTURES	SAMPLES	LITHOLOGIC DESCRIPTION																																																																												
	FORAMINIFERS	NANNOFOSSILS	RADIOLARIANS	DIATOMS																																																																																						
UPPER MIOCENE	B*													DIATOMACEOUS MUDSTONE Major lithology: diatomaceous mudstone, olive gray to dark olive gray (5Y 4/2, 5Y 3/2). Calcareous. Minor lithology: light brownish gray and olive gray (2.5Y 6/2, 5Y 5/2) dolomitic. SMEAR SLIDE SUMMARY (%): <table style="margin-left: 20px;"> <thead> <tr> <th></th> <th>CC, 14 D</th> <th>CC, 30 M</th> <th>CC, 32 M</th> </tr> </thead> <tbody> <tr> <td>Silt</td> <td>55</td> <td>25</td> <td>85</td> </tr> <tr> <td>Clay</td> <td>45</td> <td>75</td> <td>15</td> </tr> </tbody> </table> TEXTURE: <table style="margin-left: 20px;"> <tbody> <tr> <td>Silt</td> <td>55</td> <td>25</td> <td>85</td> </tr> <tr> <td>Clay</td> <td>45</td> <td>75</td> <td>15</td> </tr> </tbody> </table> COMPOSITION: <table style="margin-left: 20px;"> <tbody> <tr> <td>Quartz</td> <td>5</td> <td>5</td> <td>3</td> </tr> <tr> <td>Feldspar</td> <td>5</td> <td>5</td> <td>3</td> </tr> <tr> <td>Rock fragments</td> <td>—</td> <td>—</td> <td>2</td> </tr> <tr> <td>Mica</td> <td>Tr</td> <td>—</td> <td>—</td> </tr> <tr> <td>Clay</td> <td>45</td> <td>—</td> <td>11</td> </tr> <tr> <td>Volcanic glass</td> <td>Tr</td> <td>—</td> <td>1</td> </tr> <tr> <td>Calcite/dolomite</td> <td>15</td> <td>—</td> <td>72</td> </tr> </tbody> </table> Accessory minerals <table style="margin-left: 20px;"> <tbody> <tr> <td>Glauconite</td> <td>Tr</td> <td>Tr</td> <td>1</td> </tr> <tr> <td>Pyrite</td> <td>—</td> <td>—</td> <td>2</td> </tr> <tr> <td>Micrite</td> <td>—</td> <td>75</td> <td>5</td> </tr> <tr> <td>Diatoms</td> <td>30</td> <td>15</td> <td>—</td> </tr> <tr> <td>Radiolarians</td> <td>—</td> <td>Tr</td> <td>—</td> </tr> <tr> <td>Sponge spicules</td> <td>Tr</td> <td>Tr</td> <td>—</td> </tr> <tr> <td>Silicoflagellates</td> <td>Tr</td> <td>—</td> <td>—</td> </tr> </tbody> </table>		CC, 14 D	CC, 30 M	CC, 32 M	Silt	55	25	85	Clay	45	75	15	Silt	55	25	85	Clay	45	75	15	Quartz	5	5	3	Feldspar	5	5	3	Rock fragments	—	—	2	Mica	Tr	—	—	Clay	45	—	11	Volcanic glass	Tr	—	1	Calcite/dolomite	15	—	72	Glauconite	Tr	Tr	1	Pyrite	—	—	2	Micrite	—	75	5	Diatoms	30	15	—	Radiolarians	—	Tr	—	Sponge spicules	Tr	Tr	—	Silicoflagellates	Tr	—	—
		CC, 14 D	CC, 30 M	CC, 32 M																																																																																						
Silt	55	25	85																																																																																							
Clay	45	75	15																																																																																							
Silt	55	25	85																																																																																							
Clay	45	75	15																																																																																							
Quartz	5	5	3																																																																																							
Feldspar	5	5	3																																																																																							
Rock fragments	—	—	2																																																																																							
Mica	Tr	—	—																																																																																							
Clay	45	—	11																																																																																							
Volcanic glass	Tr	—	1																																																																																							
Calcite/dolomite	15	—	72																																																																																							
Glauconite	Tr	Tr	1																																																																																							
Pyrite	—	—	2																																																																																							
Micrite	—	75	5																																																																																							
Diatoms	30	15	—																																																																																							
Radiolarians	—	Tr	—																																																																																							
Sponge spicules	Tr	Tr	—																																																																																							
Silicoflagellates	Tr	—	—																																																																																							
		<i>Didymocyllis antepenultimus</i> Zone*																																																																																								
		<i>N. miocenica</i> Zone*																																																																																								



TIME-ROCK UNIT	BIOSTRAT. ZONE/ FOSSIL CHARACTER				PALEOMAGNETICS	PHYS. PROPERTIES	CHEMISTRY	SECTION METERS	GRAPHIC LITHOLOGY	DRILLING DISTURB. SED. STRUCTURES	SAMPLES	LITHOLOGIC DESCRIPTION																																																																																																																																																										
	FORAMINIFERS	NANNOFOSSILS	RADIOLARIANS	DIATOMS																																																																																																																																																																		
UPPER MIOCENE	Oligocene-Lower Miocene*						1					<p>POLYMICT BRECCIA/CONGLOMERATE</p> <p>Major lithology: polymict breccia/conglomerate, comprising clasts of:</p> <ol style="list-style-type: none"> 1. light olive gray (5Y 6/2) micrite. 2. gray, calcareous, diatom-bearing mudstone. 3. olive (5Y 5/3) nannofossil- and diatom-bearing mudstone. 4. grayish green (5G 5/2) calcareous mudstone. 5. light olive brown (2.5Y 5/4), (nannofossil- and) diatom-bearing muddy micrite. 6. black (N 2) diatomaceous mud (dolomitic). 7. olive gray (5Y 4/2) dolomite. 8. olive (5Y 5/4) diatomaceous mudstone. <p>Matrix: ash and diatom-bearing mudstone.</p> <p>Clast at base of CC. Finely laminated dolomitic.</p> <p>SMEAR SLIDE SUMMARY (%):</p> <table border="1"> <tr> <td></td> <td>1, 36</td> <td>1, 45</td> <td>1, 50</td> <td>1, 53</td> <td>1, 62</td> <td>1, 65</td> </tr> <tr> <td></td> <td>M</td> <td>D</td> <td>M</td> <td>M</td> <td>M</td> <td>M</td> </tr> </table> <p>TEXTURE:</p> <table border="1"> <tr> <td>Sand</td> <td>—</td> <td>20</td> <td>5</td> <td>—</td> <td>—</td> <td>—</td> </tr> <tr> <td>Silt</td> <td>50</td> <td>40</td> <td>35</td> <td>30</td> <td>30</td> <td>—</td> </tr> <tr> <td>Clay</td> <td>50</td> <td>40</td> <td>60</td> <td>70</td> <td>70</td> <td>—</td> </tr> </table> <p>COMPOSITION:</p> <table border="1"> <tr> <td>Quartz</td> <td>5</td> <td>10</td> <td>5</td> <td>3</td> <td>5</td> <td>2</td> </tr> <tr> <td>Feldspar</td> <td>5</td> <td>10</td> <td>5</td> <td>5</td> <td>5</td> <td>2</td> </tr> <tr> <td>Rock fragments</td> <td>—</td> <td>5</td> <td>2</td> <td>2</td> <td>2</td> <td>1</td> </tr> <tr> <td>Mica</td> <td>Tr</td> <td>Tr</td> <td>1</td> <td>—</td> <td>—</td> <td>—</td> </tr> <tr> <td>Clay</td> <td>50</td> <td>36</td> <td>50</td> <td>20</td> <td>55</td> <td>10</td> </tr> <tr> <td>Volcanic glass</td> <td>Tr</td> <td>20</td> <td>2</td> <td>—</td> <td>3</td> <td>—</td> </tr> <tr> <td>Calcite/dolomite</td> <td>10</td> <td>2</td> <td>—</td> <td>—</td> <td>10</td> <td>—</td> </tr> <tr> <td>Accessory minerals</td> <td>—</td> <td>2</td> <td>—</td> <td>—</td> <td>—</td> <td>—</td> </tr> <tr> <td>Pyrite</td> <td>—</td> <td>5</td> <td>2</td> <td>2</td> <td>—</td> <td>Tr</td> </tr> <tr> <td>Glaucinite</td> <td>—</td> <td>—</td> <td>2</td> <td>2</td> <td>—</td> <td>Tr</td> </tr> <tr> <td>Phosphate</td> <td>—</td> <td>—</td> <td>—</td> <td>1</td> <td>—</td> <td>—</td> </tr> <tr> <td>Micrite</td> <td>—</td> <td>—</td> <td>3</td> <td>40</td> <td>15</td> <td>80</td> </tr> <tr> <td>Foraminifers</td> <td>—</td> <td>—</td> <td>1</td> <td>1</td> <td>—</td> <td>—</td> </tr> <tr> <td>Nannofossils</td> <td>Tr</td> <td>Tr</td> <td>10</td> <td>3</td> <td>Tr</td> <td>Tr</td> </tr> <tr> <td>Diatoms</td> <td>30</td> <td>10</td> <td>10</td> <td>20</td> <td>5</td> <td>3</td> </tr> <tr> <td>Radiolarians</td> <td>—</td> <td>Tr</td> <td>2</td> <td>—</td> <td>—</td> <td>1</td> </tr> <tr> <td>Sponge spicules</td> <td>Tr</td> <td>Tr</td> <td>2</td> <td>2</td> <td>Tr</td> <td>1</td> </tr> </table>		1, 36	1, 45	1, 50	1, 53	1, 62	1, 65		M	D	M	M	M	M	Sand	—	20	5	—	—	—	Silt	50	40	35	30	30	—	Clay	50	40	60	70	70	—	Quartz	5	10	5	3	5	2	Feldspar	5	10	5	5	5	2	Rock fragments	—	5	2	2	2	1	Mica	Tr	Tr	1	—	—	—	Clay	50	36	50	20	55	10	Volcanic glass	Tr	20	2	—	3	—	Calcite/dolomite	10	2	—	—	10	—	Accessory minerals	—	2	—	—	—	—	Pyrite	—	5	2	2	—	Tr	Glaucinite	—	—	2	2	—	Tr	Phosphate	—	—	—	1	—	—	Micrite	—	—	3	40	15	80	Foraminifers	—	—	1	1	—	—	Nannofossils	Tr	Tr	10	3	Tr	Tr	Diatoms	30	10	10	20	5	3	Radiolarians	—	Tr	2	—	—	1	Sponge spicules	Tr	Tr	2	2	Tr	1
	1, 36	1, 45	1, 50	1, 53	1, 62	1, 65																																																																																																																																																																
	M	D	M	M	M	M																																																																																																																																																																
Sand	—	20	5	—	—	—																																																																																																																																																																
Silt	50	40	35	30	30	—																																																																																																																																																																
Clay	50	40	60	70	70	—																																																																																																																																																																
Quartz	5	10	5	3	5	2																																																																																																																																																																
Feldspar	5	10	5	5	5	2																																																																																																																																																																
Rock fragments	—	5	2	2	2	1																																																																																																																																																																
Mica	Tr	Tr	1	—	—	—																																																																																																																																																																
Clay	50	36	50	20	55	10																																																																																																																																																																
Volcanic glass	Tr	20	2	—	3	—																																																																																																																																																																
Calcite/dolomite	10	2	—	—	10	—																																																																																																																																																																
Accessory minerals	—	2	—	—	—	—																																																																																																																																																																
Pyrite	—	5	2	2	—	Tr																																																																																																																																																																
Glaucinite	—	—	2	2	—	Tr																																																																																																																																																																
Phosphate	—	—	—	1	—	—																																																																																																																																																																
Micrite	—	—	3	40	15	80																																																																																																																																																																
Foraminifers	—	—	1	1	—	—																																																																																																																																																																
Nannofossils	Tr	Tr	10	3	Tr	Tr																																																																																																																																																																
Diatoms	30	10	10	20	5	3																																																																																																																																																																
Radiolarians	—	Tr	2	—	—	1																																																																																																																																																																
Sponge spicules	Tr	Tr	2	2	Tr	1																																																																																																																																																																
							CC					<p>1, 82</p>	CC, 26																																																																																																																																																									
							M					<p>M</p>	M																																																																																																																																																									



SITE 685 HOLE A CORE 51X CORED INTERVAL 5529.9-5539.4 mbsl; 459.1-468.6 mbsf

TIME-ROCK UNIT	BIOSTRAT. ZONE/ FOSSIL CHARACTER			PALEOMAGNETICS	PHYS. PROPERTIES	CHEMISTRY	SECTION METERS	GRAPHIC LITHOLOGY	DRILLING DISTURB. SED. STRUCTURES	SAMPLES	LITHOLOGIC DESCRIPTION																																																																																																																																																												
	FORAMINIFERS	NANNOFOSSELS	RADIOLARIANS									DIATOMS																																																																																																																																																											
							CC				<p>BRECCIA/CONGLOMERATE with SANDY SILT</p> <p>Major lithology: breccia/conglomerate with sandy silt, containing clasts of: black (N 2) mudstone (few diatoms and radiolarians); grayish green diatomaceous mudstone; dark gray (N 4), ash, silty feldspathic sandstone; muddy quartzo-feldspathic sand; micritic sand; and veined, carbonate-cemented feldspathic sandstone.</p> <p>Matrix: gray (N 3-N 4) lithic and ash sandy silt.</p> <p>SMEAR SLIDE SUMMARY (%):</p> <table border="1"> <thead> <tr> <th></th> <th>CC. 17 D</th> <th>CC. 25 M</th> <th>CC. 29 M</th> <th>CC. 34 M</th> <th>CC. 41 M</th> </tr> </thead> <tbody> <tr> <td>Sand</td> <td>30</td> <td>5</td> <td>50</td> <td>45</td> <td>40</td> </tr> <tr> <td>Silt</td> <td>40</td> <td>25</td> <td>40</td> <td>40</td> <td>30</td> </tr> <tr> <td>Clay</td> <td>30</td> <td>70</td> <td>10</td> <td>15</td> <td>30</td> </tr> </tbody> </table> <p>TEXTURE:</p> <table border="1"> <thead> <tr> <th></th> <th>CC. 17 D</th> <th>CC. 25 M</th> <th>CC. 29 M</th> <th>CC. 34 M</th> <th>CC. 41 M</th> </tr> </thead> <tbody> <tr> <td>Sand</td> <td>30</td> <td>5</td> <td>50</td> <td>45</td> <td>40</td> </tr> <tr> <td>Silt</td> <td>40</td> <td>25</td> <td>40</td> <td>40</td> <td>30</td> </tr> <tr> <td>Clay</td> <td>30</td> <td>70</td> <td>10</td> <td>15</td> <td>30</td> </tr> </tbody> </table> <p>COMPOSITION:</p> <table border="1"> <thead> <tr> <th></th> <th>CC. 17 D</th> <th>CC. 25 M</th> <th>CC. 29 M</th> <th>CC. 34 M</th> <th>CC. 41 M</th> </tr> </thead> <tbody> <tr> <td>Quartz</td> <td>20</td> <td>5</td> <td>15</td> <td>20</td> <td>20</td> </tr> <tr> <td>Feldspar</td> <td>20</td> <td>10</td> <td>40</td> <td>30</td> <td>10</td> </tr> <tr> <td>Rock fragments</td> <td>10</td> <td>Tr</td> <td>8</td> <td>10</td> <td>10</td> </tr> <tr> <td>Mica</td> <td>Tr</td> <td>—</td> <td>—</td> <td>—</td> <td>—</td> </tr> <tr> <td>Clay</td> <td>Tr</td> <td>55</td> <td>10</td> <td>15</td> <td>—</td> </tr> <tr> <td>Volcanic glass</td> <td>30</td> <td>10</td> <td>25</td> <td>5</td> <td>5</td> </tr> <tr> <td>Calcite/dolomite</td> <td>5</td> <td>Tr</td> <td>3</td> <td>—</td> <td>—</td> </tr> <tr> <td>Accessory minerals</td> <td></td> <td></td> <td></td> <td></td> <td></td> </tr> <tr> <td> Pyrite</td> <td>—</td> <td>5</td> <td>2</td> <td>2</td> <td>—</td> </tr> <tr> <td> Glauconite</td> <td>—</td> <td>Tr</td> <td>Tr</td> <td>4</td> <td>Tr</td> </tr> <tr> <td> Barite?</td> <td>10</td> <td>—</td> <td>—</td> <td>—</td> <td>10</td> </tr> <tr> <td> Opauques</td> <td>5</td> <td>—</td> <td>—</td> <td>8</td> <td>—</td> </tr> <tr> <td> Apatite</td> <td>—</td> <td>—</td> <td>—</td> <td>—</td> <td>—</td> </tr> <tr> <td> Micrite</td> <td>—</td> <td>—</td> <td>—</td> <td>—</td> <td>50</td> </tr> <tr> <td> Diatoms</td> <td>—</td> <td>5</td> <td>—</td> <td>3</td> <td>—</td> </tr> <tr> <td> Radiolarians</td> <td>—</td> <td>5</td> <td>—</td> <td>—</td> <td>—</td> </tr> <tr> <td> Sponge spicules</td> <td>—</td> <td>Tr</td> <td>—</td> <td>—</td> <td>—</td> </tr> </tbody> </table>		CC. 17 D	CC. 25 M	CC. 29 M	CC. 34 M	CC. 41 M	Sand	30	5	50	45	40	Silt	40	25	40	40	30	Clay	30	70	10	15	30		CC. 17 D	CC. 25 M	CC. 29 M	CC. 34 M	CC. 41 M	Sand	30	5	50	45	40	Silt	40	25	40	40	30	Clay	30	70	10	15	30		CC. 17 D	CC. 25 M	CC. 29 M	CC. 34 M	CC. 41 M	Quartz	20	5	15	20	20	Feldspar	20	10	40	30	10	Rock fragments	10	Tr	8	10	10	Mica	Tr	—	—	—	—	Clay	Tr	55	10	15	—	Volcanic glass	30	10	25	5	5	Calcite/dolomite	5	Tr	3	—	—	Accessory minerals						Pyrite	—	5	2	2	—	Glauconite	—	Tr	Tr	4	Tr	Barite?	10	—	—	—	10	Opauques	5	—	—	8	—	Apatite	—	—	—	—	—	Micrite	—	—	—	—	50	Diatoms	—	5	—	3	—	Radiolarians	—	5	—	—	—	Sponge spicules	—	Tr	—	—	—
	CC. 17 D	CC. 25 M	CC. 29 M	CC. 34 M	CC. 41 M																																																																																																																																																																		
Sand	30	5	50	45	40																																																																																																																																																																		
Silt	40	25	40	40	30																																																																																																																																																																		
Clay	30	70	10	15	30																																																																																																																																																																		
	CC. 17 D	CC. 25 M	CC. 29 M	CC. 34 M	CC. 41 M																																																																																																																																																																		
Sand	30	5	50	45	40																																																																																																																																																																		
Silt	40	25	40	40	30																																																																																																																																																																		
Clay	30	70	10	15	30																																																																																																																																																																		
	CC. 17 D	CC. 25 M	CC. 29 M	CC. 34 M	CC. 41 M																																																																																																																																																																		
Quartz	20	5	15	20	20																																																																																																																																																																		
Feldspar	20	10	40	30	10																																																																																																																																																																		
Rock fragments	10	Tr	8	10	10																																																																																																																																																																		
Mica	Tr	—	—	—	—																																																																																																																																																																		
Clay	Tr	55	10	15	—																																																																																																																																																																		
Volcanic glass	30	10	25	5	5																																																																																																																																																																		
Calcite/dolomite	5	Tr	3	—	—																																																																																																																																																																		
Accessory minerals																																																																																																																																																																							
Pyrite	—	5	2	2	—																																																																																																																																																																		
Glauconite	—	Tr	Tr	4	Tr																																																																																																																																																																		
Barite?	10	—	—	—	10																																																																																																																																																																		
Opauques	5	—	—	8	—																																																																																																																																																																		
Apatite	—	—	—	—	—																																																																																																																																																																		
Micrite	—	—	—	—	50																																																																																																																																																																		
Diatoms	—	5	—	3	—																																																																																																																																																																		
Radiolarians	—	5	—	—	—																																																																																																																																																																		
Sponge spicules	—	Tr	—	—	—																																																																																																																																																																		

